

CRITICAL DESIGN ASPECTS OF PLASTIC INJECTION MOULD

Thesis

Submitted in partial fulfilment of requirements for the degree of

DOCTOR OF PHILOSOPHY

by

MURALIDHAR LAKKANNA



DEPARTMENT OF MECHANICAL ENGINEERING
NATIONAL INSTITUTE OF TECHNOLOGY KARNATAKA
SRINIVASNAGAR P.O, SURATHKAL, MANGALORE-575 025
KARNATAKA, INDIA

July 2016

DECLARATION

I hereby declare that research thesis entitled **Critical Design Aspects of Plastic Injection Mould** is being submitted to National Institute of Technology Karnataka, Surathkal in partial fulfilment towards the requirements for the award of Doctor of Philosophy in Mechanical Engineering degree is a *bonafide report of original research work carried out by me*. The material contained in this research thesis has not been submitted / formed the basis for award of any degree, diploma, associate ship, fellowship or any other similar type; either to this institute or to any other university or institution previously.

Signature of the Research Scholar

NITK Surathkal
MAY 8, 2017

Muralidhar Lakkanna
Register Number: ME10F03

CERTIFICATE

This is to *certify* that the Research Thesis entitled **Critical Design Aspects of Plastic Injection Mould** submitted by **Mr. Muralidhar Lakkanna**, (Register Number: ME10F03) as a record of the research work to be carried out by him, is *accepted as Research Thesis* submission in partial fulfilment of the requirements for the award of degree of Doctor of Philosophy.

Dr. RAVIKIRAN KADOLI
Professor, Research Guide

Dr. G C MOHAN KUMAR
Professor, Research Guide

Chairman - DRPC
(Signature with date and seal)

ACKNOWLEDGEMENT

This research work was carried out at Department of Mechanical Engineering, National Institute of Technology Karnataka with fellowship from Ministry of Human Resources Development. I'm grateful to Government of India for this award indeed it's a memorable honour on me.

I chose to convey my most sincere gratitude to Dr. G C Mohan Kumar for always being available and helping me all the while. Similarly, I'm also thankful to Dr. Ravikiran Kadoli for his reviews. I further thank my Doctorial Research Progress Committee members, Dr. V Murugan, Department of Mathematical and Computational Sciences and Dr. S M Murigendrappa, Department of Mechanical Engineering, for their encouragement. I'm offering special thanks to many professional peers for suggestions, criticisms, rewarding discussions and intellectual support.

Finally, I wish to express highest respects to my beloved father Sri Lakkanna, mother Smt. Narasamma for always encouraging and deepest gratitude to my dearest brother Dr. Yathindra Lakkanna for e'er supporting me. Finally, my special thanks to my wife Smt. Nagaveni and daughter Amrutha, whose love braved me through this insanity.

Muralidhar Lakkanna

Critical Design Aspects of Plastic Injection Mould

Abstract

To contrive parts within acceptable levels of performance and quality; proper design of injection mould feed system elements is essential and depends on {machine, material, moulding} combination including the understanding of prominent factors that conventional methods or simulating routines increasingly trust. So agnising the thermomechanical phenomenal complexities of non-Newtonian thermoplastics injection as a criterion to design feed system elements is essential to advance injection moulding technology. In regard, this strategic foresight of synchronising features on parts, behavioural properties in injectant and specifications upon machine is pursued in this dissertation. Specific arguments made here pertain to filling interval; while factoring multiple parameters like injectant viscosity, shear thinning index, injector's pressure, injection rate, impression volume and depth below parting surface. Analytical approach was adopted to deduce simple criteria for injection mould sprue and runner system design. To empathise their worthiness, they were sensitised by representatively perturbing each factor a with real combination exclusively from each aspect.

The instantaneous criterion proposed for sprue design is from the function of expansion across high-temperature and high-shear to low-temperature and low-shear injection moulding. A thorough sensitisation inquest involving most injectants asserted that pressure gradient dependent apparent viscosity was a dominant factor than shear gradient dependent thinning index.

A notable apprehension from sensitising runner size design was the dependence of assessing choice frailty on the square of in-situ state transformation behaviour against nonNewtonian mobility phenomena; and this physics was unique to each thermoplastic. Besides, the characterisation of apparent viscosity and shear thinning index combination deciphered that injection moulding configuration complexity directly provokes nonNewtonian aggression while simplicity conciliates towards Newtonian axioms.

Regardless of injection moulding combination, the explicit prevalence of afore themes were in concurrence with respective traditional cults and myths. Thus, contributing exact parametric criterion for sprue and runner systems design with respective degrees of freedom restrained from real combination. Further the ability to extend these criteria and their inferences arbitrarily to de-facto applications across many properties, needs, specifications portray value from economics, easiness and endlessness.

Contents

a.	Title Page	i
b.	Declaration	ii
c.	Certificate	iii
d.	Acknowledgement	iv
e.	Abstract	v
f.	Contents	vi
g.	List of figures	ix
h.	List of tables	xi
i.	List of symbols	xii
j.	List of acronyms	xiv
1	Introduction.	01-09
1.1.	Plastics Processing	01
1.2.	Injection Moulding Process	01
1.2.1.	Advantages	02
1.2.2.	Disadvantages	02
1.3.	Injection Moulding Physics	03
1.4.	State of art in Injection Moulding Technology	04
1.5.	Challenges in Injection Moulding	05
1.6.	Challenges in Mould Design	06
1.7.	Accessible Solutions to Design Moulds	08
1.8.	Objectives	09
2	Review of Literature and Methodology.	10-27
2.1.	Traditional Methods to Design Injection Moulds	10
2.2.	Conventional Methods to Design Injection Moulds	11
2.3.	Modern Methods to Design Injection Moulds	14
2.3.1.	Representations for Design	14
2.3.2.	Types of Calculations	16
2.3.3.	Calculated Solutions	18
2.4.	Summary of Literature Survey	19
2.5.	Prospects for Research	21
2.6.	Feed System Design	24
2.6.1.	Design Methods to Feed	25
2.6.2.	Modelling Approach to Feed System	26
3	Design of Sprue-bush	28-90
3.1.	Design of Sprue Bush Engagement	32

3.1.1.	Leak Detection.	35
3.1.2.	Seal Design Endeavours.	36
3.1.3.	Euclid Relations at Sprue Bush to Nozzle tip engagement.	37
3.1.4.	Design Characterisation.	43
3.1.5.	Design Sensitivity.	46
3.1.6.	Conclusion.	49
3.2.	Design of Sprue Conduit System.	50
3.2.1.	Sprue Conduit Design Criteria.	50
3.2.2.	Design Sensitivity Characterisation	54
3.2.2.1.	Sprue-conduit Dependence on Injectant	55
3.2.2.2.	Sprue-conduit Dependence on Machine.	64
3.2.2.3.	Sprue-conduit Dependence on Component	71
3.2.3.	Conclusion.	75
3.3.	Experimental Studies	75
3.3.1.	Methods.	76
3.3.2.	Equipment.	81
3.3.3.	Summary.	89
4	Runner Design	91-134
4.1.	Runner Cross-section Geometry Design	92
4.2.	Runner Cross-section Mechanics Design.	94
4.3.	Runner Cross-section Designing	98
4.4.	Runner Design Problem Definition.	102
4.5.	Runner Design Methodology	102
4.6.	Runner Design Criteria	104
4.7.	Non-Newtonian Injectant Behaviour in Runner Conduits Design	110
4.8.	Illustration.	113
4.8.1.	Sensitising apparent viscosity.	115
4.8.2.	Sensitising shear thinning index	116
4.8.3.	Sensitising thermoplastics de-facto range	117
4.9.	Statistical validation	119
4.9.1.	Deviation	122
4.9.2.	Variance.	123
4.9.3.	Distribution.	125

4.9.4. Summarisation	126
4.9.5. Comprehension	128
4.9.6. Standardised Residues	132
4.10. Conclusion.	134
5 Research Summary	135-138
5.1. Conclusion.	135
5.2. Limitations.	137
5.3. Recommendations for Future Work.	138
Appendix	139-140
Appendix 1 Technical Specifications of Injection Moulding Machine.	139
Appendix 2 Accuracy of injection moulding machine control system.	139
Appendix 3 Test Specimen drawing.	140
References	141-173
<i>List of Publications and Communications made out of this Phd Thesis.</i>	174-175
.....	

List of Figures

Figure 1.1	Research on Injection Mould Design	08
Figure 3.1	Schematic representation of typical sprue bush	28
Figure 3.2	Mould sprue-bush to machine nozzle-tip engagement design	38
Figure 3.3	Concave-Convex radii engagement design	38
Figure 3.4	Schematic representation of Concave Convex radii engagement	42
Figure 3.5	Recess radius design sensitivity to pinch angle (θ)	43
Figure 3.6	Max pinch-angle sensitivity to nozzle-tip orifice diameter	45
Figure 3.7	Max pinch-angle sensitivity to approach radius	46
Figure 3.8	Sprue recess radius sensitivity to pinch-angle relative to sprue approach radius for 5mm inlet orifice diameter	47
Figure 3.9	Sprue recess radius sensitivity to pinch-angle relative to sprue inlet orifice diameter for 25mm approach radius	47
Figure 3.10	Pinch Depth	48
Figure 3.11	Schematic representation of a typical sprue bush conduit region	51
Figure 3.12	Sprue bush taper angle about apparent viscosity of a thermoplastic melt	61
Figure 3.13	Sprue taper expansion about shear-thinning index of a injectant	64
Figure 3.14	Sprue taper expansion about injection rate in a machine	66
Figure 3.15	Typical Injection rate profile control for an injection moulding machine	67
Figure 3.16	Sprue taper expansion about maximum injection pressure of the machine	68
Figure 3.17	Preferable BSR versus barrel bore diameter (mm) relativity	69
Figure 3.18	Sprue taper expansion relative to machine's barrel size	70
Figure 3.19	Relative sprue taper expansion over part volume	73
Figure 3.20	Sprue taper expansion about needed sprue length	74
Figure 3.21	Experimental scheme	76
Figure 3.22	Statistical modelling of sprue expansion angle design	77
Figure 3.23	Representative photo of T11 treatment	80
Figure 3.24	Strategy of thermoplastics chosen for testing: PP, PS and POM	82
Figure 3.25	Photograph of machine used for contriving specimens	87
Figure 3.26	Elevation of mould closed assembly	87
Figure 3.27	Drawing of sprue bushes with vary expansions	88

Figure 3.28	Bottom Half plan views of mould halves assembly	90
Figure 4.1	Credible runner cross-sections adopted in practise	92
Figure 4.2	Preferential order of runner cross-section selection	92
Figure 4.3	Round cross-section exerts pressure and confines heat dissipation uniformly in all directions	93
Figure 4.4	Parabolic runner cross-section commonly adopted in practise	93
Figure 4.5	Runner radius relative to apparent viscosity	112
Figure 4.6	Feasible runner radius size relative to real world thermoplastic apparent viscosity	113
Figure 4.7	Runner radius relative to apparent viscosity	115
Figure 4.8	Runner radius relative to power law shear-thinning index (extended range)	117
Figure 4.9	Runner radius relative to shear-thinning index (across thermoplastics range)	118
Figure 4.10	Contour analysis of runner radius	119
Figure 4.11	Relative dispersion of runner radius size between actual and analytical resolute	122
Figure 4.12	Standard deviation dispersion of actual surveyed moulds	123
Figure 4.13	Normal dispersion function of CoV in runner size	124
Figure 4.14	Goodness of fit to normality of runner size CoVs	124
Figure 4.15	Pareto distribution of coefficient of runner radius size variation of actual size from analytical resolute	126
Figure 4.16	Goodness of fit to log normality of runner size CoVs	127
Figure 4.17	Histogram of runner sizes for real surveyed moulds and analytical perspective	129
Figure 4.18	Probability of congruence relative to analytical runner size	132
Figure 4.19	Normality of standardised residue	133

List of Tables

Table 3.1	Characteristics properties of ABS	65
Table 3.2	Treatment Scheme	79
Table 3.3	Treatment Matrix	80
Table 3.4	Characteristic properties of Injectants	83
Table 3.5	Characteristic property data of KOCTEL K700	83
Table 3.6	Characteristic property data of REPOL H110MA	84
Table 3.7	Characteristic property data of SC 203EL	86
Table 4.1	Apparent design purpose to proviso mapping of runner	91
Table 4.2	Possible consequences of inadequate (narrow) runner size that aggressively restrict injection	95
Table 4.3	Possible consequences of large size runner design that casually allow injection	96
Table 4.4	Sprint 650T Machine Specifications	114
Table 4.5	Comparison of various production moulds surveyed	120
Table 4.6	Consolidation and summarisation of survey	128
Table 4.7	Summarised data of surveyed production moulds	131

List of Symbols

The symbols used here follow latest recommendations of the Society of Rheology in SI units

S_n	Hemispherical abstract surface on nozzle tip	
S_s	Hemispherical abstract surface in sprue head	
R_n	Nozzle-tip approach convexity (<i>spherical</i>) external radius	m
R_s	Sprue recess concavity (<i>spherical</i>) internal radius	m
O_n	Nozzle-tip approach convexity focal centre	
D_n	Nozzle-tip aperture diameter	m
O_s	Sprue recess concavity focal centre	
D_n	Sprue conduit inlet orifice diameter	m
(x, y, z)	Co-ordinate system with origin at injection shock orifice centre	
ϕ	Pinch angle	deg
ϕ_n	Included angle between shock plane and the tangent to nozzle approach surface at engagement point	deg
ϕ_s	Included angle between shock plane and the tangent to sprue recess surface at engagement point	deg
a	Distance between nozzle tip approach (<i>hemispherical radius</i>) focal centre to injection shock plane	m
b	Distance between sprue bush recess (<i>hemispherical radius</i>) focal centre to injection shock plane	m
y_n	Tangential line to nozzle approach surface at engagement point	
y_s	Tangential line to sprue recess surface at engagement point	
P_c	Sprue-conduit entrance-pressure loss	MPa
τ	Shear injection stress	MPa
L	Sprue-bush length	m
D_{co}	Sprue passage exit orifice diameter	m
th	Impression gap thickness	m
P	Injection pressure	MPa
R	Conduit radius	m
$\dot{\gamma}$	Shear-rate of injectant	sec ⁻¹
Q	Volumetric diffusion rate	m ³ / sec
V_{Shot}	Shot volume	m ³
$t_{fill\ time}$	Fill time	sec
V_{Stroke}	Stroke volume of machine	m ³
$U_{Injection}$	Injection rate	m/sec
μ	Apparent viscosity of injectant	Pa-sec
n	Power-law index of shear-thinning behaviour in injectant	
C_p	Characteristic coefficient of a thermoplastic melt representing the extent to which conduit has to recover pressure	
E_r	Expansion ratio	

α	Half angle of conduit expansion	
(r, θ, ξ)	Cylindrical coordinate system	m
U_r, U_θ, U_ξ	Velocity components	m/sec
C_1, C_2, C_3	Integration components	
\bar{U}	Characteristic velocity	m/sec
L_r	Characteristic length of runner-conduit path	m
D	Runner Diameter	m
W_{shot}	Shot weight	gram
S	Runner-conduit surface	m ²
λ	Characteristic interval to relax injection stresses	sec
E	Modulus of elasticity of injectant	MPa
ρ	In-situ density of injectant	Kg/m ³
V_{Shot}	Shot volume	m ³
V_{Stroke}	Stroke volume	m ³
$Q[t]$	Volumetric injection-rate	m ³ /sec
t	Total injection time (fill + pack)	sec
T_0	Influx injection temperature across runner inlet	K
T	Efflux temperature across runner exit	K
T_g	Glass transition temperature (ISO 11357-2:2013)	K
μ_0	Power-law consistency factor being influx apparent viscosity at injection temperature T_0	
ΔE	Flow activation energy of injectant	
\mathbb{R}	Universal gas constant	
N	Survey sample size	
R_a	Analytically determined resolute runner size	m
R_c	Actual runner size observed on a random mould	m
σ_R	Standard deviation of surveyed mould runner size variation across its corresponding analytical resolute	m
z	Random statistical variable representing altogether differences in design, configuration, injectant and machine among the surveyed moulds	
k	Runner size category no.	
i_k	Runner size interval of k^{th} category	m
j_k	No. of moulds in k^{th} category	
π_k	Probable intensity of k^{th} category ($C_{oV} \in i_k$)	
χ_k	Discrepancy of k^{th} category	
df	Statistical degree of freedom	
$n_{C_{oV}}$	Number of moulds having similar CoV	
p	Probability of incongruence $R_c \neq R_a$	

List of Acronyms

AQL	Acceptable Quality Level	ISO 2759-1:1999
APL	Acceptable Performance Level	ISO 22514-1: 2014
OEM	Original Equipment Manufacturer	ISO 24700: 2005
PPAP	Production Part Approval Process	ISO TS 16949
CoQ	Cost of Quality	ISO TR 10014
CAD	Computer Aided Design	ISO 13567
CAE	Computer Aided Engineering	ISO 10303-233
GUI	Graphical User Interface	ISO 9241-171: 2008
BSR	Barrel-to-Shot Volume Ratio	
FEM	Finite Element Method	
FDM	Finite Difference Method	
FVM	Finite Volume Method	
BEM	Boundary Element Method	
CFD	Computational Fluid Dynamics	
PCD	Pitch Circle Diameter	
SEM	Scanning Electron Microscope	
Ra	Maximum surface roughness	ISO 4287:1997
Re	Reynolds Number	
M	Mach number at Injection shock plane	
CoV	Co-efficient of Variation	
CSM	Continuous Sensitivity Method	
Pdf	Probability distribution function	
DoE	Design of Experiments	
PLC	Programmable Logic Controller	
POM	Poly-Oxy-Methylene	CAS 9002-81-7
PP	Poly-Propylene	CAS 9003-07-0
PS	Poly-Styrene	CAS 9003-53-6

Chapter One

Introduction

1.1 PLASTICS PROCESSING

Polymer processing is producing articles of utility by applying external pressure and temperature through supporting systems. Wide diversity persists among the methods, due to extensive range of properties of polymers, great physical variety of equipment and strange needs on articles of commerce. Yet to foresee one as best suitable, its relations among design factors, controlling variables and expectations must be known thoroughly. And that idealises as the basis to process complex combination on polymer, geometries, conditions and field. Or else the process of interest often becomes "*pathological*" and requires quick intrigues, recurring redesign hiccups, raging resets and those provoke specific experiments, which typically provide only non-vult hunches to individual queries.

Many impending applications across diverse scales are increasingly prescribing plastics mainly to reduce wastes, minimise emissions, lessen dependence on fossil reserves and energy demand. Utilising plastics decouples overall environment load in relative terms of quality of life and prospects for economic growth. Owing to these preferences, plastics are eventually proving out to be a destiny for process, material and design migrations. Besides, their ability to synthesise various combination of properties is enticing adoption for many applications. Therefore, understanding plastics processing thoroughly is important to produce parts that append maximum value.

1.2 INJECTION MOULDING PROCESS

Contributions of plastics to civilisation have ranked polymer processing among the tenacious sectors of world economy and that concomitantly ensures a constant compulsion to elate sophistication, quality, performance, durability, staunch lead-time besides economising. Such adept patronage of commerce has sprung-up several polymer processing techniques; among them injection moulding technology has witnessed an unprecedented adoption rate that among every third plastic part is injection moulded. Thus it's producing parts to all facets of civilisations and that vends a broad application regime ranging from tiny nanosensors for cancer treatment

(Gordon, 2012) to gigantic marine structural hulls (Hill, 1996). These trends are sprinting the injection moulding into technical ingenuity by constantly insisting for complex and intricate processing. Like little change in a moulding wall thickness causes large swings in injection pressure distribution that would in-turn affect the shrinkage and runs out expected dimensions.

Plastic injection moulding is a purely iterant method to precisely contrive discrete identical parts from plastics through stationary field and rigid boundaries of permanent moulds under dynamic application of pressure and temperature. Plastic is fed into a heated barrel, mixed and forced into a mould; that solidifies on cooling. Whereas, plastics injection mould is an assembly of several elements that're designed specifically for the purpose. Its advantages and disadvantages are as follows,

1.2.1 ADVANTAGES

- a. It produces in bulk off a rigid mould from a few hundred to million parts per processing shift and typically has high process capability with low rejection rates, because of this it's often the most competitive method.
- b. Its well-coordinated plasticising and injection ensure excellent, gentle and continuous feeding forward across the inlet to the tip of an injection screw.
- c. Its process control is consistent and can produce accurate part dimensions with suboptimal tolerance in the conservative range from IT9 to IT14. It features good repeatability and reproducibility.
- d. Its ability to regulate injection pressure and temperature gives the liberty to produce strength ranges like flexible-to-rigid, porous-to-dense, soft-to-hard, etc.,
- e. Its through-put from one gram to one tonne features a competitive buy-to-sell ratio of less than 1.05 to produce today and shall prevail in future

1.2.2 DISADVANTAGES

- a. It involves enormous capital investment for machines, infrastructure, high expenses on moulds and long-term amortisation. Besides its intrinsic processing uncertainty owes high estimation risk on overall moulding job cost.
- b. At least two-week lead-time is needed initially and may extend depending on the configuration.
- c. Uneconomical to produce prototypes or in small batches.
- d. It creates nearly 15 to 25% of residue for recycling.

- e. It is unsuitable to produce mouldings having negative undercuts, recesses or trapped volume features.

1.3 INJECTION MOULDING PHYSICS

Fundamental elegance of plastic injection moulding physics is interesting because cyclic shear action repetitively diffuses molten streams in it. Here melt-streams refer to an identified liquefied injectant as a shot volume and melt-element represents an infinitesimal liquefied thermoplastic at any arbitrary point. The propensity to diffuse melt-streams into definite impression is moulding and the diffusing act is injection. In general, fundamental physics behind it's engaging conservative power (*thermo-mechanical*) in injector to contrive required impression features; by simultaneously contending intrinsic behaviours of injectant in transit and transition (Hsiung, et al., 1996) (Hsiung, et al., 1997). Principally thereof its concept depends on following combinatorial set of factors,

- a) Capacity of available **injector** represented by in-situ temperature and pressure gradient across machine and mould; power and velocity of injection against clamping effort.
- b) Needed **injectant**'s behavioural characteristics are described by apparent-viscosity, shear-thinness, thermal conductivity, latent heat and critical shear rate.
- c) Preferred configuration of feeding, cooling, ejection and clamping sub-system; besides each element designs on the **mould**.
- d) Functional features on mouldings represented by characteristic size, area, volume and thickness gradient of **impression**.

Expected quality, productivity and thereby frugality depend directly on all these factors and their interactions like,

- a) Injection force coerce random entanglements and distribute mass along the molecular chains that repeatedly deform and roll them down the stream in filling interval. Similarly, they deformation by untangling either partly or fully in packing interval. However, in cooling interval they recoil in coherence to injectant's state and constitutive behaviour. Such interactions subjectively contemplate as visco-elastic phenomena.
- b) Ab-initio molten state of injectant excites complex non-Newtonian characteristics that disrupt mechanical retorts. Like rapid local shear deformation rates inflate

frictional heat that raise in-situ temperature far above T_g , prolong residence time per cycle and reduces viscosity. Profound reasons for such behaviours are, (a) recoverable shear strain along melt to conduit boundary, (b) metastable hydrodynamism and, (c) intermolecular gap expansion from Van-der-Waal binding force weakening of individual chains by thermal excitements that're volatile.

- c) Inertial effects proportionately depend on the extent, location and orientation of impression region, especially at peak injection rates (Costa, et al., 2001) and neglecting it introduces significant errors.

Co-occurrence of all these in distinct scales contemplate an obvious incumbrance of metaphysics. Like suppose, free surface of molten liquid is flowing in one region, mushy porous zone is drifting over packing in some other region and, solidified moulding is already inducing residual stresses as it cools in yet another region. So, many integrities of injection-moulding are still mysterious as fundamental understandings on these phenomena that're inherent and their unknown interactions that're perhaps mostly nonlinear.

1.4 STATE-OF-THE-ART IN INJECTION MOULDING TECHNOLOGY

Today injection moulding machines, materials and mouldings are more universal and generic, despite being independent they have to flexibly manoeuvre compatibility for every combination. So, mould configuration is increasingly expected to concord speculating features, assimilating behavioural errands and restraining capacities well inside needed AQL and APL (Matin, et al., 2012). Imperatively every sub-system, element and feature of mould must be designed for a specific combination (Rees, 2002).

Ever raising OEM benchmarks expect tenacious adaptations, but with so many parameters to control; mere control resets and/or optimisations aren't relenting, instead they're making it too rigorous. So, injection moulding is envisaging progressive research to enable implicit solutions for below (*section 1.5*) challenges. The enablement from fundamental stances might ensure perfection, integrate control and offer a myriad of alternatives to explore. Such an adaptation to diverseness would warrant fresh outlooks and unfold several elates to advance technology by contributing conservancy, overdo realities and, give logical relevance to conflicting expectations. Like better use of moulding machine capacity, proper control of injectant behaviour and, contriving more intricate features on mouldings.

1.5 CHALLENGES IN INJECTION MOULDING

Ever-widening scope-to-application regime is sprouting value appendage and this is eternally challenging injection-moulding technology (Ong, et al., 1995). Its gradients of pressure and temperature rarely fulfil the spatiotemporal energy transformations through nozzle, sprue, runner, gate and moulding impression gap, for any ratio of power available in the machine to that impression requires (Campo, 2006). Instead they're often either in excess or shortage (Mattis, et al., 1996) and this is compromising performance, inflating CoQ, causing frequent disruptions and excessively burdening operations. The most horrifying challenge is the contradicting reasons are always a posteriori and frustrating challenge is the onus of curative cost and schedule often compel to helplessly endure those true causes. Nevertheless, all these mandates have to obey natural laws of physics; so understanding them better would enable progression. Following are major impeding difficulties seen,

- (a) 29% of the greatest anxieties usher from the expectation on design moulds that keeps on producing exemplarily, despite frequent product design debuts and injectant character substitutions (Popli, et al., 2009).
- (b) 26% of the anxieties occur from pruning lead-time that expect hastened mould development and cycle-time (Barlow, 1986).
- (c) 25% of failures yearn for reliable moulding that warrant perfection and insist for a good mould design well before cutting steel. It's worthwhile to realise that from an overall production view, the expense of frequent repairs and unexpected breakdowns wreak net mould cost (Thompson, 1999).
- (d) 18% of the incense is from frailness to function and endurance gouge (Metzger, 2008).

In plastic product development, mould designing usually is on a critical path and intercedes quality, productivity, frugality and value addition expectations (Mok, et al., 2008). This is because a typical mould can produce thousands of mouldings every day, but its design and manufacturing takes several months. Being a principle task, it accounts for over 26% of the total work effort and development time. Design of mould impression scoops nearly half of that than remaining activities such as configuring mould base, mould manufacturing, assembly, testing, etc. This crunch to design moulds has attracted many software apps to succour from several perspectives (Jong, et al., 2009), like automated parting surface determination, core and cavity extraction, feed-

system configuring, mould opening and mechanism for ejection, predicting distribution of pressure and temperature, coolant circulation settings, etc. Every feature design on mould element directly appends overall value, so devoting attention to it's worth towards robustness, consistency and reliability. Therefore, design of size and form on mould elements is an obvious challenge for every moulding combination or else the thronging effects become severe (Campo, 2006).

Although individual advances in mould, machine, material and moulding fronts are far matured, combined maturity and complete resoluteness is still a fiction, especially with their interactions (Britton, et al., 2001). Such expectations are still in tandem and yet to concord enough, because mould designing still amply resorts to heurism (Bikas, et al., 2002). Severeness of complexity owes enormous abstruseness to analyse and forbids comprehensive decisis; so exhaustive simulation, deliberate revisions and multifarious trails doom both interactively and iteratively, obviously they owe uncertainty (Sen, et al., 2010). Despite being prone to so many common pitfalls, conventional response ideology outlines a'posteriori mould alterations, heuristic manipulations, maintenance and modifications as active defense strategy. Therefore, propicient investigations on a'priori mould design problems are needed desperately to prevent later challenges strategically. Fundamentally, mature design criteria would enable designers to define mould specifications more accurately, swiftly synthesize robust design candidates and meticulously evaluate detailed performance and manufacturability. This research endeavour foresees that vision.

1.6 CHALLENGES IN MOULD DESIGN

Design of injection mould is a domain stark in practice but ambiguous in theory and that's often a confronted bottleneck. So it's too difficult to understand from generality to speciality because it's almost impossible to reiterate past expertise even partially for forthcoming design. Mould design standardisation and its logical reasoning often contradict as their higher order interaction pursuits are either parallel or series or both. Design of injection moulds is complicated because it has several levels of hierarchy like mould system level, subassembly level, element level and feature level. Feature-to-function mapping across the physical, control and design domains characterise only few relations are governing all of them. Instead, upper level design problems scramble over abstract purpose while lower level design problems confront specific functions

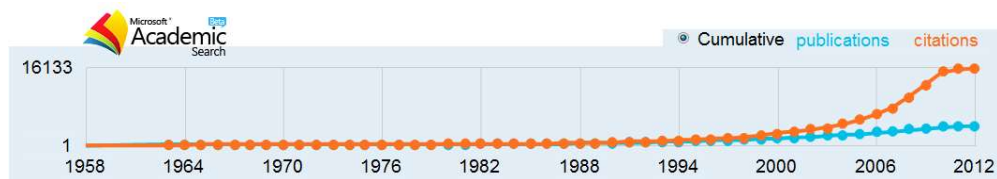
(Britton, et al., 2001), so both intent and function must prompt distinct concepts and cajole abstractions to design features. As a combination only if physical structure, semantic action and intact behaviour is synchronised, then this is possible. Or else without exact expressions, related clues or formal design criteria; semantic ambiguity always accompanies into functional objective.

Precision, accuracy, performance and efficiency depends on the degree of confidence in injection mould design. Despite so far success it's still difficult to control them because empiricism is driving most qualitative and quantitative decisions rampantly. Suppose if a mould flashes in one region as well sinks in another region, then the convention is to desperately tweak transfer position. Like adjusting injection and packing pressure, temperature or hold time till AQL and/or APL are got. Or else complicate by adopting extra hot runner manifold having dynamic feed-system with adjustable independent valves to inject selectively at different pressures to avoid flashing and increase hold pressure to evade sinking (Panchal, et al., 2010). In contrast, mould design is expected to provide quick and simple means for creating and/or adjusting configurations, intrinsically align and integrate a moulding combination. Or else the series of subjectivity, relativity, sporadity, skewity and kurtity in raw material, method and machine data will decipher into hasty decisions.

Thermoplastic injection moulding has many factors with nonlinear dependence, so associating them with complicated physical phenomena is interesting. Typical bottom-up remedial approach is often compromising, calling for undue rework and throttling actions. This is dissuading accuracy and reliability, perhaps their frailties introduce unpredictable complexities like specious semantics. Such divergence of analytical view from witnessed reality is always demanding more control or inter-alia constraints. These are also applicable to design distinct mould elements. All mould development stages are important with little variation among them, but initial conception is the most challenging one as it involves extensive intellectuality (Low, et al., 2003). In fact, with concept design sign-off, 71% or more of a mould's cost sets-in (Jackson, 2011). Essentially if that's wrong then worthwhile ingenuity opportunities are lost and tasks that follow would go horribly wrong, wreaking development budgets and schedules on havoc (Hussey, 2012). Despite so much importance of mould conception, it wasn't researched unlike the configuring, analysing, evaluating or trailing. Perhaps because

ab-initio expertise was always inept envisage proper moulds and that's the dearth in this technology.

During the last 50 years of prodigious improvements have occurred in part design, mould design and mould making mainly because of adopting microprocessor technology and extensive use of software tools. Technological advances have simplified injection mould design rigor by controlling terrible variances and dispensing expensive and tedious heuristic methods of the past. Mould making isn't an art any more instead an applied science; as fundamental laws of science, mathematical and engineering principles are becoming applicable to deal with it.



Publications: 4,313: Citation Count: 17,436

Figure 1.1: Research on Injection Mould Design (MAS, 2012).

Figure 1.1 depicts so far research attempts on injection mould design quantitatively and qualitatively. Earliest attempt to model injection moulding was around 1960s focusing on momentum, heat and mass transport. During 1970s many pioneering mathematicians studied this larger vision, purely emphasising mathematical aspects but didn't concentrate much on mould designing (Richardson, 1972). In 1971 Barrie modelled pressure gradient for dynamic feeding across the impression by evading thermal transactions and presumed a steady injection state by deliberately neglecting all periodic derivatives. However, remaining transformation equations described objective functions of mass diffusion, energy balance, constitutive hydraulics, kinetics of chemical reactions and transformations. By assuming the set of factors in them, those equations were used to predict designs through successive simulations. By 1980's significant advances in computation helped numerical simulations to get almost near solutions to injection mould design problems like representing laminar creep from single-to-multi phase mechanics (Jaworski, et al., 2010); directly setting pressure, temperature and injection velocity in proactive models; besides controlling isotropy-to-anisotropy quotient and its dispersion indirectly.

1.7 ACCESSIBLE SOLUTIONS TO DESIGN MOULDS

So far traditional and conventional methods to design moulds were good, but they're already fumbling. Mainly because the ensuing complexity isn't able to confidently specify operating factors methodically and deterring idealism. Therefore, understanding complex mechanics to design features for intrinsic attainment would connote tough to get benchmarks. Holistic mould design methods involving non-Newtonian melt mass, momentum and energy conservation that complement constitutive laws, would be better to decide conduit boundary size and geometry. Preferably, the criterion must be sophisticated to design for complex combinations and conceive robust mould features, such a notion would ensure mature mould designing with higher confidence levels, exceptional consistency, negligible degradation, low energy transactions and the best response time. Surely realising this needs a unique combination of multidiscipline philosophy, advanced skills and manufacturing expertise.

1.8 OBJECTIVES

To obtain functional value following are the objectives identified towards perfection,

- 1) Modelling criteria to design and configure most critical features in sprue and runner of feed-system by considering their functional mechanics. In sprue bush, design of engagement recess and expansion of conduit are pursued; while in the runner, conduit size and cross-section geometry are pursued.
- 2) Illustration of scope, comprehensiveness and interaction of each factor across their respective de-facto range.
- 3) Revealing their thematic rationale of injector, injectant and impression by sensitising independently beyond the natural extremes. This mathematical intelligence of exact functions prompts strategic incorporation of robustness in each design criteria.

In general, this effort contemplates analytic methods and mathematical intelligence to deal non-Newtonian behaviours of polymers, with extensive scope for extending the range of opportunities.

Chapter Two

Review of Literature and Methodology

Knowing spatio-temporal traits of injectant and coherent functions of each mould element is a prerequisite to design the real features of injection mould elements. Like non-Newtonian constitutive behaviour should be well-known for injecting swiftly and visco-elastic state behaviour should be known for gradual solidification. This behavioural parity characterises as an injectant state rise and fall bate on either sides of peak injection moment in each harmonic cycle. Thus injection and heat transfer are the major purposes of a mould to be pursued simultaneously (Chang, et al., 2001). With this rationale design concepts, philosophy and logic are set for mitigating constraints, synchronising injectant state transformation demeanours and liaising preferences (Voller, et al., 1995). Together they form ab-intio intelligence and tactical cleverness to enable following vantages,

- (a) Design of defect immune mould to get best-in-class impression orientation, parting surface, internal and external undercut recesses, feeding, ejection, cooling and venting subsystems or to configure mould base.
- (b) Outline design decision for all conceptions, choices, intuitions, etc.,
- (c) Enable true designs that are far ahead of optimality
- (d) Realise multi-attribute mould features by contouring injection around solid elements such as inserts, internal cores, venting, etc.,
- (e) Melt expansion to compression at subsonic creeping injection
- (f) Generalise solutions to low-pressure low-temperature injection issues that include conduction, convection and radiation heat transfer of transit state.
- (g) Exquisite cooling aspects for both exclusive and inclusive circuits towards complete solidification control like using a laminar-turbulent-transitional turbulence model.

2.1. TRADITIONAL METHODS TO DESIGN INJECTION MOULD

Injection mould design being an interactive task needs inter-alia knowledge on mould element functioning, manufacturing, assembling, moulding equipment and product design (Seralathan, et al., 2012). So traditionally methods relied more on compelling expertise and empirical noetism; plially they were tedious, prone to error, often prolonging and rarely appeased soaring demands (Mok, et al., 2008). Despite practising

for over half a century, they obligate grave levels of uncertainty and are less competent (Kwong, et al., 1998). Intricate mould was often too difficult for traditional methods to design unerringly. Like solving continuous mass and momentum distribution to inject melt properly against barely known empirical injectant behaviour was a daunting challenge. So initial designs were mostly vague and least logical (Thomas, et al., 2005); unfortunately, it isn't yet; because in 2011 PTC survey found 59% of current mould design projects were still derivatives of a respective forerunning mould. This happens because, before PPAP signing-off the traditional design method adopted by every mould designer was unique in their own way.

Pros of Traditional Mould Methods

Moulds are designed spontaneously at the spur of a moment with little calculations and mostly standardised solutions. From access liberty and portability sense, engineering data handbooks, manuals, templates, checklist and guides books do have matchless convenience (Rees, 2001).

Cons of Traditional Mould Methods

They are insensitive to explore alternatives and trade-offs; each design is only one design. They are treasonous either in scale or dimension, besides they have to be digitized solely or manually communicated. Contrastingly contemporary mould design realities demand more flexibility to revise, distribute seamlessly, seldom prototype and skipping iterative or heuristic controls (Hill, 1996). In fact, 61% of mould concept designs change before releasing for downstream tasks. In particular, several pareto studies have proposed with glaring themes that spur frequent revisions after detailed design. Thus, traditional methods can sparsely recognise critical needs.

2.2. CONVENTIONAL METHODS TO DESIGN INJECTION MOULD

Since traditionally methods often relied on empirical tranquil, conventional methods relied on statistical manipulation, heuristic reasoning, reviving knowledge, estimating intelligence; as they were inefficient implicitly, the erratic iterative techniques pounced over some set of parameters by intuiting as optimistic. Even powerful optimisation techniques are often deceitful as they are dependent on statistical traits. But desperate diagnostic responses methods whirl designs to immaturity. Since traditional mould design methods were mostly adopting standardised or modular strategy, conventional researchers have progressively explored expert and intelligent means to capture wisdom

and maturity (Kimura, et al., 2003). Commercially available GUIs are mostly reproducing the same traditional design methods but recursively. They often premise database retrieval schemes and empirical adjustments either on correlations or regressions; starting from simple shortcuts to full-fledged retrieval models. Their design concept decisions are from several proximate alternatives in repository archives (Ma, et al., 2003), they foresee solutions to present problems from past design knowledge (Costa, et al., 2001) and engage likely functions (Mok, et al., 2008). They expertly cascade likely axioms both serially and paralleled or either (Jong, et al., 2011). Especially, expert algorithms interact with mould configurations to assort likely advises intelligently, yet they heuristically depend on individual mould designer's own intelligence and wisdom within the decision premise (Lisjak, et al., 2009). Although most of these aps deal with specific challenges yet together make-up a sheer system. In implementation these aps interface in modular mode to promote continuous access into knowledge base and ensure relentless development or extension.

Often similar design alternatives contend to be equally feasible and deciding the best tie across the objectives is always challenging. Like development lead-time, the lowest overall cost, less operational hassle and improved performance aren't easy to get simultaneously. Even techniques like multidisciplinary optimisation of design criteria speculate (Ferreira, et al., 2010), despite adopting auxiliary tactics to fit and reasonably weigh ranges. This is mainly because, they rely on memorising experiences and intelligently educt suitable data from past solutions to meet future demands or use old cases to explain new problems. Over the years, many researchers have deciphered the whole mould design mysteries using several knowledge-based approaches {rule-based reasoning, case base, parametric design template}. Despite, simulation being too predictable and prone to the usual scale problems (Ilinca, et al., 2005), yet conventional CAE routines are a notable aid to design moulds. Indeed, CAE simulation ranks 19th among 50 top innovations having advanced injection moulding technology. Nevertheless, conventional mould design can rarely snare individual mould element design o'er in-situ function (Britton, et al., 2001).

Hybrid FEM/FDM differential methods are adopted recently on a'posteriori designs for ex-ante simulations to infer a'priori concepts for design of mould features; from structural, thermal and kinematic views for a given material, machine and moulding

combination. Whereof the direct and indirect factorisations of ex-ante simulation models pursue iterative algorithmic routines that converge gradually (Ferreira, et al., 2010) and prolong inter-alia development schedule so they are a ridiculous choice. Perhaps so many failure-trail-fix spoofs, conflict trading-off perives and successive restoring mends are together varying the objective; that's why, it's essential to adopt a priori analytical methods that focus design alternatives intelligently towards fulfilling needs (Ferreira, et al., 2013). Extensive real enquiries have revealed that ex-ante simulations are usually inaccurate, inefficient, often ineffective (Lin, et al., 2009) and more likely to mishmash (Nabialek, et al., 2006). Nevertheless, most frequent tool is tractable only at 27% because their decisions either over-or-under ride design issues. Especially with dynamic and continuous variables forfeits are more. So ex-ante trends are migrating from 2D → 2.5D → 3D; 2D planar analysis assumes uniform injection, 2.5D assumes symmetrical injection; nearly reasonable for large and thin-walled mouldings. 2.5D approximated simulations are sensitive to in-situ conditions and mould design configurations; so are inherently inaccurate to predict injection front profiles, injection streaming paths, distances and width, besides mould cooling rates and duration. Instead, 3D approach is a more aggressive and accurate apprehensive of physical phenomenon in action (Kim, et al., 2004). Adopting intricate 3D models are preferable for (i) edge influence through narrow injection conduits; (ii) transverse injection around corners or impression gap gradient influence; (iii) concentrated heat transfer around edges and narrow gaps during cooling phase and; (iv) deflections consequent to warpages. In epilogue, a comprehensive design criterion got from first principles would be trendier to deal processing challenges confidently in the design phase itself.

So far the convention was to design axiomatically, recursively simulate and revise through recurrent interactions. Besides, ex-ante analysis to evaluate a posteriori design is expensive and compels for cumbersome inter-alia expertise to identify and interpret like aligning exclusive pressure and/or temperature gradients. Such split approaches often bias results, limit intensity of discrete issues, difficult to align thoroughly and meagrely characterise key phenomena; perhaps are readily prone to chronic errors (Quadros, et al., 2001). Occasionally the progressive effort asserts few concepts from actual trials on full-scale physical prototypes. However, recent demands are increasingly mandating a priori clarity on dynamic injection effort, cooling and other

rheological behaviours, outright meddling of design is obsoleting (Hill, 1996). Although a host of ex-ante algorithms claim so, but they're barely enough and classifiable by specific results, program structure, delved knowledge and intelligence to interpret (Kazmer, 1997). Especially the perplexity of these approaches often swirls along mould configuration complexity (Ferreira, et al., 2010). Obviously even the best packages are implicit and need auxiliary expertise to decipher real mould design problem aptly in those virtual environments. Like in different guises, (*one topological model as a designer and other non-manifold topological abstract model as an analyst*) is tedious and redundant to create and deliberate. Also their GUI routines are mainly crypt for experts instead of amateurs. Therefore, tactical ignorance and adaptive difficulty perils subjectivity to design moulds better. Following two different approaches deal with these issues (Lee, 2009);

1. Development of both models simultaneously through a common intelligent modular platform though avoids extra transformation effort, but needs enormous computing time to interface. However, advances on this approach have led to dual-domain technologies that are available commercially.
2. Expert kernels smartly transform parametric type solid models into abstract models adopting medial-axis representations or generic Voronoi diagrams. These abstract models describe geometric details and identify detailed features by adopting Fourier transformations to cluster computing methods. Also using morphological techniques concurrent adjustments are made recently.

2.3. MODERN METHODS TO DESIGN INJECTION MOULDS

Modern methods rely on solving injectant characteristics, prevailing machine specifications and essential moulding features to design injection moulds under the pertinence of non-Newtonian melt injection. That naively realise mould feature design ideologically using a set of equations, initial constraints and preferences; besides are obviously exact functions. These exact functions enable concurrent balance, equilibrium and appreciate coherence of spatio-temporal traits generically instead of predicting them axiomatically.

2.3.1. REPRESENTATIONS FOR DESIGN

Influx melt diffusing into conduit has its least viscosity and is almost uniform. So, available machine velocity that dispersant diffuses it within the chosen injection

interval should together educe mould features. Injection pressure and temperature profiles differ typically across multiple sections and quickly descend to a pseudo-equilibrium state owing to (a) conductive heat transfer (*diffusion of hot injectant into a low temperature region heats-up associated mould element*) (b) regenerating frictional heat (*Convective work by shear injection stress flares frictional heat generation*). So far conventional methods have implied persuasive equilibrium and delusive injectant state profile with one section representing the entire feed system despite several injection paths. So the next logical extension being pursued currently is lofting together multiple sections like round, radial, taper, trapezoid, etc. Similar to a tree, influx melt from machine nozzle divides along injection path seamlessly into different injection paths (*like trunk, limbs, branches, twigs, etc.*) with several intermediate conditions to deduce credible designs. These multiple sections or entities infer complex representative features while fulfilling common desirability for a mould design as follows,

1. *Good injection pattern*: Best injection pattern is good directional and molecular orientation that ensues consistency and reduces variance. Its appreciation has a design significance to achieve the best balance of the feed system in multi-gating configurations. To inject the polymer into impression, thermo-rheological constraints combine with residual stress concentrations and fitting injection pattern. So, constitutive expressions can tactically design final shape, size and features of elements or entities forming conduit like number, type and location of runner.
2. *Best conduit sections*: Orienting, positioning and locating conduits with global mould layout need specific abstract consideration. Designing a correct conduit size on feeding system elements fittingly conserves the material and lessens the overall cycle time; thus contributes above 20% to the overall moulding cost. Since cooling time is dependent on the square of conduit size, agile section designs would boost productivity.
3. *Feed system variations*: Pressure distribution across the conduits ought to be balanced, so accurate designs are too critical. Like gentle injection rate balances excess latent heat across smaller sections. Thus feed system is balancing prioritises over moulding settings, processing conditions and ensures stable mould operation. Although naturally balanced feed system designs are surely desirable, achieving it has many practical hurdles like trading-offs compromising on soaring issues like mould cycle time, excess or scarce feed-to-part weights, etc. Balancing natural feed

system also appreciates the frictional heating to prevent injectant degradation. Theoretically, minimisation of pressure gradient needs large impractical conduits, so extreme feed system balance depends on other physical aspects too, such as surface roughness, cavitation, etc., Thus the models ought to introspect smaller volumetric feed rates depending on impression gap variance. The basic engineering challenge ties to either maximizing injection rate for available pressure gradient or consuming less pressure gradient for injecting a needed volume.

Normally, injection pressure applied by machine nozzle routes innately to static feed system geometry design of a mould. Multiple conduit features along the feeding system are designed to intrinsically synchronise melt injection and configure pressure gradient across each stream, mode and distinct volume. The rigor of dynamic control, overriding design issues and reliability of feed system aptness is simplified by functionally seceding injection through each mould element (*sprue, runner and gate*). Ipso-facto non-Newtonian injection irrecoverably consumes net pressure and temperature gradient throughout the feed system and that's the best metric to recognise energy transformation regions (Mattis, et al., 1996). Therefore, calculative feed system model offers an extensive ability to transpire element design decisions more thoroughly. For instance, a runner design might have an intrusive insert restricting melt injection, foregoing such complex constraints by conventional design method is tedious. In contrast analytical models can easily explore multiple conceptions and quickly find-out alternative design for such problems. As their efforts focus on idealistic overall injection mould designing and they can out-rightly specify perfect conduit size, fix potential design flaws and ensure mould performance ahead of detailed designs or creating physical prototypes. So design endeavour is intrinsically confident and overall mould operation and maintenance are also economic naturally.

2.3.2. TYPES OF CALCULATIONS

Classical 2.5D Hele-Shaw approximations is a popular isobaric hypothesises to reduce mass, momentum and energy conservation expressions (Shoemaker, 2006) by presuming invariant pressure along two injection-wise directions and locally constant across the impression gap thickness in z direction (Kennedy, 2008). Apparently, difficulty to cognise theoretical midplane makes it to be witless especially for de-facto aspect-ratios of feeding conduits (Kim, et al., 2004). Also it neglects important effects

like fountain flow, the transverse pressure gradient, stream entrapment, division, part thickness or impression gap height differences, etc., (Ilinca, et al., 2004). 2.5D Hele-Shaw approximation and reality often converge for mass conservation; rarely converge for momentum conservation and often diverge for energy conservation. These discrepancies mostly arise from misapprehension of injection stream front profile as that significantly depends on conduit design and is sensitive to conduit boundary. Although higher momentum improves injectant diffusion but better contrivance occurs from higher temperature gradient (Mattis, et al., 1996). Also superior contrivance needs prior evacuation of impression through suitable vent design. Spatial discretisation of these design aspects give implicit time integration models that led to a wide manipulation range enabling evaluation of complex surface geometries. Conversely, it also allows reverse evaluation using back propagation / race tracking and dry spotting phenomena (Voller, et al., 1995). Popular discretisation schemes adopted are FEM, FDM, FVM, and most recently control volume based BEM. Following three sequential categories summarise most notable model types for 3D geometry design in injection moulds,

Midplane models

Local 2D profile along the field boundary was estimated by positing symmetry (*using 2.5D Hele-Shaw midplane approximations*) and hybrid finite element-finite difference (FEM-FDM) schemes

2.5D surface models were extended to flat regions to avoid frequent reconstructions (Hieber, et al., 1979)

Surface models

External boundary surface (*field skin*) were iteratively traced injection-wise (Zhou, et al., 2001) (Huazim et al)

Solid models

Solid pseudo boundary was described by numerically solving the spatio-temporal momentum and state parameters (Hetu, et al., 1998)

- Melt front was patterned with Petrov-Galerkin formulation using Carreau and Arrhenius constitutive models
 - Mass convection and heat flux conduction were together patterned with Taylor discontinuous Galerkin formulation (Pichelin, et al., 1999)
 - The Eulerian theme in melt front topology was recognised by a simple segregated algorithm that implicitly discretised (*finite volume*) Navier-Stokes advection equation (Chang, et al., 2001)
 - Melt front trace was smoothed using volume fill factor (*penalty parameter*) of transient injection with
 - Non-slip interface phenomena (Han, et al., 2000)
 - With interface slip phenomena (Hwang, et al., 2002)
 - 3D/2D hybridised technique was adopted to reduce computational rigour (Friedrichs, et al., 1995) (Yu, et al., 1999)
-

Complete 3D mould design is a challenge and that's the theme behind prevailing research to advance injection moulding technology. Although several approaches were adopted to factor many direct and indirect parameters that give convincing mould designs, yet it's messy so far because considerations are still mocking generality.

2.3.3. CALCULATED SOLUTIONS

Calculating feed system design involves integrating injectant diffusion equations from injection mechanics and heat transfer based on fundamental laws of physics for each element. Control volume approach gives either best or partial equilibrium (Souza, et al., 2005). Mould configuration is conceptualised injection-wise as injectant diffuses through every element to its neighbour. Single phase injection models are better but multiphase injection mould are limited by some real complexities. So far, space and temporal patterns are segmented by unidirectional techniques along injection-wise and their solutions are aligned together effectively to model, expect and develop better mould element designs quickly.

Pros of computational methods

- (a) Features best confident than on empiricism, heurism or pragmas
- (b) Directly gets to best possible mould design
- (c) Provides access to both at local and global scale data
- (d) Offers conditional insight, that's just impossible or difficult to grasp from either conventional or tradition and even experimentation.

Cons of computational methods

- (a) Transport phenomenon presumes injectant at par with continuum matter and deals as macro scale problems. So the method isn't extrapolative.
- (b) Theoretical knowledge is incomplete to authentically model some complex phenomena, like thoroughly appreciating in-situ rheology and multiphase transportations are still pursued.

2.4. SUMMARY OF LITERATURE SURVEY

In injection moulding technology, optimism and idealism views too often have conflicting interpretations on reality and beliefs; because the methods to design injection moulds ought to take quantum leaps than relying on empiricism or pragmatism. Moreover, revising a mould design late in the development cycle is a bigger compromise than devoting early for robust design (Dacey, 1990). Advancing injection moulding technology effort relies on the likelihood of mould fulfilling aspired objectives, quick mould turnaround time and getting together other isolated developments to reap superior tooling solutions. Perfect mould doesn't exist, but a mould design can approach perfection by envisaging all known problems, defects, inferiorities and frequent uncertainties in the model. Nothing seems simpler than appreciating fundamental principles at close confidence level for configuring features on moulds from precise and accurate concepts.

Flourishing variety in injection moulding combinations and crumbling methods are together challenging the competence to design moulds. Withal, standardised and shelved propositions are undeniably impeding and compromising mould designs. They mostly recur as hierarchies, where feature designs change, alter assemblies and prolong development time. Nevertheless, associating these methods progressively to tackle specific problems that intrinsically ensue routine interoperability itself is a challenge. Despite extensive empiricism forming the basis for initial mould design, authenticate

percept differ from the prevailing methods. Thus all these methods dealing on this challenge possess certain risk of leading to disillusionment and compromise. Even after thorough analysis and exhaustive trails they at best could approach nearer to the objective, but they rarely or never converge exactly. Exact functions are necessary to design moulds that can intrinsically deal complexity ab-initio. The two main retreats of mould design methods realised are (a) it heavily relies on initial concepts (b) it can barely recognise root causes of consequences. Incidentally with many variables, constraints, objectives, preferences, perpetuating nonlinear ties to get around idealism is a herculean riddle. These challenges complicate mould design decisions and deter logical progression of systematic design effort from approaching best solutions. So the criteria to perspire from diverse views like obliging flexibility, ranging processing batch or quantity, consistent setup and optimisation procedures are still a confrontation.

Thus embroiling analytical wisdom and intelligent knowledge into mould design model can only entice a better design. Higher order interactions of spatio-temporal governing equations have to be reduced through intrinsic constraints. This would eliminate relational redundancy that otherwise recur as intense calculations and devoid the possibility of finding a solution. Often solutions rarely implicit that can uniquely strike trade-off across performance, cost and development time. True mould design criterion has to fulfil too many constraints, objectives and preferences, but functional intelligence can synthesise most concerns. So, functional intent as design intelligence is the way ahead to enable best parametric feature forms. Thus, likely decisions accreting constraints could be sensitised intuitively to spear mould design towards perfection. As sensitising the interoperability context within de-facto injection moulding range gives either exact models or parametric criteria to design features. Being an aggressive pro-active strategy, this prescripts acceptable opportunities, distinguishes efficacy and incorporates the spirits of knowledge radically to change mould design methods and best practises realised so far. Thereby mould assemblies become simple, their element designs would be specific, standard mould bases and components fit precisely without any rework. By intrinsically governing mouldability, mould designs would promptly produce their best parts in early trials itself. Thus adopting continuous sensitivity method overwhelms justification against so far inabilities as follows:

- (a) *Precise and consistent mould design*: The accuracy of mould design depends on the ability to recognise factors like injection rates (*shear*), melt state behaviour over a broad range of pressure, temperature and density much early.
- (b) *Robust mould design*: Mould designs fictitiously characterises properties of injectant's rheology that significantly depend on injection length, impression gaps, injectant temperature profile between injection phase switching and characteristic cooling times. Thus, specifically characterising injectant and choosing behavioural functions represent in-situ state demeanours.
- (c) *Design for moulding excellence*: Rigorous controls in mould design models enable material and power conservation and can thoroughly fulfil best DFX expectations.

2.5. PROSPECTS FOR RESEARCH

Feed system connects a machine's injector to the mould's impression by two prominent design stances viz geometry and mechanics. Geometry design involves configuring a parting surface, impression layout, sprue, runner and gate including their cross-section shape, longitudinal track harnessing, distributing and so on. While mechanics design parses impression filling issues and synchronises injectant characteristics, moulding features and machine specifications (Deshpande, et al., 1997). Though geometry researches subsist (Ye, et al., 2004), mechanics investigations are contrastingly abstruse (Kumar, et al., 2002). Besides, so far mechanics stance investigations were mostly on defect-to-remedial issues (Zhai, et al., 2006). This was because, preliminary perceptions were traditionally wise empirical relations mainly focused on designing a suitable mould (Pye, 1992) and accompanying obvious flaws were trounced conventionally by desperate manipulations of unrestrained processing parameters refocusing on improving the mould (Kulkarni, 2010). So the next logical method is to ensure correct design for a particular injection moulding combination. However, there's no criteria to enable sprue and runner whilst mould is designed, so even shrewd optimists aren't able to negotiate beyond some convincing compromise. Occasionally for some strange combinations, their mould configuration gets so complex that expect feed system to function from either almost equal or less than unit recovery quotient, which is the ratio of available to needed pressure gradient. Like overall feed system volume of a two-plate mould typically exceed two to three times than a similar three-plate mould alternative. Additionally, the ratio of total feed system volume to mould's overall shot volume should be as small as possible (Shoemaker,

2006); so it should be volumetrically conserved. Often such contentions compel feed system design to become inept for diffusing adequately or fill excessively into impression region. In such circumstances, rework prolongs downtime or rectifying incurs more expense or have to be scrapped feasibly (Jones, 2009). These opportunities are severely juggling design appropriateness of feed system across productivity slump and inferior quality compromise (Seow, et al., 1997). Therefore, this presents two different research outlooks that haven't been thoroughly addressed yet and presented as follows,

1. Presently design has no direct control on AQL that is essential to injection mould for a real combination. The literature review has revealed a need for more exact research to enhance confidence. This involves focus on identifying as extended sensitivities from injection moulding factors and their interactions. Although the transition from traditional to conventional has improved likelihood, but there is no guarantee of control quality. Feed system design appropriateness assertively lowers energy outlay (Weissman, et al., 2010), economises CoQ (Min, 2003) and appends reliability of overall injection moulding. Its importance bestirs with moulding dimension preciseness and spec stringency. That implies ever spurring expectations, elating acceptance benchmarks, exceeding segmentation of monitoring and standardisation of controls (Kazmer , et al., 1997) (Chin, et al., 2007) together tot for robustness in design of the feed system (Crawford, 1987). The ideal prospect is about getting all the stream races to fetch simultaneously at respective impression extremities within a mould (Beaumont, 2001). In affirmance continuous mass conveyance with balanced momentum of equilibrated energy transaction should occur concurrently (Kennedy, et al., 2013); a challenge either inept or infeasible or nearly impossible to accomplish in practice (Beaumont, 2007). Indeed, while mending design errors moulders desperately negotiate settings and often culminate at some convincing compromise of resources, efficiency, performance and quality or either (Fan, et al., 2006). As manipulations regardless of their scheme can never acclimate state nor vex design haste in-toto (Ferreira, et al., 2010). Even sophisticated control systems have marginally improved process capability (Shankar, 1978). Nevertheless, with injection dynamism being harmonic, ipso facto diligence to get all pros would surely perplex mould designing (Hassan, et al., 2010).

2. There's no clear framework or sequence of stages that will assist to the best APL. The literature clearly defines that mould performance is a knowledge intensive; however key know-how hasn't been thoroughly addressed. Ipso facto literature review provides corresponding tools and techniques, associated with injection mould design. Consequently, for a real injection moulding combination, performance is yet to be known, that ensure design for a specific APL. Intense diffusion of an injectant through rigid feeding conduits within short intervals imperil injection moulding with extreme rigor. Its shear rates are typically around 10^1 to 10^6 sec^{-1} (Zhou, 2013); localised melt temperature spikes around 200 to 400°C between shear laminates; injection rates surge at 10^3 to $10^4 \text{ }^\circ\text{C}/\text{sec}$ and 10^0 to $10^3 \text{ MPa}/\text{sec}$. Together these literal extremities flout feed system design functions extensively; where even sophisticated near characterisation methods available today become inept to fully describe in-situ interactions of actual situations; yet this challenge is unheeded so far! Perhaps accurate determination of a correct feed system design far exceeds today's technology competence (Beaumont, 2007). Consequently, designing an accurate feed system yet resorts to heurism (Khor, et al., 2010) despite independent advances in phenomenal modelling, analytical strategies and computational intelligence. Although moulding features, machine operations and material characteristics have advanced exclusively; globally resolute mould design maturity is still faraway. Primarily, because its severe complexity owes relative vagueness to analyse, inhibits collective decisiveness and that inevitably need exhaustive simulations, deliberate adjustments and multifarious trail both interactively as well as iteratively; besides together they induce uncertainties. Since empirical relation involving shot weight though vaguely ensures continuity (Huang, 2007), anguish across overshoot to short shot lingers even after several iterations (Amran, et al., 2009). Like other persecuted simulating techniques, although advanced CFD apprehensions have probed feed system functioning (Cardozo, 2008), most adaptations have merely empathised better conditions that either control defects or improve performance or both (Bezzo, et al., 2000). Processing optimisations never change feed system design; instead, they persistently arbitrate the feeding function by harnessing the in-situ state through interactions across worst-to-better mouldability (Mehat, et al., 2011).

Therefore, it's better to design intra-feed conduit from in-situ injection momentum mechanics for best mouldability. Thereby a particular {machine, material, moulding} combination with several preceding goals coalesces to inherently reduce feeding system degrees of freedom to limit its physical configuration (Crawford, 1987). Thus hardly, any scope remains for in-situ adjustment delusion instead the traditional myth of manipulating becomes redundant, though trusted by several predictive optimisers. Hence, a sophisticated criterion is critical for designing efficient conduits that diffuse injectant in its best transit state. Conscientiously feed system adaptation is a promising research avenue to advance injection-moulding technology.

2.6. FEED SYSTEM DESIGN

Feed system is an essential aspect in any mould, its purpose is to diffuse a definite quantum of injectant at a specified injection rate into a needed impression. It's difficult as characteristic design depends on the in-situ state, shear effort and large molecular weight of polymeric injectants that're behaviourally non-Newtonian. Moreover, the material or substantial function of feed system design describes a polytrophic process. In curvilinear coordinates injection is along first coordinate, the stress and velocity vary along a second coordinate and are invariant in the third coordinate. Additionally, a positive normal stress is also in the third direction owing to divergence of conduit geometry usually it's weaker with strong first normal stress and becomes substantial with weak first normal stress. Only then feed system design would depend on characteristic elasticity. Most kinetic theories on polymeric injectants don't describe this third direction stress.

A true feed system design would concurrently (a) preserve available injector's power (b) fully contrive impression features (c) synchronise injectant behaviour for diffusing and (d) engage with transit behaviour of injectant to mouldings. Besides, emphasis is on designing it with (a) flexibility to redefine design parameters in response to any in-process factor changes (b) scope for intrinsically curbing factors manipulation (c) to concede likely variance across desired levels (Akbarzadeh, et al., 2001). Thus the situation is akin to a seesaw with maximum conduit size for APL (*Acceptable performance level*) and a minimum for AQL (*Acceptable quality level*) (Kumar, et al., 2002) on either side over a design fulcrum. Like to endure injection mouldability of a chosen individual polymeric injectant, characteristic thermomechanical phase

transformation should restrain feed conduit design with the spatial factor to achieve AQL. Similarly, intrinsic non-Newtonian stress distribution pattern should conform to feed conduit design with temporal factors to achieve APL.

2.6.1. DESIGN METHODS TO FEED

Mould feed system design critically influences many dynamic phenomena such as heterogeneous solidification, capricious injection shock propagation, multimodal mobility (*across embossing, engravings, inserts, and discontinuities*), non-linear free boundary, etc., all these critically influence mould feed system design (Kazmer, 2000). Cold conduit system (*feed system*) design has to essentially appreciate specific injection wave dynamics as they propagate through conduit gap independent of melt state properties, each wave is related to a finite free melt surface (*layer*) and column head directly. The location, speed and pressure discriminate every wave from its neighbours at any instance. In particular, shock and momentum effect through preceding higher magnitude viscous effects are unfavourable to filch the best AQL and APL. Feed systems primarily diffuse injectant into impression and displace air, so functional modelling is suitable. For that resolving visco-elastic dynamics of both non-Newtonian injectant and Newtonian air that occur simultaneously is the challenge, because the locus of injectant-to-air interface have to be determined concurrently. Integrating this behavioural interface location and interaction gives a solid free surface. So a priori computing of feed system conduit with perfect dimensions is a breakthrough sophistication towards advancing mould design. As that ensures (a) efficient and effective injectant conveyance of injectant along the mould conduit, (b) best use of injectant heat and controlling solidification rates gives exciting physical features with needed characteristics and, (c) avoiding uncertain issues and reducing process dependency, thus improve process flexibility, freedom and controllability (Dym, 1987).

The impending comprehensive range of gains from thorough design of feed system justifies increased competence (Smith, 2003). Incidentally various non-linear dynamic phenomena are associated with mould feed system like large deformation free boundary motions. So integrating analytical phenomenological models ensues multiple conditions to monitor variables. However, that directly prompts to the inappropriateness of traditional or conventional methods (Petrova, et al., 1999). This is because with small Reynolds number, visco-elastic properties of injectant usually

dominate feed system momentum equilibrium states. Although the exact representation of melt injection phenomena by a descriptive model is still beyond present scientific savvy; over the preceding decennium injection modelling is gaining ample impetus. Unfortunately, most prevailing mould design criteria casually ignore inherent non-linear complexity (Petrova, et al., 1999), cascade design strategies by tactically cliquing phenomenological variables, trailing patterns (Ye, et al., 2004) and processing constraints as multiple objectives to get AQL and/or APL (Woll, et al., 1997). However, simplification and the feasibility of incorporating intelligence involves evolutionary character as multiple constraint functions need real restrictions (Cheng, et al., 2013). As usual, that resorts to heuristic scheme of tackling consequent undesirability (*defects*), either by multivariate processing or numerous trails. Even though action on melt front surface is isobaric transit thermoplastic melt jets splash, swirl and move in multiple directions consequent to discrete injection pressure (*nozzle*) fluctuation across regulated intervals. Injectant always diffuses normal to the free surface because from momentum conservation view injection velocity is directly proportional to pressure gradient across conduit ends. Since melt convection and heat extraction in feed system are consecutively cyclic, so for design perfection its geometry should be synchronous to volume, velocity profile and temperature profiles (Hirt, 1991).

Simplicities of afore traditional methods drift rheological inheritance casually that instead have complicated and significant interactions. In thermoplastic injection moulding shear and temperature dependent rheology interact at a high rate. Controlled injectant state and high rate processing limit instability, however phenomenal optimality occurs when their design can diffuse and accumulate injectant correctly at the centre of an impression. With multifarious relationships on injectant's constitutive relationship for the shear thinned injectant quickly attains a constant viscosity value at moderate shear rates. Therefore, it was essential to know feeding of a non-Newtonian injectant to design feeding optimally.

2.6.2. MODELLING APPROACH TO FEED FUNCTION

Dynamic interaction between injectant front surface and mould walls is a mysterious topic (Blake, 2006) (Ren, et al., 2010). The primary contradiction begins from transit interface of injectant-to-air and customary no-slip boundary conditions often adopted to peripheral surfaces *i.e., interface progression with rescinding injection towards solid*

peripheral surface. Overcoming the difficulty with currently available methods; the simplest Navier slip condition on the entire solid surface, slip for only dynamic contact line is adopted often. They are ad-hoc and ignore any thermodynamics considerations such as static contact angle and surface energy. However, dependence of injection effort increases steeply as injectant viscosity increases or its surface tension decreases. So, feed system of mould should be designed meticulously for proper injection through it into an impression region, while transit injectant transforms all along through filling, packing to cooling intervals. Also it's crucial to recognise and avoid injection stream wise potential risks on the lee-sides of the feed system elements. Using the highest pressure and ramping rate during filling is productive. Likewise using the lowest required pressure intensification rate during packing minimises the potential mould damages due to parts sticking or failing of moving mould elements. Hence the model to design a feed system should formally appreciate the injection mechanics. The set of thermoplastic melt injection governing equations include polymer state and constitutive equations that conserve moulding power and energy. Accordingly, an exact equation is derived specifically for sprue bush and runner that mathematically include non-Newtonian class of shear thinning character. Since characteristic dimensions of mould are bigger than intermolecular dimensions of injectant; macroscopic continuum concept is adopted to infer injectant significance on mould design. Although molecular dynamics deserve consideration; their interactions are ignored deliberately owing to afore consideration.

Continuum model allows us to describe a representative field with relevant physical quantities. Such macroscopic representations can yield best designs for any injection moulding combination. Instead, the intricacies also stretch / shrink with problem length-scales and ex post facto continuum-models aren't appropriate with length-scale changes, such as micro and Nano injection moulding.

Chapter Three

Design of Sprue-bush

Design of sprue-bush is crucial, as its features significantly influence impression contrivability. Outer head, shank and base section configurations integrate to form internal conduit geometry as schematised in Figure 3.1. Each of these must be designed keenly from characteristics of chosen thermoplastic, available machine and needed part for synchronising melt injection, its distribution and moulded part ejection.

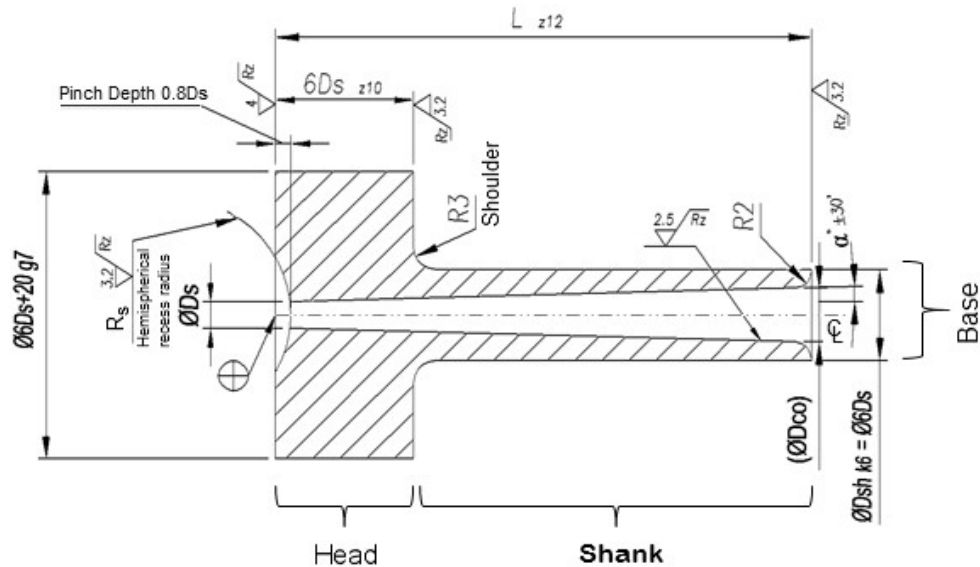


Figure 3.1 Schematic representation of typical sprue-bush (ISO 10072, 2004).

(a) Head Design

Sprue head is a positive feature having negative inlet orifice to receive melt and hold abutting nozzle-tip. Sealing its engagement with machine's nozzle is dealt here uniquely to recognise preventive design criteria.

- (i) **Shoulder Design:** Sliding injection unit of moulding machine advances barrel to abut an axial engagement thrust typically ranging from 50 to 150kN for general utility items to 200 to 300kN or even higher for engineering parts. So bigger diameter collar head form is designed with enough butting shoulder area to bear nozzle-tip sealing pressure *i.e.*, *restrain in-mould displacement*. Similarly, on barrel retrieval locating ring prevents out-of-mould disassembly owing to injection mechanics as well as welding from engagement gap leakage. Also it should be spacious enough to have heads of clamping screws over a circular PCD to overcome

axial ringing torque. Structurally collar head height and shoulder butting area ought to support extreme fatigue and impact mechanical loads by resisting shear, compression and tension deformations (Glanvill, et al., 1965). Repeated barrel engagement and disengagement of each cycle would imperil sprue head recess to severe wear possibilities. So they should be also designed for replaceability from maintenance and serviceability stances (Crawford, 1987).

- (ii) **Stress Concentration:** Rigid sprue-bush experiences undue stress concentration at the shank and head juncture much higher than those estimated by basic equations. Perhaps their accurate determination would need considerations from theory of elasticity, machining, heat treatment, etc., also gather residue stresses. So a suitable factor of safety could be imbued to homogenise stress peaks.
- (iii) **Thickness Design:** Sprue-bush wall thickness should be designed as a thick shell, because it exceeds 10% nominal conduit diameter (\bar{D}) and internal melt pressure also exceeds one-sixth of allowable stress (Howard, et al., 1981).
- (iv) **Pressure Drop:** Sprue-conduit entrance-pressure loss (P_c) is another real issue expressed as $P_c = c.\tau^m$, where c and m are empirical constants determined from popular Bagley curves for the chosen injectant and τ is shear-stress.

(b) Shank Design

Functionally sprue-bush has to mechanically and thermally engage cold mould to heated barrel with minimum energy outlay (Rubin, 1972). The phase transformation behaviour of injectant through its conduit prompts, its capillary ratio to depend on impression features below the parting surface and its interface area with mould assembly. Thus the need for either add-on sprue cooling or heating design depends on highest shearable rate of injectant for that impression (*volume and depth*) (Trifonov, et al., 2007) at best injection state (*operating pressure and temperature*). So conceit of sprue shank design criteria with mechanics of injection is essential to get almost uniform melt injection pattern despite discrete periodic stage vacillations, which has never pursued (Patil, et al., 2006) and is the main focus of this research effort. Off feed system significant fraction of in-situ pressure-recovery quotient occurs in sprue conduit geometry, conscientiously the meticulousness of spatial design criteria is where perfection hearth is for critical insight (Evans, et al., 1991). Therefore, intra-conduit in-situ melt injection momentum mechanics is the primary rationale (Strong, 2006) to

associate sprue-shank profile with material characteristics, machine specifications and part features; believing such a criterion might improve overall confidence.

- (i) **Conduit Design:** Specifying the geometry of sprue-bush conduit expansion is a prominent decision; because it tacks coefficient of pressure recovery. Like for instance, automotive component designs such as side trims, front bumpers or fenders expect superior stiffness accomplishment (Zhao, et al., 2010) from progressively accruing energy transformations through gate, runner, sprue, nozzle to moulding machine barrel; so from momentum conservation perspective that directly depends on in-mould pressure (Angstadt, et al.). This is because from dimensional assessment view of mould-function, off feed-system significant fraction of in-mould pressure head recovery from influx kinetic velocity of injection occurs in sprue-conduit region (Goodship, 2004). Thus as a prominent assessment metric the recovery quotient significantly contributes to overall mould efficiency and performance and so is an obvious element for design perfection (Haley, 2009). Besides, mould impression region being a crucial shape-contriving factor constrains the extent of injectant to diffuse through sprue-conduit by directly adjudicating fill and solidification (Bolur, 2000); aptly that extent is termed “*shot volume*”. Thus at any particular AQL and APL for perfect melt diffusion, the dimensions of expanding colder sprue-conduit passage must be configured decisively. Unfortunately, such a universal determination criterion to recover maximum pressure from the available machine, with specific behaviour of a chosen injectant and, for the needed part or impression is a void in literature. Perhaps the existing knowledge may be inaccurate, limited (ISO 10072, 2004) and inadequate for direct determination.

This enigma of abstruseness in its design criteria deceives direct determination, so mould designers intuitively assume it either arbitrarily or by wisdom and then exasperate to rectify that by deliberate manipulation or arbitrary optimisation of control factors. Therefore, this endeavour presents a generic design criterion for sprue-bush conduit. Crucial expansion ratio responsible for function was deduced quantitatively from first principles and common relations. The proposed criterion is being a simple, inexpensive, preventive would typify injecting melt specifically for a particular injection moulding combination. Further adopting “Continuous

Sensitivity Method” (CSM), the proposed criterion was sensitised over infinite scale to decipher distinct influence of each factor.

(ii) Length Design: Sprue-bush length (L) has to flush with (*cavity + bottom*) plate thickness, so at component level excess metal stock of zIT12 is provided to compensate for finish grinding upon final assembly. However, with long sprue-bush lengths thermal expansion causes “*growth*” far enough past the parting plane leading to flash. Further the nozzle contact forces exert this protrusion over the moving side of the mould to burst open clamping. So for non-sprue-gated parts, moulders should ensure sprue-bush length is within or just off parting plane at the highest operating temperature (Bozzelli, 2004). A nominal sprue length is always essential to handle moulded parts (Tewes, 2002) otherwise it’s difficult to hold fragile parts especially in an integrated work-cell automation scenario. So sprue steam is also useful to hold through downstream secondary processes, otherwise if tweezers have to directly grip moulding then coating, painting, printing or surface finishing of fragile features will consume more time besides have a risk of more rejections.

(iii) Conduit Finish: Sprue-conduit inner surface is designed smooth, furrow-less and polished to ease frictionless creep level laminar melt diffusion, simplify clean sprue stem stripping with minimum drag, sticking and friction (Dym, 1987) and nozzle-tip break off. Otherwise coefficient of frictional loss will dominate.

(c) Base Design

According to mass-momentum conservation, efflux pressure of creep level laminar melt depends directly on shank length and inversely proportional to fourth power of exit diameter. So, sprue base design is critical to preserve the pressure gradient of the available machine.

(i) **Minimum:** Sprue passage exit orifice diameter should be at least bigger than impression gap thickness (*i.e.*, $D_{co} \geq th_{max} + 1.5mm$) to ensure consistent injection rate and freeze only after impression solidifies in contrast orifice remains live to feed melt for packing (Beaumont, 2007).

(ii) **Maximum:** Excessively oversized exit sprue diameter at runner or sprue-well intersection would otherwise extend moulding cycle (Sabic, 2008). Also providing

an external (R3) fillet around sprue-bush conduit base smoothly interfaces it with sprue-well that prevent dragging melt towards walls, enables jet to be distinct, achieve highest volumetric injection rate and avoid exit turbulence (Lanxess, 2007) (Hatch, 1999).

3.1. DESIGN OF SPRUE-BUSH ENGAGEMENT

Injectant often leaks at nozzle-to-sprue engagement either during early prototyping or later, during trials (Dray Sr., 2005). ANSI B151.1, 2007 and ANSI B151.29, 2002 warns this problematic anguish as nozzle area hazard between barrel and sprue-bush. Melt leakage is irritating because it spreads all over the mould and during the spill-over either crystallizes, degrades, or contaminates. Melt leakage leads to a host of harmful begets like slow creep, drool or rapid ballooning, etc., Dangerously sprouting excess hot melt, pose higher accident likely threat to operating personnel. Consequent to leakage injection pressure is lost before diffusing injectant into impression, thus compromising product quality like packing and holding pressures insufficiency (Bozzelli, 2012). Eventually, the spill-over drool strings short-circuit heater bands, damage wires, terminals and destroy insulation blankets around the injection nozzle. Solidified drool with irregular surfaces has to be burnt-off by a gas flame blow-off torch emitting poisonous fumes and smoke. Thus complicating maintenance, laborious servicing, cost of repair and down time during service are expensive.

Perhaps primary seepage failure modes are from inadequate nozzle contact pressure, the engagement surfaces mismatch, extreme stress build-up, friction, excessive heat, surface deterioration and functional dynamics.

1. Nozzle Contact Pressure Inadequacy

Nozzle-tip of injection unit of moulding machine is designed to apply high-butting pressure when engaged over a sprue-bush of receptacle mould. This force should be higher than the resultant reaction arising from moulding on the barrel or conduit or impression boundary surface, else melt pressure will burst open. In a disastrous scenario, sprue head may accidentally detach or dislodge from nozzle-tip causing severest damage like lodging broken pieces into nozzle or clogging within sprue-conduit. Large nozzle-contact force can severely damage the top plate, so to ensure in-situ safety proper support is necessary with priority. Precautionally before engaging injection sled unit, moulds must be closed necessarily and adequately supported on

stationary side else nozzle-contact force would bend or dislocate top plate. Typically, hydraulic machines exert force and hold nozzle-contact reliably while electric machines have frequent inadequacy reports and inconsistency issues.

To estimate seating thrust for sealing-off engagement gap, injection moulding machine manufacturers are traditionally assuming an annular width and apropos diameter despite knowing its flaws, instead of considering the factual contact area. As sealing is more prudently a three-dimensional exponential decay function, rather than a finite value. Moreover, mould sealability depends on the spatio-temporal injection pressure besides early seating load over the bearing sprue surface. Thus, thicker sprue head would be stiff and forms a positive seal against whatever nozzle-tip kinetics exists. However, excessive thickness has more affinity to relax stress and form many micro-pore grooves where leakage is possible (Flitney, 2007).

In contrast, engagement purlieu damage could be avoided by considering minimum-to-maximum pressure thresholds across atmospheric pressure at ambient temperature as well as peek injection pressure at the highest operating temperature to determine the annular width to thickness ratio. Thus reckoning true 3D contact width to calculate is more likely to give adequate contact pressure, especially as the smallest pressure values considered traditionally are too conservative. Tenaciously, engagement thrust can be further determined by relating the annular width to stiffness and resilience of engaging sprue and nozzle-tip surfaces.

2. Mismatch of Engagement Surfaces

Traditionally mould designers match sprue-bush head recess with nozzle-tip inadvertently, because most processors believe just outer contact curve matching suffices to seal. However, to achieve best sealing the engaging surface forms should engage intimately over a small contact area. So the least area concentrates the entire nozzle-tip exerts constant sealing thrust to exert enormous sealing pressure (Marcus, 1967). In case if any sort off geometrical form mismatch occurs, then the engagement surface area increases forming discontinuous sealing perimeter prompting melt leakage, which flash welds exposed sprue-bush and nozzle-tip surfaces; enough to retard injection-sled unit rearwards. Such moderated engagement gap design depends on closer tolerance that's liable to raise machining cost and unreliable with frequent metal-contact movements, tremors and expansions of operating conditions (Flitney, 2007). Injection shock plane offset increases volumetric injection rates causing porous surface splay making holes in thicker moulding parts (*like polycarbonate PETP articles*).

Perhaps likely frozen layer forms a bump around inlet orifice diameter to at least 0.25 mm regardless of conduit cross section shape (Xu, 2004). So typically sprue inlet hole diameter (D_s) is 20% more than upstream injector nozzle exit tip orifice diameter (D_n) to endure smooth melt influx (Sabic, 2008). Especially because nozzle-tip area exposure to hot melt would further increase retardation pressure of injection unit backwards.

3. Extreme Stress Overt

Enormous moulding pressure induces crushing stresses that deflect engagement surface and deter sealing area. So, compressive design strength of chosen sprue material should be well above ipso facto moulding stresses (Stair, 1984). This is because conjunctural and evidential investigations consent that melt leaking force is functional scene sensitive like microstructure, texture, micro-pore shapes, asperities distribution; melt film stiffness, etc., on mating surfaces (Etsion, et al., 1999)

4. Friction

With liberal tolerances or clearances injection sled unit abutting over sprue-bush head mayn't align properly and usually needs to quiver or wobble up, down or sideway to align at true position. The ensuing friction this abuse causes gouges, burrs, hob grooves or other surface wear distortions on both nozzle-tip or sprue-bush surfaces. These eventually become passages that jet out high-pressure injectant. Therefore, injection nozzle engagement fit clearances or cushioning are controlled and periodically overseen to hold injection unit properly (Yoshioka, et al., 2007). Also excess heating of engagement surfaces decomposes the antifriction lubricant oil applied on and around sealing lips and deposit carbon residue. That usually forms a case on the atmospheric side of lip and gets squeezed mildly, this insulates heat of nozzle-tip, reduces seal friction. Suppose if the deposit is hefty then it interferes with seal-lip directly and lubricant needs a change to a grade that can bear a higher temperature.

5. Excessive Heat

Smaller surface area transmits less heat and thermally insulates, or else undue heat loss would result in many issues like stringing. According to specific transaction of local heat in mechanical face sealing, the circumference of seating surface area depends directly on intermittent heat generation and the average Nusselt number (Doane, et al., 1991). Therefore, engagement area must be preferably compact to restrain nozzle-tip heat loss into cooler sprue-bush.

6. Surface Deterioration

Reliable diagnosis investigations have revealed that cracking of engaging surface is most probably from obvious stress relaxation from either creep level laminar injection, differential thermal expansion, locating ring deflection, bolt stretch, material ageing or corrosion. So, it is essential to review in-situ handling of sealing surface, like if application is the cause then an alternate material grade with improved resistance is advisable, especially if different sprue-bush and nozzle-tip metal combinations are involved. In extreme situations, even a small fraction of contaminant in a nozzle-tip or sprue-bush materials if incompatible with injectant constituents can create high-grade alloy.

7. Functional dynamics

Engagement area is also prone to fretting damage from small, frequent and relative movements of sealing surfaces caused by vibration or rapid injection pressure recursions. So for avoiding undue momentum, it's essential to balance engagement kinetics across the sealing. Sometimes these movements are needed to improve gap sealability of engagement design. Such design flexibility would ensure sealing across de-facto operating conditions or else would eventually lead to transient leakage in operation.

From these deliberations on engagement leakage failure modes, sprue design happens to be crucial with its engagement surface form, land length as most prominent modes and is the least understood probably. Therefore, engaging recess surface form by using chosen nozzle-tip dimensions to interrelate sprue-bush design specifically for better sealing-off thermoplastic melt leakage is dealt in detail.

3.1.1. Leak Detection

Direct measurement of engagement leak is difficult, so the quick assessment adopted traditionally is "*Pinch test*", but being an empirical test it's prone to accidents. It involves inserting pressure-sensitive film between nozzle-tip and sprue-bush to assess contact pressure gradient. The inserted film gets squeezed across the whole engagement area. Later examining the impression pattern of contact area, radii mismatch and annular width variance between the concentric rings together show the disengagement. Nevertheless, a reduced inner-ring contact area is most desirable (Bozzelli, 2012).

Conventionally for detecting melt leak incidence, thermocouple probes were positioned around engagement vicinity and harnessed to external embedded-systems. Consequent to leakage, abrupt change in tunnel temperature beyond pre-set operating threshold temperature range stimulated the thermocouples (Green, 1989). Then signals from thermocouples were modulated by external connected microcontroller systems to spontaneously alert a set of relays.

Later pressure-sensitive corrosion resistant disk sensors were inserted directly across engagement area with optoelectronic or electromagnetic relays for in-situ detection of leaking melt presence or proximity. Alternatively, MEMS type strain gauge sensors were adopted for detecting leaked melt pressure to activate relays (Kennedy, et al., 1996). Melt leak detector oversees conduit-pressure across two switching thresholds (a) lower threshold is set-to sense drop consequent to leakage (b) higher threshold is set-to sense build-up across limits or blockage instance. However, both thermocouple probing and pressure sensors were infeasible because melt state (*pressure and temperature*) at the engagement junction was discretely periodic as well as intervallic.

3.1.2. Seal Design Endeavours

Literature survey on sealing design between sprue-bush and nozzle-tip reveals many a'posteriori remedial patents to overcome melt leakage hazards. Progressive design endeavours to improve engaging features have geometrically led to hemispherical concave and convex forms. Similarly, several other circumstantial investigations have prioritised positive-mechanical face seal design to intrinsically tolerate positional errors and form tightest-reliable-repeatable connexion (Dray Sr., 2002). Thus mechanical face sealing design criteria improve operational safety, functional integrity of mould and machine reliability. Emphasising resilience of injection-mould sprue-bush recess sealing design to endure operating pressure and temperature repercussions, following precepts imply getting the best sealing (Buck, 2001),

- sprue-bush recess surface hardness should be 20% less than nozzle approach surface
- sprue-bush recess and nozzle approach surfaces should be polished to achieve lowest friction coefficient that avoids in-situ intermittent heat generation and thermal expansions
- sprue-bush material should be slightly tougher than nozzle-tip material

To get better engagement sealing, most patents have disclosed several seating designs. However, those precepts were either inept or of modularised form and eventually forbid net moulding cost (Schmidt, et al., 1988). Thus, eternal demand for novel Euclidian design persists to prevent nozzle engagement leakage and thermally insulate for approaching idealistic mould performance and moulding efficiency (Kaushal, et al., 2009). Therefore, this endeavour adopts simple intelligent notion of position, extent and direction to design engagement gap seal. It's mainly dependent on persecuting context from either pursuing indifference, increasing inquisitiveness or inscrutability of Euclid conception. Nevertheless, this notion is surely definitive and mathematically precise. It involves tangential synchronisation of coaxial-convex plasticiser barrel nozzle-tip into concave bush along closed sprue inlet-orifice curve with small leakage gap (Menges, et al., 1993). Static mechanical sealing demands designing complete physical barrier for potential interface leakage path; for that hemispherical lip surfaces have to be resilient across engagement. Enough to butt innately against one another and positively form a melt tight seal without any gap for leak proof processing at static mould to machine interface without any relative movement between them.

3.1.3. Euclid Relations at Sprue-bush to Nozzle-tip Engagement

Machine nozzle-tip to mould sprue-bush intrinsic engagement design is represented schematically in Figure 3.2 to conceive Euclid feature clarity. Let us consider machine nozzle-tip approach as well as sprue-bush recess features of Figure 3.2 synonymous ($D_s = D_n$) with two distinct hemispherical abstract surfaces (S_n and S_s) that're axis symmetric along x-axis and share common radical intersection plane. By representing, the nozzle-tip approach convexity on the locus of a point that remains at a constant distance R_n (*external radius*) from a fixed-point O_n and D_n as nozzle-tip exit conduit diameter at the injection shock plane. Similarly, sprue-bush recess concavity can be represented by the locus of a point that remains at a constant distance R_s (*internal radius*) from a fixed-point O_s and D_s as sprue inlet conduit diameter at the injection shock plane.

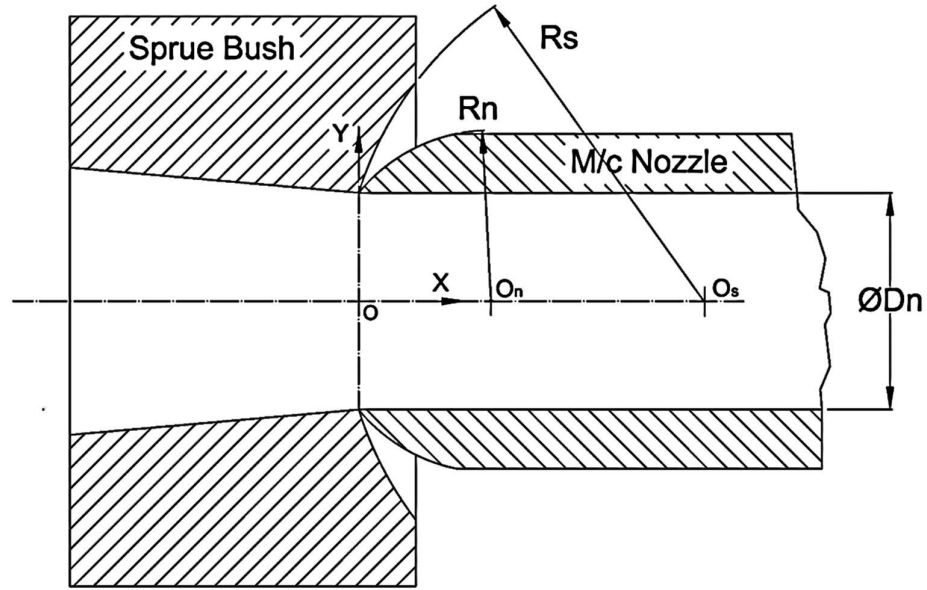


Figure 3.2 Mould sprue-bush to machine nozzle-tip engagement design.

Let us consider the centre of sprue inlet orifice as the origin of a cartesian coordinate system (X, Y, Z) as showed in Figure 3.3. Then YZ plane coincides with common radical plane of S_n and S_s as well as injection shock plane of the melt conduit.

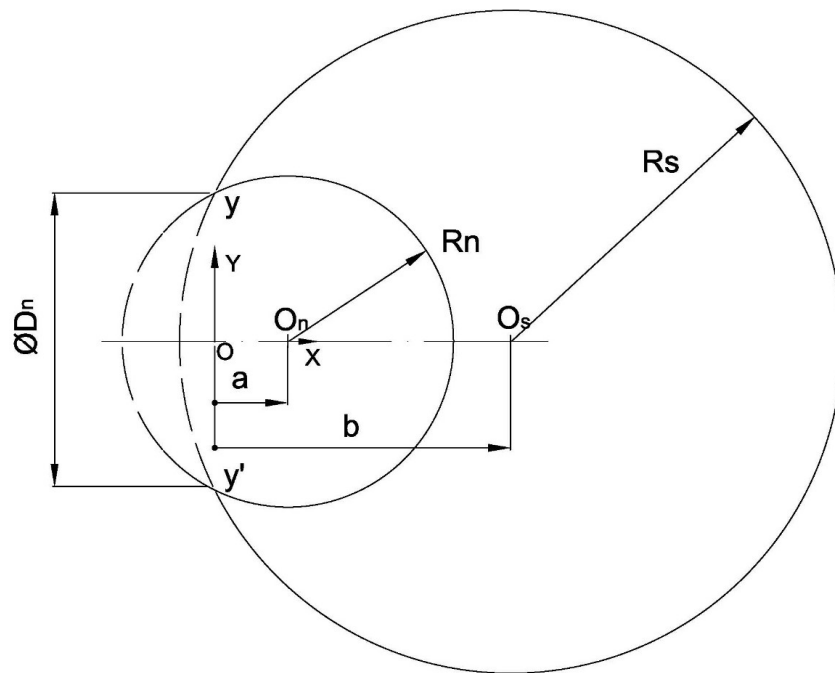


Figure 3.3 Concave-Convex radii engagement design.

Then inlet-orifice perimeter circle can be represented by equation,

$$y^2 + z^2 = \left(\frac{D_n}{2}\right)^2 \quad (3.1)$$

Also by recognising two characterise properties with equal coefficients of (x-a), y and z as well as zero coefficient of yz, zx and xy on nozzle approach geometry; convex hemisphere can be represented as,

$$S_n \equiv (x - a)^2 + y^2 + z^2 - R_n^2 = 0 \quad (3.2)$$

Similarly, by recognising two characterise properties with equal coefficients of (x-b), y and z as well as zero coefficient of yz, zx and xy on sprue-bush recess geometry; concave hemisphere can be represented as,

$$S_s \equiv (x - b)^2 + y^2 + z^2 - R_s^2 = 0 \quad (3.3)$$

Now all the coordinates of engagement interface points should satisfy both Eqn (3.2) and (3.3) i.e., $S_n - S_s = 0$ (Sommerville, 1939). So the resulting intersection curve on common radical plane in YZ direction perpendicular to engagement is given by the locus of points about both hemispheres whose centres lie on X-axis can geometrically face seal. So radial lines from x-axis to each point on sealing curve in radial plane are called radical axes.

As the quadratic circular Eqn (3.1) has two roots $\pm \frac{D_n}{2}$ that're real and distinct on either side of X-axis would share all sealing points on both S_n and S_s hemispheres. Thus Eqn (3.1) describes the engagement curve. As both S_n and S_s hemispherical radii are axis symmetric along x-axis and apart from the origin at a and b respectively; owing to engagement coincidence, their sealing point locus ought to be at constant distances from O_N and O_s . Besides, radical axes intersect both hemispheres at y and y' at x = 0 on YZ plane, so substituting Eqn. (3.1) in Eqn. (3.2) and (3.3) gives,

$$\text{for nozzle side } (x - a)^2 = R_n^2 - \left(\frac{D_n}{2}\right)^2 \quad (3.4)$$

$$\text{for sprue side } (x - b)^2 = R_s^2 - \left(\frac{D_n}{2}\right)^2 \quad (3.5)$$

Now Eqn. (3.4) and (3.5) can be solved from shared sealing point coordinates on XY plane i.e., $z=0$, $x=0$ and $y = \frac{D_n}{2}$ to get,

$$\text{for nozzle side } (0-a)^2 = R_n^2 - \left(\frac{D_n}{2}\right)^2$$

$$\text{for sprue-bush side } (0-b)^2 = R_s^2 - \left(\frac{D_n}{2}\right)^2$$

$$\text{Thus } a = \sqrt{R_n^2 - \left(\frac{D_n}{2}\right)^2} \text{ and } b = \sqrt{R_s^2 - \left(\frac{D_n}{2}\right)^2} \quad (3.6)$$

Substituting Eqn. (3.6) in Eqn. (3.2) on the nozzle side gives,

$$\left(x - \sqrt{R_n^2 - \left(\frac{D_n}{2}\right)^2}\right)^2 + y^2 + z^2 = R_n^2$$

Similarly substituting Eqn. (3.6) in Eqn. (3.3) on sprue-bush side gives,

$$\left(x - \sqrt{R_s^2 - \left(\frac{D_n}{2}\right)^2}\right)^2 + y^2 + z^2 = R_s^2 \quad (3.7)$$

$$\text{rearranging gives } 4(x^2 + y^2 + z^2) = D_n^2 + 4x\sqrt{4R_n^2 - D_n^2} \quad (3.8)$$

$$\text{and } 4(x^2 + y^2 + z^2) = D_n^2 + 4x\sqrt{4R_s^2 - D_n^2} \text{ respectively} \quad (3.9)$$

Eqn. (3.8) and (3.9) represent engaging hemispherical surfaces, where y, z varies, i.e.

$y, z \in \left[\frac{D_n}{2}, R_n\right]$ and $x \in [0, a]$ on the nozzle side as well $y, z \in \left[\frac{D_n}{2}, R_s\right]$ and

$x \in [0, b]$ on sprue-bush side. Since both hemispheres intersect at a common sealing

point; the intersection angle between their tangent planes at those points is equal to the angle between their radii. This is because tangent planes are perpendicular to the radii

(Sommerville, 1939). Further, as y and y' are two common sealing points; triangles

$O_n O_s y$ and $O_n O_s y'$ would be congruent, because the angle of intersecting points of internally engaging hemispheres is same and is an acute angle.

Therefore, all lines are tangential to hemispheres on sealing curve and pass-through conduit axis (X-axis) depends only on common apex also lying on X-axis i.e.,

$$Q_n (x^i, y^i, z^i) \text{ as well as } \left(0, \pm \frac{D_n}{2}, 0\right) \text{ for } S_n \text{ and } Q_n (x^{ii}, y^{ii}, z^{ii}) \text{ as well as } \left(0, \pm \frac{D_s}{2}, 0\right)$$

for S_s . Now $y\left(Q_n; \frac{D_n}{2}\right)$ and $y'\left(Q_s; \frac{D_s}{2}\right)$ on S_n and S_s hemispheres describe sealing curve power that's interpreted as,

$$y\left(Q_n; \frac{D_n}{2}\right) = (\text{Apex distance from centre } O_n)^2 - R_n^2$$

$$y'\left(Q_s; \frac{D_s}{2}\right) = (\text{Apex distance from centre } O_s)^2 - R_s^2$$

Where,

$$y\left(Q_n; \frac{D_n}{2}\right) = (\text{Length of tangent from } Q_n \text{ to } y^i)^2 \geq 0 \quad (3.10)$$

$$y'\left(Q_s; \frac{D_s}{2}\right) = (\text{Length of tangent from } Q_s \text{ to } y^{ii})^2 \geq 0 \quad (3.11)$$

Now equations of standard tangent lines passing through Q_n and Q_s is,

$$\text{on nozzle side as } \frac{x^2}{A^2} + \frac{y^2}{A^2} + \frac{z^2}{A^2} = 1 \Rightarrow \frac{(x_n - a)X}{A^2} + \frac{y_n Y}{A^2} + \frac{z_n Z}{A^2} = 1$$

$$\Rightarrow \frac{x_n(0)}{A^2} + \frac{y_n(D_n/2)}{A^2} + \frac{z_n(0)}{A^2} = 1 \Rightarrow \frac{y_n D_n}{2A^2} = 1 \Rightarrow y_n = \frac{2A^2}{D_n}$$

in comparison to Eqn. (3.7) with a common origin at orifice centre substituting

$$A^2 = \frac{D_n^2}{4} + (x - a)\sqrt{4R_n^2 - D_n^2} \text{ we get, } y_n = \frac{2}{D_n} \left(\frac{D_n^2}{4} + (x_n - a)\sqrt{4R_n^2 - D_n^2} \right)$$

$$y_n = \left(\frac{D_n}{2} + 4(x_n - a)\sqrt{\frac{R_n^2}{D_n^2} - \frac{1}{4}} \right) \quad (3.12)$$

$$\text{on sprue-bush side as } \frac{x^2}{B^2} + \frac{y^2}{B^2} + \frac{z^2}{B^2} = 1 \Rightarrow \frac{(x_s - b)X}{B^2} + \frac{y_s Y}{B^2} + \frac{z_s Z}{B^2} = 1$$

$$\Rightarrow \frac{x_s(0)}{B^2} + \frac{y_s(D_s/2)}{B^2} + \frac{z_s(0)}{B^2} = 1 \Rightarrow \frac{y_s D_s}{2B^2} = 1 \Rightarrow y_s = \frac{2B^2}{D_s}$$

in comparison to Eqn. (3.8) with a common origin at orifice centre substituting

$$B^2 = \frac{D_s^2}{4} + (x - b)\sqrt{4R_s^2 - D_s^2} \text{ we get } y_s = \frac{2}{D_s} \left(\frac{D_s^2}{4} + (x_s - b)\sqrt{4R_s^2 - D_s^2} \right)$$

$$y_s = \left(\frac{D_s}{2} + 4(x_s - b) \sqrt{\frac{R_s^2}{D_s^2} - \frac{1}{4}} \right) \quad (3.13)$$

Therefore, all coinciding points of engagement describing the interference Eqn. (3.1) are simultaneously tangent to both S_n and S_s hemispheres and form a closed locus of positive sealing points at contact.

Now consider triangle $O - O_n - y$ on the XY plane as sketched in Figure 3.4, let nozzle and sprue-bush radii intersection angle with orifice (shock) plane (YZ) be ϕ_n and ϕ_s respectively then,

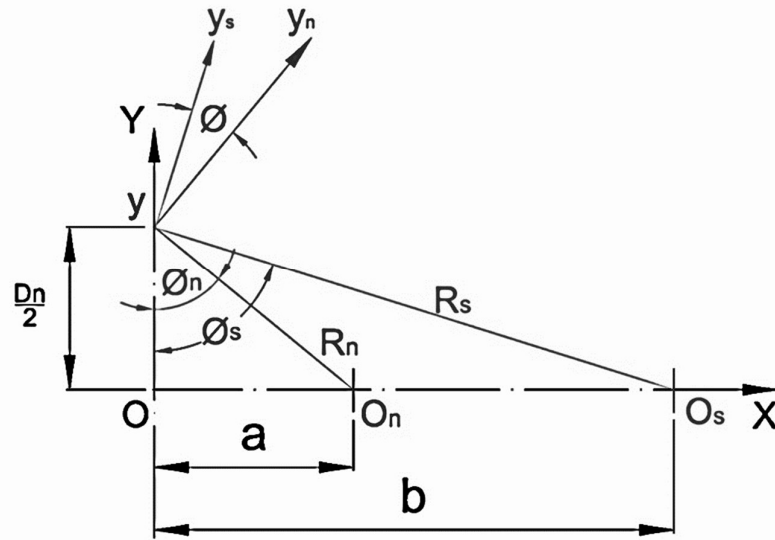


Figure 3.4: Schematic representation of concave convex radii engagement

Then slopes Y_s and Y_n would give respective inference angles at the sealing junction; so by differentiating about x respective slopes is got,

$$\text{on nozzle side } \frac{dy_n}{dx} = \tan \phi_n = 4 \sqrt{\frac{R_n^2}{D_n^2} - \frac{1}{4}} \text{ and sprue-bush side } \frac{dy_s}{dx} = \tan \phi_s = 4 \sqrt{\frac{R_s^2}{D_s^2} - \frac{1}{4}}$$

Therefore $(R_s - R_n) > (b - a)$ is the necessary condition for both tangents lines to exist at two common distinct sealing points through which unique sealing curve can exist (McCrea, 2006). Then their pinch-angle is $\phi = \phi_n - \phi_s$ and given as,

$$\phi = \cos^{-1} \left(\frac{D_n}{2R_s} \right) - \cos^{-1} \left(\frac{D_n}{2R_n} \right) \quad (3.14)$$

3.1.4. Design Characterisation

From a mathematical treatise of utilitarian Euclid Eqn (3.14), ipso facto generic pinch-angle is characterised in Figure 3.5, by considering it as dependent function $\phi = f(\cdot)$ and $\{D_n, R_N, R_s\}$ to be purely independent factors in an unbounded space. Obviously, rearranging Eqn. (3.14) gives ideal criteria for sprue-bush design as,

$$R_s = \frac{D_n}{2} \sec\left(\phi + \cos^{-1}\left(\frac{D_n}{2R_n}\right)\right) \quad 0 < D_n < R_N < R_s < \infty \quad (3.15)$$

Since Eqn. (3.15) has transcendental nature, a unique solution is indeterminate and getting R_s directly by (D_n, R_n) becomes elusive as long as $\{\phi, D_n, R_n, R_s\}$ are unbounded. So confining $\{f|\phi, D_n, R_n \rightarrow R_s\} > 0$ as real positive set obviously gives physical sense to Eqn. (3.15). Besides recognising invariance or fixate of nozzle-tip on an injection moulding machine feed unit in Eqn. (3.15) denotes $\frac{D_n}{2R_n} > 0$ to be an arbitrary real constant finite value. Thus, sprue surface “engagement form” is dependent on nozzle-tip dimensions to seal-off.

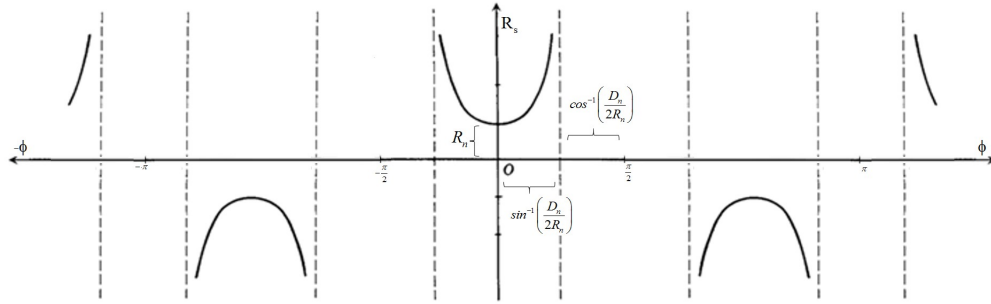


Figure 3.5: Recess radius design sensitivity to pinch-angle (ϕ).

Singularity of $R_s(\phi^\pm)$ naturally constrains pinch-angle in Figure 3.5, i.e., $\lim_{\phi \rightarrow \pm \frac{\pi}{2}} R_s(\phi)$;

$-\frac{\pi}{2} > \phi > +\frac{\pi}{2}$. Articulating the independence of nozzle-tip aperture diameter D_n ,

concave bush recess radius R_s either expands to widen or shrinks to contract pinch-angle (ϕ) for any change in nozzle-tip size. Hence the proposed relation is realistic. Thus pinch-angle of the Euclidian combination ought to be bounded between ensuing limits across which R_s always exists and is continuous as in Figure 3.5. Suppose sprue recess can't shrink instead can only expand above R_n , then its surface can only increase

to utmost be a hypothetical flat. Hence their compact sealing design criteria would principally depend on both independent orifice size and prevailing intermittent service situate as approach recess. In that stance for a random combination of $\{D_n, R_n\}; 0 < D_n < R_n < \infty$ on a nozzle-tip ensues a pinch-angle form that in turn directly determines the radius required on sprue to design engagement sealing as $R_s \propto f(\phi)$. Contextually the available machine nozzle-tip size would be survival parameter and the secant function of a thoughtfully specified pinch-angle would be the scaling function. Therefore, the wisdom to decide a particular pinch-angle is still an open issue. However, since the sprue recess design is continuous between its natural limits, at least knowing these limits would surely help deciding it.

Inferentially

1. Suppose if $R_n > R_s$, then flash forms in the entwining gap; where a chuck trap prevents demolding, retards nozzle retraction and leaks injectant profusely. Owing to progressively active friction, these effects increase, often call for discerning alignment (Menges, et al., 1993) and/or perhaps need more sealing pressure (Pye, 1992). So it's always necessary for sprue recess to exceed nozzle approach radius i.e., $R_n < R_s$.
2. Suppose if $R_s(\min) \rightarrow R_n$, then sprue recess radius should align into the exactly same size nozzle approach radius, whose radii features superimpose one-over-other, and from Eqn. (3.14) $\phi_{\min} \rightarrow 0$. In such a supposed event, the differences of S_n and S_s surfaces interlock their aspirates intimately, weld together or get distorted over repeated interfacings offering the widest ever mechanical sealing and call for lowest ever seal-off pressure. Besides, the consequent dynamics often widen clearances and eventually cause leakage. From this pretext, small pinch-angles are more likely to rub-over a narrow tolerance range (Kohler, 1975).
3. Similarly, $R_s(\max) \rightarrow \infty$ is extreme sprue-bush recess radius that almost corresponds to a flat (Glaesener, 2009) or blunt (Nakamura, et al., 1990) approach surface (Menges, et al., 1993) and from Eqn. (3.14)

$$\phi_{Max} \rightarrow \frac{\pi}{2} - \cos^{-1}\left(\frac{D_n}{2R_n}\right) = \sin^{-1}\left(\frac{D_n}{2R_n}\right).$$

Such a supposed event gives biggest radial difference between recess and approach whose physical engagement contact area is

small that in turn (a) is prone to misalignment because even slightest offset introduces a gap. Especially since $R_n \ll R_s$ highest sealing thrust is needed to endure high injection pressure and even little insufficiency leads to flash. (b) insulates heat transfer from nozzle-tip to mould, thus prevent obvious freeze up. From this pretext, bigger pinch-angles are more likely to misalign a small contact range (Kohler, 1975).

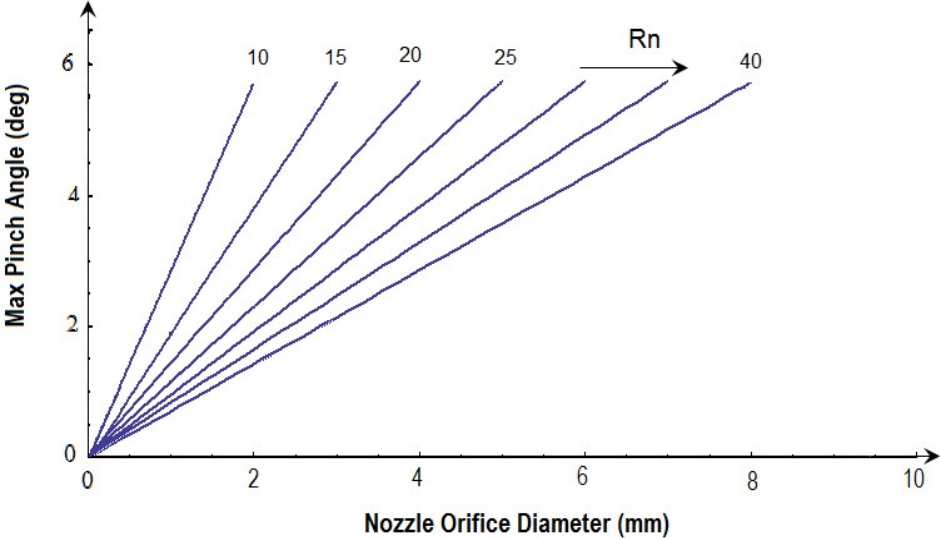


Figure 3.6: Max pinch-angle sensitivity to nozzle-tip orifice diameter.

Further, Figure 3.6 shows that the biggest possible pinch angle has direct dependence on nozzle orifice diameter with an extent (*slope*) that depends directly on approach radius. So for any given nozzle, small nozzle orifices will have little maximum possible pinch angle, thus seizing the opportunity for sprue recess to be concave *a.k.a.* the sprue recess is more likely to be almost flat for small orifices. And that’s even more obvious if nozzle approach is also smaller.

Similarly, Figure 3.7 shows that biggest possible pinch-angle has inverse dependence on nozzle approach radius across a reasonable nozzle approach radius range with an extent (*slope*) that depends directly on nozzle orifice diameter. As the characteristic curves of Figure 3.7 are hyperbolic the maximum pinch angle is too large for nozzle approach radius that’s over its orifice diameter and almost nil for bigger nozzle approach radius. So for any given nozzle, small nozzle approach radius will have big maximum possible pinch angle, thus offering the opportunity for sprue recess to be designed more concave. Therefore, big nozzle orifice diameter or small nozzle

approach radius almost smoothes engagement towards a flat interface, where beyond 6° sealing circle size tends towards the nozzle orifice radius, suggesting an abrupt contact area increase.

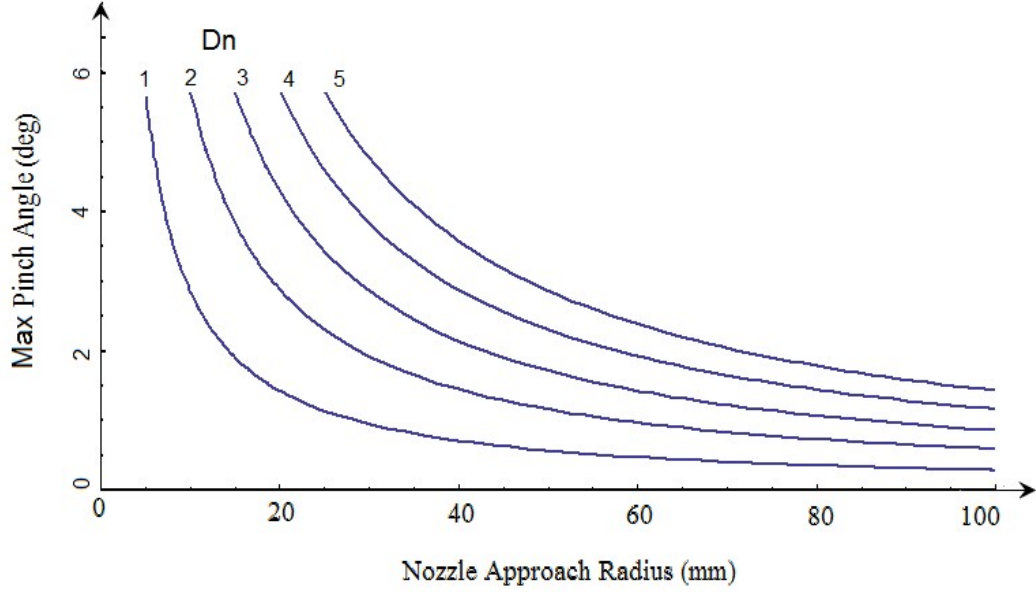


Figure 3.7: Max pinch-angle sensitivity to approach radius.

Inference

Therefore, pinch-angle must be across to align and seal,

$$0 < d\phi < \sin^{-1}\left(\frac{D_n}{2R_n}\right), \text{ i.e., } d\phi \in \left(0, \sin^{-1}\left(\frac{D_n}{2R_n}\right)\right) \quad (3.16)$$

So as $R_s \in (R_n, \infty) \Rightarrow R_s = R_n + dR_n$, where $dR_n \in (0, \infty)$

3.1.5. Design Sensitivity

As sprue radius is an independent real feature and its design could be any rational value, but for engagement sealing it depends on the nozzle approach radius and orifice diameter. Now as these two factors being independent factors, suppose if they were pure mathematical factors across an unbounded range then their Euclidian sensitivity is as plotted in Figure 3.8 and Figure 3.9. Both these plots show that characteristics curves are continuous and nonintersecting, this clearly evidences independence hypothesis, however for mechanical invariability a distinct pinch-angle exists across the engagement. Thus an exclusive influence of pinch-angle is important for sealing and it depends on the combination of nozzle-tip approach and orifice size for a given machine. However, the design of sprue recess radius is an exponentially concave sensitivity

function of nozzle approach radius and orifice diameter. This infers even minute change in pinch-angle needs large increase or decrease in sprue recess radius to seal properly, in contrast nozzle approach radius and/or its orifice diameter variety has only meagre influence. As pinch-angle widens necessary the radius of sprue recess also increases abruptly to almost flatten the recess surface, this increase aptly increases the likelihood radial misalignment as explained in section (3.1.4, 3). Similarly, at small pinch-angles engagement surface wears intensity leads to rapid distortion and eventual leakage as explained in section (3.1.4, 2). To sum up the nominal pinch-angle range between slope transition ranges would strike a perfect balance between both the extremities.

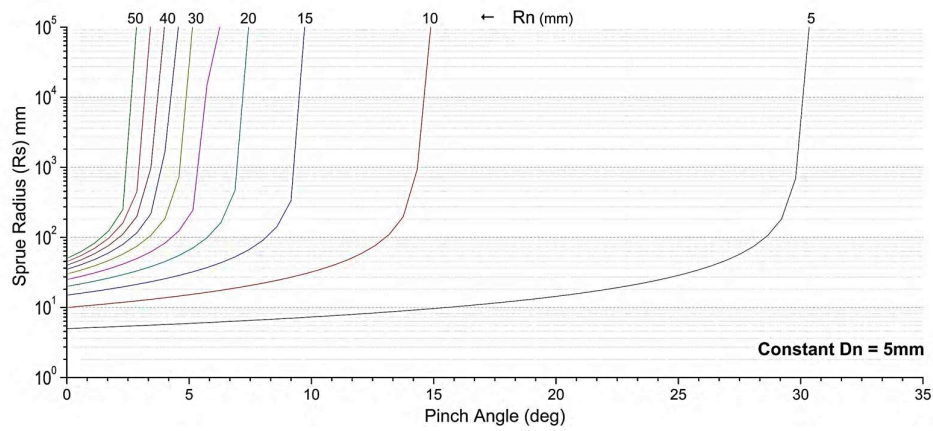


Figure 3.8: Sprue recess radius sensitivity to pinch-angle about sprue approach radius for 5mm inlet orifice diameter.

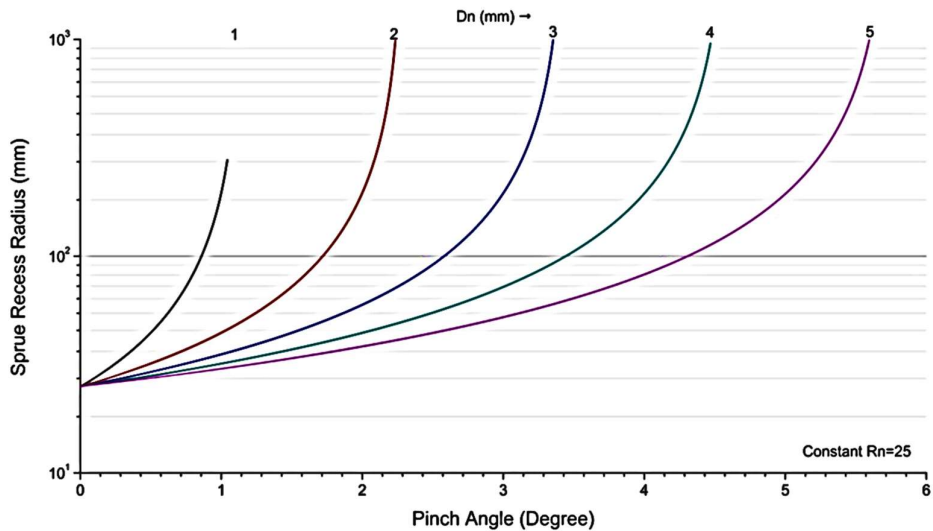


Figure 3.9: Sprue recess radius sensitivity to pinch-angle about sprue inlet orifice diameter for 25mm approach radius.

Though mechanical sealing perfection depends on pinch-angle accuracy, hemispherical concave-convex engagement difference offers the following best advantages,

- i. Positive contiguous sealing prevents excessive wear at minimum effort; the potential wear concentrates to small sealing region that normally self-compensates and in absence of abrasive contaminants, their continued rubbing action produces a lapped finish to form a closer fit.
- ii. More design flexibility can be realised to adjust little amounts of axial and/or radial misalignment, similar to rocker and socket alignment (Nakamura, et al., 1990), while remaining rigid enough to resist clearance gap extrusion between surface aspirates. Also the resilience to bear axial injection nozzle thrust avoids bending moments into either sprue or nozzle-tip.
- iii. As the engagement heat transfer depends on pinch angle, the thermal expansion of metallic sprue and nozzle elements also prompts for a conjoining seal. Thus sealing would be more efficient, despite volumetric expansion of abutting surfaces from temperature change (Glaesener, 2009).

Otherwise if by any chance injector nozzle-tip orifice diameter (D_n) exceeds sprue conduit entrance diameter (D_s), then sprue hangs-up while mould opens (Campo, 2006). So, to avoid such a mishap sprue inlet orifice (“O” diameter) is traditionally incremented by 20% of nozzle-tip exit orifice. This peeps nozzle-tip into sprue-conduit by a distance (*recess or pinch depth or engagement land as shown in Figure 3.10*)

$x_p = \sqrt{Rn^2 - \frac{Dn^2}{4}} - \sqrt{Rn^2 - \frac{(1.2Dn)^2}{4}}$. This distance spans parallel to the injection and is the ratio of tip interface length to nozzle orifice diameter and is termed as “engagement land”. Thus the engagement becomes tolerant with the possibility of providing H7h6 fit.

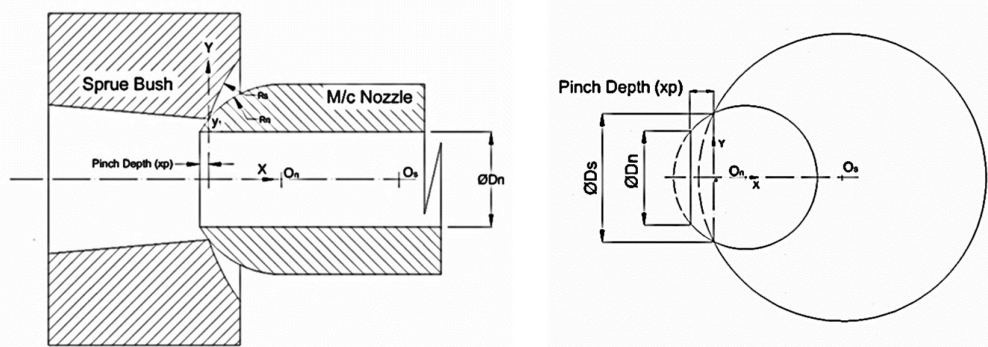


Figure 3.10 Pinch Depth.

Specific experiments in analogous situations have shown that pinch-angle increase informalises interference coax by deformation or even collapses. Ab-initio and ae-

finale pinch-angle widening steeply compromises sealing efficiency (Warring, 1981). Thus, a proper pinch-angle design would substantially increase confidence of sprue-bush engagement gap sealing. Moulds with sprue-bush designed for specific machine nozzle size are most likely to seal more accurately and therefore are less probable to leak. Suppose nozzle approach radius is 25mm and nozzle orifice is 3mm, then from Figure 3.8 and Figure 3.9, 0.05 to 0.07rad (3° to 4°) pinch-angle is enough. Further for ensuring leak proof mechanical sealing nozzle-tip is penetrated by 20% into sprue-conduit, so $D_{seal} = 1.2 D_n$, and tangent line Eqn. (3.12) and Eqn. (3.13) would also change,

$$\text{for nozzle side as } y_n = \left(\frac{3D_n}{5} + 4(x-a) \sqrt{\frac{25R_n^2}{36D_n^2} - \frac{1}{4}} \right)$$

$$\text{and } y_s = \left(\frac{3D_n}{5} + 4(x-b) \sqrt{\frac{25R_s^2}{36D_n^2} - \frac{1}{4}} \right) \text{ on sprue-bush side.}$$

Therefore Eqn. (3.15) will now become,

$$R_s = \frac{3D_n}{5} \sec \left(d\phi + \cos^{-1} \left(\frac{3D_n}{5R_n} \right) \right) \quad 0 < D_n < R_N < R_s < \infty \quad (3.17)$$

Henceforth to prevent engagement leakage, more intimate sprue-bush design is proposed with the chosen machine nozzle. Further considering pinch-angle to design sprue-bush recess compels mould designer to check and compare various nozzle-tip feature forms that might benefit the sprue-recess radius design in anyway. Ipso facto, more detailed investigation with various nozzle-tips design is needed for awareness.

3.1.6. Conclusion

Thorough pinch-angle sensitivity discussion above asserts that the possibility of parametric design for sprue-bush head to seal the engagement gap. Also designing a sprue-bush recess to an existing size and form of nozzle-tip on a machine, proper pinch-angle consideration increases confidence to prevent leak incidence. To assert this argument, various sprue recess radius and pinch-angle combinations were sensitised here to recognise leakage possibilities logically as rare and likely towards natural extremes. Wherein the choice of pinch-angle towards either extremes is more likely to leak; however, the sealing intellect wasn't yet pivotal to decisively specify a particular pinch-angle, perhaps better constraints from other factors might be needed.

Nevertheless, four distinct groups as engagement design, assembly, lip faces condition and materials are the principle factors for mechanical interface seal reliability. Possibly preventing other leakage modes might lead to those factors.

3.2. Design of Sprue-conduit System

Off the entire feed-system diverging sprue-conduit inlet orifice witnesses the swiftest volumetric shear-rate with major heat and mass transformations occurring at the shock plane (Lanxess, 2007). Narrow sprue-conduit size will rapidly shear, decrease solidification time, improve productivity (Rosato, 1997) and provokes processors to raise melt injection pressure and temperature. So sprue-bush conduit should be designed just wide enough to diffuse quickly from available pressure gradient. Mitigating melt / gas entrapment, abrupt streaming and pressure / temperature variance, vortexing, undue turbulence, discontinuous splashing of streams, self-tumbling, etc., or other challenges of dynamic characteristics of rheology to fully contrive the impression with continuous injectability. Eventually enable sprue-conduit to contrive parts that're (a) fully filled (b) superior surface finish (c) undistorted (d) denser (*minimum voids, pores and bubbles*) (e) flexible (f) superior weldmesh (g) dimensionally precise (h) uniformly shrunk (Dym, 1987).

Consequent to conduit convergence and divergence on either side of interface shock plane, greatest restraint to inject melt occurs at the interface between nozzle exit and sprue inlet orifice. So to achieve ideal throttle action shock section of sprue conduit must achieve highest shearable rate (*sonic injection*) of the chosen polymer (*perhaps $M \approx 10^{-1}$ i.e., injection velocity*). Injection shock plane Mach number depends on the rheological and shear degradation characteristics specific to chosen polymer. Convergent nozzle and divergent sprue-conduit combination acts as nozzle-diffuser in filling phase to increase melt downstream pressure at the expense of upstream velocity. A.k.a. increase diffusion rate to expand plastic melt from higher subsonic ($M < 10^{-3}$) nozzle velocity to lower subsonic ($M < 10^{-5}$) sprue filling velocity. Again the same combination acts as diffuser-nozzle to increase melt velocity at the expense of pressure during packing phase, *i.e. compress plastic melt from lower subsonic ($M < 10^{-3}$) nozzle velocity to higher subsonic ($M < 10^{-2}$) sprue compensation velocity*.

3.2.1. Sprue-Conduit Design Criteria

Analytical solution to non-trivial viscoelastic shear-thinning thermoplastic injection mould design problem is rare. This is because of complex conservancy, erratic state and

non-linear constitutive dependence; whilst even slight progress itself is a valuable contribution. So for designing sprue bush, injection problem is formulated by assuming its conduit as a generic capillary tube. Then for a pair of machine and impression, the ratio of maximum injection pressure gradient available to the limiting extent of injectable true shear-stress (τ) for chosen injectant gives its capillary ratio as

$$\frac{L}{R} = \frac{\Delta P}{2\tau} \quad (3.18)$$

Here ΔP is pressure gradient across nozzle-tip exit and sprue-well a.k.a sprue-bush conduit entrance orifice and exit orifice. While L is its length explained above and since sprue shank has linear conduit expansion its nominal diameter is an arithmetic average,

$$\text{i.e., } R = \frac{\bar{D}}{2} \text{ then, Shear Stress } (\tau) = \frac{\Delta P \bar{D}}{4L} = \frac{\Delta P}{4L} \bar{D} \quad (3.19)$$

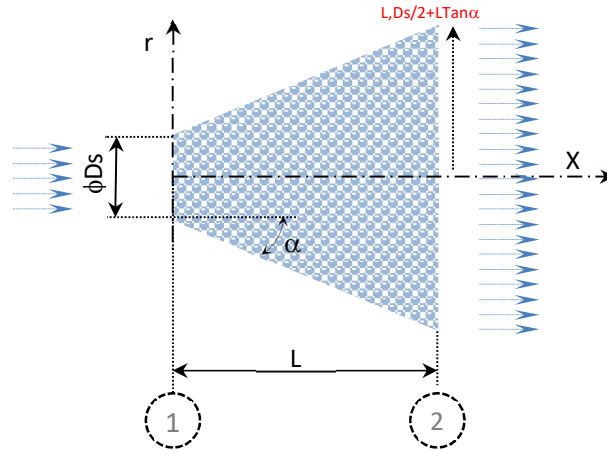


Figure 3.11 Schematic representation of a typical sprue bush conduit region.

From trigonometry for linearly expanding conduit as in Figure 3.11, its axiomatic nominal diameter \bar{D} is as follows,

$$\bar{D} = \frac{(D_s + D_s + 2L \tan \alpha)}{2} = \frac{2(D_s + L \tan \alpha)}{2} = D_s + L \tan \alpha \quad (3.20)$$

Here D_s being its inlet orifice diameter and α as its half angle or taper angle of expansion as schematised in Figure 3.11. So substituting Eqn. (3.20) in Eqn. (3.19) gives,

$$\text{Shear Stress } (\tau) = \frac{\Delta P}{4L} (D_s + L \tan \alpha) \quad (3.21)$$

Apparent shear rate (γ) for injection through a capillary conduit is (Hieber, 1987),

$$\gamma = \frac{4Q}{\pi R^3} = \frac{32Q}{\pi \bar{D}^3} = \frac{32Q}{\pi (D_s + L \tan \alpha)^3} \quad (3.22)$$

Where volumetric injection rate (Q),

$$Q = \frac{\text{Shot Volume}}{\text{Fill Time}} = \frac{V_{\text{Shot}}}{t_{\text{fill time}}}, \text{ where } t_{\text{fill time}} = \frac{\text{Stroke Volume of M/c}}{\text{Injection rate}} = \frac{V_{\text{Stroke}}}{U_{\text{Injection}}}$$

$$\text{So } Q = \left(\frac{V_{\text{Shot}}}{V_{\text{Stroke}}} \right) U_{\text{Injection}} \quad (3.23)$$

Therefore as explained in section (3.2), for designing a specific sprue-conduit, its characteristic features have to be represented by operational metrics. So melt's characteristic resistance to diffuse through sprue-conduit and specific melt strain rate response to shear injection stress are described quantitatively by apparent local viscosity (Martinez, et al., 2011). Thermoplastic melt viscosity being a true thermodynamic property varies spatiotemporally, therefore based on Sir Isaac Newton's resistance law postulated in 1687, the capillary rheologic formulation for polymer melt injection neglecting strain angle $\theta(t)$ would be (Rao, 1991),

$$\text{Apparent local viscosity } \mu \neq \frac{\text{Shear Stress } (\tau)}{\text{Shear Rate } (\dot{\gamma})} \quad (3.24)$$

Synchronous to its velocity profile slope of injection through capillary tube, shear-stress is maximum at the peripheral wall and declines towards the central core. Now substituting Eqn. (3.21) and Eqn. (3.22) in Eqn. (3.24) we get,

$$\text{Apparent local viscosity } \mu \neq \frac{\left(\frac{\Delta P}{4L} (D_s + L \tan \alpha) \right)}{\left(\frac{32Q}{\pi (D_s + L \tan \alpha)^3} \right)} \neq \frac{\Delta P \pi}{128QL} (D_s + L \tan \alpha)^4 \quad (3.25)$$

Eqn. (3.25) inequality represents non-Newtonian melt injection across nonlinear distribution of viscosity and could be equated using Weissenberg-Rabinowitsch correction (Rao, 1991) as follows (Rao, 1991),

$$\mu = \frac{\Delta P \pi}{128QL} (D_s + L \tan \alpha)^4 \left(\frac{4n}{3n+1} \right) = \frac{\Delta P \pi}{32QL} (D_s + L \tan \alpha)^4 \left(\frac{n}{3n+1} \right) \quad (3.26)$$

Here n is a behavioural index of shear-thinning flow, according to power law it's the slope of log viscosity vs. log shear-stress curve for a particular injection moulding case (Liang, 2002).

$$n = \frac{d \log_e \mu}{d \log_e \tau} \quad (3.27)$$

However, for non-Newtonian shear-thinning viscoelastic thermoplastic melts $n < 1$ (Sabic, 2008). Shear-rate dependency is a prominent injection-moulding character

that's typically around 10^1 to 10^6 per second; like high viscosity at low shear-rates in blow moulding or low viscosity at high shear-rates in extrusion (Ohlemiller, et al., 2000). So, thin viscoelastic thermoplastic melt rapidly occupies thinner mould gaps at high shear-rates. Then to fill and pack thinner-to-thicker impressions at AQL and APL; highest-to-least shear rates would be required (Cao, et al., 2008) and influx-to-efflux shear thinning behaviour of injectant (*at purge shot temperature*) has to be almost equal. Thus to inject rapidly and control at the best possible uniformity through it both gradient and variance of viscosity has to be least $\left(\nabla\mu, \frac{\partial\mu}{\partial t} \approx 0\right)$ at $x \in [0, L]$. So, despite 10^1 to 10^6 per second shear rate acting on injectant that changes violently across filling and packing stages, especially fluctuating over the cycles; and with conduit size being fixed or rigid, transit viscosity has to be adaptively moored. So logically it's essential to specifically design sprue-conduit for fastest shear-rate and preserve as much as possible uniformity conduit. Thus as conduit size is fixed, constant viscosity (μ) assumption for idealism is trustable. Therefore, rearranging Eqn. (3.27),

$$(D_s + L \tan\alpha)^4 = \frac{32\mu QL}{\Delta P \pi} \left(\frac{3n+1}{n}\right) \quad (3.28)$$

Now resolving for conduit expansion slope,

$$\tan\alpha = \frac{1}{L} \left[\sqrt[4]{\frac{32\mu QL}{\Delta P \pi} \left(\frac{3n+1}{n}\right)} - D_s \right] \quad (3.29)$$

Substituting from sound velocity definition $\Delta P = C_p P_{\text{Max}}$, where C_p is characteristic coefficient of a thermoplastic melt representing the extent to which sprue-conduit has to recover pressure and P_{Max} is rated injection pressure available in the machine (White, 2009). So substituting ΔP and Q we get,

$$\tan\alpha = \frac{1}{L} \left[\sqrt[4]{\frac{32\mu L}{\pi C_p P_{\text{max}}} \left(\frac{V_{\text{Shot}}}{V_{\text{Shot}}}\right) U_{\text{Injection}} \left(\frac{3n+1}{n}\right)} - D_s \right] \quad (3.30)$$

However, traditionally $1^0 \leq \alpha \leq 5^0$ taper is adopted arbitrarily to conserve more feed-system volume add-on expense, perhaps mayn't be idealistic (ISO 10072, 2004) (Jones, 2008). Now from Eqn. (3.30) a simplified criterion for designing expansion of sprue conduit is proposed,

$$\tan\alpha = \frac{(E_r - D_s)}{L} \quad (3.31)$$

Expansion ratio (E_r) is an important parametric quadruple ratio that collectively represents spatial change of geometry across initial nozzle-tip and off sprue-well base, cross sections (1) and (2) in Figure 3.11. Comparing Eqn. (3.30) and Eqn. (3.31) gives,

$$E_r^4 = \left(\frac{32}{\pi}\right) \underbrace{\left(\frac{3n+1}{n}\right)}_{\text{Material}} \underbrace{\left(\frac{\mu}{C_p}\right)}_{\text{Machine Setting}} \underbrace{\left(\frac{U_{\text{Injection}}}{P_{\text{Max}} V_{\text{Stroke}}}\right)}_{\text{Moulding}} \left(L_{\text{Spruc}} V_{\text{Shot}}\right) = \left(\frac{32}{\pi}\right) \underbrace{\text{Poly}}_{\text{Material}} \underbrace{\text{MS}}_{\text{Machine Setting}} \underbrace{\text{Comp}}_{\text{Moulding}} \quad (3.32)$$

According to Eqn. (3.32) sprue-conduit expansion geometry depends specifically on a particular combination {moulding, material, machine}. Like

- (a) intrinsic character and specific in-situ behaviour of the thermoplastic has representation by having directly proportional apparent viscosity and inversely proportional shear-thinning index.
- (b) machine specifications or capacity has representation by having directly proportional injection velocity and inversely proportional machine size, *i.e.*, *machine size quantified as product of maximum shot volume per stroke and maximum injection pressure.*
- (c) part features, thickness, length, volume, etc. has representation by having directly proportional part volume and depth below the parting plane.

Since each of their specific influence is quantifiable, the sensitivity discussion hereafter is reliable and valuable to responsibly configure conduit design with individual perturbations.

3.2.2. Design Sensitivity Characterisation

Conventional design criteria typically focus on direct mathematical substitution just enough to specify some discrete or numerical value. Whereas Continuous Sensitivity Method (CSM) contrasts to examine the relative sensitivity about infinite range. CSMs adopt illustrative intervention to deliberate conduit design sensitivity at wisdom level much beyond physical experimentation or classical analogy. Although its inference is still casual, analytical modelling compliments a unique perspective over prevalent myths. Independent sensitisation of each processing factor instils confidence to mould designers on their mould. However to get rational perspiration, perturbation of each factor for all three independent combinations are illustrated and discussed on de-facto scales (Bolur, 2000). So their inference provides clarity, saves time and reasonable outlay on the effects of parametric manipulations on overall process. Like sensitisation can provide information on how an increase of unit injection pressure would affect its

distribution at any particular location of the impression. Such types of information are useful to strategize following process factor change to get needed AQL and APL. Similarly, these sensitivities are also useful in algorithms of conventional variance optimisation of a chosen function (Ilinca, et al., 2004).

3.2.2.1. *Sprue-conduit Dependence on Injectant*

In general, deformation, diffusion and solidification of injection moulding need injectants in a molten state above their respective glass transition level; such a state excites intense non-Newtonian character complexity stimulating various unstable mechanical responses (Larson, 1999). Behaviours like irrecoverable shear-strain along melt-to-conduit wall interface (Bagley, et al., 1961) and hydrodynamic instability that entwine injection pattern represented by Wiesenberger number (White, 1973) are seen repeatedly. Though influx state of injectant at shear injection shock geometry zone is the principle factor; energy developed and/or absorbed later would inherently disperse melt state over 10% range (Amano, et al., 1989). Nevertheless, this dispersion depends on Barrel-to-Shot ratio (BSR) (Peischl, et al., 2004) and has direct influence on overall injection moulding yield; especially thermal characteristics of parts. Like intrusive probes in sprue-conduit have revealed that injectant pressure and temperature increase steeply during injection followed by gradual decay during packing and decrease swiftly during cooling. Such intra-conduit dynamics of volumetric injection, adiabatic compression and shear friction, imperil in-situ state to extreme volatility (Johnston, et al., 2007). So, a priori knowledge of injectant's rheological character especially apparent viscosity, shear-thinning and critical shearability rate is essential to design a sprue-conduit geometry (Liang, 2002). Therefore, sprue-conduit expansion design dependence on factors representing in-situ thermoplastic melt state in Eqn. 3.32 is true; wherein efflux shear strain ought to be a critical factor to the extent of in-mould pressure recovery needed (Liang, 1995).

Further typical injection moulding severely aggresses injectant physically at high-temperatures ($T_r > T > T_g$), high-pressures ($P_{max} > P > P_{in-mould}$) and high shear-rates ($10^6 > \dot{\gamma} > 10^1$) sec^{-1} . The extent and interval of such aggression imperils most viscoelastic shear-thinning thermoplastic melts; for instance, polyacetals easily decay under excessive shear force actions, especially at raised pressure and temperatures.

Characteristically, most thermoplastics exist in amorphous state above their glass transition temperature; nevertheless, owing to injectant decay amorphous state remain as opposed to crystallization in injection moulded part even after solidifying. Like injection moulding grade PET is in amorphous state resembling a spaghetti model or a bowl of worms, while as fibres it's in semi-crystalline state. These state dissimilarities differ their degree of molecular kinesis, local rotations, vibrations, possible translations vs. long-range (*segmental*) motion (Stevens, 1998) over injection moulding interval through filling to packing. Broad thermoplastic molecular weight distribution range and melt rheological property change from blends or co-polymers inclusion further increases likely differences during injection moulding (Tremblay, 1992). Influx polymer melt expands into sprue-conduit and witnesses extensional strain consequent to intense intra-conduit shear effort in succession (Liang, 1995). So divergence design of conduit depends specifically on rheological characteristics of injectant and should immunise undesirable defect arise. Such as wide expansion in sprue-bush design is necessary for higher molecular weight thermoplastics with greater levels of crystallinity, primary to secondary cross-link bonds that feature improved tensile strength, modulus, toughness, hardness and chemical resistance even at higher glass transition temperatures. Therefore, expansion design of sprue-conduit should ensure consequent shear-rates are within critical degradation limit of injectant, because most thermoplastic melts are prone to phase separation, morphological complexities especially about end group identities. Long-segment thermoplastic block co-polymers like polyurethane, polyetheramides, styrenic SEBS, etc., are typical injectants that need low creep level laminar shear-rates. Similarly blends like ABS with significant immiscibility do easily separate if in-situ shear-rate is high (Stevens, 1998). Therefore, expansion design of sprue-conduit has direct dependence on in-situ behaviour of injectant. Perhaps smaller expansions would orient microstructure of long molecular chains excessively as related strain levels yield or deform discretely. Conversely, rapidly diverging injection streams in wide expansion conduits lead to high compressive stress action on injectant and shrink the injectant as sprue-conduit widens toward the exit. But most thermoplastics can only bear 1 to 10 MPa as melt compared to 10MPa to 4GPa in solid-state. Besides, excess injectant inside the conduit would extend solidification time causing melt to degrade especially at low heat extraction regions, thus predating melt fracture. On the other hand, suppose if injection streams are all parallel then injectant will shear solely (Belofsky, 1995).

Since thermoplastics are in many varieties, getting a generic design criterion for all is difficult that can intrinsically inoculate respective premature freezing or impression filling-to-incompleteness through traditional and conventional methods. Like for instance molten PC having high viscosity needs larger conduit expansion than PA that has low viscosity. This happens because rigid repeating units, molecular weight, structure, etc., increase the apparent viscosity by implication constrain its mobility and dispose as degradation risk. Usually coexistence of shear and extensional rheological characteristics is riskier; sometimes even inertia also complicates further (Barnes, et al., 1989). Off recently diverging flow of non-Newtonian thermoplastic melt is studied extensively from various approaches. Like equibiaxial and planar elongations; viscosity of polymeric melts in expansion flow and; critical instabilities of diverging flow are under research. Similarly, few mathematical models for shear-thinning melt and viscosity influence on conduit size of varying complexity and form have been proposed in the literature. Some of these are straightforward approaches with curves-fit from empirical relations, while others have theoretical basis from statistical mechanics that extend kinetic theory to liquid state or theory of rate processes. Although, much of its themes are still unexplained and unknown their physical mechanisms trigger a generic criterion (Goutille, et al., 2002). Fortunately, complex in-situ viscosity decrease is often dealt by extensive adoption of power-law or Ostwald de Waele model. As it relates shear-stress and shear-rate for shear-thinning thermoplastic melt by presuming linearity on a log-log dependence over de-facto injection moulding range (Liang, 2002). Its applicable expression is,

$$\text{Apparent Viscosity, } \mu = \frac{\tau_{yx}}{\dot{\gamma}_{yx}} = k (\dot{\gamma})^{n-1} \quad (3.33)$$

Here “k” and “n” are two empirically curve-fit factors popularly known as flow thermoplastic melt consistency coefficient and power-law flow behaviour index respectively. The consistency coefficient value can be viewed as the apparent viscosity for unit shear-rate and depends on the engaged time unit (*e.g. second, minute or hour*). The index value is anywhere between 0 and 1 for thermoplastic melts, where a smaller value depicts extreme shear-thinning intensity. As this is a simplest representation, there’re several inadequacies like the fitted values are applicable over a distinct range of viscosity intensity for each thermoplastic and unsuitable to impractical extremity at zero and infinite viscosities. Thus every non-Newtonian thermoplastic is unique and its rheological behaviour must be recognised solely. Besides, consistency coefficient (k)

value depends on index (n) value, so it can't be compared independently while perturbing index (n) values. Despite these constraints, this's perhaps the most widely used model in the literature to design injection moulds.

Most viscoelastic shear-thinning thermoplastic melts are sensitive to injection force extent, especially at peek injection pressure and temperature (Whelan, et al., 1990); for instance POMs easily decay under excess shear-stress. So manipulating melt state to get uniform injection rate at some agreed interval would be essentially wisdom driven. This is because shear-injection-rate to sprue-conduit expansion combination is obvious judgement across widest for productivity and narrowest to preserve injectant quality at its best (Strong, 2006). Like thin mouldings need rapid injection rates to ensure impression gaps are filled before melt solidifies. Although higher injection rate machine is available, correct sprue-conduit design is needed to rapidly inject melt into impression gaps, while it's still as much uniform as possible to avoid differential shrinkage (Belofsky, 1995). Since thermoplastic melt is a viscoelastic shear-thinning fluid, perturbing apparent viscosity and shear-thinning index shows the exclusive influence of injectant on sprue-conduit expansion.

In-situ apparent viscosity depends significantly on shear-rate (*rated injection pressure of the machine*), temperature and pressure (*thermoplastic melt state characteristics*) and interval (*part volume*). It effectively characterises the onset of various undesirabilities (Baldi, et al., 2011) because it influences shear-rate depth deterministically (Barnes, et al., 1989). So it's worthwhile to perturb probable change in viscosity about perfect sprue-conduit expansion over de-facto range (Goutille, et al., 2002). Thereby, balancing the deformation quotient about shear-to-elongation the severity of gross melt fracture could be lessened as in Eqn. (3.24). Thereon, Eqn. (3.31) gives a suitable expansion angle to stabilize streamlines and avoid defects (Goutille, et al., 2002). To summarize, expansion design of sprue-conduit is important to prevent injectant stream splitting and gross melt fracture development, specifically adjusting the stress field. So its inference could enable injection mouldability of any polymer melts within AQL and APL (Goutille, et al., 2002). However, an in-depth exploration to know the physics of the gross melt fracture defect origination is necessary to quantify the direct and interactive influence on sprue expansion size.

1. ***Dependence on shear-rate:*** Shear-rate values distinguish the onset of upper and lower viscosity extremities depending on constitutive factors, like polymer type, concentration, molecular weight distribution, etc. In general, for any given shear-rate constant apparent viscosity high-level raises with polymer molecular weight reduction and/or molecular weight distribution becoming narrow. Conversely lower level also decreases from one thermoplastic to another. So, it's unreliable to generalise de-facto situations because every thermoplastic shows a distinct critical viscosity at its limiting shear-rate extent across 10^2 to 10^5 sec^{-1} respectively (Chhabra, et al., 2008). Injection moulding never involves shear-rates lower than 10^2 sec^{-1} because at such rates ramping time to get steady-state is too long and probably by then defects would dominate the macromolecular structure for most thermoplastics (Baldi, et al., 2011). Therefore, the ratio of injection force to product of shear-rate and nominal injectant viscosity gives characteristic size of sprue-bush to inject melt through it; as conduit radius or thickness of sheared layers (Fleming, 2004). To inject thermoplastic melt, influx shear-rate is independent of Reynolds number or sprue capillary ratio (Pérez-González, 2001), nevertheless sprue-conduit expansion governs its stability (Ramamurthy, et al., 1980). Therefore, to quickly inject nearer and just below critical shear-rate, meticulous design of sprue-conduit geometry should traverse shear-stress to shear-rate ratio towards distortion free zone (Liang, 1995).
2. ***Variation with temperature:*** Thermoplastic injection moulding involves aqueous phase just above the respective glass transition temperature that typically range from 150°C to 300°C . Thermoplastic melt viscosity has inverse dependence with temperature and that becomes more for thicker viscosity injectants (Liang, 1995). Nevertheless, the act of shearing itself produces heat between melt layers and rises the temperature enough to soften its viscosity. The rate of energy dissipated to diffuse per unit volume of injectant is the product of shear-stress and shear-rate or equivalently the product of viscosity and the square of shear-rate. Therefore, to control the extent of energy lost by heat extraction of conduit surface as melt diffuses, it's important to design sprue-bush with proper capillary ratio, conduit expansion sizes like diameter and expansion angle. It's desirable for this design to be at best possible accuracy.

3. ***Variation with pressure:*** As viscoelastic injectant diffuses into sprue-conduit its elastic energy increases and spreads by changing injectant state, this obviously reduces pressure gradient across the conduit ends. So the ability of a conduit to preserve in-mould pressure depends on elastic and rheological characteristics of injectant (Liang, 2000). However, that dependence on recoverable shear strain is specific to thermoplastic melt and usually trivial (Liang, 2000). This is because the increase of thermoplastic viscosity with pressure is exponentially small (Liang, 2001); so traditionally its effects were ignored (Liang, 2002). Nevertheless, such reasoning can't be justified always, like for long-thin-walled impressions that involve 0.5 to 1 GPa injection pressure action (Fleming, 2004). Conversely enormous injection pressure leads to excess stretching rates inciting defects. As, arbitrary intra-conduit viscosity and adherence of injectant with its interface surface (Hatzikiriakos, 1994) (Kissi, et al., 1997) divide melt into discrete injection streams (Liang, 2002). This leads to wall slipping phenomena in critical shear-stress region causing sharkskin appearance (Ramamurthy, 1986). Since in-mould pressure recovery need about available pressure gradient characterises undesirable energy transaction across the diverging sprue-conduit (Han, 1973). Efflux pressure depends on viscous dissipation and shear strain energy and that dependence increases with sprue-conduit expansion angle (Liang, et al., 2001). In other words, sprue-conduit expansion and recoverable in-mould pressure have a definite relation (Piau, et al., 1990) and that relativity becomes still more obvious as capillary ratio shortens (Liang, 1995).

Illustration

To explain the sensitivity of sprue taper expansion design criteria, a 2500 cc shot volume injection moulding part with a depth needing 80 mm sprue-bush length is assumed representatively to calculate moulding term of Eqn. (3.32) as $Comp = 0.2 \times 10^{-3}$. Similarly, Sprint series 650T horizontal injection moulding machine from Windsor Machines Ltd., Mumbai, with 2.5mm nozzle orifice is assumed representatively to calculate machine setting term of Eqn. (3.32) as $Ms = 1.4482 \times 10^{-6}$

Sensitivity to Apparent Viscosity

Viscosity of an injectant is perturbed independently over an infinite range about sprue-conduit taper. For illustration, rated injection pressure range $P_{Max} = \{1260, 2230\}$ bar and

stroke volume range $V_{\text{Stroke}} = \{3180, 8588\}$ cc of chosen 650T sprint machine are assumed to be representatively at their intermediate value of 1500bar with 50% BSR as well as 5000cc barrel stroke volume. Assuming injectant to be ABS shear-thinning power law index gets anchored to $n=0.3365$ (Shenoy, et al., 1996).

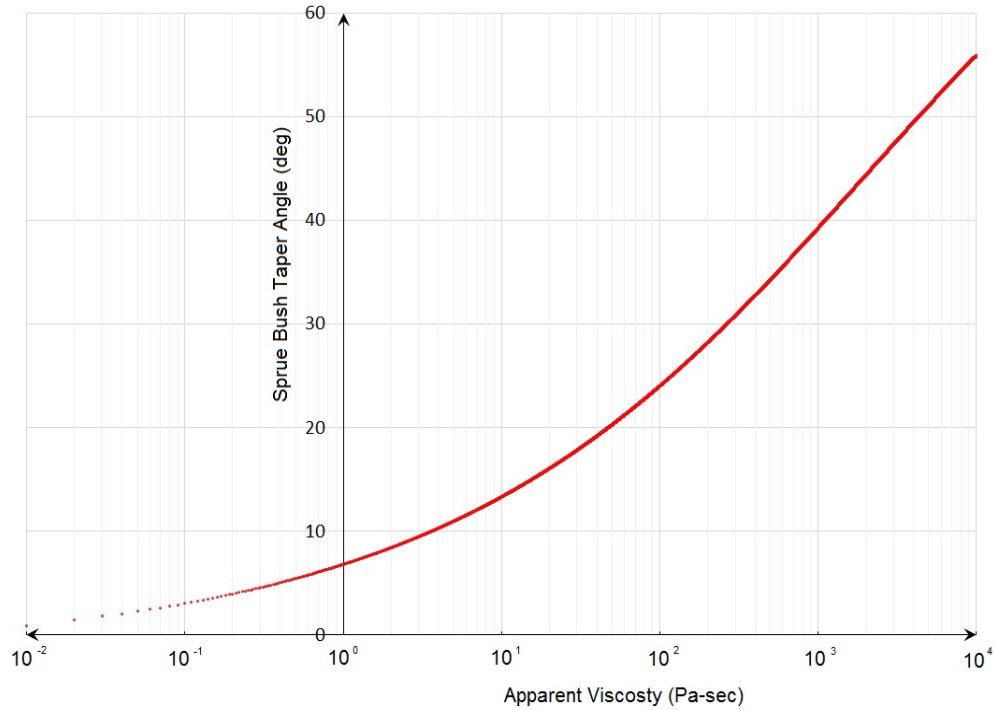


Figure 3.12 Sprue bush taper angle about apparent viscosity of a thermoplastic melt.

Perturbation of expansion angle in sprue-conduit about an injectant in Figure 3.12 has two important reasons. First one is cracking phenomenon by strangulate expansion below the curve that eventually roughens with more frequency and lesser amplitude. The second one is slip phenomenon by excess expansion above the curve that builds-up injectant along the conduit walls, detach intermittently and regularly get dragged away by the succeeding injection action (Piau, et al., 2000). Nevertheless, excess viscosity is also damaging because it orients injectant randomly and concentrates local stress making the part more susceptible to crack. For instance, ABS mouldings are often exposed to acidic solutions for electroplating, so to get a definite functional orientation sprue-conduit should expand nominally as in Figure 3.12 curve. Further transverse injection of excess viscosity superimposes subsurface orientation over primary orientation as in most real mouldings, leading to anisotropy (Belofsky, 1995), while low apparent viscosity for any shear-rate would need little expansion (Chhabra, et al., 2008).

According to Figure 3.12 expansion angle of sprue-conduit has direct exponential sensitivity with apparent viscosity of injectant. This implies to inject uniformly despite extensively changing viscosity would need proper widening. Therefore, the proposed design criterion is usefully to strategically get the best possible AQL and APL much before injectant exits sprue-bush itself, eventually fulfil mould design purpose and may thus contribute to the overall injection moulding success.

Sensitivity to Power law index

The phenomenal time-independent decrease of apparent viscosity over the shear-rate is known as “shear-thinning”; despite other analogous terms like temporary viscosity loss and pseudo-plasticity (Chhabra, et al., 2008). Most thermoplastics feature this characteristic viscosity thinning for injection rate rise (Utracki, 1982). Indeed, few reliable and outright experiments have shown that with low intensity shear-rate range the viscosity remains almost constant at its highest extent and with high intensity shear-rate range it’s at the lowest extent. These two popular extremes are described as lower and upper Newtonian regimes or first and second Newtonian regions respectively. Despite 10^4 to 10^{-1} sec^{-1} shear-rate range generic yield stress constitutive behaviour exist (Rao, 1991). So from an orphic view viscosity reaches infinite extent at zero injection effort and almost nil viscosity at enormous injection rates. However, few injectants show some unstable phenomena at interfaces and inconsistent distribution in de-facto injection moulding circumstances, that’re still contentious to concurrently achieve AQL and APL objectives. As these instabilities are associated to various defects and modern researchers are widely studying both experimentally (Shanker, et al., 1995) (Khomami, et al., 1997) and philosophically (Matsunaga, et al., 1998) to remediate by suitably designing conduit size. So extended range of shear-thinning index enables sophistication to understand conduit size sensitivity with some degree of confidence.

Temperature and pressure rise spontaneously increases individual macromolecular chain movements, relaxes chain orientation and thus improves rheological properties despite elasticity of injectant engaging in elastic deformation of influx energy. So to enable rapid injection through spue-conduit, its expansion design has to be consistent with injectant character (Liang, 2005). Thus aqueous melts could be injected even if conduit size is small, while aspic melts need reasonably wide conduit size. Even though injection of aspic melts through nominal expansions have been reported, they’re

considered uninjectable merely because of heavy viscosity owing to small shear-rate. A.k.a. in exigence a 10^0 Pa-sec viscosity takes several years to witness even slightest injection that can be seen visually (Barnes, et al., 1989). Wide-ranging shear-thinning characteristic behaviour of various thermoplastics is represented quantitatively by power law index (n) with unit reference value describing Newtonian model. As plug flow develops from almost constant influx to axially varying efflux velocity variation; the gradient behaviour reduction through thickness depicts almost constant volumetric injection (Kazmer, 2007). So apparent viscosity decline from thermoplastic melt shear-thinning decrease at any given shear-rate (*injection pressure of available machine*) could be represented by a smaller power law index. Therefore, power law index value of infinite scale depicts the complete spectrum of likely pseudo-plastic behaviours in almost all thermoplastics ever synthesised despite difficult to list and are scarce.

Obviously early melt streamlines have little and mostly linear dependence; however, as injection pattern gains momentum relative melt viscosity reduces dependence on the pressure gradient and is unique for each polymer owing to its morphology. Synergic effect of viscoelastic property variance from rheological and molecular chain structure stances suggests existence of viscosity and elasticity consequent ratios. These differences are closely dependent on the composition, constituting ratios and viscoelastic behaviour quotient. Thus sprue-conduit expansion depends on efflux shear-thinning coefficient; *a.k.a.* theory of elasticity approach is necessary to get an exact relation of conduit expansion angle with shear-thinning phenomena. Therefore, designing sprue-conduit expansion from injectant's in-situ behaviour is preventive instead of iteratively manipulating state factors as optimisation (Liang, 1995). For illustration, from the chosen 650T sprint machine specifications, rated injection pressure range $P_{Max} = \{1260, 2230\}$ bar and stroke volume range of $V_{Stroke} = \{3180, 8588\}$ cc are assumed to be representative at their nominal value of 1500bar with 50% BSR and 5000cc barrel stroke volume. Besides, holding injectant state at an apparent viscosity of $\mu = 59.589$ Pa.sec shear-thinning power law index of thermoplastic injectant is perturbed as an independent factor over an infinite range to sensitise sprue-conduit taper in Figure 3.13.

Despite extensive studies neither satisfactory models nor fundamental reasoning exist to design conduit expansion for a specific shear-thinning behaviour. So from

Figure 3.13 we can only infer that sprue-conduit expansion angle has logarithmic dependence on shear-thinning index and that's consistent with real witnesses (Liang, et al., 1997). Knowing the natural extremes across expansion less sprue-conduit with infinitely large shear-thinning flow index to (90°) expansion angle where sprue-bush conduit despairs to exist with infinitely small shear-thinning flow index is shown in Figure 3.13. However, recent investigations have shown that the sensitivity of conduit design for both the extremities *i.e.*, *rapid and gradual shear-thinning rate* is still intimidating (Takahashi, et al., 1994). Therefore, clear change in slope towards either extreme in Figure 3.13 is consistent with popular belief and is first-hand insight altogether to get an ideal sprue-conduit design, where several physical experiments are necessary to either envisage or authenticate such a view.

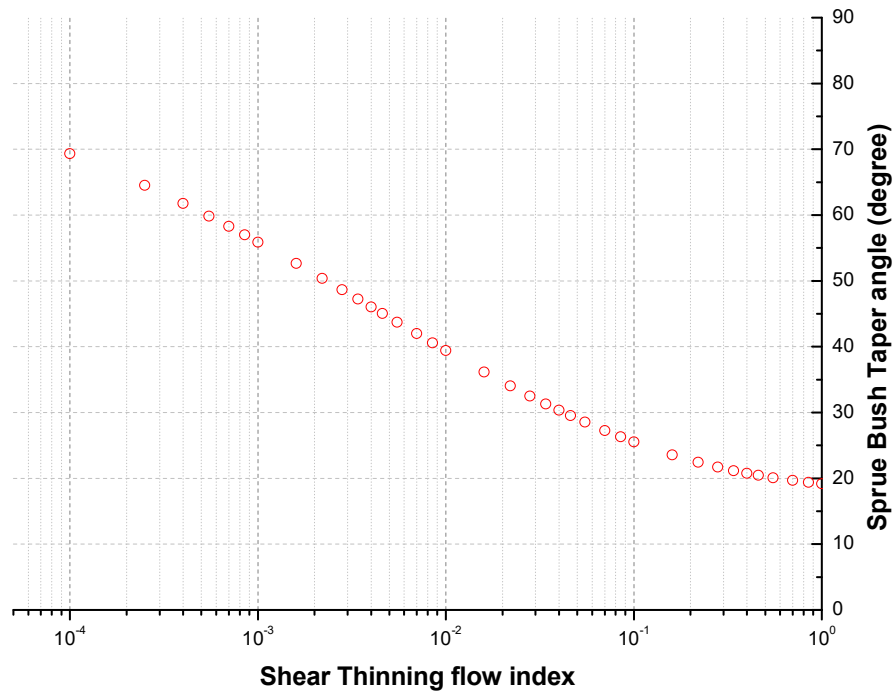


Figure 3.13 Sprue taper expansion about shear-thinning index of a injectant.

3.2.2.2. Sprue-conduit Dependence on Machine

Injection pressure delivered from moulding machine must progressively fulfil energy transformations through nozzle, sprue, runner, gate and impression (Mattis, et al., 1996). Obviously, a meticulous criterion for recovering in-situ conduit pressure is crucial to efficient mouldability, so the rational approach is to embrace its fundamental injection mechanics. Therefore to associate and recognise the sensitivity of machine specifications with taper expansion design of sprue-conduit, material and moulding is

held constant. Contending this investigation scope, injection grade acrylonitrile butadiene styrene (ABS) was assumed as representative injectant for moulding,

Table 3.1: Characteristics properties of ABS taken from MATWeb

Injection temperature	190 – 210 °C
<i>Capillary Rheometry</i>	
Power law index, n	0.2390 to 0.4340
Apparent viscosity	96.99 - 22.19 Pa - sec
In-mould injection pressure needed to contrive impression gap	4.14 – 130 MPa

Using material characteristics data listed in Table 3.1, the range in material term of Eqn. (3.32) as $Poly = \{696.786, 117.699\} = 499.682$ was calculated. Similarly, a 2500cc shot volume injection moulding part to a depth of 80 mm sprue-bush length are assumed representatively to calculate part term of Eqn. (3.32) as $C_{omp} = 80 \times 10^{-3} \times 2500 \times 10^{-6}$, $Comp = 0.2 \times 10^{-3}$. Further Windsor Machines Ltd., Mumbai, Sprint series horizontal injection moulding machine with 2.5mm nozzle orifice has been assumed representatively.

Sensitivity to Injection Rate

As most viscoelastic shear-thinning thermoplastic melts are susceptible to applied shear force extent, *like polyacetals easily decay under excess shear force action, especially at high temperatures*. Manipulating injection rate by injection pressure within an acceptable interval depends more on wisdom. This is because sprue-conduit expansion dependence on injection-rate was so far a relative judgement across maximum for productivity and minimum to preserve injectant quality at its best characteristics (Strong, 2006). Like thin mouldings need rapid injection rates to ensure impression gaps are filled before melt solidifies. Despite higher injection rate machine availability correct sprue-conduit design is critical to rapidly inject melt into impression gaps, while melt state is still as much uniform as possible to avoid differential shrinkage.

Designing sprue-conduit expansion specifically to available injection effort is pretentious, rather than scuttling probabilistically over a set of optimistic iterations. In pursuit, moulding machine's injection rate is perturbed alone over an infinite range to sensitise sprue-conduit taper. Rated injection pressure range $P_{Max} = \{1260, 2230\}$ bar and stroke volume range of $V_{Stroke} = \{3180, 8588\}$ cc for the chosen 650T sprint machine

specifications are assumed representatively to be at intermediate nominal value of 1500bar with 50% BSR and 5000cc barrel stroke volume.

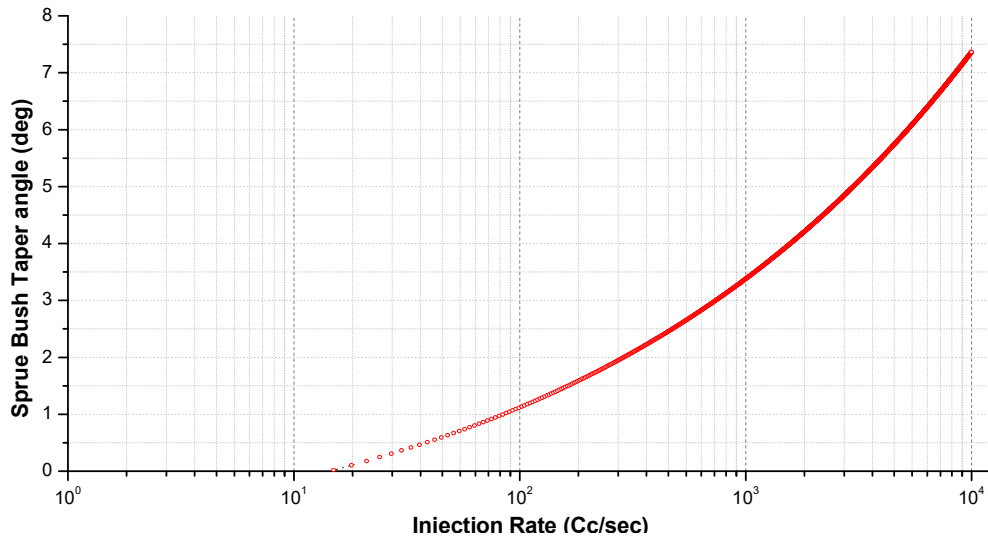


Figure 3.14 Sprue taper expansion about injection rate in a machine.

Figure 3.14 graph shows that sprue-conduit expansion has exponential dependence on injection rate extent, suggesting even a large injection rate change needs just a nominal widening. So controlling injection rate has modest influence to foreseeing sprue-conduit design perfection. Instead, excessive injection rates above the Figure 3.14 curves are damaging because they heavily orient injectant and that increases stress cracking susceptibility as explained before. For instance, ABS mouldings are often exposed to acidic solutions for electroplating, so they need to be injected at slow injection speeds to minimise any particular orientation. Further with excess speed above Figure 3.14 curves, transverse melt injection occurs superimposing subsurface orientation over primary orientation, resulting in anisotropy (Belofsky, 1995). Conversely injection rates below Figure 3.14 curves would recover inadequate in-mould pressure, extend fill time, etc., So to get the best possible performance sprue expansion design is proposed to lie on Figure 3.14 injection rate curve.

As injection rate in any available injection moulding machine is a performance limit; modern machines offer injection speed (*mm/sec*) adjustment in multiple stages. However, owing to its modest dependence on conduit expansion, the following scheme is best to get defect free mouldability.

Stage 1 Earliest injection speed has to move the screw upto 20% of its injection stroke length and gradually increase to modest injection speeds as impression gaps begin to fill, else short shots, burns, voids or weld lines might occur.

Stage 2 The screw should be moving at a modest injection speed as it reaches 40% of stroke length and so on till stage 5. Typically, injection rates reduce for the last 20% (cushion) of the stroke in stage 5, transfer position should be reached to change screw action from injection to pack (or mould).

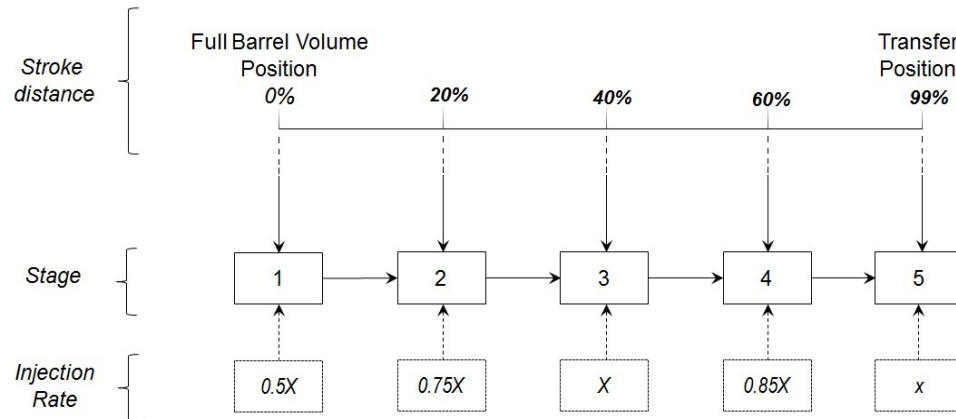


Figure 3.15 Typical Injection rate profile control for an injection moulding machine.

Injection moulding success depends on screw rotation also because controlling its RPM and tongue are important. Some low viscosity injectants (PP, PE, PS, etc.) need least torque, in contrast to viscous injectants (PC, Acrylic, etc.). So depending on melt viscosity; torque and speed have to be balanced. Besides, shear heating occurs when injecting screw moves past stage 2 to 4. Since melt viscosity changes with injection rate, obviously preserving a constant injection profile as in Figure 3.15 ensures process stability *i.e.*, to consistently fill impression gap during each shot. For this injection ram velocity or fill time has to be controlled continuously. However, velocity could also be set electronically for direct intrinsic control in few modern microprocessors based machines.

Sensitivity to Injection Pressure

Advancing injection unit screw pushes molten plastic ahead through a nozzle into sprue-conduit, so injection pressure on a moulding machine is a prominent factor (Varela, 2000). As soon as melt touches colder sprue-conduit surface it starts solidifying, so injection pressure must be enough to rapidly diffuse while melt is still in

a fluid phase. To injection-mould properly, machine should have enough injection power (*maximum injection rate x maximum injection pressure*). Like for engineering components, machines with higher injection pressure capacity are used to fill uniformly; pack more resin tightly into impression gap to reduce shrinkage; increase gate temperature to avoid short shots, surface defects, sink marks and ripples (Huang, 2007). However, energy consumption for higher injection pressure is much less than that for heating and/or cooling (Hassan, 2013), so the extent of injection pressure to a maximum of 140 MPa on older machines is often a limit. Nevertheless, most modern machines can apply 50 to 500 MPa injection pressure or even more with an assortment of barrel and screw size combinations.

So, to preserve available moulding machine's power, as an independent factor its injection pressure is perturbed over an infinite range to know the design sensitivity of sprue-conduit taper. From the chosen 650T sprint machine specifications injection rate range of $U_{\text{Injection}} = \{450, 1110\}$ cc/sec and related stroke volume range of $V_{\text{Stroke}} = \{3180, 8588\}$ cc; injection rate is assumed at an intermediate value of 700cc/sec and 5000cc barrel stroke volume for illustration.

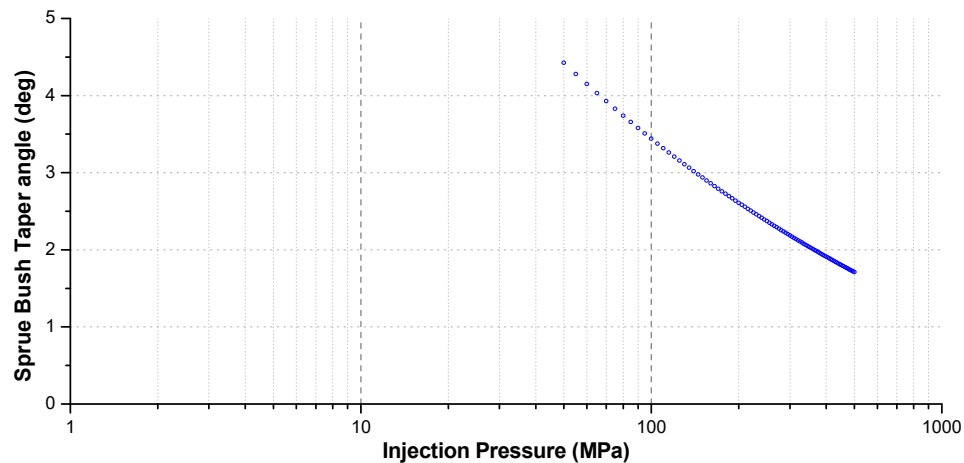


Figure 3.16 Sprue taper expansion about maximum injection pressure of the machine.

Realising from Figure 3.16 sprue-conduit expansion is inversely exponential to available injection pressure extent. This is because more pressure is needed to inject through smaller and narrow conduits than larger and wider conduits (Olmsted, et al., 2001) Figure 3.16 curve is consistent with this belief. Thus with low expansion designs below Figure 3.16 curve would risk of air trapping leading to burn marks as well as

higher moulded-in stress. Eventually these excess moulded-in stresses are likely to perpetuate as warpage, impact strength compromise and environmental stress cracking proneness. For de-facto moulding situations with critical tolerance like syringes, where core shift concerns prevail; both injection rate and injection pressure has to be configured simultaneously for smooth melt injection by properly setting screw movements (*both angular and linear*).

Conversely if sprue-conduit expansion is wider than Figure 3.16 curve then injection pressure gradient is inadequate and that leads to short shots, porosity, unacceptable shrinks, compromised stiffness, etc. Therefore, to get the best possible performance, design of expansion in sprue-conduit is proposed as in Figure 3.16 curve for an available injection pressure.

Sensitivity to Barrel Volume

Barrel volume to sprue-conduit combination adeptly needs a particular residence interval that ideally range from two to five minutes. This is because less than two minutes is rarely enough to uniformly mix melt while more than five minutes most resins break-down causing burn marks or surface defects and/or mechanical properties. So volume of barrel is important for moulding success especially with sensitive injectants like PC, ABS, PVC, Acetyls, Cellulosic, other flame retardants, etc. that're prone to burn and degrade.

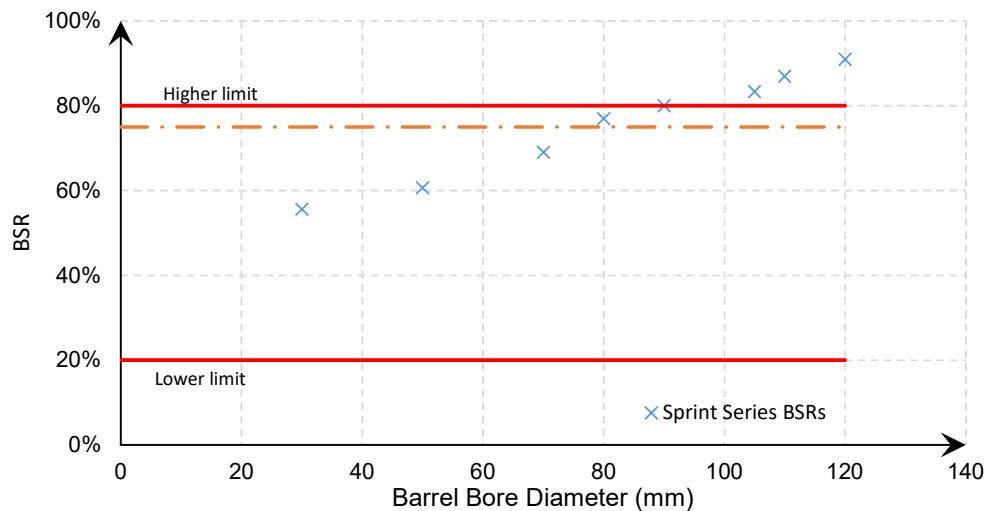


Figure 3.17 Preferable BSR versus barrel bore diameter (mm) relativity.

Occasionally machines are fitted with large screw sizes to hold more shot weight, then to get the necessary pressure recovery coefficient, sprue-conduit expansion ought

to be configured for BSR for regulating in-situ pressure gradient. So dependence of BSR choice on barrel bore size is a field-to-laboratory expertise based decision (Olmsted, et al., 2001). Therefore, current research effort intends to perturb stroke volume as an independent variable over an infinite range to sensitise sprue-conduit expansion. For which an intermediate value of 1500bar is chosen from 650T sprint machine with maximum injection pressure range of $P_{Max} = \{1260, 2230\}$ bar . Similarly, 700cc/sec injection rate is chosen from $U_{Injection} = \{450, 1110\}$ cc / sec range.

Ideal BSR range from 20% to 80% for perfect moulding, because smaller than 20% increases material residence time, prolongs shear and heat action that might degrade eventually, while more than 80% retracts screw much before mould opens causing inadequate shot size. While less than two shots of injectant in the barrel cause asymmetric melting temperature during screw metering, as a result unmelted injectant appears on the moulding compromising physical integrity (Harper, 2006). Thus, BSR should always be nominal at 50% as shown graphically in Figure 3.17 (Strong, 2006), so we propose 75% BSR as preferential choice of barrel size for the best balance of both the precludes. However, in some real situations, the ratio is beyond preferred limits for the needed part and available machine combination. So corrective measures include slowing screw rpm, lowering back pressure, lessening barrel heat in the feed zone, etc., beyond all these perfect remedial strategy is to widen sprue-conduit expansion to restrain high residence time. Therefore, it can be said that sprue-conduit expansion is exponentially dependent on barrel size on the machine.

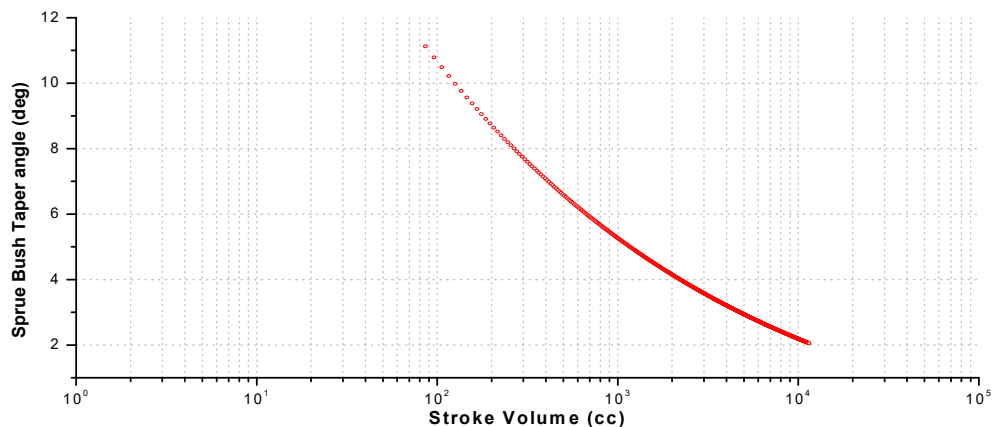


Figure 3.18 Sprue taper expansion about machine's barrel size.

According to Figure 3.18, sprue-conduit expansion dependence on stroke volume is inversely exponential. With this stroke volume above Figure 3.18 curve would compromise moulding AQL as explained before. This is because more injectant should diffuse through a strangulated sprue before solidification. Similarly, below would compromise APL as explained before. This is because injectant relaxedly diffuses through the sprue. So to get the best possible efficiency and performance, it's hereby proposed to have barrel combination or adjust stroke volume along Figure 3.18 curve.

3.2.2.3. *Sprue-conduit Dependence on Component*

Changes in impression features is more frequent on a mould, so knowing their implications is important to prevent them through design of sprue-conduit. On this theme injection grade acrylonitrile butadiene styrene (ABS) is assumed as the representative injectant to explain the dependence sprue taper expansion on part volume and depth. Material data in table 5.1 is assumed to calculate from material term range of Eqn. (3.32) as $Poly = \{159.415, 530.362\} = 344.888$. Similarly, a 650T Sprint series horizontal injection moulding machine from Windsor Machines Ltd., Mumbai is assumed representatively to calculate machine setting term of Eqn. (3.32) to be $M_s = 1.4482 \times 10^{-6}$.

Sensitivity to component volume

Injection moulded automotive parts like side trims, front bumpers or fenders expect to have the highest impact strength. That depends on peak pressure to injection mould from momentum conservation stance that in-turn is limited by impact yield strength of injectant. For sprue-conduit to configure coefficient of pressure recovery its design should obviously be a function of melt state and viscosity. Its size and shape are prominent configurable factors to respond for a particular injectant and machine (Min, 2003). So manipulating injectant and machine factors have seemingly negligible influence on the resulting part characteristics. Sprue-conduit design depends on impression volume below the parting plane because it should be enough to convect that much volume within the shortest possible interval (Schramm, et al., 2006). Thus to get better quality parts injection energy balance biased sprue-conduit form is indispensable (Barbosa, et al., 2012).

Sprue-conduit size and form effects on melt injection are little known but significant from AQL and APL views (Campo, 2006). Nevertheless, they depend on applied shear force extent and interval. For instance, thin walls or sections witness rapid shear-rates than thicker ones, such gradient filling causes diverseness of functional characteristics in moulded features. So design of conduit must intrinsically manage shear over least moulding cycle, preserve melt state and, rapidly diffuse melt through passage that's much colder than injectant for a particular extent of volume; this is typically wisdom driven.

Thus sprue-conduit has to with a complicating conduit expansion of sprue, whose size is limited severely to ensure AQL and APL. With such complications, it's almost impossible or extremely challenging to mould perplexing part shapes. Specifically, parts with large surface area and thin walls pose diathermic thermal transaction challenge for which sprue-conduit design has to achieve highest shear-rate for diffusing large volume within the shortest interval. Huge impression gap variance poses imperfect moulding risk, despite sprue-conduit being designed for thickest gap (Campo, 2006).

During melt diffusion at a particular shear-rate, necessary sprue-conduit size to get better moulding quality is inversely proportional to gap thickness. So thicker parts and a higher aspect ratio (*flow length / gap height*) impression gaps would need wider conduit expansion with more pressure recovery (Schramm, et al., 2006). While thinner parts, close tolerance level features, high degree of acceptance accuracy, negative features like undercut, recessed flow path, crouching, stream squatting, etc., would need narrow crevice conduit to get shear-rate for perfect contrivance (Barbosa, et al., 2012). This happens because cooling time depends on impression region volume or cubic wall thickness (Bolur, 2000). Restraining sprue-conduit expansion increases shear-rates to rapidly fill the mould impression that however needs higher injection pressure and temperature. Usually rapid melt injection is known to reduce impact sustenance and compromise strengths. Also melt state excitation is prone to resin characteristic degradation by shearing-off the injectants to reduce molecular weight polymer (Campo, 2006).

Part volume significantly influences the overall sprue-conduit design. Suppose if sprue-conduit has a 20° expansion then moulding a 3 litre bucket at 800cc/sec on 650T

Sprint machine, would pass drop test easily, while an 8 litre bucket despite being able to mould won't pass. To emphasise this, part volume is sensitised over expansion angle in Figure 3.19. Here rated injection pressure range $P_{Max} = \{1260, 2230\}$ bar and stroke volume range of $V_{Stroke} = \{3180, 8588\}$ cc for the chosen 650T sprint machine is assumed to be representatively at intermediate nominal value of 1500bar with 50% BSR and 5000cc barrel stroke volume. Besides, a typical 80mm sprue-bush length is assumed to show part volume sensitivity.

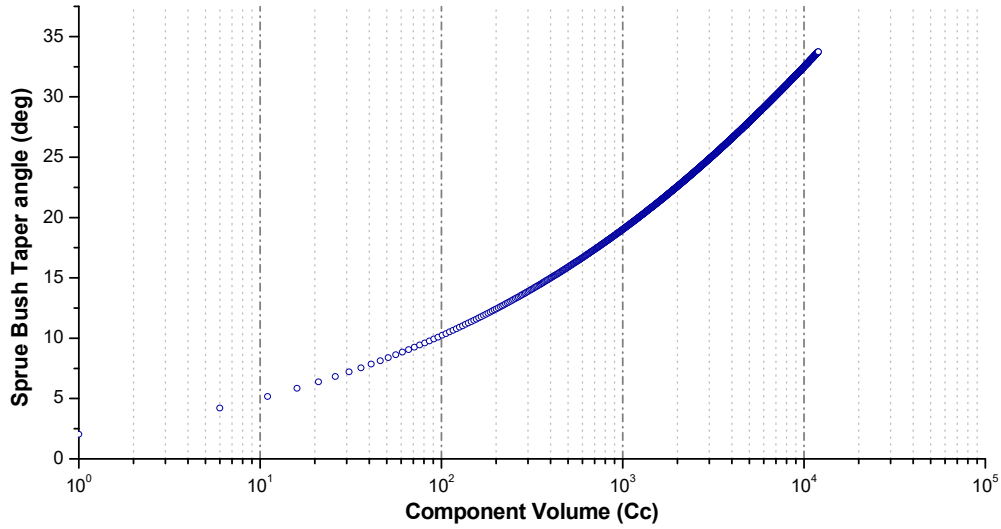


Figure 3.19 Relative sprue taper expansion over part volume.

According to Figure 3.19, sprue-conduit expansion has exponential dependence on overall impression size. Thus sprue expansion and component volume combination are suggested as Figure 3.19 curves to get the best possible AQL and APL.

Sensitivity to component depth

Ideally to achieve best performance sprue-bush has to be designed across 3 to 10 capillary ratio range (Pye, 1992). That's as explained in the beginning (*under shank design section (ii)*) depends on the impression gap or part depth below the parting plane and available nozzle size in the machine. So sprue-bush length range depends on for part depth as below,

$$3 \leq \frac{L}{\bar{D}} \leq 10, \text{ now substituting } \bar{D} = D_s + L \tan \alpha \text{ we get, } 3 \leq \frac{L}{D_s + L \tan \alpha} \leq 10 \quad (3.34)$$

$$\text{Since } \{L, D_s\} > 0, \text{ by rearranging and reciprocating we get, } \frac{1}{3} \leq \frac{D_s}{L} + \tan \alpha \leq \frac{1}{10} \quad (3.35)$$

$$\text{Resolving for } L \text{ range we get, } \frac{\left(\frac{1}{3} - \tan \alpha\right)}{D_s} \leq \frac{1}{L} \leq \frac{\left(\frac{1}{10} - \tan \alpha\right)}{D_s} \quad (3.36)$$

$$\text{Reciprocating, } \frac{D_s}{\left(\frac{1}{3} - \tan \alpha\right)} \leq L \leq \frac{D_s}{\left(\frac{1}{10} - \tan \alpha\right)} \quad (3.37)$$

Further natural extent of conduit expansion is $\alpha = \{0^\circ, 90^\circ\}$; as well as the sprue length exists as a positive value only. So for mould design perfection, the possible range of sprue length could be calculated as $L = \{0, 100\} D_s$. Injection nozzle-tip orifice typically range up to 6mm so a common nominal size of 2.5mm is reasonable consideration for illustration here.

So sprue length could be perturbed from $L = \{0, 250\}$ mm to show its sensitivity. Similarly, typical 1500cc shot volume is considered to show part depth sensitivity represented by sprue length.

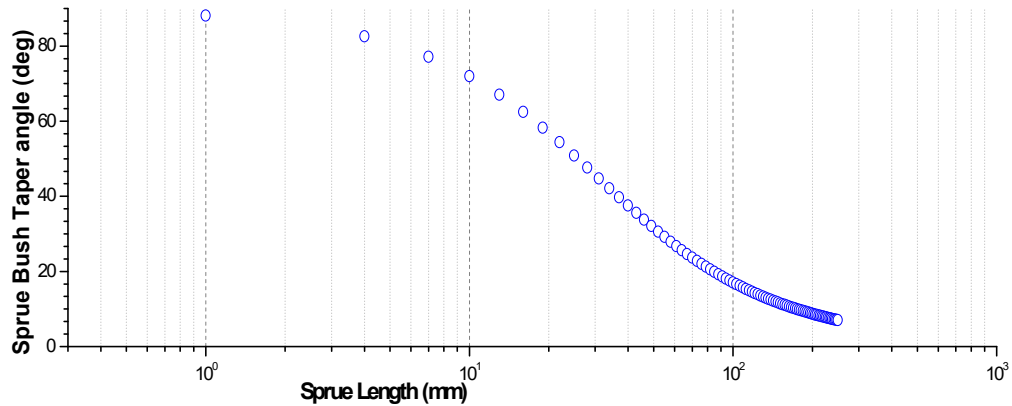


Figure 3.20 Sprue taper expansion about needed sprue length.

Figure 3.20 shows that for getting the best possible objectives, sprue-conduit expansion would have inverse dependence on part design. Also curves in Figure 3.20 clearly distinguishes short and long sprue lengths that need either extreme natural expansion angles, so are fictitious. Although Figure 3.20 plots depict short sprue (1-10mm) with wide expansion as a choice but it's impractical. So 10 to 100mm sprue length is a possible range and, conduit expansion design has almost linear negative dependence on impression depth below parting plane.

3.2.3. Conclusion

Above extensive discussion on sprue-bush design criteria shows perfectness can be approached parametrically in future. Sprue-conduit expansion criteria in Eqn. (3.31) directly recognises dependence on machine, material and moulding as independent factors. It was found that sprue-conduit expansion dependence is of exponential nature for all factors and their interactions. So Eqn. (3.31) can be used to design sprue-bush specifically for a particular injection moulding combination.

- a. Injectant's characteristic viscosity and shear-thinning index factors describe expansion design criteria for all injection mouldable thermoplastic melt in de-facto range. These two factors are given in almost all rheology studies of thermoplastics and enable designing sprue-conduit expansion conveniently for a wide-range of possible applications. Further conduit expansion has direct exponential dependence on apparent viscosity while shear-thinning index has inverse exponential dependence. Off them apparent viscosity has stronger dependence than shear-thinning index so we infer it to be more influential which is also consistent with popular practical belief (Liang, et al., 2001).
- b. Although exponential in nature injection rate is directly proportional, rated injection pressure and barrel size are inversely proportional to conduit expansion. Off them injection rate has more dominance than injection pressure and barrel size.
- c. Independent parametric sensitisation of part features portrays direct exponential dependence of expansion ratio on part volume and inversely exponential dependency on part depth below parting-off plane. Among them, part volume has more influential than part depth below the parting plane.

Besides, it's contend that the a'priori intuit on sprue-bush expansion ratio dependence would also be valuable during mould design as well as maintenance. Nevertheless, perfection is factored intrinsically into sprue-conduit design criteria to give the best possible AQL and APL benefits. This compliments many other gainable benefits through stretched competence; synchronise affective and cognitive in-situates like injection fill time, injection ramping speed for packing, controlling temperatures, compatibility, etc.,

3.3. EXPERIMENTAL STUDIES

This supplementary study intends to the examine the discrete sensitivity of sprue-bush conduit expansion. Specifically, it seeks to know the extent, expansion depends

on independent factors at expected AQL and APL placebos. Primarily to corroborate physical evidence and affirm the virtues of arguments proposed. This is so because injection capacity, injectant and impression as independent factors have to configure dependent expansion for an expected AQL and APL. Similarly, the likely implications of sprue conduit design aberrations could also be explained through disposing phenomena from erstwhile philosophy. Thus tying together, a set of isolated facts as an a’p priori sense and extend the diverse discourse as respective design criteria.

3.3.1. Methods

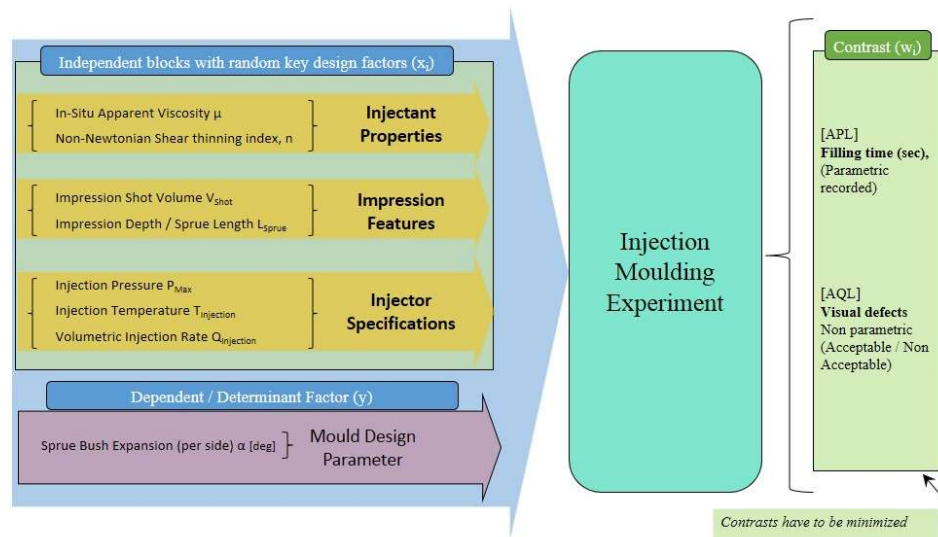


Figure 3.21: Experimental scheme

Full-scale experiments were conducted in a production machine that involved designing and developing a custom mould; selecting thermoplastics strategically and; configuring operating range. As machine control systems are mostly adapted for continuous production through a fixed set-up and run type; a sophisticated PLC controller served to run each treatment despite being fast. The PLC system could hold the parameters of injection moulding cycle-to-cycle within appendix-2 limits, while every in-situ level of experimentation strategy could be exclusively sensitized. Based on DoE approach, a reasonable structure of experimentation was designed meticulously as shown in Figure 3.21. Here AQL and APL are the two contrasts, smaller-the-better is the preferred quantitative contrast for AQL and no-defects is the preferred qualitative contrast for APL. To prevent systematic error randomisation is pursued and to reduce any likely bias removal of biasing sources is perceived retrospectively.

- Each factor (f_i) is examined for at least three equal levels as shown in Figure 3.22 to sufficiently compare the differences between them and recognise the main effect (*dependence*) of (α). So with just single degree of freedom, the “*sum of squares*” of factor-wise treatment stratifies authentic inferences. Such a segregation ensures clarity and gives more detailed insight into the nature of dependence at all levels.
- Sprue expansion (α) is deliberately varied at five levels to collectively characterise all other factors (f_i) and increase the scope of getting data on the exclusive influence of each factor. Suppose if unknown interactive influence existed then factorial design would surely avoid misleading conclusions. On the contrary even if interactive influence wasn't there, then factorial design would still yield better assessment of their influence.
- Also with more scope the inductive value of information extends individual factor influence to examine their combinatorial influence.

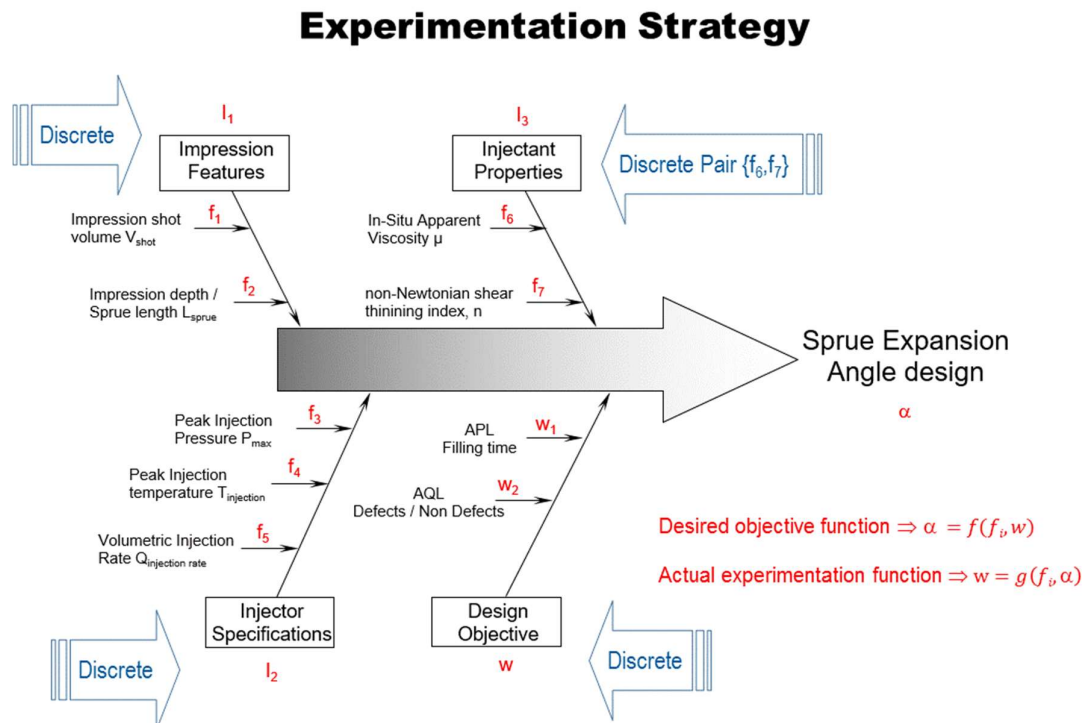


Figure 3.22: Statistical modelling of sprue expansion angle design.

General Stochastic model

Objective function or deterministic criterion for injection mould sprue bush design would be in the form of,

$$\alpha = f(f_{ij}) \text{ as } w \rightarrow \text{minimum} \quad (3.38)$$

The statistical effects model would then be,

$$\alpha = \prod_{i=1}^a F_i \cdot \prod_{j=1}^b F_j \cdot \prod_{i=1}^a F_i \left(\prod_{j=1}^b \varepsilon_{ij} \right); \text{ as } w \rightarrow \text{minimum} \quad (3.39)$$

Here,

$i = 1, 2, 3, 4, 5, 6$ and 7 is number of potential design factors

$j = 1, 2$ and 3 is number of blocks

$k = 1, 2, 3, 4$ and 5 is number of levels in each factor

$r = 1, 2, \dots, 30$ is number of replication shots per setting

$F_i = i^{\text{th}}$ inter-design factor influence (*interaction effect*)

$I_j = j^{\text{th}}$ inter-block factor (*interaction effect*)

$\varepsilon_{ij} = \text{random error} \sim \text{Normal}(0, \sigma^2)$

As blocks are independent and randomly chosen only intra-block F_i can exist and cross-examining across blocks F_i would be witless, so

$$\alpha = \prod_{j=1}^b I_j \left(\prod_{i=1}^a f(f_{ij}) \cdot F_{ij} \cdot \varepsilon_{ij} \right); \text{ as } w \rightarrow \text{minimum} \quad (3.40)$$

Taking logarithm function on both sides gives appropriate sprue bush expansion angle (α),

$$\alpha^* = \prod_{j=1}^b I_j^* + \left\{ \prod_{i=1}^a \left(f^*(f_{ij}) + F_{ij}^* + \varepsilon_{ij}^* \right) \right\}; \text{ as } w \rightarrow \text{minimum} \quad (3.41)$$

Afore injection moulding stochastic model is believed to describe adequately the underlying dependency of sprue bush expansion angle. Hence we assume it to be a design factor depending on the function of governing performance (fill time) and quality (defects). Therefore, all parameters are examined with experimental accord involving design of an expansion angle related to a particular combination of injectant, injector and impression. Fill time and quality of each experiment was recorded. As inter-block variation affects sprue expansion angle performance, different block combinations form experiments to be performed.

Factorial Design: Restraints

- a) Full factorial design seeks examining all possible combinations of the factor levels simultaneously, however the geometrical sprout in no. of experiments calls for a large experimentation effort which is impractical and expensive.

- b) Complete randomization of all factors would be strenuous, uneconomical and infeasible because it involves often changing barrel / injector pressure, temperature, injection rate as well as reconfiguring the mould besides for reloading different injectants barrel has to be purged afresh. So to avoid experimentation diversity and have homogeneity, factors are isolated by suitably blocking as Impression (I_1), Injector (I_2) and Injectant (I_3), only these blocks are chosen randomly. Perhaps such restraint may introduce “restraint error” like residual error. Nevertheless, the comparisons would be more sensible because each block naturally stratifies into distinct combinations of experiments.
- c) Main randomization control is associated with Impression (I_1), Injectant (I_3) and sprue bush expansion (α); so changing injectant, while reconfiguring mould would be reasonable. Thus, by designing the set of experiments with random mould configuration; say $\{I_1, \alpha\}$ combination and switching injectant across (I_3) factor levels; but with the same sprue or impression mould configuration (*i.e.*, either α or I_1) or rather varying both simultaneously. Hence for each mould configuration and injectant combination the entire set of experiments could be repeated, while the randomisation control associated to the pair $\{I_1, \alpha\}$ alternates as a blocked term. Thus to appreciate “**Proximity**” properly each set of proximal experiments were conducted as a block, while proximal blocks were chosen randomly.

Table 3.2: Treatment Scheme

Factors	Levels							
	1	2	3	4	5	6	7	8
Injectant	PS	POM	PP					
Sprue expansion (<i>degree</i>)	0.964	1.98	2.93	3.94	4.78			
Injection Temperature (<i>°C</i>)	205	215	225	240	255	265		
Injection Pressure (<i>MPa</i>)	1.00	3.00	4.00	5.00	6.00	6.50	7.00	7.50
Injection Speed (<i>cm/sec</i>)	0.19	0.185	0.278	0.371	0.46	0.56	0.65	0.74

According injection-moulding experiments were conducted with five different taper expanding in sprue bushes as shown in Figure 3.27, three different materials and different pressure and temperature settings for each material as tabulated in Table 3.2. However, in-situ conditions predictably vary so (a) early mouldings were discarded till operations are stable, (b) specimens were collected only after process conditions

stabilised (c) for establishment of statistical validity, reliability, replicability and consistency thirty representative shots per treatment combination were taken as shown in Figure 3.23. The general procedure followed to test injection mould sprue design is given in Table 3.3. Between each material change the hopper and barrel were cleaned by purging thoroughly.

Table 3.3: Treatment Matrix

Treatment	Injectant	Sprue expansion (degree)	Injection Temperature (°C)	Injection Pressure (MPa)	Injection Speed (cm/sec)
T1	Poly-Styrene	0.964	225	7.50	0.742
T2	Poly-Styrene	0.964	225	7.50	0.650
T3	Poly-Styrene	1.98	240	6.00	0.557
T4	Poly-Styrene	2.93	255	6.50	0.557
T5	Poly-Styrene	3.94	240	6.50	0.742
T6	Poly-Styrene	4.78	225	6.00	0.650
T7	Poly-Oxy-Methylene	0.964	225	7.00	0.557
T8	Poly-Oxy-Methylene	0.964	215	7.00	0.186
T9	Poly-Oxy-Methylene	1.98	205	5.00	0.371
T10	Poly-Oxy-Methylene	2.93	215	3.00	0.371
T11	Poly-Oxy-Methylene	3.94	205	3.00	0.186
T12	Poly-Oxy-Methylene	4.78	225	5.00	0.371
T13	Poly-Propylene	0.964	240	3.00	0.464
T14	Poly-Propylene	0.964	215	3.00	0.650
T15	Poly-Propylene	1.98	265	1.00	0.278
T16	Poly-Propylene	2.93	215	4.00	0.278
T17	Poly-Propylene	3.94	265	4.00	0.464
T18	Poly-Propylene	4.78	240	1.00	0.650



Figure 3.23: Representative photo of T11 treatment.

3.3.2. Equipment

Test Specimen

The characteristic shape of test specimen is simple injection moulded flat rectangular plaque in correspondence to ISO 10724-2 / ISO 294-3 it's type D specimen measuring 124 mm x 68 mm with a thickness of 3mm as shown in appendix 3. Test specimen is designed scouting for following impression features,

1. Mould impression size is designed to offer reasonable volume for moulding on a regular production machine, also adequately thicker for easy ejection and enough moulding interval would be available to evince the implications thoroughly on mould design.
2. The impression region is designed simple deliberately so mould constructing complication would be less and economical.
3. To avoid cores the impression doesn't have holes, recess or undercuts.
4. Test specimen is designed flat with enough limits, so impression cooling / solidification is almost equal from either sides of the mould halves.
5. Test specimen is design with uniform wall thickness to forego shrinkage, warpage, loss of dimensional accuracy and stability issues post moulding.
6. Test specimen is designed by avoiding cross section transitions, notches / stress rising corners to have less stress residues and be inherently strong.

Material

Although there are many commercial thermoplastics as competing alternatives offering a wide range of inherent benefits as well as some limits, each thermoplastic features an exclusive viscosity and shear thinning index combination. So for benchmarking design sensitivity of injectant behaviour in its mould, prospective thermoplastics were generalised across apparent viscosity versus shear thinning index in Figure 3.24. POM, PP and PS combination has almost equal dispersion interval on Figure 3.24, so they were selected to be best representative thermoplastics.

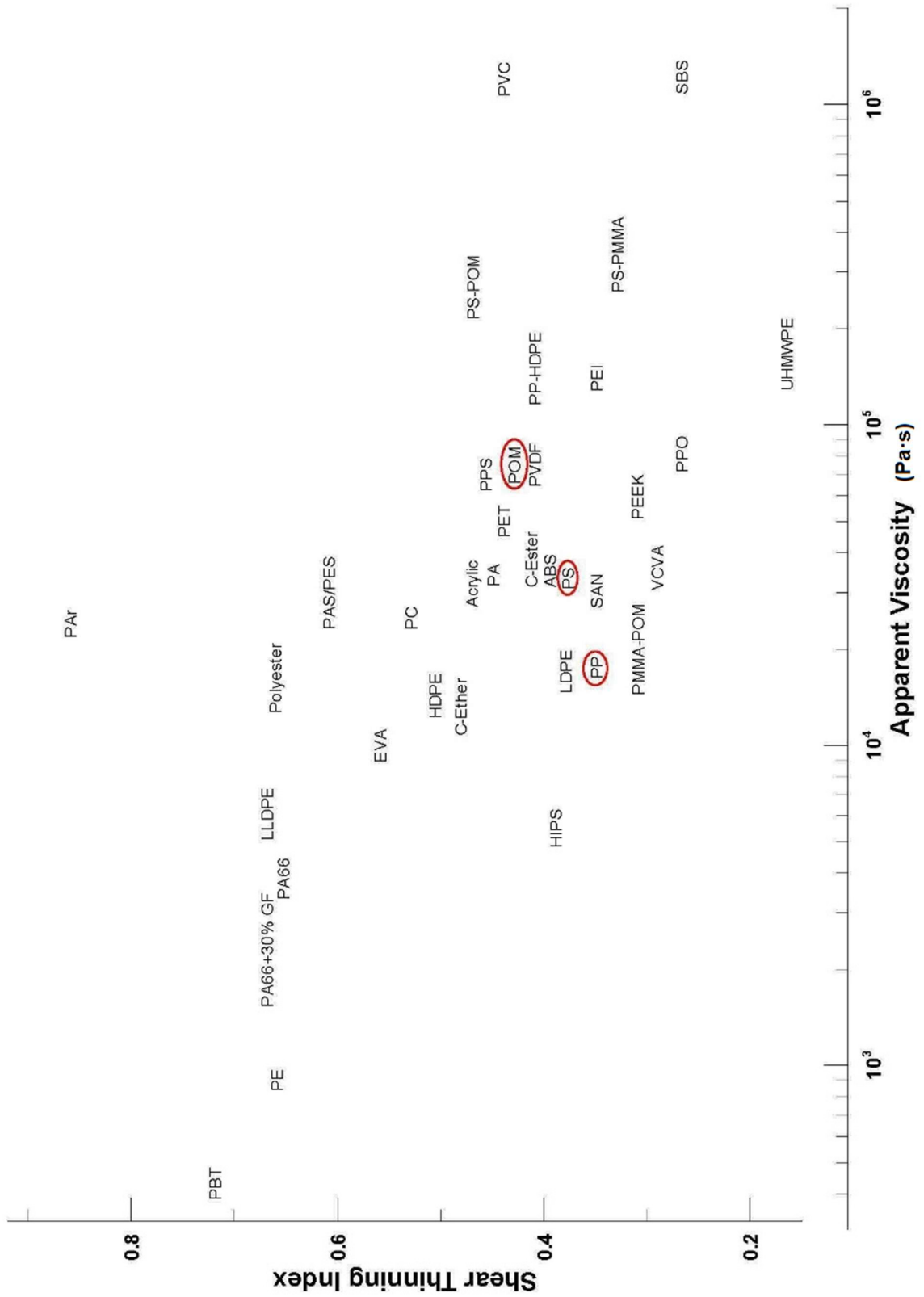


Figure 3.24: Strategy of thermoplastics chosen for testing: PP, PS and POM.

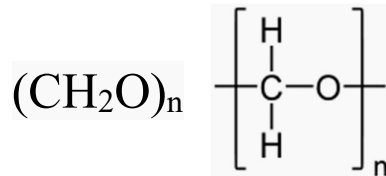
Table 3.4: Characteristic properties of Injectants.

Thermoplastic	Apparent Viscosity* (Pa-sec)	Shear Thinning Index*	Injection Temperature (°C)	
			Min	Max
Poly-Oxy-Methylene (POM)	87500	0.420	165	220
Poly-Propylene (PP)	33200	0.368	190	250
Poly-Styrene (PS)	17500	0.340	180	260

* @ injection temperature and pressure

Poly-Oxy-Methylene (POM)

Poly-Oxy-Methylene (POM) also known as Poly-Acetal (*simply acetal*) or Poly-Formaldehyde is an injection-mouldable high performance engineering thermoplastic, but more popular as glycol. It's usually polymerised by chain reaction or rarely by ring-opening polymerisation.



POM comes in a granulated form and can be contrived into the needed shapes by injection moulding (KOCETAL K700, 2014) using Table 3.5 data.

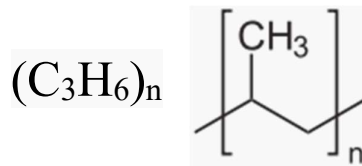
Table 3.5: Characteristic property data of KOCTEL K700

Density	(1.41 to 1.42) x 10 ⁻³ gram / mm ³	
Water absorption (23 °C, water 24 hr.)	0.22%	
Mould shrinkage	2.0 mm/mm	
Melt index (190 °C, 2160 gram)	27 gram / 10 min	
Melting point	166°C	
Heat distortion temperature	0.45 MPa	158°C
	1.80 MPa	110°C
Linear thermal expansion	13 × 10 ⁻⁵ / °C	
Rear barrel temperature	160°C - 180°C	
Middle barrel temperature	182°C - 200°C	
Front barrel temperature	190°C - 210°C	

Nozzle temperature	190 °C - 210°C
Melt temperature	166°C
Mould temperature	60°C - 100°C
Drying temperature	80°C
Dry time	3 hr
Injection pressure	68.6 – 108 MPa
Screw speed	50 – 100 rpm

Poly-Propylene (PP)

Poly-Propylene is also known as Poly-Propene, an addition thermoplastic synthesised from propylene monomer. Its properties are dependent on molecular weight, molecular weight distribution, crystallinity, type, fraction of co-monomer (*if used*) and isotacticity. PP is normally tough, flexible and has good resistance to fatigue, especially when copolymerized with ethylene. However, excess methyl group (CH₃) presence improves mechanical properties and thermal resistance, but decreases chemical resistance.



Orientation of every methyl group about alike neighbouring methyl groups in the monomer units has notable effect on their ability to form crystals. This allows PP to substitute as an alternate engineering plastic against thermoplastics like acrylonitrile-butadiene-styrene (ABS). However, it has superior specific strength, heat resistance, good surface finish and gloss on mouldings. It's rugged and remarkably endure exposure to many chemical solvents, bases and acids. At room temperature, PP is resistant to fats and almost all organic solvents, apart from strong oxidants. PP is supplied in a granulated form and can be contrived into the needed shape by injection moulding (REPOL H110MA, 2014) using Table 3.6 data.

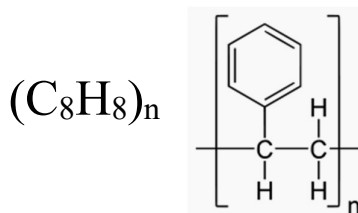
Table 3.6: Characteristic property data of REPOL H110MA.

Density	$(0.895 - 0.92) \times 10^{-3} \text{ gram / mm}^3$
Melt flow index @ 230°C / 2.16 kg	11 gram / 10 min
Spiral flow	37 cm

Xylene Soluble	4%
Young's modulus	1300 and 1800 N/mm ²
Tensile Strength at Yield @ 50mm/min	36 MPa
Elongation at Yield @ 50mm/min	10%
Flexural Modulus @ 1% secant	1.65 GPa
Notched Izod Impact Strength @ 23°C	27 J/m
Heat deflection temperature @ 455 kPa	104°C
Thermal Expansion	PP's is large but less than PE

Poly-Styrene (PS)

Poly-Styrene (PS) is a synthetic aromatic polymer synthesised from styrene monomer. They are polymerised by breaking the carbon-carbon pi bond (*in the vinyl group*) and forming a new carbon-carbon single (*sigma*) bond to interconnect as a chain. The newly formed sigma bond being much stronger than the pi bond is difficult to depolymerize. Typically, a Poly-Styrene chain consists of few thousand monomers that accrue molecular weight from 100,000 to 400,000. The long hydrocarbon chain has alternating carbon centres attaching phenyl groups (*the name given to the aromatic ring benzene*), where every chiral backbone carbon lies at the crux of a tetrahedron and has 4 bonds with its vertices. Short-range van der waals attraction between polymers chains characterises its physical properties. As the molecules are long hydrocarbon chains consisting several thousands of atoms, their total intra-molecular attractive force is large. When heated or deformed at a rapid rate, these chains slide past each other with higher degree of conformation owing a combination of viscoelastic and thermal insulation properties. This *intermolecular* weakness versus the high *intra-molecular* strength of the hydrocarbon backbone confers flexibility and elasticity. Poly-Styrene's chemical formula is $(C_8H_8)_n$ with carbon and hydrogen as main chemical elements.



Being a thermoplastic, at room temperature Poly-Styrene is in solid (*glassy*) state, easily flows above its glass transition temperature of about 100°C and hysterically regains rigidity on cooling below its glass transition temperature. This thermo-

mechanical hysteria allows Poly-Styrene to be liberally injection moulded. Although resistant to acids and bases Poly-Styrene easily dissolves in many chlorinated solvents, organic solvents and aromatic hydrocarbon solvents. Alike organic compounds, burning Poly-Styrene emits carbon dioxide and water vapour. Poly-Styrene, being an aromatic hydrocarbon, typically combusts incompletely as seen by the sooty flame.

General-purpose Poly-Styrene is clear, hard, and rather brittle. It's an inexpensive resin per unit weight. It's a poor barrier to oxygen and water vapour and has rather low melting point. PS is supplied in a granulated form and can be contrived into the needed shape by injection moulding (SC 203EL, 2014) using Table 3.7 data.

Table 3.7: Characteristic property data of SC 203EL.

Melt Flow Index @ 200°C / 5kg	8 gram / 10 min
Vicat Softening Point @ 120°C / hr., 1kg	98°C
Heat Deflection Temperature (<i>Unannealed</i>) @ 1.86 MPa	80°C
Tensile Strength @ 50 mm/mm	49 MPa
Elongation @ 50 mm/mm	2%
Flexural Strength @ 3.2mm thickness	82 MPa
Flexural Modulus @ 3.2mm thickness	2900 MPa
Izod Impact (<i>Notched</i>) @ 3.2mm thickness	20 J/m
Specific Gravity	1.04 x 10 ⁻³ gram / mm ³
Extruded Poly-Styrene is about as strong as an unalloyed aluminium, but much more flexible and much lighter (<i>1.04 g/cc vs. 2.70 g/cc for aluminium</i>).	
Melt Temperature	180°C - 260°C
Mould Temperature	40°C - 60°C

Machine

A new horizontal injection-moulding machine with reciprocating screw (*specifications are in appendix-1*) with latest version of PLC control that was just installed and tested was hired for conducting afore experimentation.



Figure 3.25: Photograph of machine used for contriving specimens.

Mould

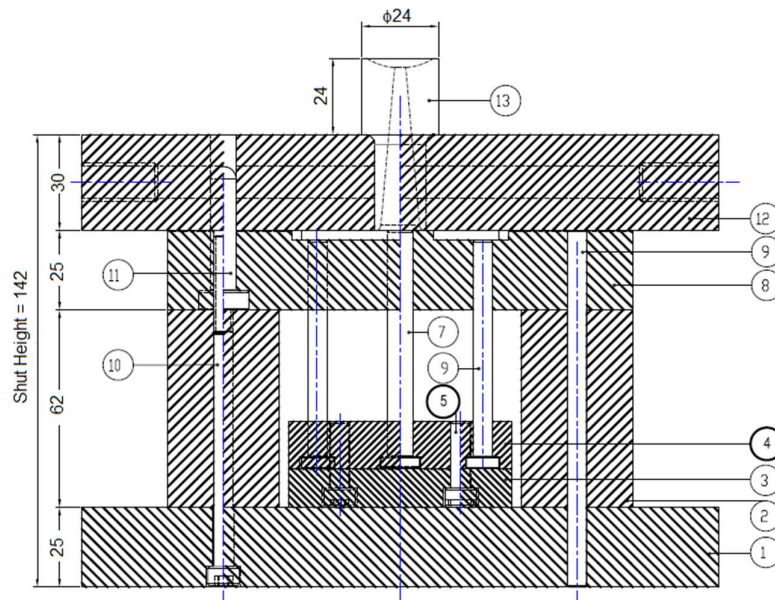


Figure 3.26: Elevation of mould closed assembly.

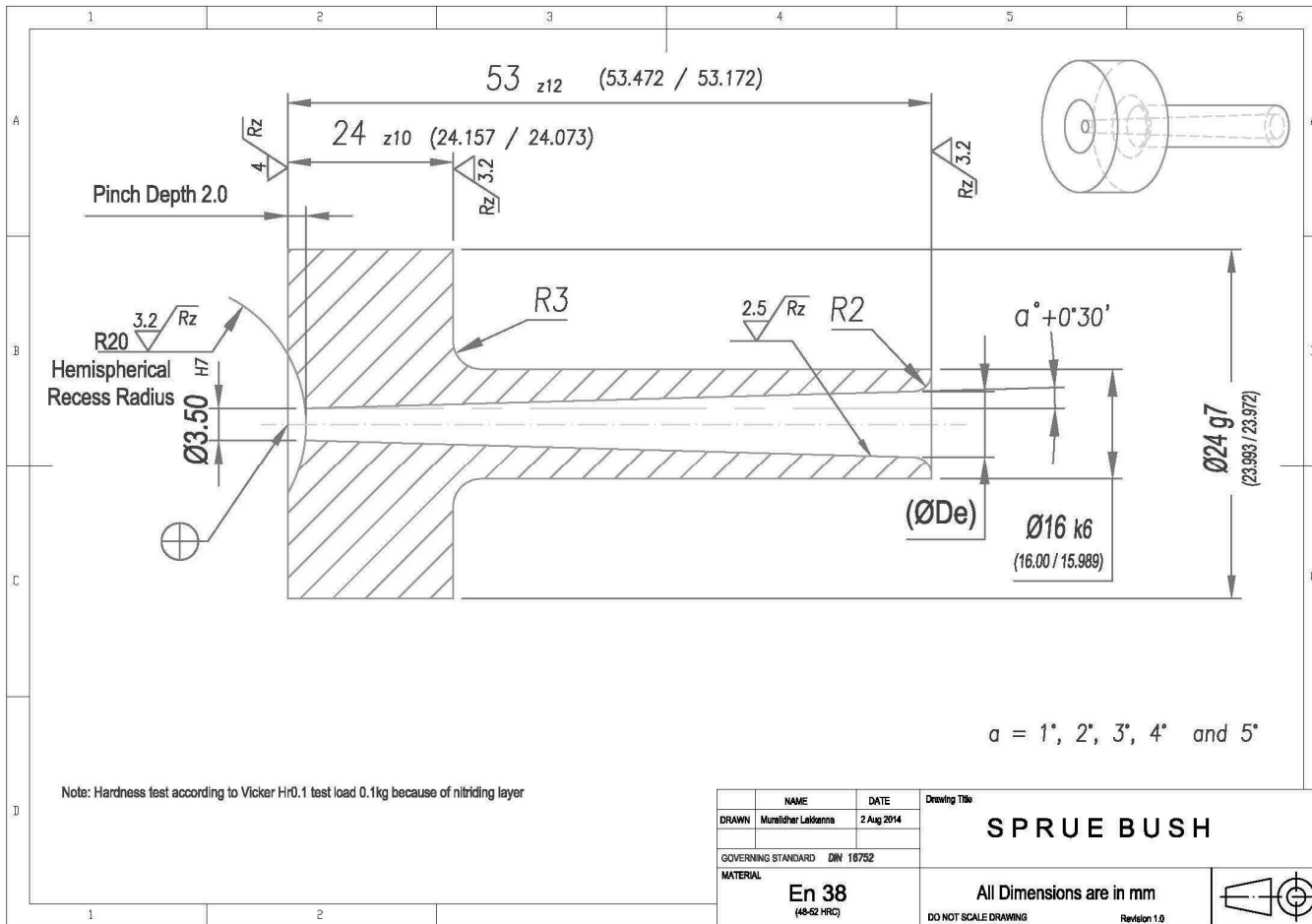


Figure 3.27: Drawing of sprue bushes with varying expansions.

A customised mould suitable for Figure 3.25 machine was manufactured with a choice to reconfigure sprue bush rapidly. Interchangeable sprue bush design specified in appendix-4 provided more flexibility and rapid transitions over the experiment combinations. Five sprue bushes were machined and their actual measurements were as in appendix-5 to 9. A single impression mould with uniform and symmetrical overall parting surface was adopted. A set of plates, pins, bushings, pillars, ejector systems and other usable elements formed the mould assembly as shown in Figure 3.28 and Figure 3.26. To ensure best reproducibility same mould was used for all experiments having same core and cavity machining tolerances for all experiments, while compensation on impression dimensions for expected shrinkage being an intrinsic character of concerned thermoplastic was ignored. A maximum draft angle of $\frac{1}{2}^\circ$ was provided along the fringes of impression. All impression surfaces and ejector pins ends were finished to $R_a = 175$ to $250 \mu\text{m}$ and surface roughness $R_z = \sim 0.12 \mu\text{m}$ for removing scars from machining to get a good light reflecting surface (SPI-SPE, B3). The experiments involve interchanging sprue bushes with varying expansions, assembled into a full-scale mould in an exact injection moulding arrangement.

Mould Cooling

Though coolant channels were designed to control point-to-point impression surface temperature differences within $\leq 5\%$. Self-sealing quick disconnect type fittings were used to connect the coolant duct to recirculating system and for maximum efficiency flow of coolant through the duct was turbulent.

3.3.3. Summary

- a. By applying principles and techniques of statistics experimental studies got through with careful planning, designing and detailed specimen preparation.
- b. Presently these specimens are under characterisation to examine variations. The observed variations would then be segregated by factors based on afore treatment matrix and random fluctuation would be eliminated.
- c. Once variations-to-factors are accounted, the dependence of sprue-conduit expansion would be physically interpreted formally.

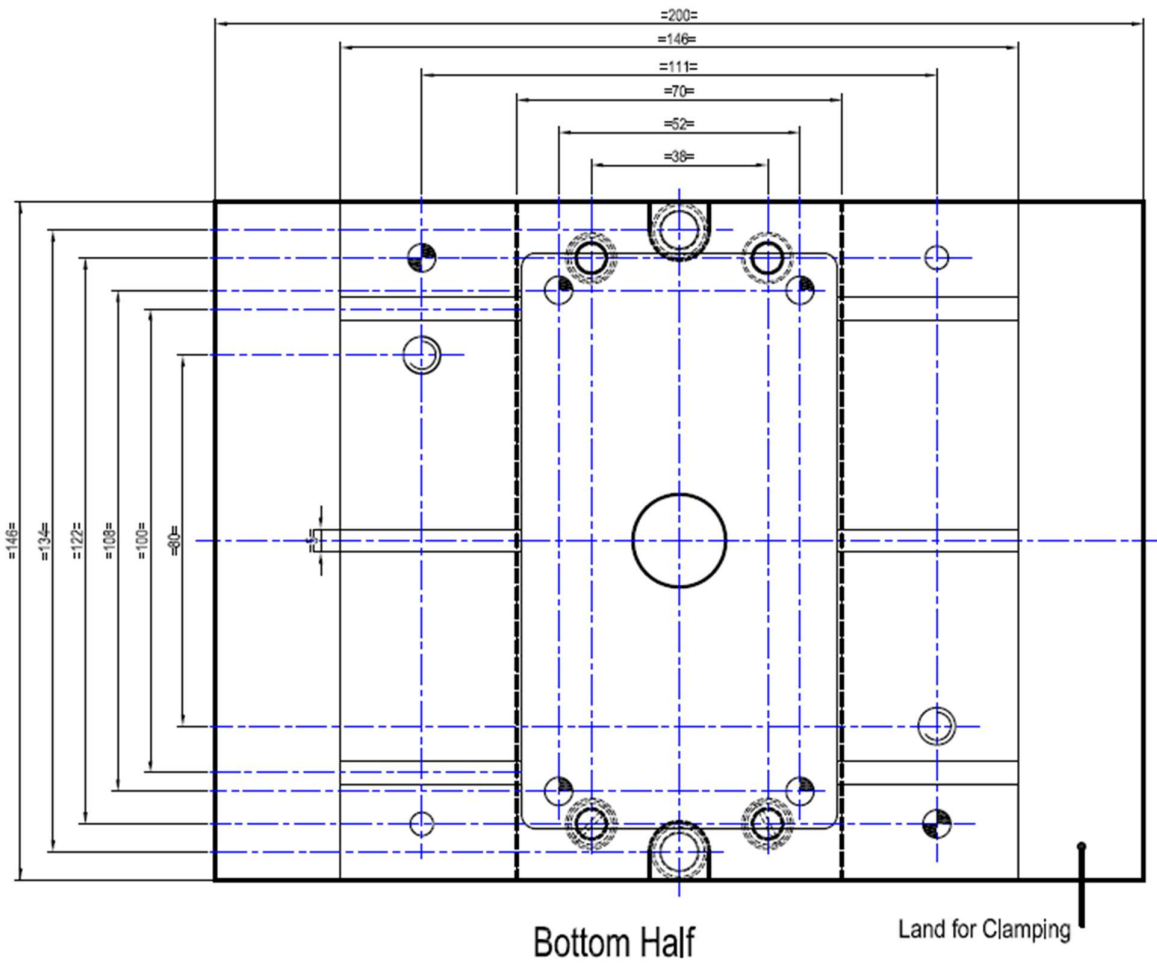
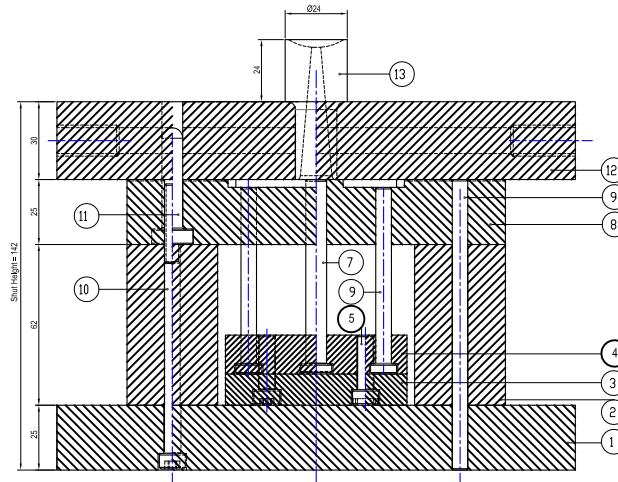
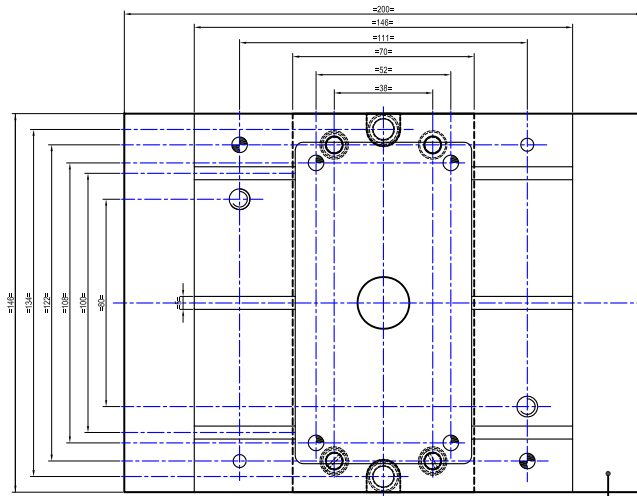


Figure 3.28: Bottom Half Plan View of mould halves assembly.

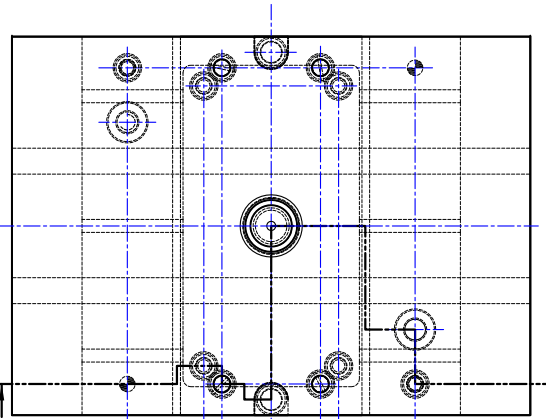


Section BB Front View

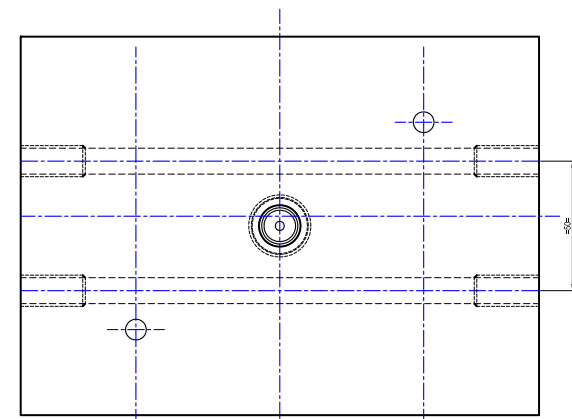


Bottom Half

Land for Clamping



Top View



Top Half

Debur and break all sharp edges
Unless otherwise specified, all dimensions are in millimeters only

Item No.	Part Description	Qty.	Material	Hardness
1	Bottom Plate	1	SAE 1030	
2	Spacer Block	2	S#42	
3	Ejector Back Plate	1	S#42	
4	Ejector Plate	1	S#42	
5	Ejector Plate Bolt: M6x27, IS2289	4	Steel 12.9	Black oxidized
6	Ejector Pin	4	CHNS	S2-S4 Hrc
7	Ejector Push Back Pin	2	S#42	
8	Cavity Plate	1	T35C-5A0/1	S#40 Hrc
9	Spacer Block Pin: DIN 16761-B	2	S#42	
10	M8x110 Bolt (Bottom Assembly)	2	Steel 12.9	Black oxidized
11	Guide Pin: DIN 16761-E	2	S#42	
12	Top Plate	1	AEI-4130	
13	Sprue Bush 5", ISD 10072	1	T110E2C1	S#40 Hrc

Drawn	Name	Date
Checked	Mohan Kumar G C	15-Nov-2014
Appr		
QA		
Released		

**Two Plate Mould
for Specimen (Plate)**

Final Assembly of Experimental Mould

SCALE: 1:1 REVISION: 0 SHEET 1 OF 1 SHEET SIZE: A1

Chapter Four

Runner Design

Typical functions and concurrent purposes of a runner system is given in Table 4.1. The ratio of total feed system volume (*including runner system*) to overall shot volume of mould should be small preferably; therefore, total runner volume has to be a small fraction of overall shot volume in general (Shoemaker, 2006). Conventionally average runner diameter should be atleast 150% of nominal impression gap height to pack adequately despite delirious phase transformation (Knepper, 2004). While its final size beside gate should be atleast 120% of biggest impression gap height, so on ejection it distorts as all other moulding features would have solidified below injectant’s glass transition temperature (Whelan, 1982). Essentially runner diameter should never exceed sprue bush exit orifice size (Rosato, et al., 2000).

Table 4.1 - Apparent design purpose to proviso mapping of runner.

<i>Design Priority</i>	More	Less
<i>Design Purpose</i>	Its purpose is to deliver molten plastic from sprue well to each gate over the parting surface for injection with minimum mechanical and thermal energy outlay	Its purpose to mechanically supporting in-processing and post-processing loads.
<i>Design Proviso</i>	Principles of melt kinematics, transition thermodynamics and injectant mobility characteristics	Principles of structural kinetics and functional dynamics

Even though individual runner stream size depends on injection effort, required shot volume and gap height of impression; its design is still ambiguous. Mainly because runner inserts despite being stationary and rigid should preserve almost homogeneous transit state to do above functions. Thus spatial heat transfers from a higher temperature injectant to a lower temperature mould, temporal momentum from high pressure influx to low pressure efflux and, the vicissitude of transit state repressing diffusion together depend on the gradients of pressure and temperature across the conduit region of runner. Thus, cross-section design depends on concurrent heat and mass transfer pattern in runner-conduit, injectant’s transit state homogeneousness trait, several a’posteriori defects on mouldings and processing hitches (Wang, 2012). Therefore, to expect utmost productivity with flawless quality; an ideal runner design should inject melt by diligently preserving pressure gradient (Bociaga, et al., 2007) and

at its best gradual chilling (Gan, et al., 2010). Meticulously designed and intrinsically governing cold runner injection moulds are worth more than expensive hot runner manifold systems (Finnie, 2011) (Zhai, et al., 2009).

4.1. RUNNER CROSS-SECTION GEOMETRY DESIGN

Shape, length, cross-section size and deliberate interactions of a runner-conduit confine injectant peregrination through it. So its design perfectness is decisive to inject, distribute melt, and then eject moulding. Typically, after defining the best promising geometric stance of each runner-conduit specifying its cross-section finalises designing as in Figure 4.1. Its cross-section area should suffice rapid diffusion with more influx and efflux; while its form perimeter ought to be less for preserving an even melt state, *i.e. relegate fringe heat transfer* (Wang, 2012). Reasoning the context is akin to a seesaw with a runner-conduit size large for APL (Haley, 2009) and small for AQL (Kumar, et al., 2002) on either side over a design fulcrum. Thus, the scalar characteristic function of area and perimeter emerges as suitable common metric for recognising injection mechanics and thermodynamics to mediate persistently between AQL and APL.

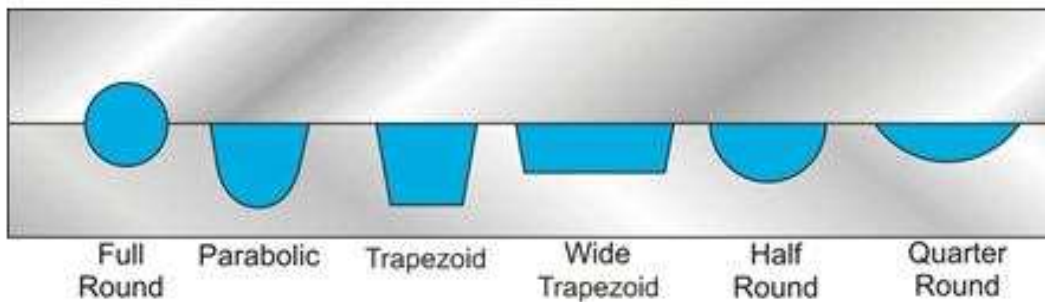


Figure 4.1 Credible runner cross-sections adopted in practise (Beaumont, 2007).

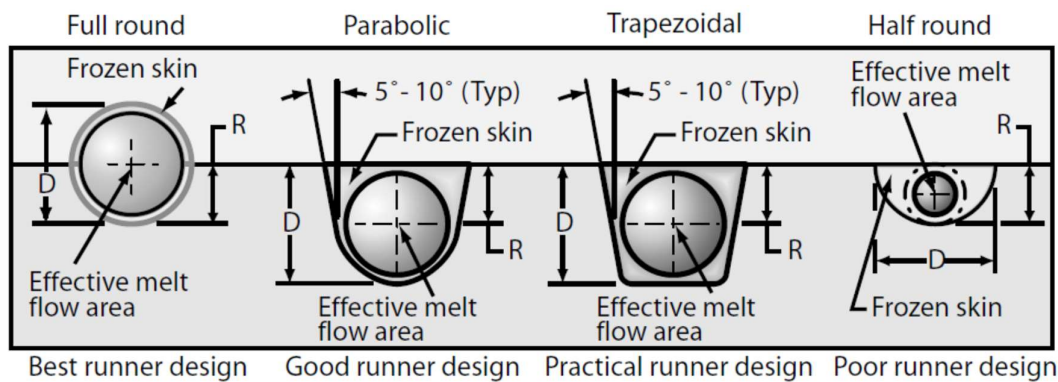


Figure 4.2 Preferential order of runner cross-section selection (Campo, 2006).

Designing runner cross section begins with deciding conduit profile among credible cross-sections satisfying the constraints of impression layout, parting surface position, location of other moulding features and criticality of runner insert(s) in mould configuration (Chen, et al., 1993) as prioritised in Figure 4.2. Typically, left-hand side profiles are preferable over right-hand side profiles in Figure 4.1, where round, parabolic and trapezoid shapes are favoured owing to their relative volume-to-surface area ratio superiority (Neely, et al., 2003). The priority elixir in runner profile decision is radial invariability along the perimeter of cross-section and adjudication of injection volume rate to transversal subsistence from shear stress ratio (Kazmer, 2007).

$$\frac{\partial}{\partial r} \left(\frac{Q[t]}{\tau} \right) \approx \text{constant} \quad \text{or} \quad \int_0^{2\pi} \left(\frac{Q[t]}{\tau} \right) dr \rightarrow \text{linear function of } r \quad (4.1)$$

The ratio of cross-section perimeter to area of a profile is its shape factor (Neely, et al., 2003); about shape factor superiority, circular (*full-round*) profile is the most efficient (Muzychka, et al., 2008) giving competing value. Its (a) small surface drag preserves pressure gradient; (b) deterrence to dissipate heat holds transverse injectant state uniformity; and (c) smooth corner-less form suppresses volumetric friction easing ejection (Neely, et al., 2003). Thus, tranquillises the distortion of transit injectant state because it exerts even pressure and balances heat dissipation in all directions as shown in Figure 4.3.

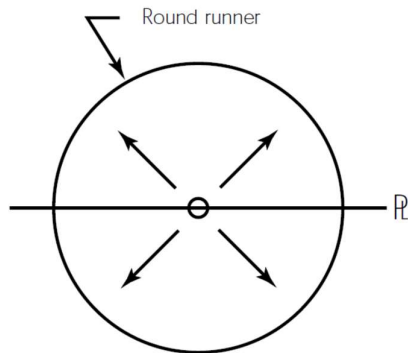


Figure 4.3 Round cross-section exerts pressure and confines uniform heat dissipation all around.

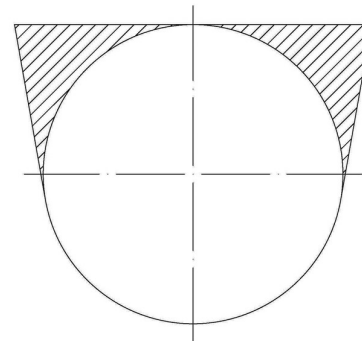


Figure 4.4 Parabolic runner cross-section commonly adopted in practise.

Although round runner is a best choice, designers usually choose either a parabolic or trapezoid as competing substitutes (Ziobro, 2013) to avoid the inconvenience of machining (Chiang, et al., 2006) and nuisance of accurately aligning it on both halves of the parting surface (Neely, et al., 2003). That's because they combine afore convenience of machining only on mould's ejector half and having a cross-section area of almost equal to or else envisaged circular profile. Despite ceding from a full round to a parabolic or trapezoid profile, as relative

index designers correlate their depth to width average at par with full round diameter. As 10° draft inclusion on each side exceeds the overall runner cross-section area of about 20% shown as shaded area in Figure 4.4 but mostly it's ignored in practice. Suppose if injection was through any other afore or regular polygonal or irregular profiles then their sharp corners physically divide injection streams (McKee, et al., 2006) that either induce vortices or delaminate. Thus the extent of residual stress embedded into finished moulding clearly depends on runner cross-sectional profile deterrence from roundness.

Since contrived parts should have less stress residue, non-circular runner profiles are viable choices; only if moulding product design can tolerate surfeiting stress residue. Even though moulded-in residual stress eventually relaxes overtime (Bryce, 1998). However, variation of transverse stress action along the periphery both squeezes cruising polymer molecules in some regions and relaxes at other locations. Thus they deform divergently and fill the impression with radially gradient properties of moulding (Bryce, 1998). This phenomenally complicates injection physics beyond relative shape conciliation (Syrjala, 2002). In contrast, the circular profile realms only boundary layer injection stream fractioning across upper and lower streams (Vaz Jr, et al., 2003). Therefore, by *assumption (d)* an axis-symmetric tube is presumed to represent individual runner domain for mass conveyance, transform momentum and dissipate energy through it.

4.2. RUNNER CROSS-SECTION MECHANICS DESIGN

Beyond continuity, runner cross-section geometry is also responsible for bulk transfer and impression contrivance (Trifonov, et al., 2008). Its characteristic size determination inextricably depends on the gradients across influx and efflux pressures; core of transit injectant stream and runner insert boundary temperature; morphology of injectant's structure and intrinsic behavioural characteristics; and impression features mandating mould configuration. Similarly, its inner surface reduces the tribological deterrence of pressure and temperature gradients; and the adhesion of transforming phase. Usually it's either polished to smoothness (Ra) within 0.8 to 1.8 μm (Wang, 2012) and hardened or occasionally chrome plated to smooth finish (Ra) within 16 to 20 μm (Menges, et al., 1993) because some injectant additives like fillers erode chrome plating (Whelan, 1982). With most modern injection-moulding machines offering programmable control, to get thro' several effects listed in Table 4.2 and Table 4.3 the demand for robustness in runner size design is even more (Nightingale, 1978).

Table 4.2 - Possible consequences of inadequate (narrow) runner size that aggressively restrict injection

-
- a. Its stern resistance surges mechanical effort that massively orient polymer molecules (Malloy, 1994), stretch, decompose (Yang, et al., 1998), inflict damage to morphological structure (Inn, et al., 1998) and infiltrate several defects. Like stiffened mouldings (Kolnaar, et al., 1997), especially while moulding heat-sensitive and long-molecular-chain injectants (*like PC*), narrow runner designs often exceed shear-rate beyond the critical limit of injectant.
 - b. Small runner around sprue well substantially affects feeding continuance (Beaumont, 2007) *i.e. large cross-sectional gradient between sprue exit to runner entrance risk mobility departure from assumption (e) and (i)*.
 - c. Concentric laminar shear mobility along stationary restraining conduit walls possibly inflates uncontrolled heating.
 - i. Their large temperature gradient often dissipates heat quickly and freezes runner stem prematurely even before fully diffusing into the impression region (Tang, et al., 2006). This eventually
 - contrives short shots owing to inadequate volume injection (Kenig, 1972)
 - desists packing owing to inadequate shrink compensation that spurs aesthetic defects like warpage, flow marks, sink, voids, etc., (Knepper, 2004)
 - ii. Their fringe friction from injecting reheats low flash injectants to occasionally char, splay or form local silver streaks. These compromise functional features like electrical, optical, etc., on mouldings (Goodship, 2004). In contrast, constrictive reheating domination makes-up for in-runner injectant temperature decrease of high flash injectants; instead sometimes it even combines to raise through filling interval, despite lowering the barrel temperature (Goodship, 2004).
 - d. Restrained melt injection embeds excess stress into injectant's microstructure that often infiltrates into impression region, credibly persists as residue and causes anisotropy (Collier, 1973). Altogether, they compromise moulding strength at a rigor that rages with reducing runner size (Yao, et al., 2004).
 - e. It intensifies intra-conduit injection impulse to diffuse injectant rapidly towards impression region much before air could escape through vents and apparently traps remnants as local blisters. Consecutive packing impulse enormously compresses these

blisters and quickly flares up their temperature. Perhaps this ignites, burns surrounding melt or thermally deteriorates injectant until entrapped air deflates or evacuates.

- f. Its brisk injection rips injectant off runner-conduit edges, buckles spouting streams that contain diverse melt states across modes or folds creating local welds; classically this is described as jetting in practise (Jones, 2009).
- g. It perhaps clenches machine's injectability by either throttling fill time or choking feed system (Yang, et al., 1996).

Table 4.3 - Possible consequences of large size runner design that casually allow injection

- a. Traditionally processors deemed large runners produce a superior finish, ebb weld lines, flow lines, sink marks, and avert internal stresses on mouldings. But their volumetric increase sabotages available machine capacity, like injector's effort exertion per stroke, barrel's heating capacity to plasticise per hour (Rosato, et al., 2000), etc.,
- b. Its reasonably gentle pressure gradient would possibly tranquilise injection and prompt post filling defects with possibilities (Yablochnikov, et al., 2014) like,
 - i. Inconsistent packing deprives mould texture aping at gently packed regions typically termed cloudiness (Bryce, 1997).
 - ii. Uneven injection differs temperature gradient across impression's concave and convex surfaces that eventually wrap mouldings (Gordon Jr, 2010).
 - iii. Gradient packing effort distorts moulding off its shape that eventually affects uniform ejection action (Gordon Jr, 2010).
 - iv. Local wavelets variedly propagate to injection path extremities within impression region creating rippled solidified layers like fingerprints.

Contrarily, suppose if pressure and temperature are manipulated (*raised*) to pack effectively then larger runners stuff excess injectant into thicker regions of impression causing to flash.

- c. Its excess scrap volume quotient squanders energy; at first for plasticising and then prolongs cooling interval to extract undue heat for pre-ejection solidification (Khor, et al., 2010). Also, its regrinding, granulating and added handling is prone to contaminate later. Thus runner volume or size excessiveness has direct repercussions on mould competitiveness (Cheater, 1978).
- d. Besides coupling moment of extravagant runner projected area position on parting surface needs proportionately extra capacity to clamp (Zombade, et al., 2007).

- e. Excessively liberal designs create "intra-conduit dead slugs" around race termini or junctions that are difficult to clean (Imihezri, et al., 2006) on consecutive shots.
-

Runner system though volumetrically small its either leeway as listed in Table 4.2 and Table 4.3 hesitate injection, consume more energy or eventually deprive function (Tadmor, et al., 2006). So to design a proper runner system, AQL and APL together are to be adjudicated together as expectant factors. This is because from SEM images of runner stem morphology, nucleation rate, microstructure, granular fineness, density and phase multiplicity are direct ensues of injection speed $\left(\frac{\partial P}{\partial t}\right)$. Similarly their homogeneity to heterogeneity quotient is a direct percussion of thermodynamic stability $\left(\frac{\partial T}{\partial t}\right)$ (Shimbo, 2000). Classical plug flow concentrates conveyance to runner-conduit centre and diverge shear stress around its walls (Johannaber, 2008). Melt pressure intensifies temporally rivalling to gradient change from available injector action and subsides temporally rivalling to its gradient change from moulding relaxation while solidifying. Similarly melt temperature subsides temporally rivalling to fringe gradient reduction across transit injectant and spatially constant mould element. So, simultaneous conservation of injectant's tenacious mass transition and persistent energy transformation would mandate design of conduit. As smallest filling and packing interval is enough to inject shot volume, reciprocal of highest injectable volumetric shear-rate (*pressure and temperature*) available with the machine would restrict the preferable runner of least size (Bozzelli, 2012). Like,

- a) If impression thickness is too less and needs gentle holding pressure, then injectant should fill quickly at higher velocity, as it freezes instantly. And its corresponding runner size should be small, barely enough to inject rapidly from the available machine's capability as well as overcome Table 4.3 hitches. This technique is referred as starve feeding (Jones, 2009) and, for such mould designs often shot volume is almost equal to impression volume.
- b) Else, if impression thickness is too much, then injectant must fill slowly allowing more time for liquid to solid phase transformation. So its corresponding runner size should be big enough to delay solidification deliberately until thick impression sections pack adequately as well as avoid Table 4.2 hitches. A technique referred as sluggish feeding (Jones, 2008) and often in such mould designs shot volume would far exceed impression volume that too commensurate to gap height. Also such heavy runners might need

exclusive pins for positive ejection (Nightingale, 1978) and designing coherent cooling system for it becomes difficult as cooling intervals becomes difficult (Jones, 2008).

Thus injectant conveyance and its phase transformation together rein an exclusive conduit geometry design. Besides each consecutive runner segment delivers lesser injectant than its preceding segment, so logically the subordinate runners have to be relatively smaller (Rosato, et al., 2000). However, abrupt differences across runner segments along injection stream should preferably be also avoided (Whelan, 1982). Essentially, runner stems must solidify slower than the moulding, usually cooling rates around runners are 30 to 80 % of impression region (Beaumont, 2007), so on ejection they don't cling to either mould surface or moulding. For ease of extraction, they are expected to be stiff enough to bear the ejection effort and amply tough to deflect along injectant's elastic modulus. So runners should solidify at an interval just above two atleast (*fastest*) to three times utmost (*slowest*) of their respective impression's (Shoemaker, 2006).

From the preceding section (4.1) and (4.2) deliberations, it's clear that designing accurate runner size is a delicate problem that most mould designers typically encounter (Postolache, et al., 2009). Thus ab runner size determination is valuable to judiciously trade-off between small (*ref. Table 4.2*) and large (*ref. Table 4.3*) size implications.

4.3. RUNNER CROSS-SECTION DESIGNING

Conventional runner-conduit designing casually neglects afore apprehension. Most popular empirical criterion adopted to estimate primary runner size is $2R = D = \frac{\sqrt[2]{W_{shot}} \sqrt[4]{L_r}}{3.7}$, where W_{shot} is shot weight in grams and L_r is longest runner length in mm that're typically around $1 \leq R \leq 6$ mm (Pye, 1989). They simply intrust either independent (Rosato, et al., 2000) or arbitrary substitution (Beaumont, 2007), or empirical approximation (Kamal, et al., 1989), and inevitably warrant optimisation about successive heuristics (Huang, et al., 2008). Mainly because empirical equation to calculate runner conduit size was deduced by correlating capillary Newtonian flow at quasi-steady approximation to melt injection. Such reliance on subjective intuition or immanent wisdom makes them manipulative; essentially limiting them across definite confidence levels involves extensive heurism with exhaustive iterations that prolong lead-time and proliferate errors, besides risking non-optimality (Zhai, et al., 2009). Thus proper size determination difficulty causes most temporal and local fluctuations as well as AQL and APL run-outs or either compromises (Johannaber, 2008). Nevertheless for

overcoming deterrents, most mould designers are adopting various simulative methodologies for analysing injection mechanics, tactically predicting implications (Zdanski, et al., 2008) and then strategically optimising them with suitable multiple objective functions (Ziobro, 2013). Few researchers have correlated ipso-facto defects and their aftermath corrections to acclaim salient perfection constraints as phenomenal reconnaissance (Kim, et al., 1995). Most of these studies primarily focus on tackling AQL and APL or either aberrance by reverting to ipso-facto knowledge (Chen, et al., 2009). So at a definite AQL and APL or either, optimum design needs countless iterations, irrespective of the repressing methods adopted (Sun, et al., 2015). This is because many factorial setups and start-ups constrain each successive repression's variability that evidently per se chaos and cumbersomeness (Packianatheri, et al., 2000). Their complexities involve arbitrating many design alternatives to negotiate a best trade-off for that either examining individually (Gastrow, et al., 2006) or assessing all together (Kim, et al., 1995) being simply impossible. The solution sets typically have too many alternatives with multiple implications that are unpalatable by traditional or strategic optimisation techniques and experimentally assessing so many is bizarre. Perhaps even sophisticated evolutionary approaches (*stochastic*) impeach to specify a probable alternative (Zhai, et al., 2009). Yet design of runner systems in injection mould relies on several heuristics and knowledge retrieval systems (Bozdana, et al., 2002). Like recently ANNs were adopted widely for improving the quality (*such as warpage, shrinkage and sink marks*) of plastic injection-mouldings by deliberately optimising runner size. However, from goal, scope and interpretation perspective, they're exhaustive, computationally subjective as their aptnesses are inherently circumstantial; and judgmental as their discretions are problem-specific (Beaumont, 2007). Unfortunately, the basic generalisation involved in such schemes led to wild inaccurate estimates and fragmentary disconcerts (Akbarzadeh, et al., 2001) as alluded in preceding Table 4.2 and Table 4.3. For instance, even same volume impressions differing in topographies need exclusive runner design despite (Sun, et al., 2015) having identical {Mould, Material, Machine} configuration (Bozdana, et al., 2002).

Pragmatic attempts have been mostly futile or speculative on implications consequent to design errors of runner size; ipso-facto interpretations from them are ridiculous and unreliable because of rampant circumstantial biases (Rhee, et al., 2006). Thus, their general opinion is that a proper runner design realised from {material, machine, moulding} configuration would predispose controllable / variable factors (Beaumont, 2007). Therefore, finding an accurate

runner size and predicting its configured interaction for a particular combination by experimentation would need countless treatments and that's irrational (Morgan, 2002).

In early 1970s, many mould runners were calculated as unidirectional design problems by presuming them as injection-wise conduits (Broyer, et al.). However, as variance of their aspect ratio became large and sometimes multimodal; designing runners became difficult and remediating de-facto complexities was often beyond maker's wisdom. As in family moulds that require inconsistent feed system design like filling very high or low injection aspect ratio (*length / thickness ratio*) and varying thickness impressions, particularly thick/thin part challenges. Later in 1980s, researchers overwhelmed by such an extent of conduit design intricacies, injection-wise discrete cross-sections were sequenced along the runner layout configuration (Kim, et al., 1995) and hypothesising each section as an independent bidirectional design problem (Varner, 1981). Yet thorough runner design optimisation at system level was unavoidable because all stream race sections with varying designs had to be still combined. Similar propositions had several other schemes, among them injection-wise weighed sharing of pressure gradient across all segmented races was the most popular approach. However, these was insensitive to individual race stream length, as it intuitively gave runners too small towards the gates and too large towards the sprue well. To overcome this pressure gradient was shared across the ratios of segment lengths. Although simple, this approach ignored post processing discrepancies and eventual defects that err often-ripled as mould configuration complexity (Kazmer, 2007). Like overall feed system volume in a 2-plate mould typically exceed 2 to 3 times than a similar 3-plate mould alternative (Nightingale, 1978). Principally because, the total length and cross-section size of runners were supposed to be smaller for getting AQL and only the cross-section size had to be larger for achieving APL (Campo, 2006). Most contemporaneous software apps that're simulating mould fill presume 2.5D circular cross-section profiles to analyse runner systems and their algorithms casually reduce all other profiles to an equivalent circular cross-section. Although pretentious for calculation sake, such a reduction was accepted widely despite the risk of definite thermal and mechanics computation error around accosts (Kennedy, et al., 2013). 2.5D runner approximations neglect cross-section corner effects by generalising radial variations as negligible and instead posits theoretical coefficients. So most characteristic properties on mouldings are potentially inconsistent owing to the injection-wise streaming passeul, despite contriving them on the same multi-cavity mould (Beaumont, 2001). Filling and packing inconsistencies were prominent consequences of such design lapses owing to improper shear

and thermal stratifications across each impression sub-region (Beaumont, 2007). In estimating the smallest runner-conduit size necessary to fill, reliabilities of most commercial mould simulation software apps are sporadic as they analyse shear-rate and safely limit it below criticalness of polymeric injectant. However, they are treacherous to estimate near conduit size extent needed for an acceptable level packing.

Therefore inferring from literature survey, determination of an ideal runner size depends on solving complex combinatorial functions having exclusive symbolic multi-level conditions with each level having distinct constraints. Combinatorial functions involve nonlinear injection moulding conservation equations, idiosyncratic viscoelastic shear thinning injectant state equation (*like Tait's equation*) and constitutive intricacy of moulding equations (*like power law equation*). To append at best predesign value the runner design criteria should thoroughly ensure consistent injection velocity and coherent heat transfer (Kennedy, et al., 2013). Instead of speculating while designing or panicking after designing, it's worth reasoning some critical design facets that are unique and simple. Like inoculating several defects existences, improving design flexibility, reviving ability to confront higher risks and ingeniously conceptualising worthier configurations that eventually reach newer levels of quality and performance. To the best of our knowledge investigations to adopt such an intuitive integrated approach of regulating a polymeric injection through runner-conduit design wasn't ventured neither by deducing an exact runner size nor implying predictive process settings. Such an exclusive design criterion that exploits the best ability of the machine's injector, dexterity of the injectant, for producing alluring component features at expected AQL and APL (Bociaga, et al., 2007) is needed desperately. Obviously that should also economise accrues like appending scrap, cycle terms, CoQ weal, complement value (Jones, 2009) and supplement mould designer with abilities to inculcate engineering views. Possibly, it should also bait algorithms for designing moulds, while its corollary must recognise ideal processes control data determination at system level. Thus, create a unique scheme that adapts and improves over broad regime of processing as well as prompt several important theoretical persuasions on mould feeding systems.

With that, we intend to deduce a comprehensive independent criterion for proper design of runner system that achieves multiple objectives simultaneously. Believing, these critical insights into runner design benefits mould designers, analysts and simulation routine / kernel cryptologists. Eventually this intellect might shorten mould commissioning time, quicken

moulding development lead-time, boost productivity, improve customer satisfaction, and together achieve AQL, APL or both goals.

4.4. RUNNER DESIGN PROBLEM DEFINITION

- a. Realise criteria to design a suitable runner cross-section size from a set of thumb rules (*got from hard astute wisdom and affirmed by classical knowledge, traditional myths, trusted evidences, factual witnesses, etc.* (Beaumont, 2007)) to a set of scientific criteria (*got by understanding the complex interactions of factor-to-conduit and affirmed by philosophical methods, theories, laws, lemmas, etc.*)
- b. Deduce a definite criterion from its function and in-situ interaction. Use proven analytical principles for dynamic injection of incompressible (Tadmor, et al., 2006), visco-elastic, nonlinear shear-thinning injectant, with non-isothermal conditions (Gan, et al., 2010) to commensal all issues explained in the beginning. Considering mould element wall temperature as constant (Tadmor, et al., 2006) (Kumar, et al., 2002) while injectant's phase transforms from fluid to solid amid laminar creeping transit speed ($10^{-6} < Re < 10^{-1}$) (Deshpande, et al., 1997).
- c. Emphasise instantaneous injection mechanics to deduce generic constraints and strategically preclude recognised fall-outs or defect instances.
- d. Colligate moulding features, machine specifications and material properties as independent factors to enable mathematical intelligence advantage for deducing deterministic runner design function suitable for even complex moulds.

4.5. RUNNER DESIGN METHODOLOGY

Despite small volumetric diffusion-rate, consistent intra-conduit extensional strain is essential to inject a definite mass through the fixed conduit region of runner. This implies runner cross-sectional design has more dependence on apparent viscosity of injectant than its length design. So, length was repressed deliberately (*as assumption (b)*) as constant factor at its minimum here (*as assumption (f)*) to prune intra-conduit viscous heating and transit phase transformation anxieties. Similarly substituting the steady state velocity profile (*as assumption (d)*) reduced transient injection (*filling*) effort estimation to a deterministic function of the injectant's critical shear limit. For restraining consequent shear-rate (Campo, 2006) just below critical degradation limit (*see Table 4.2 (a)*) (Bociaga, et al., 2007), shear-thinning index is chosen for an intended transit melt state (Liang, 2002) (*as assumption (e)*). Simultaneously, modelling injection effort against non-Newtonian flow resistance and conjugate transit heat transfer for a particular shot

volume led to a sophisticated analytical solution. Available machine specifications, regarded injectant characteristics and desired moulding features are implicitly associated for parametric design of a proper runner cross-section radius (*as in Eqn (4.20)*). Later to restrain the hassle of running myriad mould trails with yearning experimental treatments and dynamic optimisation across the entire operating regime; material, machine and moulding variables were grouped as exclusive factors and explicitly categorised criterion (*as in Eqn (4.26)*) to propose as an analytically model. Its computational intelligence advantage uniquely synchronises processing demurs and corresponding behaviours as independent factorial stimuli to predict a confiding response (Mehat, et al., 2011). Besides, its corollary enables determination of optimum setting for controllable parameters that inherently avert noise factors. By that mould designers could judiciously specify a runner-conduit size and the moulder could be aware of critical processing limits for injection pressure, melt and mould temperature, volumetric injection rate (*as in Table 4.2(a)*) and moulding features (Hoffman, et al., 2013). Therefore, the fully functional criterion involving afore dynamically varying parameters is more adept to tackle design challenges (Yablochnikov, et al., 2014) like freedom to position or configure gate almost anywhere on the impression's parting surface premise. Like with multi-gated moulds (*as contemplated in section (4.3)*) weld and meld line defects could be avoided remarkably by designing runner-conduit size to divide volumetric injection rate suitably, depending on individual runner stream lengths or gate positions. Further, the criterion is also extendable to design many other runner systems with non-circular cross-sections and segmented lengths or either. Like to balance in-mould pressure induced moments of multi-impression or multi-gated moulds that have unlike impression regions or diverse transit volume fractions.

The intuit from afore proposed criteria indeed has triple implications on system, parameter, and tolerance design. Among these parameter design being the most imperative (Kim, et al., 2000) was emphasised explicitly here by assessing respective principal sensitivities. For that purpose, an illustrative intervention at a definite AQL and APL was hypothesised to sensitise the proposed criteria over infinite range that led to worthwhile insights for idealism. In addition, the proposed criteria over infinite range that lead to worthwhile insights for idealism. In addition, the proposed intuit corollary was also useful to specify suitable processing range or control tolerance limits for sustaining consistency like influx melt state (*barrel temperature and injector pressure*), filling time, switchover points, packing duration, coolant circulation and so forth (Hassan, et al., 2010). Besides, research and development outlay also subdues as

its sensitisation enquiries en-masse on multiple parameters per treatment instead of specific treatments as did in traditional methods (Kim, et al., 2000).

4.6. RUNNER DESIGN CRITERIA

The runner system configuration being a network of streams was seen as a set of contiguous tubular elements differing in lengths (Zdanski, et al., 2008). These sequentially aligning or associating elements with varying lengths were represented by an arbitrary symbolic function ($\xi = f(r, \theta, z)$) along the entire injection trace. Conduit being tubular for descriptive simplicity of governing equations (*as in assumption (d)*), cylindrical coordinate system (r, θ, z) was embraced. For injecting melt into the mould impression region, intra conduit resistance was constituted by adopting the Generalised Newtonian Fluid (GNF) Ostwald-de-Waele model over the power-law fluid regime with reasonable coincidence to de-facto situations (Zdanski, et al., 2011).

Assumptions

- a. Typical runner stem weights are merely a small fraction of shot weight so gravitational forces are neglected (Kleindel, et al., 2014)
- b. Instantaneous volumetric injection rate $Q[t]$ is kept constant deliberately to ensure continuous filling (Yeager, 2014)
- c. By adopting a reliable injector control system, pseudo-steady state would be implicit (Seo, et al., 2011)
- d. Thermoplastic melt injection through circular section runner-conduit having its central axis along ξ -direction produces angular invariance with symmetrical momentum and thermal profile, as deliberated in the preceding section (4.5). Also as flow profile being irrotational, stirring from rotational component of velocity vector is neglected throughout the conduit passage (Trifonov, et al., 2008), $U_\theta = 0$
- e. Melt injected into runner-conduit from sprue well is almost uniform especially at creep level ($10^{-6} < Re < 10^{-1}$) Reynolds's number (Yang, et al., 1994)
- f. In subsistence to the preceding section (4.3) review, injection through runner-conduit is presumed as fully developed (Deshpande, et al., 1997), because its representative length is short (*as explained in preceding section 4.5*) (Osswald, et al., 2006), $\frac{\partial U_\xi}{\partial \xi} = 0$.

- g. Injected polymer melt would to be isotropic (Zhu, et al., 2004), $\frac{dE}{dS} = 0$
- h. Interface wall slip is neglected, $U_{\xi}[r \rightarrow R] = 0$ (Zheng, et al., 2011)
- i. From the preceding section (4.3) review, suppressing transit injectant's shear stress interaction complexity around runner domain boundary prevents injection insularity at extreme junctions (Graebel, 2001). So, runner-conduit race edge transition from sprue-well to gates are assumed to have seamless gradience from either termini or else pressure gradient reduces as in adjunct "plug" flow from convergence, divergence or both.

Mathematical Formulation

The resultants of injection effort across sprue-well exit *or runner-conduit entrance orifice* and gate entrance *or runner-conduit exit orifice* being two equal and opposite dynamic forces act along injection wise ξ -direction. They stimulate instantaneous melt injection, provoke injectant's behaviour and are proportionate to impression's volume (*shot*). Together they also control runner-conduit injection continuity and momentum balance. So the general mass conservation expression is,

$$\frac{\partial \rho}{\partial t} + \nabla(\rho \bar{U}) = 0 \quad (4.2)$$

From assumption (d) and (e) Eqn (4.2) reduces to,

$$\frac{\partial \rho}{\partial t} + \frac{\partial}{\partial \xi}(\rho \bar{U}_{\xi}) = 0 \quad \Rightarrow \quad \frac{\partial \rho}{\partial t} + \rho \frac{\partial \bar{U}_{\xi}}{\partial \xi} + \bar{U}_{\xi} \frac{\partial \rho}{\partial \xi} = 0 \quad (4.3)$$

Suppose assumption (b) $\frac{\partial \bar{U}_{\xi}}{\partial \xi} = 0$ were true then Eqn (4.3) further reduces to,

$$\frac{\partial \rho}{\partial t} + \bar{U}_{\xi} \frac{\partial \rho}{\partial \xi} = 0 \text{ after rearranging we get, } \bar{U}_{\xi} = - \frac{\partial \rho / \partial t}{\partial \rho / \partial \xi} \Rightarrow U_{\xi} = \frac{\partial \xi[t]}{\partial t} \quad \therefore \text{ assumption (e)}$$

So instantaneous melt front position would be $\xi[t] = \frac{1}{\pi R^2} \int_0^{t_{inj}} Q[t] dt$ (4.4)

Differentiating Eqn (4.4) with injection interval we get, $\frac{\partial}{\partial t}(\xi[t]) = \frac{Q[t]}{\pi R^2} = \bar{U}_{\xi}$ (4.5)

As discussed in section (4.5), radial component of velocity is inexistent for circular conduits,

$$\frac{\partial(r U_r)}{\partial r} = 0 \quad (4.6)$$

Integrating Eqn (4.6) gives $r U_r = C_1$; but since rigid and fixed conduit confine injection, assumption (h) led to conforming boundary condition $U_r[r \rightarrow R] = 0$ that accedes $C_1 = 0$. Besides from assumption (d), transverse mobility is also absent $U_r = 0$ throughout the conduit (Postolache, et al., 2009). Thence U_{ξ} is lone velocity component existing that also as an exclusive function of r coordinate. With that rate of deformation tensor reduces to,

$$\text{Shear-rate } \dot{\gamma} = \begin{bmatrix} 0 & 0 & \frac{dU_\xi}{dr} \\ 0 & 0 & 0 \\ \frac{dU_\xi}{dr} & 0 & 0 \end{bmatrix} \Rightarrow \dot{\gamma} = \sqrt{\frac{(\dot{\gamma} : \dot{\gamma})}{2}} = \sqrt{\left(\frac{dU_\xi}{dr}\right)^2} = \left|\frac{dU_\xi}{dr}\right| = -\frac{dU_\xi}{dr} \quad (4.7)$$

Now, the scalar product of tensor $\dot{\gamma}$ is $2\left(\frac{dU_\xi}{dr}\right)^2$ and always negative $\dot{\gamma} < 0$ for tubular conduits, depicting shear dependence. We now consider Navier stokes equation of motion for momentum conservation as below (Bird, et al., 1960),

In r direction

$$\rho \left(\frac{\partial U_r}{\partial t} + U_r \frac{\partial U_r}{\partial r} + \frac{U_\theta}{r} \frac{\partial U_r}{\partial \theta} - \frac{U_\theta^2}{r} + U_\xi \frac{\partial U_r}{\partial \xi} \right) = -\frac{\partial P}{\partial r} - \left(\frac{1}{r} \frac{\partial}{\partial r} (r \tau_{rr}) + \frac{1}{r} \frac{\partial}{\partial \theta} (r \tau_{r\theta}) - \frac{\tau_{r\theta}}{r} + \frac{\partial \tau_{r\xi}}{\partial \xi} \right)$$

In θ direction

$$\rho \left(\frac{\partial U_\theta}{\partial t} + U_r \frac{\partial U_\theta}{\partial r} + \frac{U_\theta}{r} \frac{\partial U_\theta}{\partial \theta} + \frac{U_r U_\theta}{r} + U_\xi \frac{\partial U_\theta}{\partial \xi} \right) = -\frac{1}{r} \frac{\partial P}{\partial \theta} - \left(\frac{1}{r^2} \frac{\partial}{\partial r} (r^2 \tau_{r\theta}) + \frac{1}{r} \frac{\partial}{\partial \theta} (r \tau_{\theta\theta}) + \frac{\partial \tau_{\theta\xi}}{\partial \xi} \right)$$

In ξ direction

$$\rho \left(\frac{\partial U_\xi}{\partial t} + U_r \frac{\partial U_\xi}{\partial r} + \frac{U_\theta}{r} \frac{\partial U_\xi}{\partial \theta} + U_\xi \frac{\partial U_\xi}{\partial \xi} \right) = -\frac{\partial P}{\partial \xi} - \left(\frac{1}{r} \frac{\partial}{\partial r} (r \tau_{r\xi}) + \frac{1}{r} \frac{\partial}{\partial \theta} (r \tau_{\theta\xi}) + \frac{\partial \tau_{\xi\xi}}{\partial \xi} \right)$$

Substituting velocity components in Eqn (4.8) reduces to,

$$\left. \begin{aligned} \frac{\partial P}{\partial r} &= 0 \text{ in r direction} \\ \frac{\partial P}{\partial \theta} &= 0 \text{ in } \theta \text{ direction} \\ \frac{\partial P}{\partial \xi} &= -\frac{1}{r} \frac{\partial}{\partial r} (r \tau_{r\xi}) \text{ in } \xi \text{ direction} \end{aligned} \right\} (4.9)$$

With influx pressure action in ξ direction alone $P[0,0,\xi]$ becomes an exclusive function of ξ , thus only $\frac{\partial P}{\partial \xi}$ remains in LHSs of Eqn (4.9). Contrastingly its RHS being exclusive function of r resolves to a finite value. Also individually r and ξ being independent coordinates, for mathematical equivalence LHS and RHS together have to convene at a constant value. Thus pressure gradient invariability along the tube implies ordinary differentials. So on integrating about r we get,

$$\tau_{r\xi} = -\left(\frac{r}{2}\right) \frac{dP}{d\xi} + C_2 \quad (4.10)$$

From assumption (d) core velocity is rapid (Kumar, et al., 2002) then in Eqn (4.10) shear stress won't exist at the crux $r \rightarrow 0, \tau_{r\xi} \rightarrow 0$; as a boundary condition this removes integration constant as $C_2 \rightarrow 0$.

$$\tau_{r\xi} = -\left(\frac{r}{2}\right) \frac{dP}{d\xi} \quad (4.11)$$

Eqn (4.11) now describes an asymptotic dispersion of shear stress from nothing at core to severe along the boundary. Suppose if the entire runner-conduit were a distinct element then injection effort applied across its length $\xi \in [0, L_r]$ should diffuse injectant at creep rate ($10^{-6} < Re < 10^{-1}$) that too as regular concentric annular laminates (Imihezri, et al., 2006) (*to forego Table 4.2 (c) impasse*). That's because convection momentum of those cylindrical tubular shaped laminates across either ends should merely overcome injectant's inter-annular surface viscous shear resistance according to assumption (i). There each differential laminate with accordant cross-section (*having internal radius r and external radius $r + \delta r$*) witnesses representative apparent viscosity $\mu[t, \mathbb{S}(r, r + \delta r)]$ resistance along its cylindrical surface $\mathbb{S}(r, r + \delta r)$ (Osswald, et al., 2006). However from power law, provocation of injectant's constitutive behaviour by injector's shear effort is responsible for shear mobility that responds as true velocity in ξ direction (Abel, et al., 2009).

$$\tau_{r\xi} = -\mu \gamma^{n-1} \frac{dU_\xi}{dr} \quad (4.12)$$

With that substituting Eqn (4.7) in Eqn (4.12) we get,

$$\tau_{r\xi} = -\mu \left(\frac{dU_\xi}{dr} \right)^{n-1} \frac{dU_\xi}{dr} \quad (4.13)$$

So by combining Eqn (4.11) and Eqn (4.13) gives,

$$-\mu \left(\frac{dU_\xi}{dr} \right)^{n-1} \frac{dU_\xi}{dr} = -\frac{r}{2} \frac{dP}{d\xi} \quad (4.14)$$

Simplifying Eqn (4.14) gives,

$$-\frac{dU_\xi}{dr} = \sqrt[n]{-\frac{r}{2\mu} \left(\frac{dP}{d\xi} \right)} \quad (4.15)$$

Integrating Eqn (4.15) about r gives,

$$U_\xi[r] = \frac{n r}{1+n} \sqrt[n]{\frac{r}{2\mu} \left(-\frac{dP}{d\xi} \right)} + C_3 \quad (4.16)$$

Now by applying fringe boundary condition $U_\xi[r \rightarrow R] = 0$ (*assumption (h)*) C_3 as below,

$$C_3 = -\frac{n R}{1+n} \sqrt[n]{\frac{R}{2\mu} \left(-\frac{dP}{d\xi} \right)} \quad (4.17)$$

Substituting Eqn (4.17) in Eqn (4.16) and on simplification we get,

$$U_{\xi}[r] = \frac{n(r^{\sqrt[n]{r}} - R^{\sqrt[n]{R}})}{1+n} \sqrt[n]{\frac{1}{2\mu} \left(\frac{dP}{d\xi} \right)} \quad (4.18)$$

Similarly, by integrating Eqn (4.5) about conduit radius gives volumetric injection-rate as,

$$Q[t] = \int_0^R 2\pi r U_{\xi}[r] dr \quad (4.19)$$

Now by substituting Eqn (4.18) in Eqn (4.19), and then evaluating, we get

$$Q[t] = -\frac{n\pi R^3}{(1+3n)} \sqrt[n]{\frac{R}{2\mu} \left(-\frac{\partial P}{\partial \xi} \right)} \quad (4.20)$$

As transverse (*tumbling*) and angular (*stirring*) pressure effort are dormant, afore partial derivative relegates to an ordinary differential equation as,

$$Q[t] = -\frac{n\pi R^3}{(1+3n)} \sqrt[n]{\frac{R}{2\mu} \left(-\frac{dP}{d\xi} \right)} \quad (4.21)$$

Suppose if influx injection pressure P_0 thrusts normally at the crux of runner-conduit inlet cross-section surface dS_0 at $\xi=0$ then net force action across complete surface $S_0[r, \theta, \xi]$ is $F_0 = \int_0^S P_0(-\hat{n})dS$, where \hat{n} is the unit normal vector and its -ive sign denotes inward action of

influx force. Similarly, at exit surface with $\xi = L_r$, $F_{L_r} = \int_0^S P_{L_r}(\hat{n})dS$. Combining them using

Gauss divergence theorem gives $\sum F = -\int_0^V \nabla P \cdot dV$ and for achieving hydrodynamic equilibrium

net injection effort should repress to $\sum F = 0$ (Deshpande, et al., 1997) that results in $\int_0^V \nabla P \cdot dV = 0$

. Implying that net pressure gradient persists regardless of conduit volume or size and with the absence of radial (*as in section (4.5)*) and rotational (*assumption (d)*) macroscopic mass

mobility is independent of r and θ . Thus $\left\{ \frac{dP}{dr}, \frac{dP}{d\theta} \right\} = 0$, then its temporal pressure difference

function remaining is $\partial P = (P_0 - P_{L_r})$, and as it's dependent solely on conduit length (ξ) resolves

as $-\frac{dP}{d\xi} = \frac{(P_{L_r} - P_0)}{L_r}$ and substituting that in Eqn (4.21) gives,

$$Q[t] = -\frac{n\pi R^3}{(1+3n)} \sqrt[n]{\frac{R}{2\mu} \left(\frac{(P_{L_r} - P_0)}{L_r} \right)} \quad (4.22)$$

Eqn (4.22) is power law equivalent of the celebrated Newtonian Hagen-Poiseuille equation,

where its Newtonianess could be verified by substituting $n=1$. Pressure gradient extent being

intra-impression difference across sprue-well exit and gate entrance is expressed as a relative

quotient fraction of rated injection pressure P_{\max} available in the machine as $\nabla P = C_p P_{\max}$. Here

C_p being characteristic coefficient controlling pressure intensity needed by injectant to contrive

fully $C_p = \frac{P_{\max} - P_{\text{in-mould}}}{P_{\max}}$, which instead is described by velocity of sound through injectant. Now

substituting afore analogy in Eqn (4.22) gives,

$$Q[t] = \frac{n\pi R^3}{(1+3n)} \sqrt[n]{\frac{R C_p P_{Max}}{2\mu L_r}} \quad (4.23)$$

Similarly from design perspective, $t_{fill\ time} = \frac{\text{Stroke Volume of M/c}}{\text{Injection rate}} = \frac{V_{Stroke}}{Q_{injection}}$ and $\frac{1}{\underbrace{\dot{\gamma}}_{AQL}} \leq \frac{V_{Shot}}{Q[t]} \leq \frac{V_{Stroke}}{\underbrace{Q_{injection}}_{APL}}$

Suppose if APL was decisive then to prance available intact capacity, with the convenience of assumption (b) instantaneous volumetric injection rate could be constrained safely at machine's rated capacity as,

$$Q[t] \leq Q_{injection} \left(\frac{V_{Shot}}{V_{Stroke}} \right) \quad (4.24)$$

So we equate Eqn (4.23) and Eqn (4.24) to get,

$$\left(\frac{V_{Shot}}{V_{Stroke}} \right) Q_{injection} = \frac{n\pi R^3}{(1+3n)} \sqrt[n]{\frac{R C_p P_{Max}}{2\mu L_r}} \quad (4.25)$$

Now resolving for R we get, $R = \left(\frac{(3n+1)Q_{injection}}{\pi n} \left(\frac{V_{Shot}}{V_{Stroke}} \right) \right)^{\frac{n}{3n+1}} \left(\sqrt[n]{\frac{2\mu L_r}{C_p P_{max}}} \right)$

$$R = \underbrace{\left(\left(\frac{Q_{injection}}{V_{Stroke}} \right)^n \sqrt[n]{\frac{Q_{injection}}{C_p P_{max} V_{Stroke}}} \right)^{\frac{n}{3n+1}}}_{\text{Injector}} \underbrace{\left(\left(\frac{(3n+1)}{\pi n} \right)^n \sqrt[n]{\frac{2\mu(3n+1)}{\pi n}} \right)^{\frac{n}{3n+1}}}_{\text{Injectant}} \underbrace{\left((V_{Shot})^n \sqrt[n]{L_r V_{Shot}} \right)}_{\text{Impression}} \quad (4.26)$$

Thermal energy outlay equilibrium mainly depends on morphological structure of the injectant. Like for accounting in-situ heat transfer significance of semi-crystalline, linear flexible homo-polymer at injection temperature (*above its respective melting point*); Arrhenius type relation in Eqn (4.27) should be incorporated in Eqn (4.26)

$$\mu = \mu_0 e^{\left(\frac{\Delta E}{R} \left(\frac{1}{T} - \frac{1}{T_0} \right) \right)} \quad (4.27)$$

Similarly, for amorphous linear flexible homo-polymer at $T_g < T \leq (T_g + 100^\circ C)$ Williams-Landel-Ferry (WLF) equation is suitable. So, a thermodynamic behavioural model fitting to injectant's morphological structure would combine with Eqn (4.26). Efflux temperature (T) being non-observable is inept to describe (*shot*) volumetric heat transfer of transit injectant through the conduit for prevailing thermal conductance of mould configuration. So the proposed design criterion embraces constraints that're specific to a particular injectant and mould configuration, however to be generic in consensus with our objective this endeavour pauses here.

However, the noteworthy elite facet of the proposed runner-conduit radius criterion is congregation of cognitive factors. That coherently combine available machine (*injection pressure*), preferred injectant rheological behaviour of preferred injectant (*apparent viscosity and shear-thinning index of influx melt*), component features (*like runner length along parting*

plane and overall moulding volume), and being restrained by AQL and APL or either. Similarly, familiarising Eqn (4.26) quantitatively as an explicit function of such cognitive factors shows comprehensibility in apt runner-conduit size designing as described in section (4.4). Like balancing the deformation quotient of shear-to-elongation would suppress transit variability. Like molten PC having high viscosity needs bigger conduit size than PA that has rather low viscosity. Because PC's rigid repeating units, heavy molecular weight, fibrous structure and so forth would increase apparent viscosity and oppose mobility across its characteristic limits. Lower to limit shear strain and higher limit beyond which defects like degradation, microstructure diversity, anisotropy, yield surface quality and so forth would be probable (Boronat, et al., 2009) (*see Table 4.2(a)*). Similarly, PP shear thins quickly enabling rapid injection through narrow conduit irrespective of melt to mould temperature gradient. Contrastingly PC that shear thins gradually needs ridiculously large conduits with little temperature gradient and gentle injection effort to contrive fully, especially those impressions having cosmetic features (Henz, 2013). Because principally thermoplastic injectants either elastically gather or relieve strain energy during transit depending on runner conduit design (*see Table 4.2(d)*) by splitting melt streams at the expense of some energy (Liang, et al., 2001). Therefore non-Newtonian behavioural trait (*represented by shear thinning index*) should be a prominent factor to design a runner conduit size (Liang, 1995) (Martinez, et al., 2011). Therefore, Eqn (4.26) ascribes a proper size that can possibly stabilise productivity and control quality as expected in the beginning.

4.7. NON-NEWTONIAN INJECTANT BEHAVIOUR IN RUNNER-CONDUITS DESIGN

Conventionally plastic moulds are ab-designed for Newtonian injectants by hypothesising equal distribution of injection stress in all directions for isotropic subterfuge as well as exclusive pressure dependence (*i.e, shear components dominating normal components*) for injection rate to be linear. Despite such continuum hypothesis in-situ momentum and energy conservation nonlinearity defy exact solution; urging mould designers to embrace informal solution criteria and methodologies based on asymptotic intuition or wisdom. Nevertheless during injection non-Newtonianity of higher molecular weight injectant manifests as viscoelasticity through quadratic shear-rate term $\dot{\gamma} = \lambda \mu \left(\frac{\bar{U}}{L_r} \right)^2$; wherein traditionally neglected inertia and elastic stresses dwarf in elasticity term, $\frac{\lambda \mu}{\rho L_r^2}$ which if $\frac{\lambda \mu}{\rho L_r^2} \gg 1$ then injectant's

elastic stresses would dominate or if $\frac{\lambda \mu}{\rho L_r^2} \ll 1$ then injectant's inertia stresses would dominate or if $\frac{\lambda \mu}{\rho L_r^2} \approx 1$ then both elastic and inertia stresses would be equally existent. Likewise normal stress differences and anisotropy are also non-Newtonianity manifestations causing phenomena such as die-swell, tubeless siphon, elastic recoil, rod climbing, etc. Additionally non-Newtonianity also manifests under certain circumstances as multiple injection regimes discriminated by Deborah / Weissenberg number as well as secondary or tertiary injection and instabilities; few injectants also exhibit length scale (*or time scale*) behaviours changes. Therefore in lieu of such pragmatic criticality appreciating non-Newtonianity to design plastic injection mould feed systems especially to inject ubiquitous injectants is still a perplexing knowledge gap for modern engineering research portfolio. This associates nonlinear injectant behaviour in classical hypothesis. Injection mould design problems are quite unique because of the constitutive structure. The recent advancements in non-Newtonian injectant mechanics are helping to pursue both fundamental and experimental curiosities that are directing plastic injection mould design toward maturity. Like injectate swell, multi-phase liquid-liquid or gas-liquid injection, yield-elastic stress of injection are presently researched in injection moulding premise. Therefore this endeavour aims to emphasise the qualitative distinctness of non-Newtonian injectant behaviour in general and discriminates polymeric and nonpolymeric aspects of injectants.

Contention and Discussion

Figure 4.7 schematises ideal runner size sensitivity to in-situ apparent viscosity with corresponding shear-thinning index curves in relevance to our objective of emphasising the criticality of appreciating non-Newtonian behaviour upfront, especially those arising in actual injection-moulding in contrast to just Newtonian behaviour on infinitely extending dimensional scale. Although the curves literally appear to be linear, actually they are exponential by nature. Since the corresponding curves are discrete, shear-thinning index and the apparent viscosity pair cognitively have negligible interactive sensitivity towards ideal runner size. Also the curves with differing slopes intersect at some large viscosity, beyond which their slope proliferate. However, real-world thermoplastic melts having apparent viscosity ranging from 10^2 to 10^6 Pa-sec (Cogswell, 2003) will certainly have a distinctive ideal runner size continuously existing. Such a runner size would be almost directly proportional to injectant state (*represented by both viscosity*) whose scale and intensity being acutely oppressed by non-

Newtonianity quotient (*represented by shear-thinning index*). This is also evident in Figure 4.5, because the curve slope increases as injectant shear thins more and more, indicating a narrow conduit would be enough for high shear-thinning ($n < 1$) and that being significantly dependent on injection rate available in machine. On the contrary shear thickening ($n > 1$) behaviour of injectant tends the slope to zero, indicating conduit size approaches a constant finite value with reducing dependency on injectant viscosity. The logarithm plot of runner radius to injectant viscosity was found to be linear as in Eqn (4.26) with a slope ranging between $0 < \tan \varphi < \frac{2L_r}{C_p P_{max}}$. Thus, we now conclude that injectant's non-Newtonianity would be very crucial to design runners for any mould configuration.

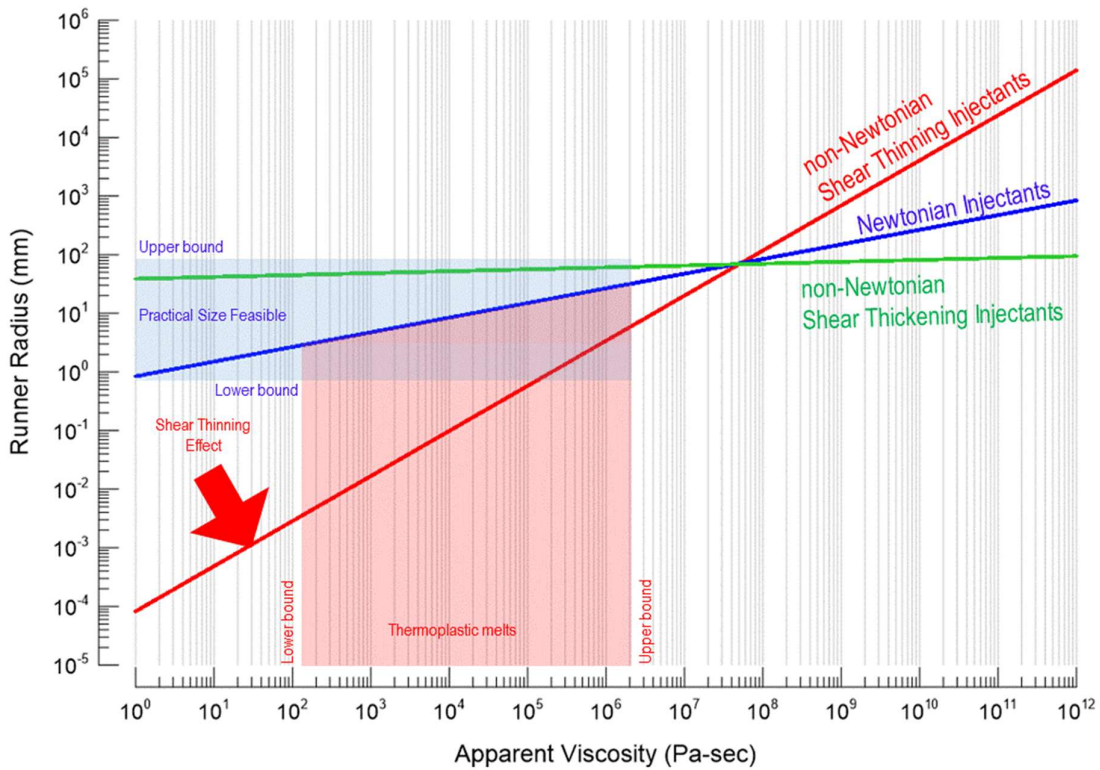


Figure 4.5 Runner radius relative to apparent viscosity.

Nevertheless, within practically feasible runner size range being 1 to 50mm for all most all injection mouldable thermoplastic melts having an apparent viscosity from 10^2 to 10^6 Pa-sec, the deliberation aspect has been clearly emphasised by capturing the region of interest in Figure 4.6. Hence it would be evident to conclude that a priori appreciation of non-Newtonian behaviour has definite advantages over casually neglecting it and then trying to optimise for perfection. Therefore the casualness of neglecting non-Newtonian behaviour to designing feed system irrespective of injectant's character by trusting empirical myths would obviously

compromise perfection (Kamal, et al., 1975). It can also be inferred that even after optimising the moulding quality accomplished would be at the cost of performance, perhaps over time as the performance increase moulding quality would deteriorate. Such as excess runner size would lead to flash or undersize would prematurely freeze prior to occupying impression gap. Perhaps if mould performance and mould quality are scrupulously optimised concurrently then dynamic issues like inconsistent shrinkage or warpage occurrence would be most probable (Tang, et al., 2006).

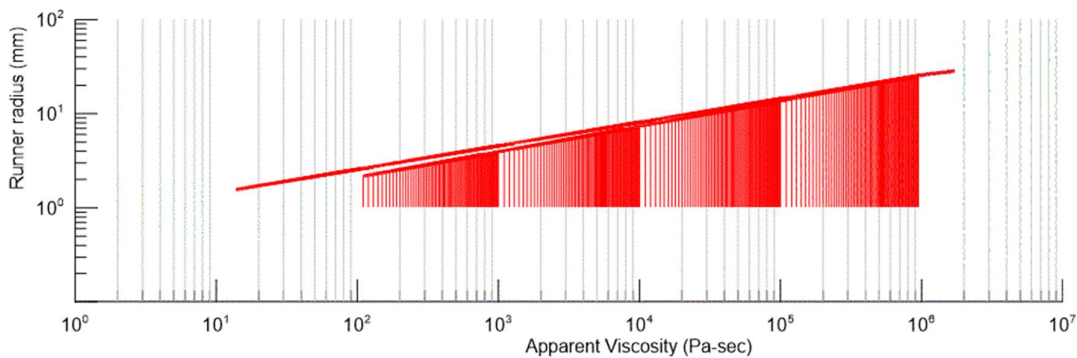


Figure 4.6 Feasible runner radius size relative to real world thermoplastic apparent viscosity.

4.8. ILLUSTRATION

From runner-conduit size design perspective, the onsets of several concerns have deterministic attributions to in-situ transit state of injectant that prolifically characterises the injection-moulding combination prominence. Therefore, distinct perturbation of injection-moulding combinations would enounce sensitivity intellect that we hope enables the prudence to specify an accurate runner size for any particular combination. For example, thorough appreciation of injectant's behavioural character before diffusing through a runner is better than rectifying its consequent defects after occurrence (Liang, 1995) and eventually striving to improve the overall mould design. The preceding literature review in section (4.3) connives two enthrals for designing a runner-conduit (Isayev, et al., 1987), (i) inoculating in-situ phenomenal defects rouse (ii) restraining the injection effort that otherwise incites indiscriminate mobility such as detaching or dragging away.

So sensitising a runner-conduit size over its rational range endures physical relevance and associated uncertainty to decisiveness. However, for discussing the sensitivity of such a complex design parameter both conventional pragmatic examination and classical philosophical inquests stumble. Mainly because traditional analogy presumes it independent and casually substitutes finite runner sizes well enough to fathom some discrete design, then

corrects it across expected AQL and APL or either. In contrast, CSM regards its function and in-situ interaction wisely across infinite range much beyond what pragmatic experimentation or classical philosophy could achieve. So for inquisitiveness, CSM was adopted with an illustrative intervene to deliberate conduit design sensitivity thorou'ly across intra-conduit in-situ injectant states. Even though complete analytical inference is still abstruse; the intervention supplements a curious perspective over prevailing myths. Through power law parameters in Eqn (4.26), the progressive thermodynamics also has deterministic prominence over rheology in injection moulding. Thus runner-conduit size sensitivity across de-facto polymeric character or astute in-situ behavioural range endures judicious decision on design adeptness at distinct extent for a chosen injectant. That sensitivity intellect is valuable to configure conduit size by stabilizing streamlines in the design stage and lessen defects amplitude. Such a priori association of intrinsic characteristics of polymeric material to runner-conduit size is better (Liang, 1995).

In pursuit of comprehensiveness, they (*apparent viscosity and shear-thinning index*) are sensitised by perturbing independently to know their exclusive bias (Turgeon, et al., 2002), while assuming all other factors at a certain level as espoused below,

- a. Windsor Sprint series horizontal injection-moulding machine has been adopted representatively,

Table 4.4: Sprint 650T Machine Specifications (Windsor, 2013)

Injection Pressure	P_{Max}	147 to 211.5 MPa
Pressure intensity (<i>from BSR</i>)	C_p	75 %
Barrel Stroke Volume	V_{Stroke}	3770 to 5430 cm ³
Volumetric Injection Rate	$Q_{injection}$	483 to 720 cc/sec
Nozzle orifice	D_n	2.5mm

Now considering machine term of Eqn (4.26) and substituting Table 4.4 ranges, we get

$$M_s = \left(\frac{(Q_{injection})^{\frac{n}{3n+1}}}{\sqrt[3n+1]{C_p P_{max}}} \right) = \frac{(\{483, 720\} \times 10^6)^{\frac{n}{3n+1}}}{\sqrt[3n+1]{0.5 \{147, 211.5\} \times 10^6}} m(m/N)^{\frac{1}{1+3n}} \quad (4.28)$$

For mathematical simplification, restraining Eqn (4.28) at nominal values gives,

$$M_s = \frac{(601.5 \times 10^6)^{\frac{n}{3n+1}}}{\sqrt[3n+1]{89.625 \times 10^6}} m(m/N)^{\frac{1}{1+3n}} \quad (4.29)$$

- b. Adopting a typical representative injection moulded part with 80mm hypothetical runner length (L_{Runner}), 2500 cc impression shot volume (v_{Shot}) and by substituting them in material term of Eqn (4.26); we get,

$$\text{Comp} = \sqrt[3n+1]{L_r} = \sqrt[3n+1]{0.08} \text{ m}^{\frac{1}{3n+1}} \quad (4.30)$$

Now substituting Eqn (4.29) and Eqn (4.30) in Eqn (4.26) we get,

$$R = \left(\left(\frac{(3n+1) 601.5 \times 10^6}{\pi n} \right)^{\frac{n}{3n+1}} \sqrt[3n+1]{1.785216\text{E-}9 \mu} \right) 10^3 \text{ m} \quad (4.31)$$

Runner design dependence on in-situ influx injectant viscosity and shear-thinning index is evident from Eqn (4.31). So their corresponding behavioural divergence and uncertainty would obviously affect efflux state and transforming phase variance; thus compromising AQL and APL or either (Boronat, et al., 2009). Therefore, Eqn (4.26) is proposed to calculate an ideal runner size, suppose if the injectant was ABS with (n) respectively at 0.33, then $R = 0.23681665 \times 10^{-3} \mu^{0.497636228} \text{ m}$.

4.8.1. Sensitising apparent viscosity

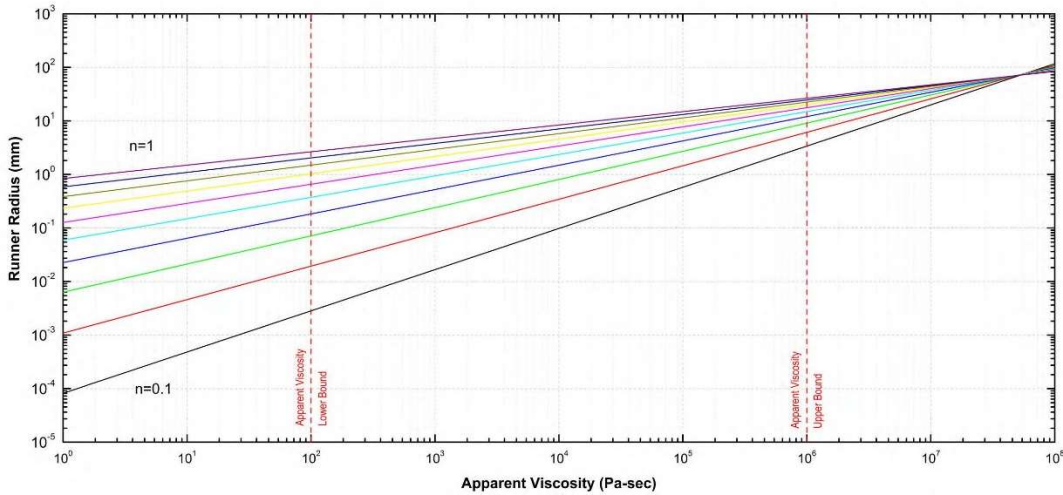


Figure 4.7 Runner radius relative to apparent viscosity.

Across de-facto thermoplastic bounds (Hoffman, et al., 2013), the aggressive influence of apparent viscosity (*representing in-situ injectant state*) on runner size features was prophesied to be almost asymptotic (Falah, 2014). Perhaps that pretence came from the literal appearance in describer's terse ranges (Postolache, et al., 2009). Principally because for non-Newtonian thermoplastics with viscoelastic shear-thinning behaviour (Bozzelli, 2012) their relation can never be linear as eluded so far, instead it has to be characteristically exponential. The abiding exponential function would have apparent viscosity at its base and the shear-thinning index as

a prominent factor entwining its coefficient sub-function representing survival or existence altitude and its exponent sub-function representing scaling intensity. So the conjugate pair of apparent viscosity and shear-thinning index together characterise injectability of thermoplastic injectant as trusted traditionally (Brincat, et al., 1998). However, shear-thinning index dependent coefficient and exponent pair aggresses apparent viscosity (*base factor*), besides assorting in-situ state across its de-facto range of injectant. Figure 4.7 shows these facets by perturbing in-situ apparent viscosity for ideal runner size arrayed with corresponding shear-thinning index curves. Also the tradition of prudently specifying a default small size to conserve runner volume expense could be subjectively convincing for aqueous commercial polymers, while surely fallacious for aspic and diversely non-Newtonian engineering polymers.

For specific pertinence to all real injection-moulding situations, abscissa was extended much beyond de-facto range of 10^2 to 10^6 Pa-sec (Cogswell, 2003). Prima facie evince of Figure 4.7 curves foretells a direct exponential dependence between them and the ideal design is surely possible across de-facto apparent viscosity range. Also each curve featured a distinct slope and intersected at some hypothetical gloopy value beyond this their slopes proliferated and that affirmed first order interactive sensitivity of apparent viscosity and shear-thinning index pair towards idealism was visibly negligible. Alike popular practise belief (Gastrow, et al., 2006), aqueous injectants needed narrow runner sizes than aspic injectants. Therefore, mere in-situ viscosity manipulation can never crap aptness of runner size design.

4.8.2. Sensitising shear-thinning index

Injectant's in-situ shear-thinning index dominance on runner design criterion is obvious from Eqn (4.26), because its behavioural divergence and uncertainty disposes efflux state and affects APL, while its behavioural instability affects the transforming phase and overruns AQL. Figure 4.8 illustrates these facets by perturbing in-situ shear-thinning index about ideal runner size with an array of apparent viscosity curves. In relevance to our objective of thorou' inquest across all injectants, sensitisation was extended beyond de-facto range. We infer from Figure 4.8 plots that in-situ shear-thinning behaviour vividly influences injection mouldability, especially across practicable conduit range. Prima facie observation of Figure 4.8 plots shows that curve slopes tow invariability towards behavioural extremeness (*gradualness and perilousness*), thus ceding the prominence of injectant's shear-thinning index on runner designs. Also, each curve has a distinct slope and is non-intersecting specifically within a characteristic de-facto region this affirms first order interactive sensitivity of apparent viscosity

and shear-thinning index pair towards an ideal runner size is also visibly negligible. Nevertheless, Figure 4.8 shows incessant persistence of ideal design across de-facto shear-thinning range ($0.1 < n < 1$) (Cogswell, 2003) and direct exponential dependence of runner size on shear-thinning index (*representing in-situ injectant state*).

Logically, intense shear-thinning type of injectant reduces power-law index, in correspondence conduit size should shrink for whichever injectant viscosity. It even closes runner existence itself towards natural extreme of zero size as shown in Figure 4.8. So to enfold APL, a liberally shear-thinning injectant needs almost narrow conduit design with much dependence on intrinsic viscosity, while a firmly stubborn injectant with almost no shear-thinning behaviour needs a large conduit design with less dependence on intrinsic viscosity.

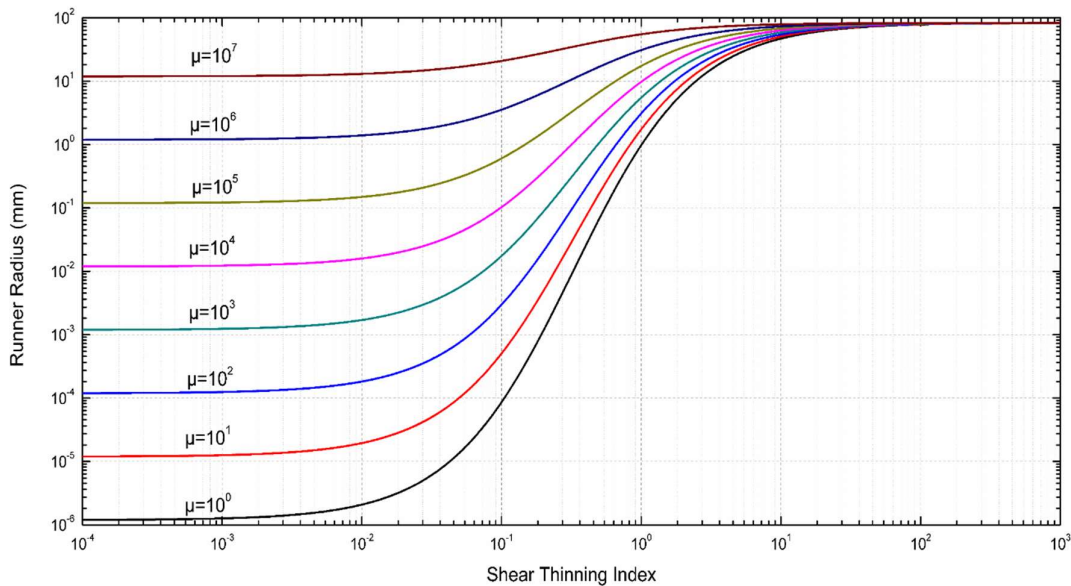


Figure 4.8 Runner radius relative to power law shear-thinning index (extended range).

4.8.3. Sensitising thermoplastics de-facto range

If injectants shear thin then ($1 > n \rightarrow 0$) else if they shear thicken then ($1 < n \rightarrow \infty$), but de-facto characteristic range for thermoplastics is ($0.1 < n < 1$). Similarly, thermoplastics de-facto characteristic apparent viscosity range happens to be 10^2 to 10^6 Pa-sec (Cogswell, 2003). In pretence to our objective (*in section 4.4*) of thorou'ly assessing thermoplastics for injection-moulding; apparent viscosity is considered as a random factor and shear-thinning index as a nested factor, in afore hypothesised case. Figure 4.9 presents their factorial sensitivities, where their slopes together appear almost equivalent. Although entailing slopes asymptote in appearance indeed they're appallingly complex and characteristically exponential; because design aberrance of runner size surely compromises AQL and APL or either. However, the

altitude changes in apparent viscosity disperse wider than shear-thinning dispersion and its characteristic dispersion broadly encompasses the entire range across both shear-thinning behavioural index as well as practicable bounds. Suitably, we infer that it's rather more influential and that's also consistent with pragmatic belief. So altogether runner size sensitivity across these de-facto ranges in Figure 4.9 decipher their incessant existence and exponential complexity.

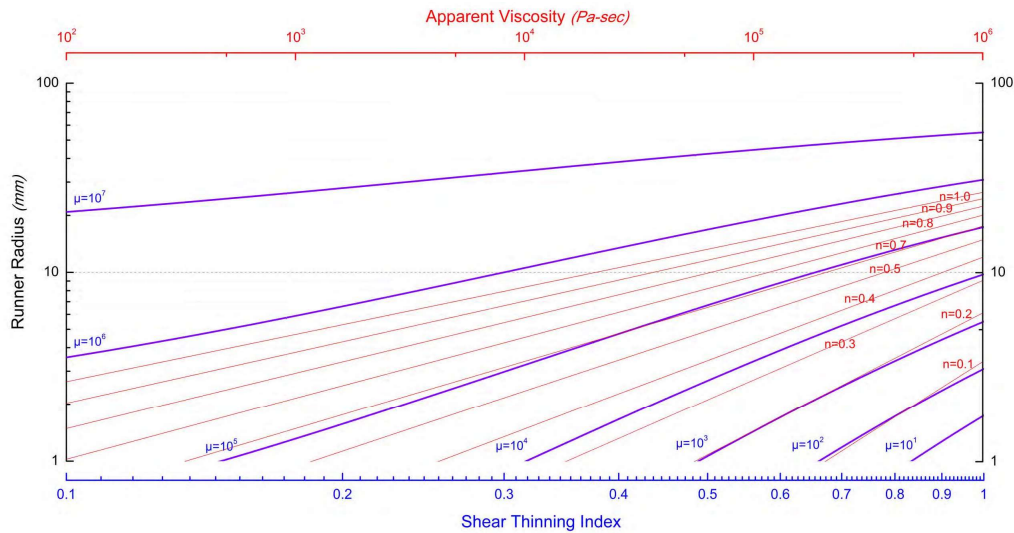


Figure 4.9 Runner radius relative to shear-thinning index (across thermoplastics range).

Apparent viscosity and shear-thinning index sensitivities assimilation in Figure 4.10 congregate to form true response contour surfaces ordering equal runner radii. Design conformance to regions within these contours depict the best arbitration as expected in section (4.4) that was a design mystery so far because huge data was necessary to portray a similar design region. That enervates both experimentation and simulation routines (*as reported in literature section (4.3)*) as meliorating injectant's state successively through so many iterations become irrational (Morgan, 2002). Also, recognition of the unerring possibility to design proper runner sizes across de-facto range for whichever endured injectant character from Figure 4.10 is surely worthwhile. Therefore, validity of the proposed criterion becomes logically obvious and generically applicable to all injection moulds irrespective of the combination {material, moulding, machine}.

Despite so much implicit relativity of salient factors to runner design, fundamental description is still unheard. Specific elucidations on runner-conduit design sensitivity at either extremities *i.e.*, *rapid and gradual shear-thinning rate* are still daunting. Therefore, the current endeavour describes an altogether first-hand insight to improve the robustness in designing

runners. Predicting or addressing these arguments through pragmatic and classical approaches would need myriad interventions. Thus, the tempting practice of spontaneously manipulating in-situ transit state might have reasonable influence on the overall runner-conduit size design error (Hoffman, et al., 2013). Instead even the largest envisaged tweak atoned APL or AQL or both slightly (Henz, 2013). Like for regulating shear-thinning behavioural influence, the following strategies are adopted (a) preserving melt temperature uniformity (b) controlling melt injection rate steadiness (c) adjusting pressure and injection rate amplitude and (d) stabilising melt injection consistency (*against cycle intervals*). The tradition of ignoring injectant's character or merely specifying it from empirical myths would often compromise AQL and APL or either and therefore ideal runner size is unique. So it's evident that with proper design of feed systems all thermoplastics are injection mouldable.

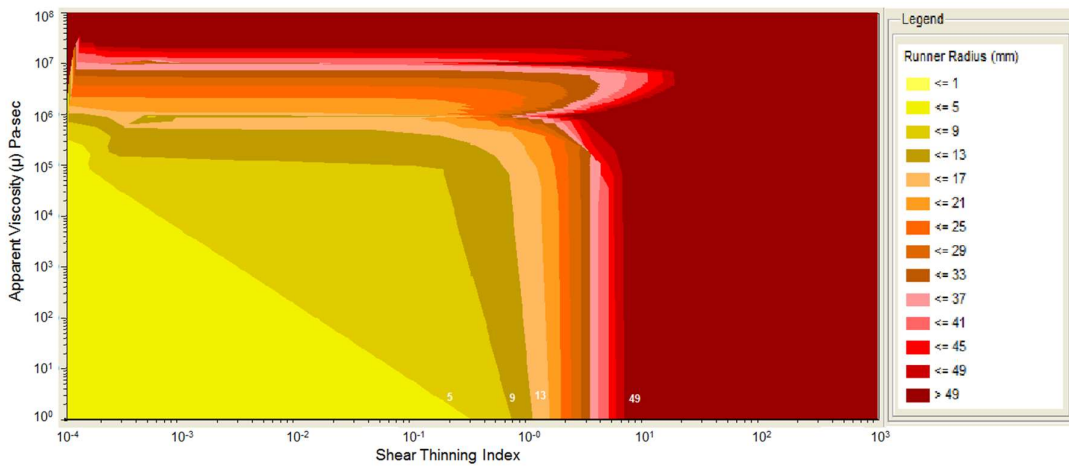


Figure 4.10 Contour analysis of runner radius

4.9. STATISTICAL VALIDATION

Successive statistical techniques were used to authenticate reliability of the proposed analytical criteria as well as appropriateness of inferred decipherments from afore illustration. Expecting their implicitness would spontaneously lead to commendable design judgements. So to prove implicit scientific intelligence and supplement confidence on the proposed proper runner design criterion, random on-production moulds were surveyed and corroborated as exclusive runner design cases. Those moulds were designed empirically ab-initio and the respective size was optimised later over several iterative trails, corrections and adjustments; perhaps engaging design of experiments approach. From each mould trail cards at M/s Prime Tooling, Bengaluru, final runner design data (*sample size N=34*) observed is in Table 4.5. Their corresponding analytical resolute were also inversely determined by substituting injectant accorded power law parameters (Tan, 2006) in Eqn (4.26).

Table 4.5 – Comparison of various production moulds surveyed

Mould No.	Injectant	Power law parameters (Mark, 2007) (Tan, 2006)		Machine parameters (Windsor, 2013)		Runner length mm	Moulding parameter		Runner radius R (mm)	
		Shear-thinning index	Viscosity consistency factor	Injection pressure	Volumetric injection-rate		Wall thickness	Component volume	Analytical resolute	Measured
		n	(Pa sec)	N/m ²	cm ³ /sec		mm	mm ³		
1	ABS	0.25	39,000	213	514	90	(4.0 ~ 1.4) ≈ 3.0	217,890.09	1.23	12.34
2	PA66+ 30%GF	0.66	2,300	1840	99	51.5	(4.8 ~ 0.75) ≈ 2.5	2,303.57	0.76	1.44
3	ABS	0.25	39,000	180	222	8	≈ 1.0	1,492.00	0.30	3.00
4	PC	0.74	920	180	100	100	≈ 1.0	3,596.60	1.96	1.91
5	PA66	0.66	4,000	180	222	170	≈ 1.0	1,276.74	3.54	3.98
6	PA66	0.66	4,000	220	169	49.2	≈ 1.2	19,040.00	2.05	3.35
7	POM	0.42	7,500	180	222	74	(4.0 ~ 2.0) ≈ 3.0	25,763.00	1.30	4.77
8	ABS	0.25	39,000	220	169	222	≈ 1.0	10,030.00	1.73	7.77
9	PP	0.28	22,000	213	514	8.9	≈ 1.8	326,660.00	0.32	2.53
10	HIPS	0.38	5,500	180	100	90	≈ 1.0	4,860.00	0.86	2.00
11	PA66	0.66	4,000	180	222	25	(2.5 ~ 1.5) ≈ 2.0	8,893.00	1.86	2.86
12	PP	0.28	22,000	180	222	14	≈ 1.0	13,400.00	0.39	1.95
13	PC	0.74	920	180	222	28	(1.54 ~ 1.05) ≈ 1.5	6,760.00	1.58	2.78
14	PA66+ 30%GF	0.66	2,300	220	50	66	(4.0 ~ 2.0) ≈ 3.0	7,513.60	1.44	4.02
15	POM	0.42	7,500	180	222	30	(5.4 ~ 3.0) ≈ 3.6	35,460.00	0.87	8.00
16	PP	0.28	22,000	180	100	27.4	≈ 1.2	21,630.00	0.50	2.90
17	PA66+ 30%GF	0.66	2,300	180	222	65	(6.0 ~ 4.0) ≈ 5.4	91,000.00	2.13	2.68
18	PBT	0.71	430	180	222	19	(2.0 ~ 1.0) ≈ 1.75	13,095.00	0.99	1.48
19	PC	0.74	920	230	224	103	(8.0 ~ 1.0) ≈ 2.0	30,500.00	2.20	7.00
20	PP	0.28	22,000	180	222	50	≈ 1.5	35,641.44	0.78	5.00
21	PA66+ 30%GF	0.66	2,300	180	222	19	(2.8 ~ 0.3) ≈ 1.55	14,136.00	1.41	5.65
22	ABS	0.25	39,000	190	200	30	≈ 2.5	119,060.00	0.61	7.13
23	ABS	0.25	39,000	220	169	450	≈ 2.5	101,000.00	2.58	10.00
24	ABS	0.25	39,000	200	335	40	(5.0 ~ 2.8) ≈ 4.0	292,200.00	0.75	6.00

25	ABS	0.25	39,000	200	335	50	≈ 1.0	4,860.00	0.86	2.00
26	PA66	0.66	4,000	220	169	19.5	≈ 1.0	6,500.00	1.51	1.55
27	ABS	0.25	39,000	1840	99	15	≈ 1.2	16,627.00	0.10	1.21
28	ABS	0.25	39,000	213	514	25.8	≈ 3.0	57,460.00	0.60	5.33
29	PP	0.28	22,000	230	224	320	≈ 2.5	107,750.00	1.87	6.47
30	POM	0.42	7,500	230	280	25	≈ 4.0	43,000.00	0.75	5.38
31	PP	0.28	22,000	220	169	200	≈ 3.0	57,922.00	1.42	8.58
32	PP	0.28	22,000	213	514	58.5	≈ 1.0	13,330.00	0.88	5.84
33	PP	0.28	22,000	200	335	50	≈ 1.0	4,860.00	0.78	2.00
34	PC	0.74	920	180	222	30	≈ 1.0	10,317.00	1.62	3.50

4.9.1. Deviation

Although actual over analytical resolute runner sizes plot on identical scale must limn asymptotic dispersion with unit slope for absoluteness, contrarily Figure 4.11’s peculiarity swerve portrayed nonlinearity. Also density contours confined 90% of the survey to a particular region of interest that aptly isolated sceptical outliers or illogical extremes (Janke, et al., 2005); thus retaining only coherent deviations for statistical intervention.

More explicitly overlooking injectant behaviour, machine specifications and moulding features Figure 4.11’s density contours surmised runner size design preference across quartile sub-ranges

$$\frac{dR_c}{dR_a} > 1, \frac{d^2R_c}{d^2R_a} > 0 \begin{cases} 1 < R_c < 10 \text{ mm} \\ 0 < R_a < 3 \text{ mm} \end{cases} \quad (4.32)$$

So to perspire more insight from Figure 4.11 surmise, respective runner size standard deviation for each surveyed mould was contrasted directly in Figure 4.12 across Eqn (4.32)’s symbolic region of interest.

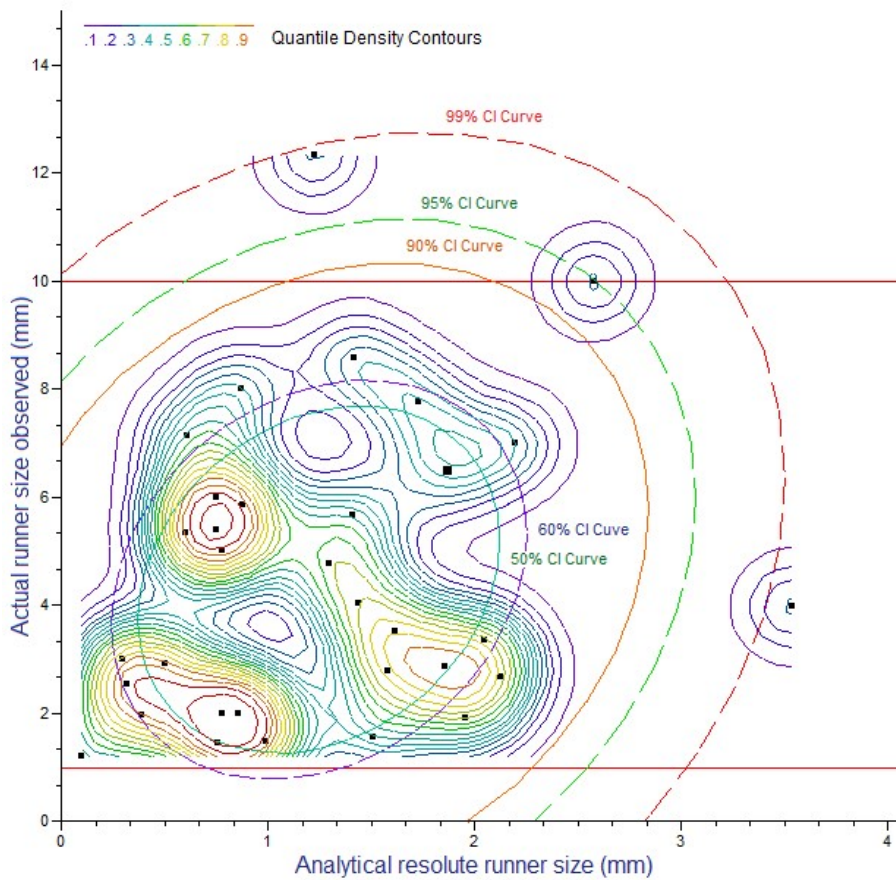


Figure 4.11 Relative dispersion of runner radius size between actual and analytical resolute.

Dispersion of standard deviations in Figure 4.12 illustrates distinctness, discreteness, randomness and independency of survey. Here again with 90% confidence,

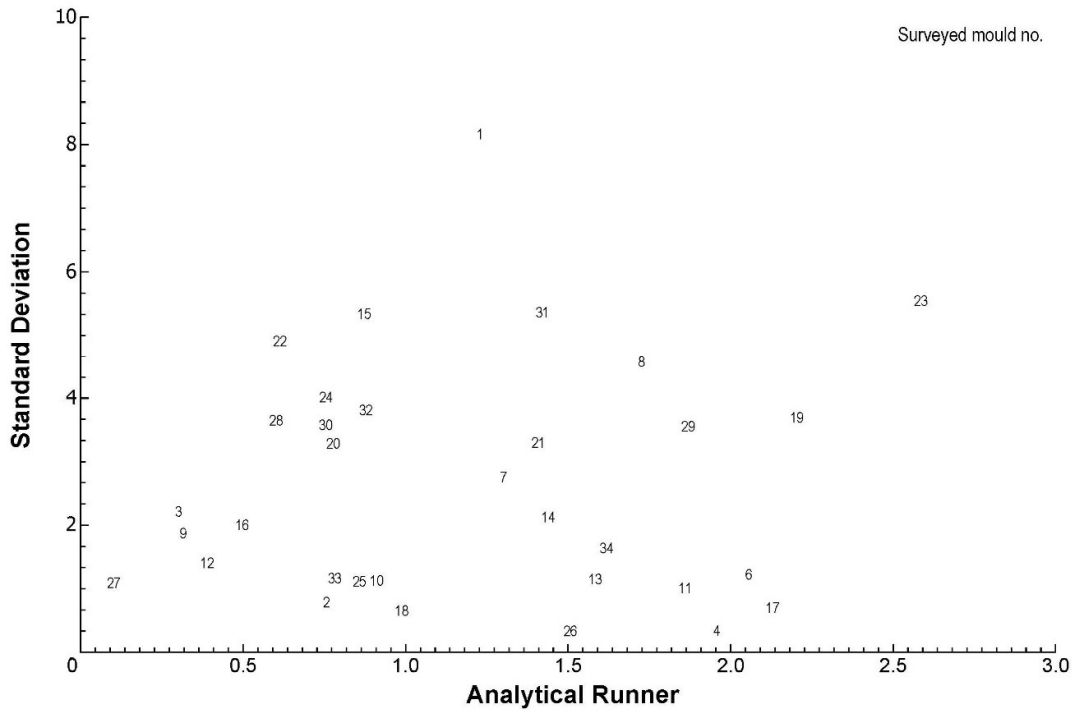


Figure 4.12 Standard deviation dispersion of actual surveyed moulds.

$$\frac{d\sigma_R}{dR_a} > 1, \frac{d^2\sigma_R}{d^2R_a} > 0 \begin{cases} 0 < \sigma_R < 6 \text{ mm} \\ 0 < R_a < 3 \text{ mm} \end{cases} \quad (4.33)$$

Thus Eqn (4.32) and Eqn (4.33) together affirm moderate congruence of survey data and presence of their higher order moments suggest absolute impertinence is unlikely.

4.9.2. Variance

Despite design, configuration, injectant and machine differences in surveyed moulds their incongruence cause must be understood because actual size over analytical resolute has wide dispersion in Figure 4.11. So their deviations are summarised and abstracted for stochastic judgement. Pertinently for at par succinct characterisation of runner size exhaustiveness and its variance, exclusive coefficient of variation (CoVs) were determined as an assessment metric of interest. Respective CoV of each representative mould in the sampled survey set by quantitatively removing their ensuant combinatorial bias and standardised them in general.

$$\text{CoV} = \frac{R_a}{\sigma_R} \quad (4.34)$$

Implicitly to begin apprehending Eqn (4.32) and Eqn (4.33) disperse, determinant CoV mean(s) and standard deviations were assessed over standard normal distribution function representatively,

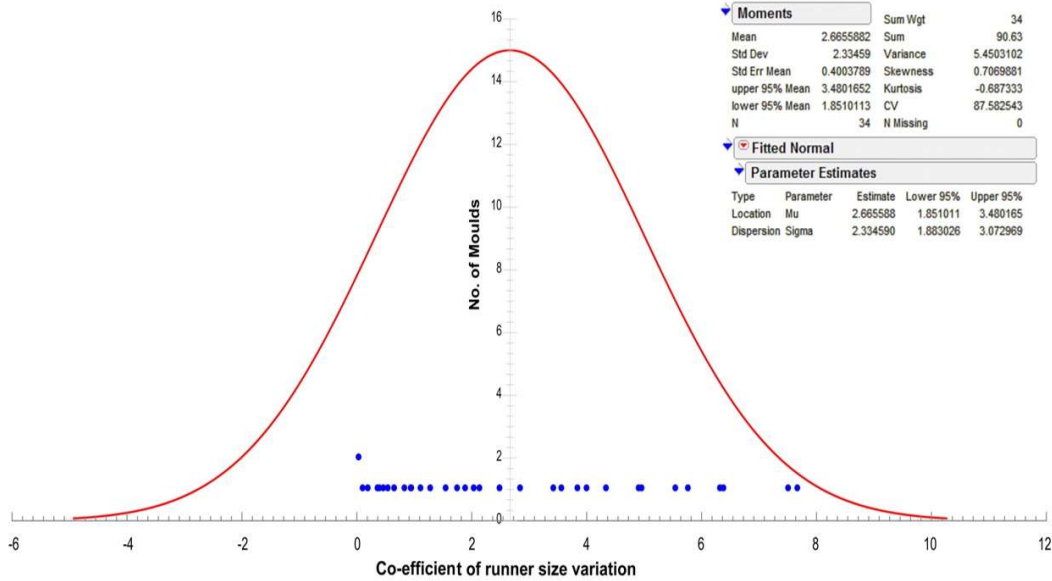


Figure 4.13 Normal dispersion function of CoV in runner size.

$$\text{CoV} \sim N\left(\overline{\text{CoV}}, \sigma_{\text{CoV}}^2\right), \begin{cases} -\infty < \overline{\text{CoV}} < \infty \\ 0 < \sigma_{\text{CoV}} < \infty \end{cases} \quad (4.35)$$

Consistently CoV disperse normalisation in Figure 4.13 prompt the following observations,

- Though runner size CoV was unpredictable its dispersal density had an order and statistical pattern that implies consistence.

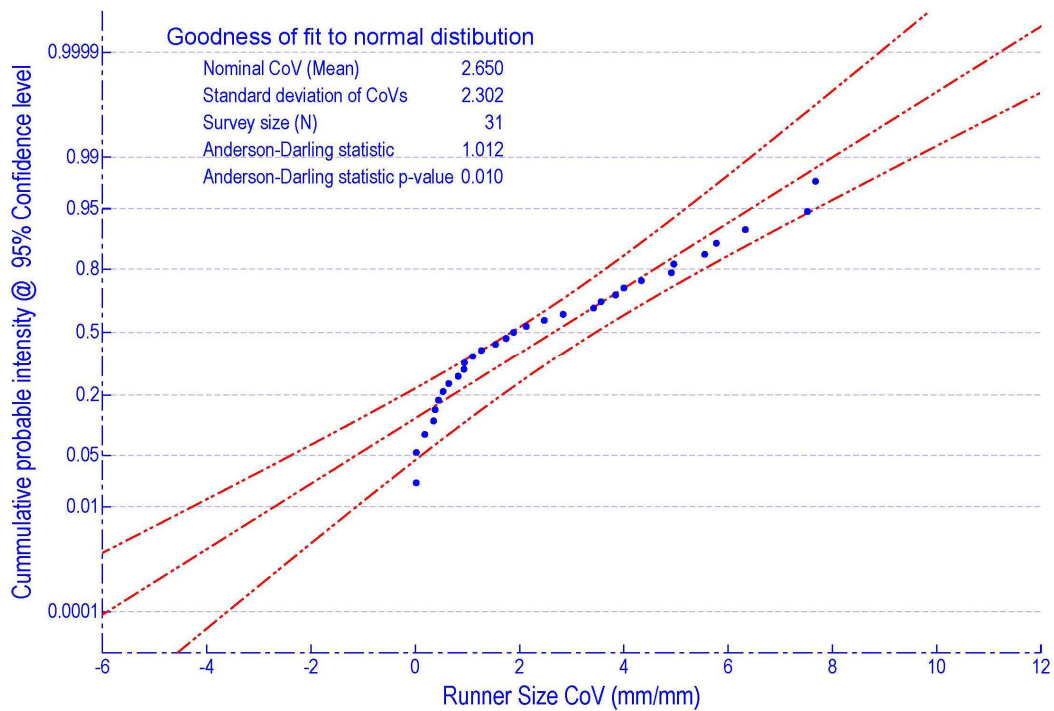


Figure 4.14 Goodness of fit to normality of runner size CoVs.

- b. Highly skewed ($\beta_1 = 0.707$) and positive definite $\text{CoV} > 0$ implies nominal incongruence is often and large incongruence is occasional.

$$\lim_{k \rightarrow 0} j_k \rightarrow N ; \text{CoV} \rightarrow \overline{\text{CoV}} \text{ and } \lim_{k \rightarrow \infty} j_k \rightarrow 0 ; \text{CoV} \rightarrow \infty \quad (4.36)$$

- c. Suppose if large spurs of large incongruence occur in some strange moulds designs, then they are mostly independent of the survey sample set size as slouched kurtosis (*platykurtic* $\beta_2 = -0.687333$) has almost flat ends (*section 4.9.4 deliberates this exquisite characteristic facet specifically*).

$$\frac{dj_k}{d\text{CoV}} \rightarrow 0 \begin{cases} \text{CoV} \rightarrow \pm \infty \\ \text{CoV} = \overline{\text{CoV}} \end{cases} \quad (4.37)$$

4.9.3. Distribution

Essentially, to corroborate the arguments in preceding section (4.9.2), dispersion must be unbiased with runner size as a standard random variable. However, that contradicts irrational traditional contemplation as to runner size was an arbitrarily random variable (Pye, 1989). Hence to generalise conformance, CoV frequency distribution was formalised for asymptotic consistency with Gaussian or standard normal distribution function and was assessed adopting applicable Shapiro–Wilk test as follows (Shapiro, et al., 1965),

Null Hypothesis : CoV deviation tendency and generic *incongruity* were characterised independently by normal distribution function,
 $H_0 : \text{CoV}_e \in N\left(\overline{\text{CoV}}, \sigma_{\text{CoV}}^2\right); \{\text{CoV}_1, \text{CoV}_2, \dots, \text{CoV}_N\}.$

Alternate Hypothesis : CoV deviation tendency and generic *incongruity* couldn't be characterised by normal distribution function
 $H_1 : \text{CoV}_e \notin N\left(\overline{\text{CoV}}, \sigma_{\text{CoV}}^2\right); \{\text{CoV}_1, \text{CoV}_2, \dots, \text{CoV}_N\}.$

Descriptive statistics : Moments in Figure 4.13 legend

Statistical Inference : Shapiro-Wilk normality test statistic was 0.89967 and its corresponding likelihood value ($< w$) for $N=34$ was 0.0045 that being much below the acceptable alpha level of 0.05, null hypothesis had to be rejected.

However, as survey sample size ($N=34$) biases p-value in the Shapiro–Wilk test; so we can still interpret that statistical evidence wasn't enough to accept coefficient of runner size variations as a normally distributed in general.

4.9.4. Summarisation

CoV normality features large intra category (*i*) frequency disparity in Figure 4.13 because thrice the standard deviation far exceeded the frequent mean $3\sigma_{i_{CoV}} > \overline{CoV}$ and $\overline{CoV} - 3\sigma_{i_{CoV}} < 0$. Incidentally such rarity was unseen among the survey data; instead, real runner size always exceeded its analytical resolute. So CoVs of survey set were sorted and their ensuing dispersion range was grouped distinctly across *k* classes with sub-ranges having a definite interval ($\delta i = 1.78046875$) incisively enough (*minimum*) to stabilise a continuous Pdf (Johnson, et al., 1994). Then real moulds having runner size CoV across each category range were segregated as in Table 4.6. Among them almost congruent category was the most frequent whereas extensively deferring being the most erratic; that implied CoV frequency distribution function was asymmetric. So Eqn (4.36) gets revised as;

$$\lim_{k \rightarrow 0} j_k \rightarrow N ; CoV \rightarrow 0 \text{ and } \lim_{k \rightarrow \infty} j_k \rightarrow 0 ; CoV \rightarrow \infty \quad (4.38)$$

Similarly, Eqn (4.37) now revised as;

$$\frac{dj_k}{dCoV} \rightarrow 0 ; CoV \rightarrow +\infty \text{ and } \frac{dj_k}{dCoV} \rightarrow +\infty ; CoV \rightarrow 0 \quad (4.39)$$

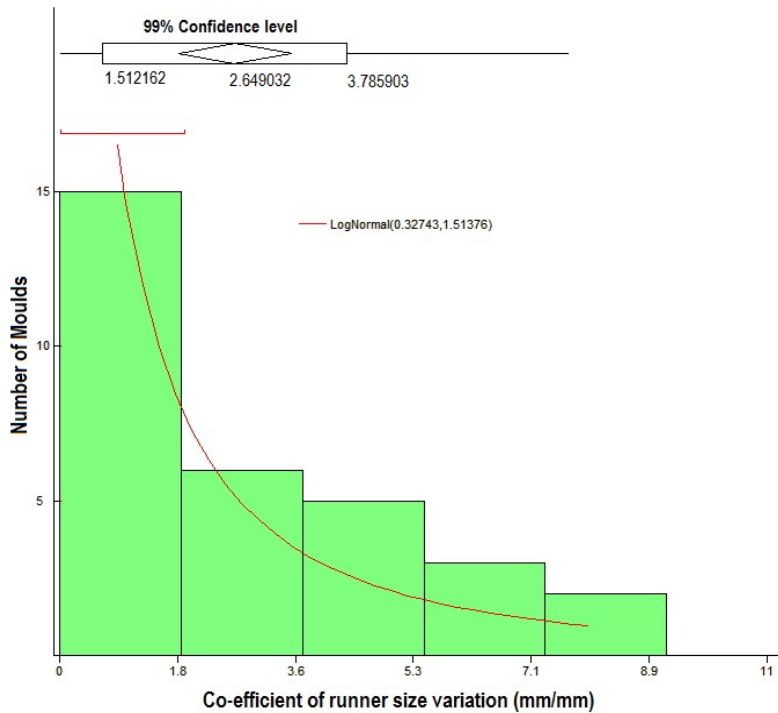


Figure 4.15 Pareto distribution of coefficient of runner radius size variation of actual size from analytical resolute.

Thus, Eqns (4.38) and (39) summarise the extent of randomness in runner radius size CoV per mould, where the number of moulds per category j_k congregates CoV scale stochastically

across natural extremes. Therefore, for a sample set of 34, its frequency distribution was judged reasonably (Montgomery, 2005) to be Galton's continuous distribution with lognormal function (Crow, et al., 1988) with definite local and scaling parameters. Figure 4.15 Pareto chart thorou'ly describes this qualitative concoction,

Thus for a general population of real moulds, local parameter at 0.32743 mm/mm represent CoV median (*where chances of CoV to either exceed or be lesser than 0.32743 mm/mm are equal* $p(n_{CoV} > 0.32743) \approx p(n_{CoV} < 0.32743)$), while $(n_{CoV} > 0.32743, n_{CoV} < 0.32743) \in N$. Likewise, 1.51376 mm/mm monotone scaling parameter rage severe endurance and aggressive conformance of CoVs to Pdf (Crow, et al., 1988). Thus, the repressing local parameter, dominant scaling parameter and Eqn (4.33) together collude to a logical interpretation that CoV would be a locally self-similar attribute (Constantine, et al., 1994). Also this intuit substantiates afore Eqn (4.32) observation that a local preferential range persists to design runners for every moulding combination. Despite surveyed moulds differing in design, configuration, injectant and machine; afore proposed criteria evidently articulates casualness in weirdly large CoV (*law of rare events*) and persistence in typically small CoV (*law of distribution convergence*). However, too small spectral deviance exaggerates range dependence and large spectral deviance disparages range dependence; such ineptness to characterise absolute extremes explicitly implies unbounded range of CoV distribution.

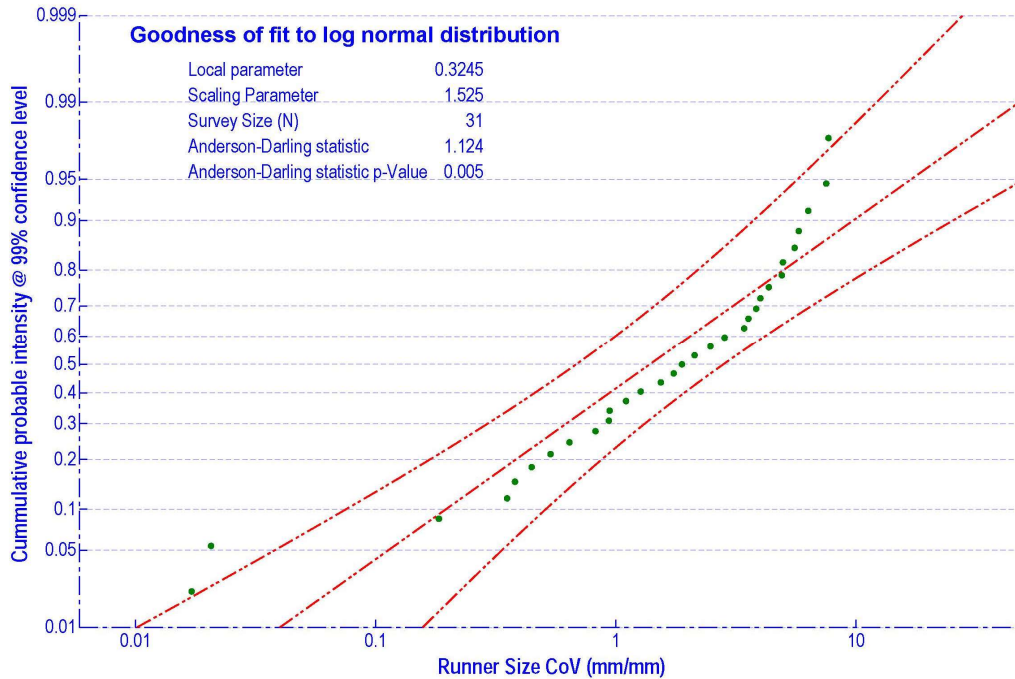


Figure 4.16 Goodness of fit to log normality of runner size CoVs

Finally, log normality plot of CoV distribution showed a good fit to straight line in Figure 4.16, while Anderson-Darling statistic p-value being 0.005 was smaller than its normal counterplot of 0.01 in Figure 4.14. Thus, afore judgement of a log normal function representing CoVs distribution was reasonable. Besides normal plot outlined too large or small runner size radicals are insignificant because of their deceptive erring in the survey data set. Therefore, the congruence function is characteristically exponential (*nonlinear*) and its inconsistency represents wide factorial aberrance among the surveyed moulds. Also, actual size to analytical resolute relativity was rationalised as $R_c = (1 + 2e^{0.32743 + 1.51376Z})R_a$, with $Z > 0 \sim N(0.32743, 1.51376)$ and determinant stretching index (*constant*) was two. This relation is useful to strategize improvement or troubleshoot maintenance and ease outlining heuristic manipulations. Further, the relation is useful to assess defect dispositions as DfM revisions on product design such as excess or scant pressure gradient.

Table 4.6 - Consolidation and summarisation of survey

Category no. k	Category interval i_k	No. of moulds j_k	Probable category intensity $\pi_k (CoV \in i_k)$	Chi-square test statistic $\sum \chi_k^2$
1	$0 < CoV \leq 1.8$	14	0.4516	0.9674
2	$1.8 < CoV \leq 3.6$	5	0.1613	16.7698
3	$3.6 < CoV \leq 5.4$	7	0.2258	51.9355
4	$5.4 < CoV \leq 7.2$	3	0.0968	106.4646
5	$7.2 < CoV$	2	0.0645	180.3570
Total no. of moulds (N)		31	Degree of freedom, df	4
Mean no. of moulds per category (\bar{j}_k)		6.2		
		Nominal CoV	0.32743	
		(local parameter of log normal distribution)		
		Probability of CoV distribution function being lognormal		≈ 1

4.9.5. Comprehension

Though R_c and R_a are solutions to the same runner design problem of same the mould, they were determined separately from different criteria conceptions. Yet from afore analysis, they are neither completely congruent $R_c \approx R_a$ nor extensively incongruent $R_c \neq R_a$; instead a tersely small local discrepancy might persist between them. So homogenate metric CoV was determined for every mould and adopted to summarise and categorise quantitatively as in Table 4.6. The tabulated abstraction was now multinomial because,

- a. N moulds were categorised among k sub-ranges parsing at par CoV (for authenticity $0 < k < N$) with each k^{th} category or i^{th} interval having j_k moulds while $\sum j_k = N$. These categories were mutually exhaustive and exclusive because moulds were classified each into a single category. Besides for reliability, Yate's correction was also adopted for categories having fewer than 5 moulds, $j_k < 5$.
- b. Despite each mould selection being sequential, neither preceding nor consecutive mould choices biased its runner size CoV; instead its basis was independent, atypical and invariant. The expected deviation of actual runner size differing from its corresponding analytical resolute for any randomly selected discrete mould was mutually exclusive among k categories and together congregate as $\sum \pi_k = 1$.
- c. For all N moulds, their respective runner size CoV surely belonged to either of the intervals or anyone k category $CoV \in i_k; 1 < k < N$ and belonging to multiple categories was impossible. So the intensity of each class was definite with a concurring probability of every runner size belonging to a k^{th} category $0 < \pi_k < 1$. Then there is a high risk of wrongly rejecting atleast anyone of them because the nominal runner sizes of all intervals are ordered.

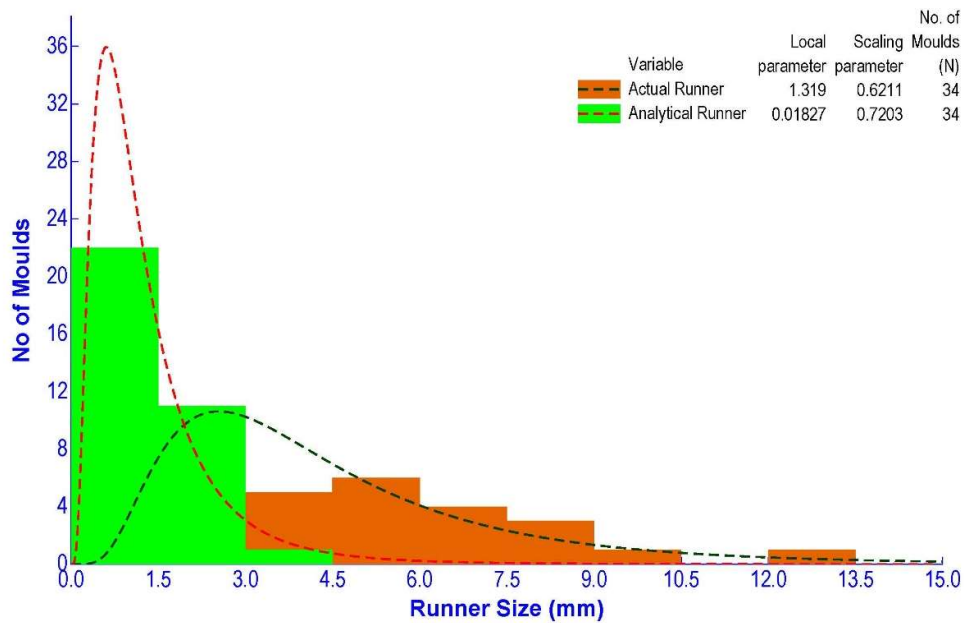


Figure 4.17 Histogram of runner sizes for real surveyed moulds and analytical perspective.

Above assertions together imply, though complete congruence of actual and analytical runner size across indefinite range $R_c \neq R_a; 0 < R < \infty$ is unlikely instead likeliness persist around some intermediate range as seen in Eqn (4.32). So from an inquisitive interpretation of Mendel's law,

systematic intra-class discrepancies and their subduing inconsistencies subsist all over the survey range; perhaps randomly because individual mould selection was random or without preference or bias. Therefore, by presuming log normal distribution ($R_a \sim \text{Log N}(\bar{R}_a, \sigma_{R_a})$ and $R_e \sim \text{Log N}(\bar{R}_e, \sigma_{R_e})$) the frequencies of subsets is plotted in Figure 4.17.

If above avowed intent was reliable then many runner measurements on real moulds and their corresponding analytical resolute would be congruent across each runner size category. To ascertain that Cochran's theorem based standard normal random statistic (*chi-square*) of each runner size class is used to characteristic intra-class incongruence among discrepancies (Bapat, 2000).

$$\text{Chi-square test statistic, } \chi_k^2 = \sum_{k=1}^N \left\{ \frac{(N_k \{R_e\} - N_k \{R_a\})^2}{N_k \{R_a\}} \right\} \quad (4.40)$$

Now in each runner size class if chi-square test statistic is near zero then congruency is statistically likely; otherwise if it's faraway then congruency is statistically unlikely. Of-course, that depends on survey size (Janke, et al., 2005); because normal density peaks near zero.

Null Hypothesis : The actual optimised runner size frequency per class is *congruous* with its corresponding analytical resolute, $H_0 : N_i \{R_e\} \approx N_i \{R_a\}$ *i.e.* R_e and R_a are *pertinent*.

Alternate Hypothesis : The actual optimised runner size frequency per class is *incongruous* towards its corresponding analytical resolute, $H_1 : N_i \{R_e\} \neq N_i \{R_a\}$ *i.e.* R_e and R_a are *impertinent*.

Descriptive statistics : See Table 4.7

Statistical Inference : Though the Pearson's probability of overall incongruence in this survey is acceptable at the most only 5%, the data in converse has likely incongruence of atleast 99.63%, this enounces enough statistical evidence to reject the null hypothesis H_0 .

Although actual runner size and its corresponding analytical resolute are independent, perhaps the entire survey set altogether may be less congruent. However from Figure 4.18, some almost congruent moulds may be expected in first, second and third categories (Harter, 1960) amongst the nine statistically (*using Chi-square test statistic*) fragmented sub-ranges. But for the first and third categories, expected incongruence were atleast 99.99% and 98.76% respectively that testifies enough stochastic evidence to reject $H_0 : N_i \{R_e\} \approx N_i \{R_a\}; \begin{cases} i \rightarrow 0 < R_a \leq 1.5 \\ i \rightarrow 3 < R_a \leq 4.5 \end{cases}$.

Table 4.7 - Summarised data of surveyed production moulds

Runner Size Class	Runner size interval (mm)	No. of Moulds in i^{th} class		Class Intensity $P(R_c \rightarrow R_{a,i})$	Chi-square Statistic with Yate's correction for continuity	Discrepancy	Statistical degree of freedom	Probability of Incongruence for i^{th} Class	Probability of Congruence for i^{th} Class
		With actual runner size	With analytical runner size						
k	I	$N_i \{R_c\}$	$N_i \{R_a\}$	π_i	χ_i^2	χ_i	df_i	p_i	$1 - p_i$
1	$0 < R \leq 1.5$	3	22	0.65	16.41	4.05	0	0.999948960	0.01 %
2	$1.5 < R \leq 3$	12	11	0.32	0.09	0.30	1	0.236975399	76.30 %
3	$3 < R \leq 4.5$	4	1	0.03	6.25	2.50	2	0.987580669	1.24 %
4	$4.5 < R \leq 6$	7	0	0.00	Indeterminate	Indeterminate	3	Indeterminate	≈ 0 %
5	$6 < R \leq 7.5$	3	0	0.00	Indeterminate	Indeterminate	4	Indeterminate	≈ 0 %
6	$7.5 < R \leq 9$	3	0	0.00	Indeterminate	Indeterminate	5	Indeterminate	≈ 0 %
7	$9 < R \leq 10.5$	1	0	0.00	Indeterminate	Indeterminate	6	Indeterminate	≈ 0 %
8	$10.5 < R \leq 12$	0	0	0.00	Indeterminate	Indeterminate	7	Indeterminate	≈ 0 %
9	$12 < R \leq 13.5$	1	0	0.00	Indeterminate	Indeterminate	8	Indeterminate	≈ 0 %

However, with an utmost probability of 76.3% congruence, second category testifies ample stochastic evidence and averts $H_0 : N_i \{R_e\} \approx N_i \{R_a\}; i \rightarrow 1.5 < R_a \leq 3 \mid \chi_{23.70\%}$ rejection despite considerable type II error risk (*at least 23.7%*) (Pearson, 1900). Yet the promisingly accurate interpretation from the theory of probabilities is that if analytical runner sizes were from 1.5 to 3 mm then those few real moulds would still probably be congruent. Perhaps the slight deviations are mere accrues from the likely errors often caused by factors common in these mould designs.

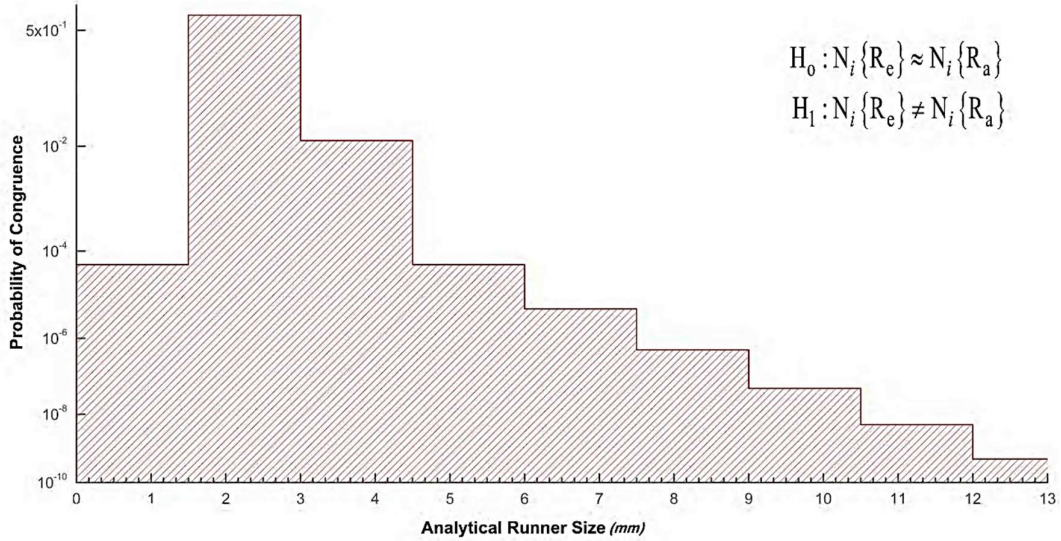


Figure 4.18 Probability of congruence relative to analytical runner size.

4.9.6. Standardised Residues

The argument enduring in preceding section 4.9.5, implies that runner sizes of real moulds differ more from their corresponding analytical resolute, Figure 4.18 features a weak congruence for most categories or sub-ranges. Although credible explanation for such enigma is complicated, our clarification is too small (*ref. Table 4.2*) and large (*ref. Table 4.3*) runner size designs though unintentional might ascend from digressing factors like totting design, configuration, injectant and machine differences among the surveyed moulds. Thus, some mysterious factors in observed runner designs are prepossessing appropriateness of proposed analytical design criteria because incongruence is wailing over. Therefore, it's worth examining the existence of any discreet residue among the deviations across runner sizes. Pertinently, exclusive standardised residue for each category was determined as;

$$r_i = \frac{N_i \{R_e\} - n \pi_i}{\sqrt{n \pi_i (1 - \pi_i)}} = \frac{N_i \{R_e\} - N_i \{R_a\}}{\sqrt{N_i \{R_a\} (1 - \pi_i)}} \quad (4.41)$$

Suppose if categorical residue was independent then $\{r_i\}$ spreads normally with nominal residue (*mean*) $\bar{r}_i = 0$ and residual standard deviation $\sigma_{r_i} = 1$, $r_i \sim N(0,1)$ portraying a symmetric

unimodal distribution. That's because if deviation's residual explicitness sways natural then its dispersion pattern would confine its density to the region under the normal curve else $\{r_i\}$ might disperse abnormally or scatter randomly.

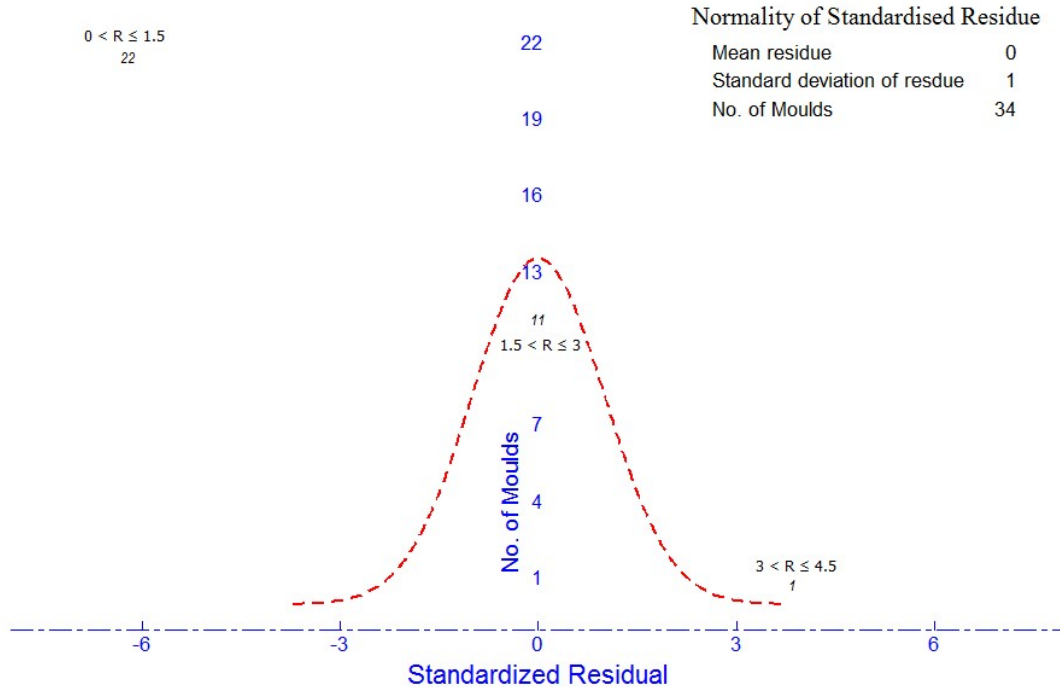


Figure 4.19 Normality of standardised residue.

Normal distribution function plot of standardised residues in Figure 4.19 couldn't represent 67.65% of the surveyed moulds, so they don't have residual standardised deviation. This asserts statistical evidence isn't enough to assume deviations are fully independent; instead they have some intra-categorical explicit residual deviation. While 32.35% of the surveyed moulds have standardised deviation residues, moreover they belong to a particular interval. Therefore, moulds with analytical runner sizes less than 1.5mm and more than 3mm would be incongruent without any residual standardised deviation. Thereof analytical runner size from 1.5 to 3 mm are likely to be tentatively congruent with some explicit deviation residue; incidentally this intuit synchronises with Eqn (4.32) as well as Figure 4.18 inference. That validates our proposed analytical criteria with an acceptable confidence, because runner size designs in most moulds are in that sub-range.

Reportedly, it enounces that congruence estimation undeniably involves variance σ_R^2 regardless of mould design type. Statistical contemplations reveal that even large survey size ($N \rightarrow \infty$) would modestly reduce nominal CoV *a.k.a. infinite survey size is necessary to feature*

congruence of actual and analytical runner sizes. Similarly, heuristic optimisation involves myriad trails or revisions for achieving the ideal design, because randomly or arbitrarily espoused ab-initio gestates are unlikely to realise perfection. Such a contrasting asymmetric diversity evidently recognises that despite rigorous optimisation empirical design is only a best estimate but can never converge into perfection. Therefore, the proposed analytical design criterion is more reliable than the traditional custom of succumbing to empiricism and then venturing never enough heuristic trails to optimise perplexing parameters. Besides the proposition being characteristically generic, parametrically engrosses machine, material and moulding sensitivity.

4.10. CONCLUSION

The series of extensive justifications above logically concludes that amid plastic injection mould development, the rationality of designing coherent runner-conduit analytically from power law parameters surely leads to better performance and superior quality. The proposed a priori criterion (*as in Eqn (4.26)*) balances mechanics and resolves an exclusive runner radius for a particular injection-moulding case. In addition, sensitising a hypothetical case explained its consistency across a de-facto range. Its statistical corroboration with real runners from production moulds affirmed 76.3% likely design congruence across 1.5 and 3mm sub-range. So, the proposed design criterion is valid by its relevance to general application possibilities. Although sensitivity plots don't insist potential designs; they instead reveal likely consequences or reliably imply incorporation of robustness. We hope this will endow mould designer with an auxiliary ability to recognise nonlinear interaction behaviour of the injectant clearly; that was impossible so far. Thus, henceforth ab-factoring will incorporate confidence and prods up the challenge of developing better moulds.

Chapter Five

Research Summary

At the outset, the purpose of this research was to study the critical design aspects of plastic injection mould. Based on the review of erstwhile literature, feed system features were perceived to be the most critical aspect to advance the rationale. Foretelling the importance of genericness and idealism of design criterion in injection moulding context limns the related speculate skill necessary to develop a mould.

Here the critical aspects to improve designing was to study the intriguing mechanics in sprue bush and runner insert. Applying well-known analytical solutions of functional mechanics gave explicit design criteria. These criteria progressed beyond retrieving proximate solutions from bygone knowledge to deterministically recognising the significance of present needs, resources, performance and quality expectations; besides it also led to earnest perceptions and arguments. That was essential because past knowledge retrieval is almost exhaustive to address all problems of the future, especially in a near net shape premise. Moreover, asserting subjective axioms like apprehending “*no-flow*” or “*transition*” regions is too indiscernible. Despite persistent debates on the refining ex-ante simulations contribute to mould designs, in reality they just endure vulnerable solution to a prevailing deprive, that too after rigorous analysis. Their benefits are neither comprehensive nor imitable in future; that’s why exact models were proposed across real configurable range of factors combinations for designing sprue and runner conduits. Since their inferences are specific, they’re summarised besides respective content discussion. Their sensitivities were explored beyond intrusion and rational grasp, using mathematical intelligence. The accuracy and precision of these pre-empted led to contributing an elaborate discourses on each aspect in the appending list of publications.

5.1. CONCLUSIONS

After thoroughly investigating the engagement of sprue-bush to nozzle-tip, where feed-system begins; it was found that the ability to mechanically seal mould engagement depends on pinch-angle between sprue-bush recess and nozzle-tip approach radii. That pinch-angle was able to discriminate leakage possibilities logically as rare and likely. An analytical criterion was deduced on expanding sprue-conduit with a combination of three factors that have independent significance levels. So forth, severe dependence of sprue-conduit expansion design on independent factors representing injectant character, capacity of injector and

impression features was the motivation for fifth publication. The dependence of injection-wise expansion in sprue-conduit on behavioural viscosity and characteristic shear thinning index was motivation for second publication. In general, this was because a comparative study of their sensitivity showed sprue-conduit expansion should widen for viscous incrust and narrow for shear thinning encrust. A critical investigation across de-facto injection moulding range found apparent viscosity had relative dominance among them. However, this dependence was found to be particularly sensitive to the way in which specific combinations were parameterised. Such a design criterion to improve likelihood specifically at the best AQL and APL is just the first time proposition towards idealism.

The critical consequences of neglecting non-Newtonian character in early designing of runner conduits were the motivation for the first publication. It was possible to empathetically describe the effects of shear thinning in thermoplastic injection across filling and packing interval using Power-law constitutive model and Hagen-Poiseuille solution. To avoid designing excursions, the criterion was bounded across a recursive range. The specific co-occurrence patterns of slope range on a log-log plot for runner-conduit radius over viscosity was able to distinguish the effects of Newtonian, non-Newtonian shear thinning and non-Newtonian shear thickening. The important observation there was the partial interference of de-facto region of thermoplastics and the region of rational runner size. This interference region made us to interpret that ideal runner design was achievable for every thermoplastic behaviour ever synthesised. Consideration of apparent viscosity with power-law description of generalised Newtonian concept to design runner-conduit for injection moulding thermoplastics was a motivation for the third publication. Sensitising runner design across de-facto thermoplastics range extended the direct relationship between runner-conduit size and in-situ melt state from so far believed linearity to exponential with discrete slope and altitude combination for each thermoplastic. This probably reflects the number of possibilities as well as flexibility of repertoire of inclusiveness. The aggressive dependence of injectant characteristics on cylindrical runner-conduit was the rationale in fourth publication. An exclusive design sensitisation of apparent viscosity and characteristic shear thinning index affirmed that a best design exists across de-facto injection moulding range for every real combination. Moreover, the proposed criteria and real runners from production moulds corroboration showed statistically likely design congruence.

Therefore, the criteria to design injection mould elements though depends on the accuracy of in-situ behaviour appreciation, would ultimately affect AQL and APL. This happens because all the factors and the sensitivities that follow presage that are continuously liable for every possible combination and discreetly existing throughout the de-facto range. Moreover, AQL and APL are mere relents in traditional and conventional criteria, but that's possible to expect in the proposed criteria. However, the need for managing proper combinations and smoothing the variances of each factor is ever recurrent. So, kinesis intervention was worth else if neglected becomes a prime reason for discrepancies. Nevertheless, accurate description of local behaviours like stiffness function of wall geometry, boundary function of transit injectant and phase interactions seeking original contributions from the theory of multiphase creep are real challenges. Thus, following statements are made in summarisation from the contributions of this study.

- a) The possibility to explain overall design sensitivities of each factor that configure a feed system in a mould was the main outcome. The design criterion proposed for sprue and runner conduit were able to override the need for assuming them empirically. The thematic criteria functions were able to fragment complexity and the proposed concept allows accuracy over almost all possible injection moulding configurations.
- b) Design sensitisation across de-facto extent validates the comprehensiveness of true criteria. As each factor in the parameterised model is itself a source of discussion, they individually become important in a specific local context. The pattern and sequence of sensitivity curves infer design important implications surging from functional-axioms, including amongst many other applications detection of defects enfolding likeliness from similarities with a known cause and effects in literature. Thus, this work can be seen as part of a broad knowledge on the design of moulds in which our understanding of a particular feature either in sprue or runner is proposed as a predictive model.
- c) Conversely the potential congruity of this true criterion on real moulds from production complements it's as an alternate opinion and is valuable to practise. Like it could also be used to improve flexibility, capacity and productivity of an existing mould.

5.2. LIMITATIONS

Non-linear conservation in plastic injection mould design depicts unique challenges to represent physical transformations through various tasks that are the basis for apt design from both theoretical and applied stances. This studies form an evaluative perspective on critical aspects of plastic injection mould through CSM. As its direct consequence following few

limitations was found, like around the natural extremes of characteristic size representing the conduit, singularity was shown for all factors in the proposed models. Although this affirms the validity of contentions in some sense, however the constraints apprehending both ex-ante and pragmatic endures are the ones that bind phenomenal diversities. It's likely that either extreme of the de-facto range for a physical parameter is speculative in real injection mould design situation. A considerable discrepancy challenge persists between the analytical solution and pragmatic astute, for whichever model is used. In contrast, despite ideal criteria contributions proposed here led us few steps ahead in the search for getting perfection, perhaps offering a generic framework. Therefore, we believe the sensitivity notions presented here are recurrently open for future investigations to become more explicit. As it's sensitivities doesn't necessarily offer direct substitutes, but their patterns here are consistent with both traditional and conventional beliefs.

Even though the proposed design criteria are effective, it begets accuracies from injectant properties, machine specifications and moulding features. Although the assumptions limit the aptness and precision to achieve expected better congruence. The salient lacunae affecting arguments and interpretations differ between the in-situ conditions and those involved in designing. *For example, peak injection speed is inherently slower than the speed expected.*

5.3. RECOMMENDATIONS FOR FUTURE WORK

Future research would focus on deterministic functions to compute feeding conduit designs for a typical injection mould context with an overall aim to achieve desired accuracy and precision. Besides all a posteriori aspects of inciting imperfections and compromising consequences have to be systematically analysed and thoroughly tied either quantitatively and/or qualitatively. Since rigorous treatment of exponential sensitivities is far beyond current state of research, it's more important to discuss the ideas that can eventually lead to determination of an ideal criteria. Such as uniqueness, compatibility, boundedness and well-posedness. As all factors have de-facto boundedness the immediate challenge is to determine comprehensive limits for each mould feature as well. Nevertheless, intercepting the characteristics of exact solutions to gain tangible AQL and APL benefits would always be recurring interest.

Appendix

Appendix 1 Technical Specifications of Injection Moulding Machine

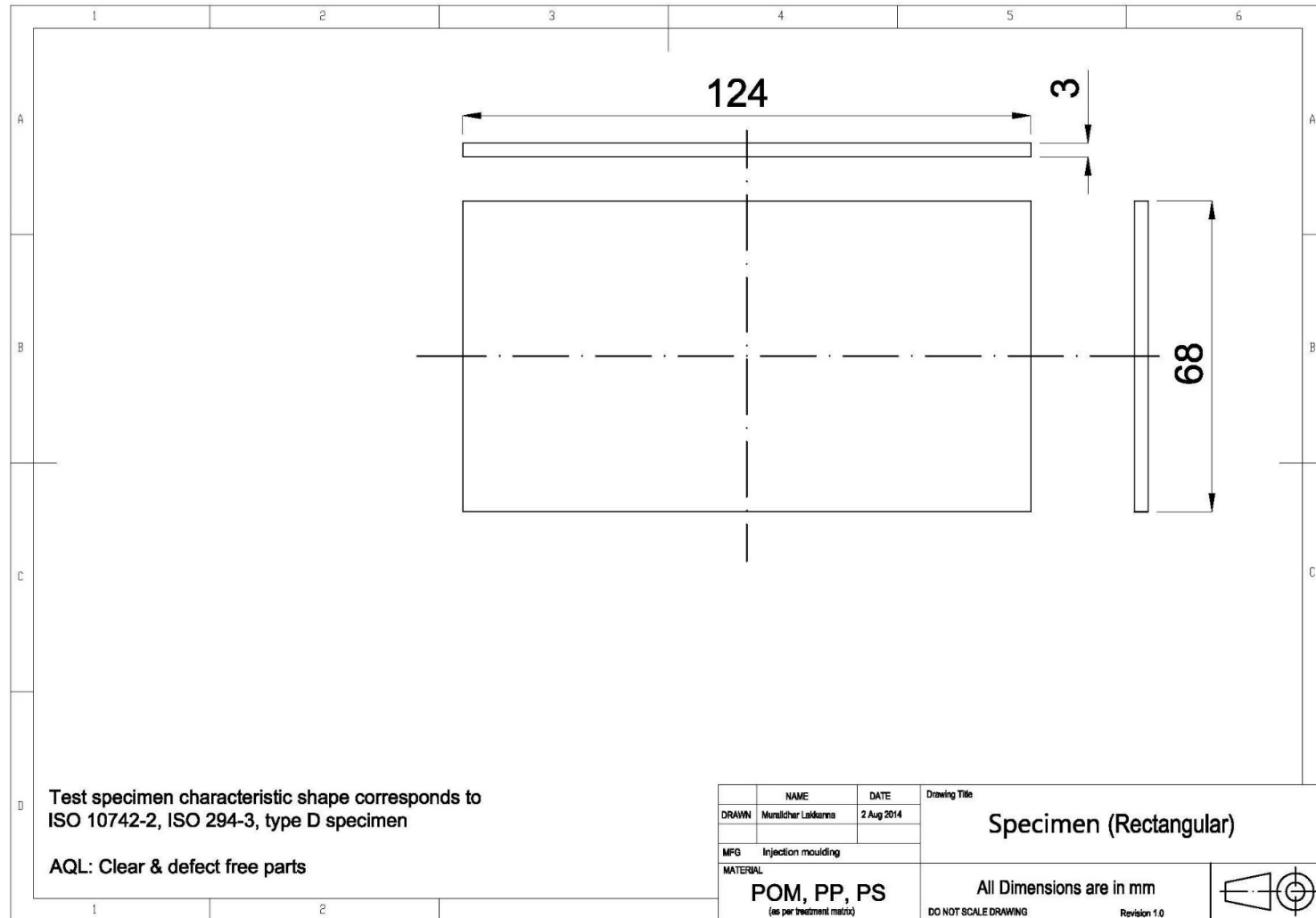
Futura series injection moulding machines (Futura'90, 2015)

Screw diameter	35 mm
Screw length	19 mm
Stroke volume	$130 \times 10^3 \text{ mm}^3$
Injection weight max	123 gram
Injection rate	$127 \times 10^3 \text{ mm}^3/\text{sec}$
Plasticising rate	15 gram/sec
Injection pressure $\pm 2 \%$	1592 bar
Rotational speed of screw	275 rpm
Clamping force	900 kN
Mould operating stroke	320 mm
Distance between tie bars H x V	360 x 360 mm
Mould thickness, min/max.	100 – 350 mm
Ejector stroke	100 mm
Ejector force	29.4 kN
Ejector number	5 pcs
Pump drive	9.78 kW
Installed heating capacity	6.46 kW
Total connected power	16.24 kW
Machine dimensions (L x W x H)	3.8 x 1.6 x 1.8 m
Oil tank capacity	190 litre
Net weight (without Oil)	3.9 t

Appendix 2: Accuracy of injection moulding machine control system

Melt temperature	$\pm 3^\circ \text{C}$
Mould temperature	$\pm 3^\circ \text{C}, \leq 80^\circ \text{C}$ $\pm 5^\circ \text{C}, \geq 80^\circ \text{C}$
Hold pressure	$\pm 5 \%$
Injection time	$\pm 0.1 \text{ sec}$
Hold time	$\pm 5 \%$
Shot weight	$\pm 2 \%$

Appendix 3: Test specimen drawing



References

Abel M Subhas, Datti P S and Mahesha N (14 Feb 2009), Flow and heat transfer in a power law fluid over a stretching sheet with variable thermal conductivity and non-uniform heat source, *Intl. jour of heat & mass transfer*, 52(11-12):2902-2913, doi: 10.1016/j.ijheatmasstransfer.2008.08.042, ISSN: 0017-9310, Elsevier Science Publishers B V, Amsterdam, The Netherlands.

Akbarzadeh A and Sadeghi M (June 2011), Parameter study in plastic injection molding process using statistical methods and IWO algorithm, *Intl. jour of model optimisation*, 1(2):141–145 (1022406), doi: 10.7763/IJMO.2011.V1.25, ISSN 2010-3697.

Amano Osamu and Utsugi Shirou (25 Feb 1989), Temperature measurements of polymer melts in the heating barrel during injection moulding Part 2: 3D temperature distribution in the reservoir, *Polymer Engineering & Science*, 29(3):171–177, doi: 10.1002/pen.760290304, ISSN: 1548-2634, Society of Plastics Engineers, NY, USA.

Amran, M A; Hadzley, M; Amri, S; Izamshah, R; Hassan, A; Samsi, S; Shahir, K (29 May–1 June 2009) Optimisation of gate, runner and sprue in two plate family plastic injection mould, *American Institute of Physics conference proceedings*, Langkawi, Kedah, Malaysia, 1217:309, doi: 10.1063/1.3377834

Angstadt D C and Coulter J P (1999), Cavity pressure and part quality in the injection moulding process, 89:7-18, *Symposium on the science, automation, and control of material processes involving coupled transport and rheology changes*, ed. Ilegbusi O J, Oyeleye G O and Coulter J P, Nashville, TN, ISBN: 0791816621, Transactions of the ASME, NY, USA.

Bagley E B and Schreiber H P (March 1961), Effect of die entry geometry on polymer melt fracture and extrudate distortion, *Journal of Rheology*, 5(1):341–353, doi: 10.1122/1.548904, ISSN: 0148-6055, The Society of Rheology, New Jersey, USA.

Baldi Francesco, Franceschini Anika and Bignotti Fabio (1 Oct 2011), On the measurement of the high rate flow properties of organo-clay platelet filled polyamide 6 melts by capillary rheometer, *Polymer Testing*, 30(7):765–772, doi: 10.1016/j.polymertesting.2011.07.002, ISSN 0142-9418, Elsevier Science Publishers B V, Amsterdam, The Netherlands.

Bapat Ravindra B (2012), *Linear algebra and linear models*, 3ed., doi 10.1007/978-1-4471-2739-0, ISBN 978-1-4471-2739-0, Springer-Verlag Ltd, London, UK.

Barbosa Carlos Nuno, Julio C. Viana, Markus Franzen, and Ricardo Simoes (8 Aug 2012) Towards improved impact performance of injection moulded parts, *Plastics Research*, doi: 10.2417/SPEpro.004288, Society of Plastics Engineers, NY, USA.

Barlow Sir William (1986) Engineering design for profit, *International Journal of Technology Management*, 1(3/4):341-9, doi: 10.1504/IJTM.1986.026115, ISSN 0267-5730, InderScience Publishing.

Barnes Howard A, Hutton John Fletcher and Walters Kenneth (2005), *An introduction to rheology*, Volume 3 of Annals of Discrete Mathematics, Rheology series, 1ed, 7 Impression, doi:10.1016/B978-0-444-87469-6.50001-9, ISBN 0-444-87469-0, Elsevier Science Publishers B V, Amsterdam, The Netherlands.

Beaumont John P (2001) Revolutionizing runner designs in hot and cold runner molds, *ANTEC*, 59:3680-3687, Society of Plastics Engineers, NY, USA.

Beaumont John P (2007) *Runner and Gating Design Handbook*, 2ed., ISBN 13 978 1 56990 421 3, Carl Hanser Verlag GmbH & Co. KG, Munich, Germany.

Belofsky Harold (01 April 1995) *Plastics: Product Design and Process Engineering*, ISBN 1-56990-142-2, Carl Hanser Verlag GmbH & Co. KG, Munich, Germany.

Bezzo F, Macchietto S, Pantelides C C (July 2000) A general framework for the integration of CFD and process simulation, *International Journal of Computer Applications in Chemical Engineering*, 24(2-7):653-658, doi:10.1016/S0098-1354(00)00372-0, ISSN: 0098-1354, Elsevier Science Publishers B V, Amsterdam, The Netherlands.

Bikas Athanasios, Pantelelis Nikos and Kanarachos Andreas (5 March 2002) Computational tools for the optimal design of the injection moulding process, *Journal of Materials Processing Technology*, 122(1):112–126, doi:10.1016/S0924-0136(01)01248-1, ISSN: 0924-0136, Elsevier Science Publishers B V, Amsterdam, The Netherlands.

Bird Robert Byron, Stewart Warren E and Lightfoot Edwin N (2007), *Transport phenomena*, 2ed (rev.), ISBN 978-0-470-11539-8, John Wiley & Sons, Inc., NY, USA.

Blake Terence D (1 July, 2006) The physics of moving wetting lines, *Journal of colloid and interface science*, 299(1):1-13, doi: 10.1016/j.jcis.2006.03.051, ISSN: 0021-9797, Elsevier Science Publishers B V, Amsterdam, The Netherlands.

Bociaga E and Jaruga T (Feb 2007), Experimental investigation of polymer flow in injection mould, *Archives of material science & engineering*, 28(3):165-172, ISSN 1897 2764, International OCSCO world press, Poland.

Bolur Prabodh C (2000) *A Guide of Injection Moulding of Plastics*, 3ed, ISBN 81-7764-000-3, Allied Publishers Ltd, India.

Boronat T, Segui V J, Peydro M A and Reig M J (1 March 2009), Influence of temperature and shear-rate on the rheology and processability of reprocessed ABS in injection molding process, *Jour of mat. proc. tech.*, 209(5):2735 2745, doi: 10.1016/j.jmatprotec.2008.06.013, ISSN: 09240136, Elsevier Science Publishers B V, Amsterdam, The Netherlands.

Bozdana A Tolga and Eyercioglu Omer (6 Oct 2002), Development of an expert system for the determination of injection moulding parameters of thermoplastic materials: EXPIMM, *Jour of mat. proc. tech.*, 128(1-3): 113–122, doi: 10.1016/S0924-0136(02)00436-3, ISSN: 0924 0136, Elsevier Science Publishers B V, Amsterdam, The Netherlands.

Bozzelli John (July 2004), How to Stop Flash, *Plastics Technology*, 50(7);50-51, ISSN: 0032 1257.

Bozzelli John P (June 2012), Understanding polymer flow: Interpreting the viscosity curve, *Plastics tech.*, 58(6); 23-25, ISSN: 0032 1257.

Brincat Paul, Friedl Chris and Talwar Kapil (26-30 April 1998), Extensional viscosity modeling for injection molding simulation, in *Proceedings of 56th ANTEC*, Atlanta, GA, Part 1 (of 3);552-556, Society of Plastics Engineers, NY, USA.

Britton G A, Tor S B, Lam Y C, Deng Y M (15 Aug, 2001) Modelling functional design information for injection mould design, *International Journal of Production Research*, 39(12):2501–2515, doi:10.1080/00207540110048954, ISSN 0020 7543, CRC Press, Taylor & Francis Ltd., Singapore.

Britton G A, Tor S B, Lam Y C, Deng Y M (15 August 2001) Modelling functional design information for injection mould design, *International Journal of Production Research*, 39(12):2501–2515, doi:10.1080/00207540110048954, ISSN 0020 7543, CRC Press, Taylor & Francis Ltd., Singapore.

Broyer E, Gutfinger C and Tadmor Z A (1975) Theoretical Model for the Cavity Filling Process in Injection Molding, *Transactions of society Rheology*, 19(3):423.-444, doi:10.1122/1.549379, ISSN: 0038-0032, The Society of Rheology, New Jersey, USA.

Bryce Douglas M (1997), *Plastic injection moulding, Vol II Material selection and product design fundamentals*, ISBN 0-87263-488-4, SME, Dearborn, MI, USA.

Bryce Douglas M (1998), *Plastic injection moulding, vol III: Mould design and construction fundamentals*, ISBN 0-87263-495-7, SME, Dearborn, MI, USA.

Buck S G (2001), Material for Seal Faces, *Pumps & Systems*, Cahaba Media Group, Birmingham, AL, UK.

Campo Edgar Alfredo (2006) *The complete part design handbook for injection moulding of thermoplastics*, doi: 10.3139/9783446412927, ISBN-13: 978-3-446-40309-3, Carl Hanser Verlag GmbH & Co. KG, Munich, Germany.

Cao Wei, Shen Changyu, Zhang Chunjie and Wang Lixia (May 2008) Computing flow-induced stresses of injection molding based on the Phan–Thien–Tanner model, *Archive of Applied Mechanics*, 78(5):363–377, doi: 10.1007/s00419-007-0167-4, ISSN: 0939-1533, Springer-Verlag Ltd, London, UK.

Cardozo D (30 Sept 2008) Three models of the 3D filling simulation for injection Molding: A Brief Review, *Journal of Reinforced Plastics & Composites*, 27(18):1963-74, doi: 10.1177/0731684408092386, ISSN 0731 6844, SAGE Publications, NY, USA.

Chang Rong-yeu, Yang Wen-hsien (30 Sept, 2001) Numerical Simulation of Mould Filling in Injection Moulding using 3D finite volume approach, *International Journal of Numerical Methods in Fluids*, 37(2):125-148, doi: 10.1003/flid.166, ISSN: 1097-0363, John Wiley & Sons, Inc., NY, USA.

Cheater G (1978), Economic material use in injection moulding, in *Developments in injection moulding*, 1ed., Pp. 155-168, doi 10.1007/978-94-009-9649-6_6, ISBN 978-94-009-9651-9, Applied sci pub ltd, Shrewsbury, UK.

Chen Chin Piao, Chuang Ming Tsan, Hsiao Yun Hsiang, Yang Yung Kuang, Tsai Chih Hung (Sept 2009), Simulation and experimental study in determining injection molding process parameters for thin-shell plastic parts via design of experiments analysis, *Expert sys. with applns*, 36(7):10752–10759, doi: 10.1016/j.eswa.2009.02.017, ISSN: 0957 4174, Elsevier Science Publishers B V, Amsterdam, The Netherlands.

Chen L L, Chou S Y and Woo T C (Dec 1993), Parting directions for mould and die design, *Computer aided design*, 25(12):762–768, doi: 10.1016/0010-4485(93)90103-U, ISSN: 0010 4485, Elsevier Science Publishers B V, Amsterdam, The Netherlands.

Cheng Jin, Liu Zhenyu, Tan Jianrong (May 2013) Multiobjective optimisation of injection molding parameters based on soft computing and variable complexity method, *International journal of advanced manufacturing technology*, 66(5):907-916, doi:10.1007/s00170-012-4376-9, ISSN 0268-3768, Springer-Verlag Ltd, London, UK.

Chhabra Rajendra P and Richardson J F (2008) *Non-Newtonian Flow and Applied Rheology*, 2ed., ISBN: 978-0-7506-8532-0, Butterworth Heinemann.

Chiang S M, Huang C H, Chiu K Y and Hung S Y (2006), Runner system for a plastic injection mould, *US Patent* 0198922A1.

Chin K S, Mok C K, Zu Xu (Sept. 2007) Modelling and performance simulation of mould design process, *International journal of advanced manufacturing technology*, 34(3-4);236-251, doi:10.1007/s00170-006-0584-5, ISSN 0268-3768, Springer-Verlag Ltd, London, UK.

Cogswell F N (2003), *Polymer melt rheology*, doi: 10.1533/9780857092984.frontmatter, ISBN: 978-1-85573-198-1, Woodhead publishing ltd, Cambridge, UK.

Collier J R (9-10 Oct 1973), Predicting plastics performance, in *EP & S Division technical conf.*, Downingtown, PA, Pp 79-85, Society of Plastics Engineers, NY, USA.

Constantine A G and Hall Peter (1994), Characterizing surface smoothness via estimation of effective fractal dimension, *Journal of the Royal Statistical Society: Series B (Methodological)*, 56(1):97-113, ISSN: 0035 9246, Royal Statistical Society, UK.

Costa C A, Young R I M (2001) Product range models supporting design knowledge reuse, *Journal of Engineering Manufacture*, Proceedings of the IMECHE Part B, 215(3):323–37, doi:10.1243/0954405011515406, ISSN: 0954-4054, Professional Engineering Publishing.

Costa Franco S, Ray Shishir, Friedl Chris, Cook Peter S, Xu Shoudong (6-10 May 2001) The Effect of Inertia on fill pattern in injection molding, *ANTEC*, Dallas, Texas, vol III Special areas M5P1:454-459, Society of Plastics Engineers, NY, USA.

Crawford Roy J (1987), *Rubber and plastic engineering design and application*, ISBN 10 - 0852985711, Allied Publishers, London, UK.

Crow Edwin L and Shimizu Kunio (1988), *Log-normal distributions: theory and application*, ISBN 0-8247-7803-0, Marcel Dekker Inc, NY, USA.

Dacey W E (1990), Cost of Engineering Changes at Various Stages of Electro-Mechanical System Development, *Proceedings of 4th Design for manufacturability conference*, Dallas, TX, USA.

Deshpande Shailesh V and Iyer Kannan N (1997), Mathematical Modeling of flow in trapezoidal runners, in *7th Asian congress of fluid mechanics*, Pp. 601-603, ISBN 8170237327, Indian Institute of Technology, Chennai.

Doane J C, Myrum T A and Beard J E (April–May 1991), An experimental-computational investigation of heat transfer in mechanical face seals, *International Journal of Heat Mass Transfer*, 34(4/5):1027-1041, doi:10.1016/0017-9310(91)90014-6, ISSN: 0017-9310, Elsevier Science Publishers B V, Amsterdam, The Netherlands.

- Dray Sr. Robert F (2 July 2002) Shut Off Valves, *US Patent 6413076 B1*.
- Dray Sr. Robert F (March/ April 2005), 4 worst plastic injection mould design, *Plastics Machinery & Auxiliaries*, Canon Communications Llc., TX, USA.
- Dym Joseph B (1987) *Injection Moulds & Moulding: A practical manual*, 2ed., ISBN 10-0442222238, Van Nostrand Reinhold publisher, NY, USA.
- Etsion Izhak, Kligerman Y and Halperin G (1 January1999), Analytical & Experimental Investigation of Laser-textured Mechanical Seal Faces, *Tribology Transactions*, 42(3):511-516, doi:10.1080/10402009908982248, ISSN 1040-2004, CRC Press, Taylor & Francis Ltd., Singapore.
- Evans J R G and Hunt K N (January 1991), A heated sprue bush for ceramic injection moulding, *Journal of material science letters*, 10(12):730-733, doi:10.1007/BF00722783, ISSN 0261-8028, Kluwer Academic Publishers, Boston, USA.
- Falah Ahamad (Jan-March 2014), Behaviour and melt viscosity of PC/LDPE blend in capillary flow, *International Journal of ChemTech Research*, 6(1):316-323, ISSN 0974 4290, Sai Scientific Communications, Mumbai, India
- Fan Bingfeng, Kazmer David O, Nageri Ranjan (April 2006) An Analytical Non-Newtonian and Nonisothermal Viscous Flow Simulation, *Polymer-Plastics Technology and Engineering*, 45(3):429-438, doi:10.1080/03602550600554018, ISSN 0360-2559, CRC Press, Taylor & Francis Ltd., Singapore.
- Ferreira Irene, Cabral Jose A, Saraiva Pedro M (26-28 June 2013) Axiomatic design as a creative innovation tool applied to mold design, *7th International conference on axiomatic design*, ICAD-2013-25:169, doi: 10.1002/pen.760352303, Worcester, MA, USA.
- Ferreira, Irene; Weck, Olivier de; Saraiva, Pedro; Cabral, Jose (2010) Multidisciplinary optimisation of injection molding systems, *Structural Multidisciplinary Optimisation*, 41(4):621–635, doi: 10.1007/s00158-009-0435-8, ISSN 1615-147X, Springer-Verlag Ltd, London, UK.

Finnie Richard (6-7 Dec 2011), Advantages of a cold runner system, *Silicone Elastomers*, Chicago, IL USA.

Fleming Don J (19 April 2004) Polymer Rheology, *Expert Lecture*, at Telford Polymer Association for Rapra Technology.

Flitney Robert (11 July 2014) *Seals & Sealing Handbook*, 6ed., doi:10.1016/B978-0-08-099416-1.00008-5, ISBN: 978-0-08-099416-1, Butterworth-Heinemann, Elsevier Science Publishers B V, Amsterdam, The Netherlands.

Friedrichs B, Guceri S I (Dec 1995) Hybrid numerical technique to model 3D flow fields in resin transfer molding processes, *Polymer Engineering & Science*, 35(23):1834-1851, doi: 10.1002/pen.760352303, ISSN 1548-2634, Society of Plastics Engineers, NY, USA.

Futura'90, (2015) Electronica Plastic Machines Limited, Gat No. 399, Hissa No. 1 & 2, Bhare. Tal Mulshi, Dist Pune 412 115, Serial Number 2567, FU00900056 at Om Vinayaka Industries. - Timber yard layout, Mysore road, Bangalore.

Gan T W, Choudary I A and Nukman Y (2010), Mold Filling analysis by using finite volume method, in *11th Asia pacific industrial engg & mngt. sys. conf.*, Int. foundn. for prodn res., Meleka, Malaysia, Pp 512.

Glaesener Pierre (20 Oct 2009) Moulding machine & melt channel interface, *US Patent 7604477 B2*.

Glanvill A B and Denton E N (1965) *Injection Mould Design Fundamentals*, American edition, ISBN-10 0831110333, Industrial Press Inc, NY, USA.

Goodship Vanessa (2004), *Arburg practical guide to injection moulding*, ISBN 1-85957-444-0 – 9781859574447, iSmithers Rapra Publishing, Shropshire, UK.

Goodship Vanessa (2004), *Troubleshooting injection moulding*, 15(4), ISBN 185957470X, 9781859574706, iSmithers Rapra Publishing, Shropshire, UK.

Gordon Guthrie (2012) Multi-Scale Nano-processing of Polymeric Products, *Ph.D. Thesis*, National Science Foundation Grant No 0425826, UML Nanomanufacturing Centre,

Department of Plastics Engineering, University of Massachusetts Lowell, Lowell, Massachusetts 01854, USA,

Gordon Jr M Joseph (2010), *Total quality process control for injection moulding*, 2ed., ISBN 0470584483- 9780470584484, John Wiley & Sons, Inc., NY, USA.

Goutille Yannick and Guillet Jacques (12 January 2002), Influence of filters in the die entrance region on gross melt fracture: extrudate and flow visualization, *Journal of Non-Newtonian Fluid Mechanics*, 102(1):19–36, doi:10.1016/S0377-0257(01)00125-2, ISSN 0377-0257/02, Elsevier Science Publishers B V, Amsterdam, The Netherlands.

Graebel William I (19 Jan 2001), *Engg fluid mechanics*, Intl. student ed., ISBN 9781560327110, CRC Press, Taylor & Francis Ltd., Singapore.

Green Thomas M (3 Aug 1989), Injection moulding machine having nozzle leak detecting system construction, *US Patent 4921416 A*.

Haley John E (Fall 2009), The importance of mould design to productivity, *Production*, AQA Corporation, USA.

Han Chang Dae (May 1973), Influence of the die entry angle on the entrance pressure drop, recoverable elastic energy, and onset of flow instability in polymer melt flow, *Journal of Applied Polymer Science*, 17(5):1403–1413, doi: 10.1002/app.1973.070170508, ISSN: 1097-4628, John Wiley & Sons, Inc., NY, USA.

Han Ruihua, Shi Linhuo, Gupta Mahesh (Mar 2000) Three-dimensional simulation of microchip encapsulation process, *Polymer Engineering & Science*, 40(3):776-785, doi: 10.1002/pen.11207, ISSN 1548-2634, Society of Plastics Engineers, NY, USA.

Harper Charles A (2006), *Handbook of Plastic Processes*, doi: 10.1002/0471786586, ISBN 13:978-0-471-66255-6, John Wiley & Sons, Inc., NY, USA.

Harter H Leon (Dec 1960), Critical values for Duncan's new multiple range test, *Biometrics: Journal of the International Biometric Society*, 16(4):671-685, doi: 10.2307/2527770, ISSN: 1541-0420.

Hassan Handy (July 2013), An experimental work on the effect of injection moulding parameters on the cavity pressure and product weight, *International journal of advance manufacturing technology*, 67(1):675-686, doi: 10.1007/s00170-012-4514-4, ISSN: 0268-3768, Springer-Verlag Ltd, London, UK.

Hassan Handy, Regnier Nicolas, Le Bot Cedric, Defaye Guy (Jan 2010), 3D study of cooling system effect on the heat transfer during polymer injection molding, *International journal of thermal sciences*, 49(1):161–169, doi: 10.1016/j.ijthermalsci.2009.07.006, ISSN 1290-0729, Elsevier Masson SAS, Elsevier Science Publishers B V, Amsterdam, The Netherlands.

Hatch R (Sept 1999) Trouble Shooter Part 34 // Sinks inside a moulded plug, *Injection Moulding*, 7(9):106-111, USA.

Hatzikiriakos Savvas G (October 1994), The onset of wall slip and sharkskin melt fracture in capillary flow, *Polymer Engineering & Science*, 34(19): 1441–1449, doi: 10.1002/pen.760341902, ISSN: 1548-2634, Society of Plastics Engineers, NY, USA.

Henz Joe (June 2013), What's different about molding engg plastics, *Plastics tech.*, ISSN: 0032 1257.

Hetu, J F, Gao D M, Garcia-Rejon A, Salloum G (Feb 1998) 3D finite element method for the simulation of the filling stage in injection molding, *Polymer Engineering & Science*, 38(2):223-236, doi: 10.1002/pen.10183, ISSN 1548-2634, Society of Plastics Engineers, NY, USA.

Hieber C A, Shen S F (1979) A finite element/finite difference simulation of the injection-molding filling-process, *Journal of Non-Newtonian Fluid Mechanics*, 7(1):1-32, doi:10.1016/0377-0257(80)85012-9, ISSN: 0377-0257, Elsevier Science Publishers B V, Amsterdam, The Netherlands.

Hieber Cornelius A (29 June 1987) "Melt viscosity characterisation and its application to injection molding", Pp 1- 129, in *Injection & comp. molding fund.*, ed Isayev Avraam I, ISBN 0 8247 7670 4, Marcel Dekkar Inc, NY, USA.

Hill D (20 Oct, 1996) Further studies of the injection moulding process, *Applied Mathematical Modelling*, 20(10): 719–730, doi:10.1016/0307-904X(96)00069-8, ISSN: 0307-904X, Elsevier Science Publishers B V, Amsterdam, The Netherlands.

Hirt C W (1-2 May 1991) A Flow-3D study of the importance of fluid momentum in mould filling: Numerical Simulation of Casting solidification in automotive applications, *18th Annual Automotive Materials Symposium*, FSI-91-00-02, Kellogg Centre, Michigan State University, East Lansing, Michigan, USA.

Hoffman David A and Beaumont John P (Aug,2013), A new look at evaluating fill times for injection molding, *Plastics tech.*, 59(8):22-29+41-44, ISSN: 0032 1257.

Howard Black Paul and Eugene Adams Otto (6 Dec 2007), *Machine Design*, 3ed, Mechanical Engineering Series, ISBN 0-07-085037-2, McGraw-Hill, NY, USA.

Hsiung C M and Sheng Q (Sept 1997) A rectilinear flow model approach to the simulation of the injection molding process, *Journal of Reinforced Plastics & Composites*, 16(13):1242-51, doi: 10.1177/073168449701601308, ISSN 0731 6844, SAGE Publications, NY, USA.

Hsiung C M, Cakmak M and Ulcer Y (Sept 1996) A structure oriented model to simulate the shear induced crystallization in injection molding polymers: A Lagrangian approach, *International Journal for the Science and Technology of Polymers*, 37(20):4555-71, doi:10.1016/0032-3861(96)00291-1, ISSN: 0032-3861, Elsevier Science Publishers B V, Amsterdam, The Netherlands.

Huang Ming Shyan (23 March 2007) Cavity pressure based grey prediction of the filling-to-packing switchover point for injection moulding, *Journal of Materials Processing Technology*, 183(2-3):419–424, doi: 10.1016/j.jmatprotec.2006.10.037, ISSN: 0924-0136, Elsevier Science Publishers B V, Amsterdam, The Netherlands.

Huang Ming-Shyan and Lin T Y (Dec 2008), Simulation of a regression-model and PCA based searching method developed for setting the robust injection molding parameters of multi-quality characteristics, *Intl. jour of heat & mass transfer*, 51(25-26):5828– 5837, doi: 10.1016/j.ijheatmasstransfer.2008.05.016, ISSN: 0017 9310, Elsevier Science Publishers B V, Amsterdam, The Netherlands.

Hussey Lance (2012) 5 Must have feature in your concept design, *White Paper*, PTCorp, Pp. 1-4.

Hwang C J, Kwon T H (Jan 2002) A full 3D finite element analysis of the polymer injection molding filling process including slip phenomena, *Polymer Engineering & Science*, 42(1):33-50, doi: 10.1002/pen.10926, ISSN 1548-2634, Society of Plastics Engineers, NY, USA.

Ilinca Florin, Héту Jean-François (1-5 May 2005) Optimization of the injection molding process using design sensitivity analysis, *ANTEC, Boston, Massachusetts, Injection Molding -23T4, Process 2*, 101663: 2129-2133, ISBN: 9781604234527, Society of Plastics Engineers, NY, USA.

Ilinca Florin, Héту Jean-François and Pelletier Dominique (14 July 2004) Design sensitivity analysis for the optimization of the injection moulding process, *International polymer processing journal*, 20(1):86-92, doi: 10.3139/217.1864, ISSN 0930-777X, Carl Hanser Verlag GmbH & Co. KG, Munich, Germany.

Imihezri S S S, Sapuan S M, Sulaiman S, Hamdan M M and Zainudin E S (2006), The simulation study of the effect is single and double gated moulds on pressure and temperature in injection molding of polymeric composite clutch pedals, *Multidiscipline modeling in materials & structures*, 2(3):355-362, doi: 10.1163/157361106777641350, ISSN: 1573-6105, Emerald Insight.

Inn Y W, Fischer R J and Shaw M T (1998), Visual observation of development of sharkskin melt fracture in polybutadiene extrusion, *Rheologica acta*, 37(6):573-582, doi: 10.1007/s003970050144, ISSN: 0035 4511, Springer-Verlag Ltd, London, UK.

Isayev Avraam I and Upadhyay Ram K (1987), "Flow of polymeric melts in juncture regions of injection molding", Pp 137- 226 in *Injection & comp. molding fund.*, ed Isayev Avraam I, ISBN 0-8247-7670-4, Marcel Dekkar Inc, NY, USA.

ISO 10072:2004, *Tools for moulding, Sprue Bushes, Dimensions*, 2ed. International Organisation for Standardisation, Geneva, Switzerland.

Jackson Chad (July 2011) Trends in Concept Design, *Survey based study including 214 mould making individuals response*, PTCorp, <http://www.ptc.com/go/concept-design>.

Janke Steven J and Tinsley Frederick C (July 2005), *Introduction of linear models and statistical inference*, doi: 10.1002/047174011X, ISBN: 978-0-471-66259-4, John Wiley & Sons, Inc., NY, USA.

Jaworski Zdzislaw, Zakrzawska Barbara (24 May 2010) Towards Multiscale Modelling in Product Engineering, *International Journal of Computer Applications in Chemical Engineering*, 35(3):434-445, doi: 10.1016/j.compchemeng.2010.0.5.009, ISSN: 0098-1354, Elsevier Science Publishers B V, Amsterdam, The Netherlands.

Johannaber Friedrich (2008), *Injection moulding machines*, 4ed., doi: 10.3139/9783446450110, ISBN: 978-3-446-22581-7, Carl Hanser Verlag GmbH & Co. KG, Munich, Germany.

Johnson Norman L, Kotz Samuel and Balkrishan N (Oct. 1994), *Continuous univariate distributions*, vol 1, ISBN: 978-0-471-58495-7, John Wiley & Sons, Inc., NY, USA.

Johnston Stephen, David Kazmer, Zhaoyan Fan and Robert Gao (6-11 May 2007), Causes of melt temperature variations observed in the nozzle during injection moulding, *ANTEC*, Cincinnati, Ohio, 2:1073-1077, ISBN 978-0-9753707-5-9, Society of Plastics Engineers, NY, USA.

Jones Peter (2008), *Mould design guide*, ISBN 978-1-84735-087-9, iSmithers Rapra Technology, Shropshire, UK.

Jones Peter (2009), *Budgeting, costing and estimating for the injection moulding industry*, ISBN 1847352111 - 978-1-84735-211-8, iSmithers Rapra Publishing, Shropshire, UK.

Jong Wen-Ren, Wu Chun-Hsien and Lee Ming-Yen (2011) Feature-based integration of conceptual and detailed mould design, *International Journal of Production Research*, 49(16):4833-4855, doi:10.1080/00207543.2010.504421, ISSN 0020-7543, ISSN 0020 7543, CRC Press, Taylor & Francis Ltd., Singapore.

Jong Wen-Ren, Wu Chun-Hsien, Liu Hung Hsun and Li Ming-Yan, (4 March 2009) A collaborative navigation system for concurrent mold design, *International journal of advanced manufacturing technology*, 40(3-4): 215-225, doi:10.1007/s00170-007-1328-x, ISSN 0268-3768, Springer-Verlag Ltd, London, UK.

Kamal M R, Mashelkar R A and Mujumdar A S (1989), *Transport phenomena in polymer systems*, Pp. 133–217, ISBN 0-7458-0663-5, John Wiley & Sons, Inc., NY, USA.

Kamal M R, Youti K and Doan P H (Dec 1975) The Injection moulding behaviour of thermoplastics in thin rectangular cavities, *Polymer Engineering & Science*, 15(12):863-868, doi: 10.1002/pen.760151208, ISSN 1548-2634, Society of Plastics Engineers, NY, USA.

Kaushal Hitesh and Ursu Douglas (5 March 2009) Injection moulding nozzle wedge seal, *US Patent 20100227019 A1*.

Kazmer David O (1997) Best Practices in Injection molding, *Journal of Injection Moulding Technology*, doi:10.1.1.586.1712, Society of Plastics Engineers, NY, USA.

Kazmer David O (2016) *Injection Mould Design Engineering*, 2ed, doi: 10.3139/9781569905715, ISBN 13 978 1 56990 417 6, Carl Hanser Verlag GmbH & Co. KG, Munich, Germany.

Kazmer David O (21-23 June 2000) Axiomatic design of the injection molding process, *1st International Conference on Axiomatic Design*, 991:123-9, Cambridge, Institute for Axiomatic Design, MA, USA.

Kazmer David O and Speight Russell G (1997) Polymer Injection Molding Technology for the Next Millennium, *Journal of Injection Molding Technology*, 1(2):81-90, Society of Plastics Engineers, NY, USA.

Kenig S (1972), Injection moulding of thermoplastics, *Ph.D. Thesis*, Department of Chemical Engineering, McGill University.

Kennedy Gerard P and Donnelly John P M (6 Aug 1996) Leak Detector for Injection Moulding Machine, *US Patent 5542835 A*.

Kennedy Peter Kenneth (2008) “Practical & Scientific aspects of injection molding simulation”, *PhD Thesis*, ISBN 978 90 386 1275 1, Technische Universiteit Eindhoven, Eindhoven, The Netherlands.

Kennedy Peter Kenneth and Zheng R (May 2013), *Flow analysis of injection moulds*, 2ed., ISBN: 978-156990512-8, Carl Hanser Verlag GmbH & Co. KG, Munich, Germany.

Khomami B and Ranjbaran M M (July 1997), Experimental studies of interfacial instabilities in multilayer pressure driven flow of polymeric melts, *Rheologica Acta*, 36(4):345-366, doi: 10.1007/BF00396323, ISSN: 0035 4511, Springer-Verlag Ltd, London, UK.

Khor C Y, Ariff Z M, Che Ani F, Mujeebu M Abdul, Abdullah M K, Abdullah M Z, Joseph M A (Feb 2010) Three-dimensional numerical and experimental investigations on polymer rheology in meso-scale injection molding, *Intl. conrn. in heat & mass transfer*, 37(2):131–139, doi: 10.1016/j.icheatmasstransfer.2009.08.011, ISSN: 0735-1933, Elsevier Science Publishers B V, Amsterdam, The Netherlands.

Kim B H and Ramesh M C (01 Nov 1995), Automatic runner balancing of injection molds using flow simulation, *Journal of engineering for industry*, 117(4):508–515, doi: 10.1115/1.2803528, ISSN: 0022 0817, Transactions of the ASME, NY, USA.

Kim Sang-Woo, Turng Lih-Sheng (19 April 2004) Developments of three-dimensional computer-aided engineering simulation for injection moulding, *Modelling & Simulation in Materials Science & Engineering*, 12(3): 151-173, doi: 10.1088/0965-0393/12/3/S07, ISSN: 0965-0393, Institute of Physics Publishing, Bristol, UK

Kim Y J and Cho B R (Nov 2000), Economic consideration on parameter design, *Quality & reliability engg intl.*, 16(6):501–514, doi: 10.1002/1099-1638(200011/12)16:6, ISSN: 0748 8017, John Wiley & Sons, Inc., NY, USA.

Kimura F, Ariyoshi H, Ishikawa H, Naruko Y, Yamato H (2003) Capturing Expert Knowledge for Supporting Design and Manufacturing of Injection Molds, *CIRP Annals - Manufacturing Technology*, 53(1):147–150, doi:10.1016/S0007-8506(07)60665-9

Kissi N El, Piau J M and Toussaint F (February 1997), Sharkskin and cracking of polymer melt extrudates, *Journal of Non-Newtonian Fluid Mechanics*, 68(2–3):271–290, doi:10.1016/S0377-0257(96)01507-8, ISSN 0377-0257/02, Elsevier Science Publishers B V, Amsterdam, The Netherlands.

Kleindel S, Eder R, Schretter H and Hochenauer C (22 Jan 2014), Elastic mold deformation during the filling and packing stage of the injection molding process, *Smart science*, 2(1):44-53, doi: 10.6493/SmartSci.2014.158, ISSN: 2308-0477, Taiwan Association of Engg & Tech Innovation.

Knepper P C (16-20 May 2004), The effect of runner diameter on packing of a plastic part with injection molding, in *ANTEC*, Chicago, IL, USA, 1;702-706, Society of Plastics Engineers, NY, USA.

KOCETAL K700 (2014) General Purpose POM 1018 from KonLon Plastic Inc, Eungmyeong-dong, Gimcheon-si, Gyeongsangbuk-do, Korea.

Kohler Arthur (28 Oct, 1975) Alignment Assemblies for Plastic Injection Moulds, *US Patent 3915610 A*.

Kolnaar J W H and Keller A A (April 1997), A temperature window of reduced flow resistance in polyethylene with implications for melt rheology Part-3: Implications for flow instabilities and extrudate distortion, *International Journal for the Science and Technology of Polymers*, 38(8):1817–1833, doi:10.1016/S0032-3861(96)00707-0, ISSN: 0032-3861, Elsevier Science Publishers B V, Amsterdam, The Netherlands.

Kulkarni Suhas (2010) *Robust Process Development and Scientific Molding*, Carl Hanser Verlag GmbH & Co. KG, Munich, Germany.

Kumar Amit and Ghoshdastidar P S (15 Oct 2001), Numerical simulation of polymer flow into a cylindrical cavity, *Jour of fluids engg*, 124(1):251-262, doi:10.1115/1.1445796, ISSN: 0098 2202, Transactions of the ASME, NY, USA.

Kumar Amit, Ghoshdastidar P S, Maju M K (15 Jan 2002) Computer simulation of transport processes during injection mould-filling and optimisation of the molding conditions, *Journal of Materials Processing Technology*, 120(1-3):438-449,

doi:10.1016/S0924-0136(01)01211-0, ISSN: 0924 0136, Elsevier Science Publishers B V, Amsterdam, The Netherlands.

Kwong C K, Smith G F (April 1998) A Computational system for process design of injection moulding: Combining blackboard-based expert system and case based reasoning approach, *International journal of advanced manufacturing technology*, 14(4):239-246, doi: 10.1007/BF01199878, ISSN 0268-3768, Springer-Verlag Ltd, London, UK.

Lanxess Corporation (2007) *Engineering plastics part & mould design guide*, Pp. 168, Pittsburgh, PA 15275, USA.

Larson Ronald G (1999) *The Structure and Rheology of Complex Fluids*, ISBN 13: 9780195121971, Oxford University Press Inc, NY, USA.

Lee Sang Hun (15 May 2009) Feature-based non-manifold modeling system to integrate design and analysis of injection molding products, *Journal of Mechanical Science & Technology*, 23(5):1331-41, doi:10.1007/s12206-009-0407-3, ISSN 1738-494X, Springer-Verlag Ltd, London, UK.

Liang Ji Zhao (2002) Characteristics of melt shear viscosity during extrusion of polymers, *Polymer Testing: Material Characterisation*, 21(3):307-311, doi:10.1016/S0142-9418(01)00088-5, ISSN 0142-9418/02, Elsevier Science Publishers B V, Amsterdam, The Netherlands.

Liang Ji-Zhao (2002), The melt elastic behaviour of polypropylene/glass bead composites in capillary flow, *Polymer Testing: Material Behaviour*, 21(8):927-931, ISSN: 0142-9418, doi:10.1016/S0142-9418(02)00036-3, Elsevier Science Publishers B V, Amsterdam, The Netherlands.

Liang Ji-Zhao (April 2001), Pressure effect of viscosity for polymer fluids in die flow, *International Journal for the Science and Technology of Polymers*, 42(8):3709-3712, doi:10.1016/S0032-3861(00)00507-3, ISSN: 0032-3861, Elsevier Science Publishers B V, Amsterdam, The Netherlands.

Liang Ji-Zhao (June 2005), Estimation of entry natural converging angles during capillary extrusion flow of carbon black filled NR/SBR compound, *Polymer Testing: Material*

Behaviour, 24(4):435–438, doi: 10.1016/j.polymertesting.2005.01.011, ISSN: 0142-9418, Elsevier Science Publishers B V, Amsterdam, The Netherlands.

Liang Ji-Zhao (June–July 1995), Effect of the die angle on the extrusion swell of rubber compound, *Journal of Materials Processing Technology*, 52(2-4):207-212, doi:10.1016/0924-0136(94)01610-D, ISSN 0924-0136, Elsevier Science Publishers B V, Amsterdam, The Netherlands.

Liang Ji-Zhao (September 2000), Estimation of die-swell ratio for polymer melts from exit pressure drop data, *Polymer Testing: Data Interpretation*, 20(1):29–31, doi:10.1016/S0142-9418(99)00074-4, ISSN: 0142-9418, Elsevier Science Publishers B V, Amsterdam, The Netherlands.

Liang Ji-Zhao and Ness J N (April 1997), Studies on melt flow properties of low density and linear density polyethylene blends in capillary extrusion, *Polymer Testing*, 16(2):173–184, ISSN: 0142-9418. doi:10.1016/S0142-9418(96)00041-4, Elsevier Science Publishers B V, Amsterdam, The Netherlands.

Liang Ji-Zhao, Chan J S F and Wong E T T (20 July 2001), Effects of operation conditions and die angles on the pressure losses in capillary flow of PS melt, *Journal of materials processing technology*, 114(2);118-121, doi:10.1016/S0924-0136(01)00731-2, ISSN 0924-0136, Elsevier Science Publishers B V, Amsterdam, The Netherlands.

Lin Huang-Ya, Young Wen-Bin (Sept 2009) Analysis of the filling capability to the microstructures in micro-injection molding, *Applied Mathematical Modelling*, 33(9):3746-3755, doi: 10.1016/j.apm.2008.12.012, ISSN: 0307-904X, Elsevier Science Publishers B V, Amsterdam, The Netherlands.

Lisjak D, Godec D, Pilipovic A (2009) Application of artificial intelligence in conceptual mould design, *7th International conference on industrial tools and material processing technologies, ICIT&MPT 2009*, Pp. 277-280, Slovenian tool and die development centre, Slovenia, Ljubljana.

Low Maria L H, Lee K S (2003) Application of Standardisation for initial design of plastic injection moulds, *International journal of production research*, 41(10):2301-2324,

doi:10.1080/0020754031000077338, ISSN 0020–7543, CRC Press, Taylor & Francis Ltd., Singapore.

Ma Yong-Sheng, Tor Shu Beng, Britton Graeme A (02 Aug 2003) The development of standard component library for plastic injection mould design using an object-oriented approach, *International Journal of Advanced Manufacturing Technology*, 22(9):611–618, doi:10.1007/s00170-003-1555-8, ISSN 0268-3768, Springer-Verlag Ltd, London, UK.

Malloy Robert A (1994), *Plastic part design for injection molding*, ISBN: 978-344640468-7, Carl Hanser Verlag GmbH & Co. KG, Munich, Germany.

Marcus Paul (31 July 1967) Moulding Apparatus Valve & Nozzle, *US Patent 3535742 A*.

Mark James E (2007), *Physical properties of polymers handbook*, 2ed., doi: 10.1007/978-0-387-69002-5, ISBN 978-0-387-31235-4, Springer-Verlag Ltd, London, UK.

Martinez A, Castany J and Mercado D (Dec 2011), Characterization of viscous response of a polymer during fabric IMD injection process by means a spiral mold, *Measurement*, 44(10):1806–1818, doi: 10.1016/j.measurement.2011.09.011, ISSN 0263-2241, Elsevier Science Publishers B V, Amsterdam, The Netherlands.

MAS, Microsoft Academic Search, (Accessed on 1 May 2012), Microsoft

Matin Ivan, Hadzistevic Miodrag, Hodolic Janko, Vukelic Djordje, Lukic Dejan (Nov 2012) A CAD/CAE-integrated injection mold design system for plastic products, *International journal of advanced manufacturing technology*, 63(5):595–607, doi:10.1007/s00170-012-3926-5, ISSN 0268-3768, Springer-Verlag Ltd, London, UK.

Matsunaga K, Kajiwara T and Funatsu K (July 1998), Numerical Simulations of Multi-Layer Flow for Polymer Melts: A Study of the Effects of Viscoelasticity on Interface Shape of Polymers within Dies, *Polymer Engineering & Science*, 38(7):1099-1111, doi: 10.1002/pen.10277, ISSN: 1548-2634, Society of Plastics Engineers, NY, USA.

Mattis James, Sheng Paul, Di Scipio William, Leong Ken (6-8 May 1996), A framework for analysing energy efficient injection moulding die design, *Proceedings of International Symposium on Electronics & Environment*, Dallas, TX, USA, INSPEC Accession No:

5323698;207-212, doi:10.1109/ISEE.1996.501879, ISBN: 0-7803-2950-3, IEEE Transactions.

McCrea William H (27 Jan 2012), *Analytical Geometry of Three Dimension*, ISBN 0-486-45313-8, Dover Publications, NY, USA.

McKee Raymond W and Hoover Joshua A (7-11 May 2006), Effect of sharp corners and runner length on melt flow imbalances, *ANTEC*, Charlotte, NC, 5;2868-2872, Society of Plastics Engineers, NY, USA.

Mehat Nik Mizamzul, Kamaruddin Shahrul (24 Mar 2011) Investigating the effects of injection moulding parameters on the mechanical properties of recycled plastic parts using the Taguchi method, *Materials & Manufacturing Processes*, 26(2):202-209, doi:10.1080/10426914.2010.529587, ISSN: 10426914.

Menges, Georg, Michaeli, Walter, and Mohren, Paul (2001) *How to make Injection Moulds*, 3ed, doi: 10.3139/9783446401808, ISBN: 978-3-446-21256-5, Carl Hanser Verlag GmbH & Co. KG, Munich, Germany.

Metzger Michael W (02 Dec 2009) Plastics one has the vision, *Quality Digest*, Plastics One, Melville, New York, USA.

Min B H (10 May 2003), A study on quality monitoring of injection-moulded parts, *Journal of material processing technology*, 136(1-3):1-6, doi: 10.1016/S0924-0136(02)00445-4, ISBN 0924 0136, Elsevier Science Publishers B V, Amsterdam, The Netherlands.

Mok C K, Chin K S and Lan Hongbo (Feb 2008) An internet based intelligent design system for injection moulds, *Robotics & computer integrated manufacturing*, 24(1):1-15, doi: 10.1016/j.rcim.2006.05.003, ISSN: 0736-5845, Elsevier Science Publishers B V, Amsterdam, The Netherlands.

Montgomery Douglas C (July 2012), *Introduction to statistical quality control*, 7th ed International student version, ISBN: 978-1-118-32257-4, John Wiley & Sons, Inc., NY, USA.

Morgan Wilhelm O (18-19 March 2002), Profit from redesign tooling and leadership change, in *Advances in plastic injection moulding tech*, Process optimisation and simulation techniques session, Barcelona, Spain, ISBN 1-85957-314-2, iSmithers Rapra Publishing, Shropshire, UK.

Muzychka Y S and Edge J (Nov 2008), Laminar non-newtonian fluid flow in noncircular ducts and microchannels, *Jour of fluids engg*, 130(11);1112011-7, doi: 10.1115/1.2979005, ISSN: 0098 2202, Transactions of the ASME, NY, USA.

Nabialek J, Koszkul J (30 Nov, 2006) Model optimisation for mould filling analysis with application CAE package Mould, *Journal of Achievements in Materials & Manufacturing Engineering*, 19(1):75-82: 1.630, International OCSCO World Press, ed. University Czestochowa Technical. - al Armii Krajowej 19c, Czestochowa, Poland.

Nakamura Susumu, Yokoi Kochi and Nakamura Hejime (17 April 1990) Nozzle Touch Sprue Bush Device, *US Patent 4917595 A*.

Neely Amanda and Hennebicque Mark (4-8 May 2003), The effect of runner shape on mold filling and product variation, Proceedings of 61st ANTEC, Nashville, TN, USA, 3;3368-3372, Society of Plastics Engineers, NY, USA.

Nightingale J (1978), *Mould design and manufacture, in Developments in injection moulding*, 1ed., by Whelan Anthony and Craft J L, Pp.71-100, doi: 10.1007/978-94-009-9649-6_3, ISBN 978-94-009-9651-9, Applied sci pub ltd, NJ, USA.

Ohlemiller T J, Shields J, Butler K, Collins B and Seck M (15-18 Oct 2000), Exploring the role of polymer melt viscosity in melt flow and flammability behaviour, in *Proceedings of new developments & key market trends in flame retardancy*, Fire Retardant Chemicals Association, Ponte Vedra, FL, USA, Pp1-28.

Olmsted Bernie A and Darvis Martin E (14 March 2001), *Practical Injection Moulding*, ISBN-13: 000-0824705297, CRC Press, Taylor & Francis Ltd., Singapore.

Ong S K, Prombanpong S, Lee K S (Feb 1995) An object-oriented approach to computer-aided design of a plastic injection mould, *Journal of Intelligent Manufacturing*, 6(1):1-10, doi: 10.1007/BF00123672, ISSN: 0956-5515, Springer-Verlag Ltd, London, UK.

Osswald Tim A and Hernández-Ortiz Juan P (2006), *Polymer processing - modeling and simulation*, ISBN-13: 978-1-56990-398-8, Carl Hanser Verlag GmbH & Co. KG, Munich, Germany.

Packianather M S, Drake P R and Rowlands H (Dec 2000), Optimizing the parameters of multilayered feed forward neural networks thru' taguchi design of experiments, *Quality & reliability engg intl*, 16(6):461–473, doi: 10.1002/1099-1638(200011/12)16:6<461: AID-QRE341>3.0.CO;2-G, ISSN: 1099-1638, John Wiley & Sons, Inc., NY, USA.

Panchal Rahul, Kazmer David O (29 Nov 2010) In-situ shrinkage sensor for injection molding, *Journal of manufacturing science & engineering*, 132(6):6-064503, doi:10.1115/1.4002765, ISSN:1087-1357, Transactions of the ASME, NY, USA.

Patil Pramod D, Feng J James and Hatzikiriakos Savvas G (15 November 2006) Constitutive modelling and flow simulation of PTFE paste extrusion, *Journal of Non-Newtonian fluid mechanics*, 139(1-2):44–53, doi: 10.1016/j.jnnfm.2006.05.013, ISSN: 0377-0257, Elsevier Science Publishers B V, Amsterdam, The Netherlands.

Pearson Karl (1900), On the criterion that a given system of deviation from the probable in the case of a correlated system of variables is such that it can be reasonably supposed to have arisen from random sampling, *Philosophical magazine series 5*, 50(302):157-175, doi:10.1080/14786440009463897, ISSN: 1941-5982, CRC Press, Taylor & Francis Ltd., Singapore.

Peischl G C and Bruker I (25 August 2004) Melt homogeneity in injection moulding: Application of a ring-bar device, *Polymer Engineering & Science*, 29(3):202-208, doi: 10.1002/pen.760290308, ISSN: 1548-2634, Society of Plastics Engineers, NY, USA.

Pérez-González José (2001) Exploration of the slip phenomenon in the capillary flow of linear LDPE via electrical measurements, *Journal of Rheology*, ed. Colby Ralph H., 45(4):845, doi: 10.1122/1.1380259, ISSN 0148-6055, The Society of Rheology, Victoria, Australia.

Petrova Tatiana, Kazmer David (1999) Incorporation of phenomenological models in a hybrid neural network for quality control of injection moulding, *Polymer-Plastics*

Technology & Engineering, 38(1):1-18, doi:10.1080/03602559909351556, ISSN: 0360-2559, CRC Press, Taylor & Francis Ltd., Singapore.

Piau J M, Kissi N El and Nigen S (June 2000) Effect of die entrance filtering on mitigation of upstream instability during extrusion of polymer melts, *Journal of Non-Newtonian Fluid Mechanics*, 91(1):37–57, doi:10.1016/S0377-0257(99)00083-X, ISSN 0377-0257, Elsevier Science Publishers B V, Amsterdam, The Netherlands.

Piau J M, Kissi N El and Tremblay B (1990), Influence of upstream instabilities and wall slip on melt fracture phenomena during silicones extrusion through orifice dies, *Journal of Non-Newtonian Fluid Mechanics*, 34(2):145–180, doi:10.1016/0377-0257(90)80016-S, ISSN 0377-0257/02, Elsevier Science Publishers B V, Amsterdam, The Netherlands.

Pichelin E, Coupez T (July 1999) Taylor discontinuous Galerkin method for the thermal solution in 3D mold filling, *Computer Methods in Applied Mechanics & Engineering*, 178(1-2):153-169, doi:10.1016/S0045-7825(99)00011-0, ISSN: 0045-7825, Elsevier Science Publishers B V, Amsterdam, The Netherlands.

Popli G S, Rao D N (26 July 2009) Strategies for enhancing competitiveness of Indian Plastic Processing in post WTO regime, ID 1439092, *Sustainable Social Research Network*, New Delhi, India.

Postolache Ion, Fetecau Catalin, Stan Felicia and Nedelcu Dumitru (Dec 2009), Study of the polymer flow through tubular runner, *Materiale plastice*, 46(4):458-461, ISSN: 0034-7752, Society of Chemistry, Bucharest, Romania.

Pye Ronald George William (1992), *Injection Mould Design Manual for the Thermoplastics Industry*, 4ed, ISBN 0-582-01611-8, Longman Scientific & Technical (John Wiley & Sons, Inc., NY, USA) in association with the Plastics and Rubber Institute, UK.

Quadros W R, Gurumoorthy B, Ramaswami K, Prinz F B (July 2001) Skeletons for representation and Reasoning in Engineering Applications, *Engineering with computers*, 17(2):186-198, doi:10.1007/PL00007200, ISSN 0177-0667, Springer-Verlag Ltd, London, UK.

Ramamurthy A V (April 1986) Wall Slip in Viscous Fluids and Influence of Materials of Construction, *Journal of Rheology*, 30(2):337-358, doi: 10.1122/1.549852, ISSN: 0148-6055, The Society of Rheology, NJ, USA.

Ramamurthy A V and McAdam J C H (1980), Velocity Measurements in the Die Entry Region of a Capillary Rheometer, *Journal of Rheology*, 24(2):167-189, doi: 10.1122/1.549561, ISSN: 0148-6055, The Society of Rheology, Victoria, Australia.

Rao Natti S (2004) *Design Formulas for Plastics Engineers*, 2ed., doi: 10.3139/9783446413009, ISBN: 978-3-446-22674-6, Carl Hanser Verlag GmbH & Co. KG, Munich, Germany.

Rees Herbert (2001) *Understanding Injection Mould Design*, ISBN 1-56990-311-5, Carl Hanser Verlag GmbH & Co. KG, Munich, Germany.

Rees Herbert (2002) *Mold Engineering*, 2ed, ISBN 3 446 2 1 659 6, Carl Hanser Verlag GmbH & Co. KG, Munich, Germany.

Ren Weiqing, Hu Dan and Weinan E (Oct 2010) Continuum models for the contact line problem, *Physics of fluids*, 22(10): 102103, doi:10.1063/1.3501317, ISSN: 0031-9171, American Institute of Physics, NY, USA.

REPOL H110MA, (2014) General Purpose Polypropylene, from Reliance Industries Ltd., Mumbai, India.

Rhee B O, Park H P, Cha B S and Lee K (7 - 11 May 2006), An experimental study of the variable-runner system, in *ANTEC*, Charlotte, NC, USA, 2(103364); 1113-1117, Society of Plastics Engineers, NY, USA.

Richardson S (Dec 1972) Hele Shaw flows with a free boundary produced by injection of fluid into a narrow channel, *Journal of Fluid Mechanics*, 56(4):609-618, doi: 10.1017/S0022112072002551, ISSN: 0022-1120, Cambridge University Press, Cambridge, UK.

Rosato Dominick V, Rosato Donald V and Rosata Marlene G (2000), *Injection moulding handbook*, 3ed, Kluwer academic publishers, Massachusetts, ISBN 0-7923-8619-1 - 9780792386193.

Rosato Donald V and Rosato Dominick V (1990), *Plastic Processing Data Handbook*, 2ed, doi:10.1007/978-94-010-9658-4, ISBN: 978-94-010-9660-7, © Van Nostrand Reinhold, Springer International Publishing AG, Netherlands.

Rubin I Irvin (27 April, 1973), *Injection Moulding - Theory & Practice*, Volume 7 of SPE Monographs, ISBN: 978-0-471-74445-0, John Wiley & Sons, Inc., NY, USA.

Sabic (2008) *Injection moulding processing guide*, SABIC Innovative plastics IP BV.

SC 203EL (2014), General Purpose Polystyrene (GPPS), from Supreme Petrochem Ltd., 17/18, Shah Industrial Estate, Veera Desai Road, Andheri (West), Mumbai- 400 053, India.

Schmidt Harald H and Rozema Henry J (26 April 1988) Sealing & Retaining bush for injection moulding, *US Patent No 4740151*.

Schramm Dana E and Vadlamudi Raghu (1 July 2006), Reshaping devices with microfeatures, *Medical Device and Diagnostic Industry News*.

Sen Chiradeep, Ameri Farhad, Summers Joshua D (30 Sept 2010) An entropic method for sequencing discrete design decisions, *Journal of Mechanical Design*, 132(10):101004:1-14, doi:10.1115/1.4002387, ISSN:1050-0472, Transactions of the ASME, NY, USA.

Seo Jaho, Khajepour Amir and Huissoon Jan P (11 Nov, 2011), Identification of die thermal dynamics using neural networks, *Jour of Dyn. Sys., Meas., Control* 133(6):061008, doi:10.1115/1.4004045, ISSN:0022-0434, Transactions of the ASME, NY, USA.

Seow L W, Lam Y C (15 Dec 1997) Optimising flow in plastic injection moulding, *Journal of Materials Processing Technology*, 72(3):333-341, doi:10.1016/S0924-0136(97)00188-X, ISSN: 0924-0136

Seralathan V, Jegadheesan C (July 2012) A framework of experts decisions in injection molding design: A neuro-fuzzy approach, *European journal of scientific research*, 82(4):474-484, ISSN 1450-216X, EuroJournals Publishing, Inc., Seychelles.

Shankar (1978) Dynamic modelling and control of injection molding machines, *Doctoral Dissertation*, Carnegie-Melton University, USA.

Shanker R and Ramanathan R (7 to 11 May 1995), Effect of die geometry on flow kinematics in extrusion dies, *ANTEC, Boston, Massachusetts*, S42700/962601:65-68, 012SPE, Extrusion Division; vol 1- Processing, ISBN 978-1566763196, Society of Plastics Engineers, NY, USA.

Shapiro Samuel Sanford and Wilk Martin B (1965), An analysis of variance test for normality (complete samples), *Biometrika*, 52(3-4):591-611:(593), doi: 10.1093/biomet/52.3-4.591, ISSN 0006-3444.

Shenoy Arun V and Saini D R (23 Aug 1996) *Thermoplastic Melt Rheology and Processing*, ISBN 9780824797232, Marcel Dekker Inc., New York, USA.

Shimbo Minoru, Kawashima H and Yoshitani S (24-25 Oct 2000), Foam injection technology and influence factors of microcellular plastics, in *2nd Intl. conference on thermoplastic foam FOAMS 2000*, Thermoplastic Materials & Foams Division, NJ, Session III (1); Pp162-168, Society of Plastics Engineers, NY, USA.

Shoemaker Jay (2006), *Mouldflow design guide*, doi: 10.3139/9783446418547, ISBN: 978-3-446-40640-7, Carl Hanser Verlag GmbH & Co. KG, Munich, Germany.

Smith Douglas E (21 May 2003) Design sensitivity analysis and optimization for polymer sheet extrusion and mold filling processes, *International Journal for Numerical Methods in Engineering, Special Issue: Design Sensitivity and Optimization of Large-Scale Problems*, 57(10):1381-1411, doi: 10.1002/nme.782, ISSN: 1097-0207, John Wiley & Sons, Inc., NY, USA.

Sommerville D M Y (25 Feb 2016) *Analytical geometry of Three Dimension*, Cambridge University Press, London, UK, ISBN 9781316601907

Souza Araújo André Luíz de, Matos Gurgel José Maurício Alves de, Marcondes Francisco (6-11 November 2005) Mould filling simulation using a control volume FEM, *18th International Congress of Mechanical Engineering*, Proceedings of COBEM 2005, 6-11:8, Ouro Preto, MG, Brazil.

SPI-SPE Mold Finish Comparison Standard, ver B3, Society of the Plastics Industry & Society of the Plastics Engineers, USA.

Stair W K (2010), "Dynamic seals" in *Handbook of Lubrication: Theory & Design*, edited by E Richard Booser, Vol 2, doi: 10.1201/9781420050448.ch31, ISBN 978-0-8493-3902-8, Society of Tribologists and Lubrication Engineers & American Society of Lubrication Engineers, CRC Press,

Stevens Malcolm P (19 Nov 1998), *Polymer Chemistry: An Introduction*, 3ed., ISBN-13: 978-0195124446, Oxford University Press, NY, USA.

Strong Brent A (2006), *Plastics: Materials & Processing*, 3ed., ISBN-13: 9780131145580, Pearson Prentice Hall, Ohio, USA.

Sun Guo Gong, Liu Chang Hua and Li Qiang (March 2015), Optimal design of runner for shell of mobile telephone based on moldflow software, *Applied Mechanics & Materials*, 741:191-194, doi: 10.4028/www.scientific.net/AMM.741.191, ISSN: 1662-7482, Trans Tech Publications Inc. Switzerland.

Syrjala S (Jan 2002), Accurate prediction of friction factor and nusselt number for some duct flows of power-law non-newtonian fluids, *International Journal of Computation & Methodology, Numerical heat transfer Part A: Applications*, 41(1):89-100, doi:10.1080/104077802317221456, ISSN: 1040-7782, CRC Press, Taylor & Francis Ltd., Singapore.

Tadmor Zehev and Gogos Costas G (2006), *Principles of polymer processing*, 2ed., ISBN 0470355921, 9780470355923, John Wiley & Sons, Inc., NY, USA.

Takahashi Yoshiaki, Shinichi Kitade, Naoki Kurashima and Ichiro Noda (Nov 1994), Viscoelastic properties of immiscible polymer blends under steady and transient shear flows, *Polymer Journal*, 26(11):1206–1212, doi:10.1295/polymj.26.1206, ISSN: 0032-3896, Nature Publishing Group, The Society of Polymer Science, Japan.

Tan Victor (June 2006), "Rheological and thermophysical properties of polymers", in *Principles of Polymer processing*, ed by Zehev Tadmor, Costas G. Gogos, 2ed., Pp 887-913, ISBN: 978-0-471-38770-1, John Wiley & Sons, Inc., NY, USA.

Tang S H, Kong Y M, Sapuan S M, Samin R and Sulaiman S (20 Jan 2006), Design and thermal analysis of plastic injection mould, *Jour of materials process tech*, 171(2):259-267, doi: 10.1016/j.jmatprotec.2005.06.075, ISSN: 0924 0136, Elsevier Science Publishers B V, Amsterdam, The Netherlands.

Tewes Otto (Feb 2002), On par with the automotive industry, *Engel Injection magazine for plastic industry*, Pp. 26-27.

Thomas Eltzer, Denis Cavallucci, Emmanuel Caillaud (1 - 5 May 2005) Improvement of mould design: A new method based on contradictions, 63rd ANTEC, Hynes Convention Center, Boston, Massachusetts, Processing Section, Mold Making and Mold Design Division, New Ideas for Improvements, 1(35) T8; 899-903, ISBN: 978-1604234527, Society of plastics engineers, NY, USA.

Tremblay Bernard (May 1992) Visualization of the flow of linear low density polyethylene blends through sudden contractions, *Journal of Non-Newtonian Fluid Mechanics*, 43(1):1–29, doi:10.1016/0377-0257(92)80015-P, ISSN 0377-0257/02, Elsevier Science Publishers B V, Amsterdam, The Netherlands.

Trifonov Dimitar S and Kostadinov Kostadin (2008), Computer modeling and simulation of the process of information microstructure replication for optical data storage, *Cybernetics & information technologies*, 8(4), ISSN: 1311-9702, Bulgarian academy of sciences, Sofia.

Trifonov Dimitar S and Toshev Yuli E (3-5 Oct 2007), An approach for predicting the correct geometry and parameters of the sprue system of an optical disc mould by use a computer aided design and simulation, *4M2007: 3rd International Conference on Multi-Material Micro Manufacture*, PID367152:221-224, Process Modelling and Simulation / ed. Dimov S, Menz W and Toshev Y, Whittles Publishing Ltd., Borovets, Bulgaria.

Turgeon E, Pelletier D and Borggaard J (7 June 2002), A general continuous sensitivity equation formulation for complex flows, *International Journal of Computation and Methodology, Numerical heat transfer Part B: Fundamentals*, 42(6):485-498, doi:10.1080/10407790260444787, ISSN 1040-7790, CRC Press, Taylor & Francis Ltd., Singapore.

Utracki L, M R Kamal (February 1982), A Melt rheology of polymer blends, *Polymer Engineering & Science*, 22(2):96–111, doi: 10.1002/pen.760220211, ISSN: 1548-2634, Society of Plastics Engineers, NY, USA.

Varela A E (January 2000), Self-tuning pressure control in an injection moulding cavity during filling, *Chemical engineering research design*, Official Journal of the European Federation of Chemical Engineering, Institution of Chemical Engineers (UK), 78(1):79–86, doi:10.1205/026387600526906, ISSN: 0263-8762, Elsevier science publishers B V, Amsterdam, The Netherlands.

Varner Arnold (5-8 May 1980), MOLDFLOW - Computer age approach to design of moulds and plastics parts, 38th ANTEC, NY, 27:598-599, Society of Plastics Engineers, NY, USA.

Vaz Jr M and Gaertner E L (Nov 2003), Rheological instability of polymer melt flow in circular channels, *International Communications in Heat & Mass Transfer*, 30(8): 1051-9, doi: 10.1016/S0735-1933(03)00171-4, ISSN: 0735 1933, Elsevier science publishers B V, Amsterdam, The Netherlands.

Voller V R and Peng S (Nov 1995) An algorithm for analysis of polymer filling of molds, *Polymer Engineering & Science*, 35(22):1758-1765, doi: 10.1002/pen.760352205, ISSN 1548-2634, Society of Plastics Engineers, NY, USA.

Wang Jian (23 March 2012), *Some critical issues for injection moulding*, doi: 10.5772/2294, ISBN 978-953-51-0297-7, InTech Publishing.

Warring, Ronald Horace (1981), *Seals and sealing handbook*, 1ed, ISBN 0-87201-801-6, Gulf Publishing Company, Book Division, Houston, USA.

Weissman Alexander, Ananthanarayanan Arvind, Gupta Satyandra K, Sriram Ram D (12 May 2010) A Systematics methodology for accurate design stage estimation of energy consumption for injection molded parts, *Proceedings of the International design engineering technical conferences & computers and information in engineering conference (IDETC/CIE 2010)*, Montreal, Quebec, Canada, DETC 2010-28889: 1-13, doi:10.1115/DETC2010-28889, Transactions of the ASME, NY, USA.

Whelan Tony and Goff John (1990), *Injection moulding of thermoplastics Materials -1*, ISBN 978-1-4757-0582-9, Van No strand Reinhold, NY, USA.

Whelan W (1982), *Injection moulding materials*, ISBN 13-978-94-009-7360-2, doi:10.1007/978-94-009-7358-9, Applied sci pub ltd, NJ, USA.

White Frank M (16 Jan 2016), *Fluid Mechanics*, 8ed, ISBN: 978-1-2591-6992-2, Tata McGraw Hill Education Pvt Ltd., New Delhi, India.

White James Lindsay (23-26 August 1972), Critique on flow patterns in polymer fluids at the entrance of a die and instabilities leading to extrudate distortion, *US-Japan Seminar on Polymer Processing and Rheology*, Applied polymer symposia 20(9): 155–174, ed by Donald C. Bogue, Misazō Yamamoto, James Lindsay White, University of Tennessee, Knoxville and at Gatlinburg, Tennessee, NCID BA13905646, John Wiley & Sons, Inc., NY, USA.

Windsor Machine specifications, (accessed in 2013), www.windsormachines.com, *Windsor machines ltd, Mumbai*,

Woll Suzanne L N, Cooper Douglas J (May 1997) Pattern-based closed loop quality control for the injection molding process, *Polymer Engineering & Science*, 37(5):801-812, doi: 10.1002/pen.11723, ISSN 1548-2634, Society of Plastics Engineers, NY, USA.

Xu Guojun (2004), Study of thin wall injection moulding, *PhD Thesis*, ISSN 0496668943, Department of Chemical Engineering, Ohio State University, Columbus, OH, USA.

Yablochnikov E I, Pirogov A V, Vasilkov S D, Andreev Y S and Barvinsky L A (8 - 12 September 2014), Studies of design and technology influence on optical properties of injection molding parts by simulation, in *Shaping the future by engg, 58th IWK Ilmenau scientific colloquium*, Technische Universität Ilmenau.

Yang S Y and Nien L (Sept 1996), Experimental study of injection compression molding of cylindrical parts, *Advances in polymer tech*, 15(3):205–223, ISSN: 0730 6679, John Wiley & Sons, Inc., NY, USA.

Yang W J, Mochiziki S, Nishiwaki N and Mujumdar A S (1994), "Transport phenomena in manufacturing and materials processing", A Volume in *Transport processes in engg*, ISBN: 978-0-444-89358-1, Elsevier Science Publishers B V, Amsterdam, The Netherlands.

Yang X, Wang S Q, Halsa A and Ishida H (1998), Fast flow behavior of highly entangled monodisperse polymers, Part-1 Interfacial stick-slip transition of polybutadiene melts, *Rheologica acta*, 37(5):415–423, doi: 10.1007/s003970050128, ISSN: 0035 4511, Springer-Verlag Ltd, London, UK.

Yao D and Kim B (Nov 2004), Scaling issues in miniaturization of injection molded parts, *Jour of mfg sci. & engg*, 126(4):733-739, doi: 10.1115/1.1813479, ISSN: 10871357, Transactions of the ASME, NY, USA.

Ye X G, Lee K S, Fuh J Y H, Zhang Y F (19 Feb, 2004), Automatic initial design of injection mould, *International Journal of Materials and Product Technology*, 15(6):503-517, doi:10.1504/IJMPT.2000.001259, ISSN 0268-1900.

Yeager Mark (Summer 2014), Variothermal temperature control more gloss, less weld lines, *Molding views, Injection molding division*, 22-27, Society of Plastics Engineers, NY, USA.

Yoshioka Mitsushi and Kawasaki Tatsuya (23 Oct 2007) Aligning device for an injection nozzle, *US Patent 7284977 B2*.

Yu Yun-Wey, Liu Ta-Jo, Hsu Chang-Liang, Yang Yeon-Sheug (8 Apr 1999) Hybrid 3D/2D finite element technique for polymer processing operations, *Polymer Engineering & Science*, 39(1):44-54, doi: 10.1002/pen.11395, ISSN 1548-2634, Society of Plastics Engineers, NY, USA.

Zdanski P S B and Vaz Jr M (May 2011), A numerical method for simulation of incompressible three-dimensional newtonian and non-newtonian flows, *International Journal of Computation and Methodology, Numerical heat transfer Part B: Fundamentals*, 59(5):360-380, doi: 10.1080/10407790.2011.572727, ISSN: 1040 7790, CRC Press, Taylor & Francis Ltd., Singapore.

Zdanski P S B, Vaz Jr M and Inácio G R (2008), A finite volume approach to simulation of polymer melt flow in channels, *Engg computations*, 25(3):233 - 250, doi: 10.1108/02644400810857074, ISSN: 0264 4401.

Zhai M, Lam Y C and Au C K (2009), Runner sizing in multiple cavity injection mould by non-dominated sorting genetic algorithm, *Engg with computers*, 25(3):237–45, doi: 10.1007/s00366-008-0120-3, ISSN: 0177 0667, Springer-Verlag Ltd, London, UK.

Zhai M, Lam Y C and Au C K (May 2006) Runner sizing and weld line positioning for plastics injection moulding with multiple gates, *Engineering with computers*, 21(3):218-224, doi:10.1007/s00366-005-0006-6, ISSN 0177-0667, Springer-Verlag Ltd, London, UK.

Zhao Zhenyu, Xushu He, Mingjun Liu, Bai Liu (4-6 June 2010), Injection mould design and optimisation of automotive panel, *3rd International Conference on Information and Computing*, IEEE Computer Society, Vol 3, INSPEC Accession No. 11433441: 119-122, doi: 10.1109/ICIC.2010.214, ISBN: 978-1-4244-7081-5.

Zheng Rong, Tanner Roger I and Fan Xi Jun (2011), *Injection molding, Integration of theory and modelling methods*, doi: 10.1007/978-3-642-21263-5, ISBN 978-3-642-21263-5, Springer-Verlag Ltd, London, UK.

Zhou Huamin M, Li Dequn Q (4 April 2001) Numerical simulation of the filling stage in injection molding based on surface model, *Advances in polymer technology*, 20(2):125-131, doi: 10.1002/adv.1010, ISSN: 1098-2329, John Wiley & Sons, Inc., NY, USA.

Zhou Huanmin (Feb 2013) *Computer modeling for injection moulding*, ISBN 978-0-470-60299-7, John Wiley & Sons, Inc., NY, USA.

Zhu Peng Wei and Edward Graham (April 2004), Morphological distribution of injection moulded isotactic PP: A study of synchrotron small angle X-ray scattering, *International Journal for the Science and Technology of Polymers*, 45(8):2603-2613, doi: 10.1016/j.polymer.2004.02.031, ISSN: 0032-3861, Elsevier Science Publishers B V, Amsterdam, The Netherlands.

Ziobro J (2013), Design modification of the flow system of injection moulds for rubber in the aspect of improving performance, *Proceedings of the Lviv Polytechnic*, National University, Lviv, Ukraine, 772;73-79.

Zombade N, Bean R, Thompson A and Kazmer D O (6-11 May 2007), Analysis and validation of mold design guidelines for cooling time and runner sizing, in *ANTEC*, Mold making and mold design D35 division, Cincinnati, OH, USA, 5:2567-2571, Society of Plastics Engineers, NY, USA.

List of Publications and Communications made out of this Phd Thesis

Peer-reviewed journal publications

1. Muralidhar Lakkanna, Mohan Kumar G C, Ravikiran Kadoli (03 July 2015)
Criticality of appreciating non-Newtonianity in plastic injection mould conduit design, *International Journal of Fluid Mechanics Research*, 42(4):301-314, ISSN 1064-2277, doi: 10.1615/InterJFluidMechRes.v42.i4.20, Begell House, Inc. USA.
2. Muralidhar Lakkanna, Mohan Kumar G C, Ravikiran Kadoli (23 Dec 2014)
Computational design of mould sprue for injection moulding thermoplastics, *Journal of Computational Design and Engineering*, 3(1):37-52,
doi:10.1016/j.jcde.2015.06.006, Society of CAD/CAM Engineers, Elsevier Science B V, Amsterdam, The Netherlands.
3. Muralidhar Lakkanna, Mohan Kumar G C, Ravikiran Kadoli (10 Dec 2014) Simple viscosity criterion for injection moulding thermoplastics, *Polimeri: Plastics and Rubber Journal*, 35 (1-2): 29-33, ISSN: 0351-1871, Society of Plastics and Rubber Engineers, Zagreb, Croatia
4. Muralidhar Lakkanna, Ravikiran Kadoli, Mohan Kumar G C (31 Jul 2013)
Configuring Sprue Conduit Expansion in Plastic Injection Mould Design, *International Journal of Applied Research in Mechanical Engineering*, 3 (1) 14-21, ISSN 2231 – 5950, Interscience Research Network, India.

Peer-reviewed conference presentations

5. Muralidhar Lakkanna, Mohan Kumar G C, Ravikiran Kadoli (25-26 Apr' 14)
Viscosity biased runner conduit design for Plastic Injection Moulding, *6th National conference on advanced in polymeric materials*, OP-89:132,
doi: 10.13140/2.1.1036.8964, Dept of Polymer Science and Technology, Sri Jayachamarajendra college of engineering, Mysore.
6. Muralidhar Lakkanna, Mohan Kumar G C, Ravikiran Kadoli (12-14 Feb 2014)
Influence of Thermoplastic Shear Thinning Behaviour on Sprue Conduit Expansion in

- Plastic Injection Moulding, *25th AGM Symposium of Materials Research Society of India*, doi: 10.13140/2.1.1462.8808, Indian Institute of Science, Bangalore.
7. Muralidhar Lakkanna, Mohan Kumar G C, Ravikiran Kadoli (06-07 Feb 2014)
Viscosity Biased Sprue Conduit Expansion for Plastic Injection Moulding, *27th National convention of metallurgical & materials engineering & National seminar on multifunctional & adaptive materials*, doi: 10.13140/2.1.1593.9523, Institution of Engineers (India), Karnataka State Centre, Bangalore.
 8. Muralidhar Lakkanna, Mohan Kumar G C, Ravikiran Kadoli (18-20 Dec 2013)
Design of Sprue Bush for a Plastic Injection Mould: A Machine Perspective, *1st International and 16th National Conference on Machines and Mechanisms*, 336 (Design-112):241-248, doi: 10.13140/2.1.2871.9046, Indian Institute of Technology Roorkee, India.
 9. Muralidhar Lakkanna, Mohan Kumar G C, Ravikiran Kadoli (21-22 Jun 2013)
Governing Equations to Inject Thermoplastic Melt Through Runner Conduit in a Plastic Injection Mould, *National Conference on Innovations in Mechanical Engineering*, Pp 327-337, doi: 10.13140/2.1.4756.0645, ISBN: 978 93 82163 00 8, Mech Engg Dept, MIT&Sci, Madanapalle, Andhra Pradesh, India.
 10. Muralidhar Lakkanna, Mohan Kumar G C, Ravikiran Kadoli (02 Jun 2013) Design Sensitivity of Sprue Conduit Expansion in Plastic Injection Mould, *International Conference on Mechanical and Industrial Engineering*, Pp 1-7, doi: 10.13140/2.1.5018.2083, ISBN 978-93-83060-05-4, Interscience Research Network, Bengaluru, India.
 11. Muralidhar Lakkanna, Mohan Kumar G C, Ravikiran Kadoli (07-08 May 2013)
Design Sensitivity of Sprue Bush in a Plastic Injection Mould, *National conference on emerging trends in materials, manufacturing and design*, DE08;36, doi: 10.13140/2.1.2527.8409, Mech Engg Dept, MEPCO, Sivakasi, Tamilnadu, India.